Operational Aspects, Failures and Design of Radiant Tube Heater Systems in a Continuous Strip Annealing Furnace

W. Michael James

Thesis submitted to Cardiff University
in fulfilment of the requirements for the degree of
Engineering Doctorate

Cardiff University
June 2011

DECLARATION

This work has not previously been accepted in substance for any degree and is not concurrently submitted in candidature for any degree.

Signed …… (candidate)

Date ……

STATEMENT 1

This thesis is being submitted in partial fulfilment of the requirements for the degree of EngD

Signed …… (candidate)

Date ……

STATEMENT 2

This thesis is the result of my own independent work/investigation, except where otherwise stated.

Other sources are acknowledged by explicit references.

Signed …… (candidate)

Date ……

STATEMENT 3

I hereby give consent for my thesis, if accepted, to be available for photocopying and for inter-library loan, and for the title and summary to be made available to outside organisations.

Signed …… (candidate)

Date ……

SUMMARY

The focus of this Engineering Doctorate Thesis is the investigation into how the radiant tubes installed in the Continuous Annealing Process Line (CAPL) at Port Talbot steel works were failing and what measures could be taken to improve tube life.

Radiant tube replacement and associated maintenance costs were one of CAPL's biggest annual expenditures, with on average 33 tubes changed every year. Tube longevity was as low as 4 years in the hotter furnace zones, while in comparison, the cooler regions of the furnace had all original tubes still in operation after 12 years of service.

A benchmarking process identified that most annealing furnaces were replacing on average 10% of total furnace tubes per year, while tube designs varied according to furnace manufacturer and tube supplier. Segal Galvanising line in Belgium, replaced the least amount at approximately 8.5%, through increasing material grades and subtle design changes

Temperature analysis of the furnace at CAPL, highlighted that tube temperatures reached above 1000ºC with differentials of up to 75ºC across tube length in normal operation. Analysis of failed material identified that the tubes had been subjected to excessively high temperatures, which affected the microstructure and properties of the material, resulting in cracking failures at the end of the firing leg.

Stress analysis showed that tube life was in the region of 4 years with current designs and maximum temperatures of 1000ºC. Installation of expansion bellows and increasing material grade resulted in longevity of the tube to increase by over double.

Improvements have been made to the tube design and material specification throughout the project, with further changes employed in trial tubes, currently in use at CAPL furnace, with the aim of confirming theory discussed in this thesis and improving tube longevity.

ACKNOWLEDGEMENTS

Firstly, I would like to thank the project sponsors EPSRC and Tata Steel for the opportunity to conduct an interesting research project, which I have thoroughly enjoyed. I have worked closely with Tata personnel, namely Gareth Morgan, Darryl Lewis, Andrew Radford and my industrial supervisor Andrew Thomas, whom have contributed towards this thesis and shared the passion for improving radiant tube life at Port Talbot.

At Cardiff University, School of Engineering, huge thanks must go to my academic supervisor Prof Tony Griffiths whose experience, expertise and help has guided the progress of this project. Thanks must go to Prof Keith Williams for his help and to Malcolm Seaborne who I worked closely with in developing the temperature cycling testing rig.

Thanks to a travel grant from the Welsh Livery Guild, I was able to travel to Japan and gain valuable experience in visiting another global steel manufacturer, Sumitomo Metals Ltd, to discuss my project and research and appreciate the work being undertaken at Sumitomo in improving radiant tube life. Thanks to Asano-san and his colleagues for their welcome during my visit.

I have made some wonderful friends during this project and met many characters along the way. To Piia, Chris, Dai and Lee, I have thoroughly enjoyed working with you and shared many memorable moments during the EngD.

I would like to thank my parents for supporting my decision to go to Cardiff University to study Mechanical Engineering and always showed interest and enthusiasm in my work.

Last, but by no means least, I would like to thank my Wife, Sam, who I met and fell in love with through the Engineering Doctorate scheme. We shared some memorable moments together and thank you for all your encouragement, support and love during this project.

Contents

1 Introduction 1

1.1 Background 1
1.2 Motivation 2
1.3 Structure of Thesis 2

2 Background and Literature Review 5

2.1 Radiant Tubes 5
2.1.1 Introduction 5
2.1.2 Combustion 6
2.1.3 Heat Transfer Considerations 14
2.1.4 The Manufacture of Radiant Tube Heating Elements 17
2.1.5 Material Choice 19
2.1.6 Radiant Tube Designs 29
2.1.7 Fuels 31

2.2 Radiant Tube Annealing Furnaces 32
2.2.1 The Requirement for Annealing 33
2.2.2 Continuous Annealing 35
2.2.3 Radiant Tube Furnaces 36

2.3 Summary 37

3 Case Study Site: Port Talbot Works, Continuous Annealing Process Line 38

3.1 Introduction 38
3.2 Tata Steel Port Talbot Works 38
3.2.1 Raw Materials to Steel Making 39
3.2.2 Hot Rolling 40
3.2.3 Cold Rolling 40
3.2.4 Annealing 41

3.3 The Continuous Annealing Process Line 42
3.3.1 Process Sections 42

3.4 Port Talbot Furnace History 47
3.4.1 Introduction 47
3.4.2 Failure History 48

3.4.3 Radiant Tube Designs 51
3.4.4 Material Specifications 59
3.4.5 Failure Types 61
3.4.6 Radiant Tube Failures at Other Sites 63
3.5 Summary 68
4 Analysis of Existing Radiant Tube Furnaces 69
4.1 Introduction 69
4.2 Radiant Tube Furnaces within Tata 69
4.2.1 Tata Packaging, Trostre 69
4.2.2 Tata Steel, Llanwern – "Zodiac" 78
4.2.3 Segal, Liege, Belgium – Galvanising Line 80
4.3 Sumitomo Metals Ltd., Kashima Works, Japan 85
4.3.1 Continuous Annealing Line 86
4.3.2 No.2 Continuous Galvanising Line 88
4.3.3 No.3 Continuous Galvanising Line 89
4.3.4 Radiant Tube Discussions at Kashima Works 89
4.3.5 Radiant Tube Improvements 93
4.4 Summary of Findings 95
5 Radiant Tube Temperature Analysis 99
5.1 Introduction 99
5.1.1 Multi Thermocouple Radiant Tube 99
5.1.2 Data Acquisition 101
5.1.3 Data Presentation 102
5.2 Areas of Investigation 103
5.3 Temperature Analysis and Results 104
5.3.1 Introduction 104
5.3.2 Maximum Temperatures 104
5.3.3 Average Temperature Profile 105
5.3.4 Weekly Analysis 106
5.3.5 Temperature Differential 108
5.3.6 Temperature Differential during Periods of Downtime 109
5.3.7 Furnace Heating and Cooling 112

5.3.8 Tube Temperature Profile....116
5.3.9 Furnace Temperature....120
5.3.10 Frequency of Temperature Variation....122
5.3.11 Heating Rate Trial....124
5.4 Discussion....127
5.5 Summary of Investigation....129
6 Radiant Tube Metallurgical Failure Analysis....130
6.1 Introduction....130
6.2 Background....130
6.3 Experimental....131
6.3.1 Sample Selection....131
6.3.2 Sample Preparation....133
6.3.3 Sample Analysis....134
6.3.4 Visual and Dimensional Examination....134
6.4 Results....135
6.4.1 Weld Failures....135
6.4.2 Deformed Failures....138
6.4.3 Dimensional Analysis....139
6.4.4 Compositional Check....141
6.4.5 Mechanical Testing....143
6.4.6 Microstructure Analysis....145
6.4.7 Scanning Electron Microscope (SEM) Analysis....161
6.5 Discussion....164
6.6 Summary....167
7 Finite Element Modelling of a Radiant Tube....169
7.1 Introduction....169
7.1.1 Building the Model....169
7.1.2 Designs....170
7.1.3 Boundary Conditions....171
7.2 Results and Discussion....173
7.2.1 Deformation....173
7.2.2 Stress Analysis....175

7.2.3 Temperature 179
7.2.4 Heating and Cooling 180
7.3 Design Development 182
7.3.1 New Support Design 182
7.3.2 Expansion Bellows 184
7.4 Radiant Tube Life Prediction and Comparison 187
7.5 Summary of Findings 191
7.5.1 Future Work 192
8 Temperature Cycling of Heat Resistant Material 193
8.1 Introduction 193
8.2 Test Rig Design and Manufacture 193
8.3 Equipment 195
8.3.1 Test Rig Equipment 195
8.3.2 Monitoring Equipment 197
8.4 Test Samples 199
8.5 Test Methods 201
8.5.1 Temperature Cycling 201
8.5.2 Heat and Hold 202
8.6 Results 203
8.6.1 Test Rig Problems 203
8.6.2 Cyclical Temperature 204
8.6.3 Heat and Hold 207
8.7 Discussion 209
8.8 Summary of Findings 211
9 Conclusions and Further Work 212
9.1 Conclusions 212
9.2 Further Work 214
9.2.1 Mixing Element Radiant Tube 214
9.2.2 Ceramic Inserts 215
9.2.3 Radiant Tube Monitoring 216
9.2.4 Different Radiant Tube Designs and Burner Arrangements 217
10 References 218

11 Appendices 227

11.1 Appendix A 227
11.2 Appendix B 228
11.3 Appendix C 228
11.4 Appendix D 230
11.5 Appendix E 231
11.6 Appendix F 232
11.7 Appendix G 234
11.8 Appendix H 236
11.9 Appendix I 238
11.10 Appendix J 239
11.11 Appendix K 240
11.12 Appendix L 241
11.13 Appendix M 242

Index of Tables

Table 4-1 - Process Line Capability 89
Table 4-2 - Description of Radiant Tube Installed 90
Table 4-3 - A summary of the various radiant tube parameters discussed: 98
Table 5-1 - Periods of Downtime 109
Table 6-1 - General information regarding failed samples taken for further analysis 133
Table 6-2 - Table of composition of heat resistant stainless steel grades used at CAPL Port Talbot 142
Table 8-1 - Dimensions and chemical composition of the grades received from Kubota Metals 199
Table 11-1 - Material composition of radiant tube material 227
Table 11-2 - Semi-quantitative EDS microanalysis results of sample 5 OS 6.1 231
Table 11-3 - Calibration chart for the thermocouple voltages 240
Table 11-4 - Temperature cycling log 241
Table 11-5 - Combustion ratios to be considered for the heat cycling test rig 244

Index of Figures

Figure 2-1 - Schematic showing a radiant tube being used to anneal strip steel 5
Figure 2-2 - The change in adiabatic flame temperature with equivalence ratio..... 8
Figure 2-3 - Recuperator heat exchanger recovering heat energy from the hot exhaust gases and transferring them to the incoming combustion air 10
Figure 2-4 - Temperature profile comparison of a radiant tube with regenerative and recuperative systems..... 11
Figure 2-5 - Regenerative burners being utilised in a radiant tube application..... 12
Figure 2-6 - Schematic displaying the design of a burner head..... 12
Figure 2-7 - WS self regenerative burner for radiant tube applications..... 13
Figure 2-8 - Example of a plug-in recuperator used in a radiant tube application 15
Figure 2-9 - Figure displaying the effect of preheating the combustion air on adiabatic flame temperature..... 15
Figure 2-10 - Heat transfer within a typical radiant tube furnace..... 17
Figure 2-11 - Image showing a spin-casting machine able to produce cast tubes. Note different size moulds in background to produce various diameters of tubes 18
Figure 2-12 - Image of a 'W' shaped fabricated tube used in the galvanizing line at Tata Steel, Llanwern..... 19
Figure 2-13 - The role of each major element in a heat resistant alloy material 21
Figure 2-14 - Designation and composition of heat resistant alloys..... 22
Figure 2-15 - Influence of stress and temperature on creep behaviour..... 24
Figure 2-16 - Stress versus rupture lifetime for a particular material at three different temperatures..... 25
Figure 2-17 - Stress versus steady state creep rate at three different temperatures 26
Figure 2-18 - Oxide layer formation which protects the base metal..... 27
Figure 2-19 - The mechanism of spalling as identified by the schematic diagram above. This is the response of the oxide when loaded in compression: (a) Buckling of the oxide (b) Shear cracking of the oxide, and (c) plastic deformation of the oxide and alloy..... 28
Figure 2-20 - A single ended radiant tube with a reverse annulus flow for the exhaust gases. 30
Figure 2-21 - The various radiant tube designs and types that are available and used in furnaces today..... 31

Figure 2-22 - Dislocation movement along slip plane due to applied stress 33
Figure 2-23 - Grain boundary migration during recrystallisation and grain growth.35
Figure 2-24 - Schematic displaying the operation of a W shaped radiant tube in a typical vertical annealing furnace to provide the necessary heat treatment to the steel 36
Figure 3-1 - Heavy end process route for the manufacture of steel slabs from raw materials at Port Talbot Works 39
Figure 3-2 - Hot rolling mill at Llanwern Integrated Steel Works 40
Figure 3-3 - The Continuous Annealing Process Line (CAPL) at Port Talbot Integrated Steel Works 42
Figure 3-4 - Schematic depicting the CAPL (Port Talbot) sections 43
Figure 3-5 - Steel grade heating cycles 44
Figure 3-6 - Drawing showing the radiant tube location within the furnace..... 45
Figure 3-7 - Number of radiant tubes changed per year at the continuous annealing line, Port Talbot..... 48
Figure 3-8 - Number of radiant tubes changed per furnace zone..... 50
Figure 3-9 - Average age of failed radiant tube when replaced per furnace zone 51
Figure 3-10 - Stein Heurtey original radiant tube design with 'Hook and Eye' support 52
Figure 3-11 - First radiant tube design proposed by Almorgroup 53
Figure 3-12 - Inter tube link used on DVL-1 galvanising line in Ijmuiden..... 54
Figure 3-13 - Proposed inter tube design for use on Port Talbot CAPL radiant tubes 54
Figure 3-14 - Modified Almorgroup radiant tube..... 55
Figure 3-15 - Final radiant tube design proposed by Almorgroup 56
Figure 3-16 - FAI manufactured radiant tube for Port Talbot CAPL 57
Figure 3-17 - Improving methods of thermal resistance 58
Figure 3-18 - Radiant tube design for high temperature and high combustion load... 59
Figure 3-19 – Failure type of the Stein Heurtey radiant tube (Failure type 1) 61
Figure 3-20 - Failure types of Almorgroup radiant tubes (Failure type 2 & 3)..... 62
Figure 3-21 - Failure types resulted from poor quality control at Almorgroup..... 63
Figure 3-22 - Drawing displaying the layout of the galvanising heating/soaking section..... 63
Figure 3-23 - Schematic view of radiant tube and support mechanisms..... 66
Figure 4-1 - Radiant tube design used at the CAPL at Trostre Works..... 70

Figure 4-2 - Pictures indicating the common failures of tubes at Trostre; (A) cracking of the firing leg and (B) of the weld region of the 1st return bend 71
Figure 4-3 - The number of radiant tubes replaced each year since CAPL was commissioned until 2006 72
Figure 4-4 - The number of radiant tubes changed per zone 72
Figure 4-5 - Schematic displaying CAL layout at Tata Packaging, Trostre 77
Figure 4-6 - A deformed firing leg in location inside furnace 78
Figure 4-7 - A typical failure of Zodiac radiant tube. Deformation of firing leg, which in location, inside furnace, is the uppermost leg 79
Figure 4-8 - A refurbished fabricated radiant tube used in the furnace of Zodiac, Llanwern. Note: Green colour on tubes/bends indicate old part of radiant tube 80
Figure 4-9 - Bellows fitted to the firing leg of the Segal radiant tube allowing expansion along the length of the tube 81
Figure 4-10 - Creep strength comparison of firing leg materials 82
Figure 4-11 - New support design adopted by Segal, where the top return bend is supported by the lower support via a tubular link/rod 83
Figure 4-12 - Number of radiant tubes replaced per year - Segal Furnace 84
Figure 4-13 - Original Radiant tube design employed by the Drever furnace at Segal Works, Liege, Belgium 84
Figure 4-14 - Revised radiant tube design currently used by Segal. Note the expansion bellows on burner flange and elongated rod which provides support for the upper bend 85
Figure 4-15 - Plant Layout of Kashima Steel Works 86
Figure 4-16 - Continuous Annealing Line No.2 at Kashima Works 88
Figure 4-17 - Radiant tube design used at Kashima Works 90
Figure 4-18 - Cracked radiant tube where weld are has failed 91
Figure 4-19 - Failed radiant tubes showing signs of deformation in the firing and second leg 92
Figure 4-20 - Schematic showing the operation of the inspection camera 93
Figure 4-21 - New bend support design aimed at reducing the bending force in the tube 94
Figure 5-1 – Image displaying the radiant tube fitted with 20 thermocouples installed into zone 7 of the furnace for data acquisition 100
Figure 5-2 - Image displaying the location and purpose of each thermocouple 101

Figure 5-3 – Pi ProcessBook image displaying radiant tube schematic and live thermocouple readings.....102
Figure 5-4 – Pi ProcessBook image displaying continuous log of thermocouple readings.....103
Figure 5-5 – Figure displaying the maximum thermocouple temperatures recorded for each month.....105
Figure 5-6 – Figure displaying the average thermocouple temperature for each month 106
Figure 5-7 - Average thermocouple temperature for June (Month and Week) 107
Figure 5-8 - Radiant tube average temperature profile for continuous week in each month.....107
Figure 5-9 – Figure displaying the maximum and average radiant tube temperature differential for each month and continuous operational week.....108
Figure 5-10 – Figure displaying the behaviour of the radiant tube during furnace cooling and heating, for the period 11th – 14th March 2008 110
Figure 5-11 - Radiant tube behaviour during furnace cooling and heating, for the period 26th – 31st October 2008.....111
Figure 5-12 – The figure displays zone 7 temperature during three separate furnace cool down cycles 112
Figure 5-13 – The figure displays the tube temperature profile during a typical furnace cool down cycle 113
Figure 5-14 – The temperature of zone 7 during three separate furnace heating cycles 114
Figure 5-15 – Figure displaying the response of the radiant tube during a furnace heating cycle 115
Figure 5-16 – The figure displays the tube temperature profile with time during a typical furnace heating cycle 116
Figure 5-17 – Showing the zone 7 and radiant tube temperature and demand during the production of 1815mm wide x 1.15mm gauge strip. (Zone Power Demand of 100% indicates that all installed thermal power is utilised). 117
Figure 5-18 – Figure displays the zone 7 and radiant tube temperature and demand for the annealing of the 1071mm wide strip (Low power demand). (Zone Power Demand of 100% indicates that all installed thermal power is utilised). 118

Figure 5-19 – The figure shows the radiant tube temperature profile during high and low firing scenarios 120
Figure 5-20 - A comparison of furnace zone temperatures from heating from ambient to production temperatures 121
Figure 5-21 – Frequency of temperature variation for the 11 months of operation...123
Figure 5-22 - Histogram of temperature data for each radiant tube leg 124
Figure 5-23 - Temperature data for radiant tube profile from reduced heating rate trial 125
Figure 5-24 - Comparison of temperature parameters during heating trial.....126
Figure 6-1 - Example of failure at weld region between firing leg and the first return bend 132
Figure 6-2 - Example of deformed firing leg, which has resulted in a crack 132
Figure 6-3 - Pictorial representation of failures at the respective burner positions ...135
Figure 6-4 - Very low levels of deformation visible in weld failure samples 136
Figure 6-5 - Colour difference visible on inside surface 137
Figure 6-6 – Scale layer on inside surface of tube 6 MS 8.1.....138
Figure 6-7 - Severe deformation of firing leg leading to cracking (not shown).....138
Figure 6-8 - Internal surface defects of a deformed radiant tube. Visible signs of wall thinning through deep crevices and pits 139
Figure 6-9 - Circumference of failed tubes in as received condition.....140
Figure 6-10 - Maximum and minimum tube wall thickness of each sample.....141
Figure 6-11 - Nickel and chromium content of each sample.....143
Figure 6-12 - Vickers hardness values across the tube wall thickness.....144
Figure 6-13 - Vickers hardness comparison of new as cast samples versus failed samples 145
Figure 6-14 - Light optical micrograph of the general structure of as-cast HP grade material 146
Figure 6-15 - Low magnification micrographs of sample 5 OS 6.1, indicating (a) internal oxide layer breaking away from base metal (b) external surface of radiant tube which is exposed to reducing atmosphere.....147
Figure 6-16 - Example of how the oxide layer breaks up and cracks and eventually breaking off exposing fresh metal underneath to further oxidation.....148
Figure 6-17 - High magnification micrograph of crack displayed in sample 5 OS 6.1 in Figure 6-14 (a) 149

Figure 6-18 - Backscattered electron image of area near the inner surface of sample 5 OS 6.1. 151
Figure 6-19 - Region of aligned voids at the weld fusion line in sample 5 OS 6.1 ...152
Figure 6-20 - Micrographs of sample 3 OS 8.2 displaying the formation of a crack between the weld filler and tube metal. 153
Figure 6-21 - Preferential oxidation along the grain boundaries resulting in metal loss in sample 3 OS 8.2 154
Figure 6-22 - High magnification micrographs of sample 7 MS 8.4 interior displaying the presence of voids at grain boundaries....155
Figure 6-23 - Crack in sample 3 MS 3.4 which is propagating along the network of voids 156
Figure 6-24 - Higher magnification inspection of void formation in interior of sample 157
Figure 6-25 - Interior structure of sample 3 MS 3.4. Evidence of considerable void formation through sample....158
Figure 6-26 - Interior structure of 3 OS 8.4 (A) and 5 MS 6.3 (B) with large amounts of voids present 158
Figure 6-27 - Deep crack in sample 6 MS 6.3, initiated due to a failure in the oxide layer and progresses along the grain boundaries following voids which have developed in the structure due to creep deformation 160
Figure 6-28 - SEM image of sample 3 OS 8.2 at the weld root showing the lack of weld penetration and cracks at the weld root....161
Figure 6-29 - SEM images of cracks formed in the scale at the base of a weld (A), Close up of crack (B) and highly porous oxide layer (C)....162
Figure 6-30 - Cracks highlighted in fracture surface of sample 5 MS 6.3 163
Figure 6-31 - Cracking propagating from the inner surface towards the external face in sample 6 MS 6.3....164
Figure 6-32 - Schematic representation of the five stages of microstructural degradation in carbon-oxygen-containing environments 166
Figure 7-1 - Images of the various supports used as part of the development of the radiant tube undertaken by Port Talbot CAPL. 171
Figure 7-2 - Displaying the three temperature profiles used to simulate radiant tube conditions within the furnace. Temperature profiles were taken from multi thermocouple tube installed in zone 7 172

Figure 7-3 - Figure shows the expansion of the radiant tube structure due to applied temperature fields. Expansion along the x-axis (length of tube) A, expansion in the z-axis, B and deformation in the y-axis, C. Ghost image showing original position in image A.....173
Figure 7-4 - Total displacement in the x axis with varying tube temperature profiles 174
Figure 7-5 - Total displacement along the z axis with varying tube temperature profile 175
Figure 7-6 - Stress generated in the bottom surface of the firing leg. The location for all failure types experienced at Port Talbot CAPL 176
Figure 7-7 - Failure type of Stein Heurtey designed tubes at Port Talbot CAPL.....177
Figure 7-8 - Failure type of Almor designed tubes at CAPL Port Talbot 178
Figure 7-9 - Stress generated in the lower surface of the firing leg at various profile temperatures.....180
Figure 7-10 - Profile of the stresses generated in the lower surface of the firing leg during the heating phase of the radiant tube from ambient temperatures 181
Figure 7-11 - Profile of stresses generated in the lower surface of the firing leg during the cooling cycle of the radiant tube 182
Figure 7-12 - The modelling software allows the simulation of new radiant tube designs and supports. Here a support is trialled at all return bends 183
Figure 7-13 - Stress generated in new design displayed in Figure 7-12 compared with the current tube design used at CAPL 184
Figure 7-14 - The model allowed for the analysis of expansion bellows which can be fitted to the end of the flanges.....185
Figure 7-15 - A comparison of the stress generated in the firing leg with and without the attachment of expansion bellows at the firing and exhaust leg.....186
Figure 7-16 - A prediction of the tube material life from documented creep rupture data for material grade HP.....187
Figure 7-17 - A comparison of tube rupture life for various material specifications at a particular stress magnitude 189
Figure 7-18 - A comparison of tube life prediction with and without the attachment of expansion bellows, for material grade HP.....190
Figure 8-1 - Image showing the heat cycling test rig fitted with a natural gas burner, but without thermal insulation 194

Figure 8-2 - Schematic displaying the general layout of the heat cycling testing rig 194
Figure 8-3 - Electric fan fitted with rotameters, capable of delivering 4500L/min of air 196
Figure 8-4 - Natural gas rotameters to indicate pilot gas and main burner gas flows (L/min).....197
Figure 8-5 - Natural gas burner fitted with pilot burner for main burner ignition.....197
Figure 8-6 - Image displaying the layout of the samples within the test rig 198
Figure 8-7 - Test Samples received from Kubota Metals for heat cycling experiments. A - HK40 with inner machined bore. B -KHR35H with as-cast inner surface. C - KHR48N with as-cast inner surface.....201
Figure 8-8 - Problems with lighting the main burner were experienced during preliminary tests.....203
Figure 8-9 - The thermal lining cracked, distorted and worked loose from the Inconel structure during thermal cycling experiments 204
Figure 8-10 - Sample temperatures during heat cycling between 1000ºC and 500ºC. Cycles 11 to 17 shown.....205
Figure 8-11 - Images displaying the microstructure of the HK40 sample (A) after 100 cycles compared to an as cast sample of HP material (B).....205
Figure 8-12 - Image displaying the comparison of samples of each material after 1 and 100 cycles 206
Figure 8-13 - Sample temperatures during the heat and hold experiment 207
Figure 8-14 - Dark coloured scale littered on chamber floor after final heat and hold cycle. (A) General view of chamber, (B) Close up of scale.....208
Figure 8-15 - Differences between an as-cast surface (KHR48 and KHR35) to a machined inner bore surface (HK40).....210
Figure 9-1 - Image displaying a section of a MERT radiant tube showing the continuous weld bead on the inside of the tube surface.....214
Figure 9-2 - Side and front views of the Spyrocor ceramic insert.....215
Figure 9-3 - The effect of installing a ceramic insert into an exhaust leg.....216

1 Introduction

1.1 Background

The Steel industry has gone through some turbulent times recently with over capacity in supply and substantially reduced profit margins[1]. Reduced shift working and plant closures have been the by-product of the down turn in business. The supply of steel products has also changed in many sectors, where quality and reliability is now a fundamental prerequisite in the market place. The automotive sector is one such example, where pressed body panels require exacting material specifications, thus quality and costs are under great pressure and hence the steel industry, especially that of strip steel. Greater pressures are put on the manufacturing processes to develop ever increasing quality at reduced process costs.

Radiant tube furnaces are predominantly the chosen method of heating in industrial applications such as annealing furnaces for steel manufacture and reforming furnaces in the petrochemical industry. Heat energy can be transferred to the load indirectly via the radiant tube from a source of energy. This allows the load to be heated in a protective atmosphere, allowing for an excellent product quality and eliminates inherent effects from exposure to the heat source. This is typical of a continuous strip annealing process.

Failures in radiant tubes range from severe deformation to cracking of the tube material, leading to a reduction in product quality and yield, reduction in process throughput and increase in process costs. Research into radiant tube heaters and heat resistant alloys is quite extensive, especially in the petrochemical industry, with investigations into failure mechanisms[2-7] and prolonging material life[8-13]. The development of a radiant tube therefore, can be beneficial both financially to the company and improve product quality.

This thesis focuses on the problems encountered with radiant tube heater systems employed at a case study site, Tata Steel – Port Talbot, and the subsequent development opportunities that can be undertaken to improve tube longevity.

1.2 Motivation

The steel industry has had to endeavour tough times of late due to increasing production costs, increasing raw materials costs, tougher environmental legislation and a more competitive global market. At Tata Steel Port Talbot, great emphasis has been put on generating savings within the company by reducing purchasing, maintenance and production costs, improving the productivity of process lines and generating value from waste.

The replacement of radiant tubes is one of the largest annual maintenance expenditures at the Continuous Annealing Process Line (CAPL), which also require long maintenance durations for removal and installation. Broken or deformed radiant tubes incur further costs through strip surface damage and surface quality defects.

As a result, the aim of this research is to investigate the following:

- Understand how radiant tubes fail
- Identify the root cause of failure
- Operating conditions of the furnace
- Suggest improvements to tube design
- Increase tube longevity

1.3 Structure of Thesis

The chapters hereafter, discuss the process from understanding the in-service conditions of radiant tubes in the Port Talbot annealing furnace, nature of radiant tube failures within the Tata Steel group and numerous other annealing furnaces and recommendations for the improvement of radiant tube longevity.

Chapter 2 provides the background knowledge needed to understand the subsequent chapters. The theory commences with an introduction of the radiant tube and how via a combustion process, the tube can be utilised for heat transfer. The differing manufacturing techniques for the radiant tube are evaluated, highlighting the opportunities and limitations posed by the differing routes.

Similarly, material selection for the manufactured radiant tube is of paramount importance, as the reviewed literature is discussed, emphasising the influence on in-service performance. Subsequently, the application of radiant tubes in annealing furnaces is introduced in the final section of this chapter. The relevance of all the theoretical dimensions previously explained, highlights their suitability to the use in such a process.

Building upon the introduction to radiant tube furnaces in an annealing application, Chapter 3 introduces Tata Steel Port Talbot Works, discussing briefly the processes and production routes through this integrated steel works. The importance of the annealing process is highlighted and the radiant tube furnace is discussed in detail. Key parameters of the furnace are outlined allowing a full understanding of the severity of the problem encountered with failing radiant tubes.

Having discussed the important role of the radiant tubes in the continuous annealing process at the Port Talbot Works, the nature and impact of radiant tube failure is investigated. The location, design and material specification of radiant tube failures is collated into a 'Port Talbot Furnace History' highlighting early trends in failure types.

To determine the performance of Port Talbot's radiant tube furnace, a comparison of service conditions, design, material specifications and failures of other radiant tube furnaces was required. The comprehensive benchmarking investigation in Chapter 4 builds upon the findings in Chapter 3, now encompassing other radiant tube annealing furnaces. A benchmarking study across numerous sites within Tata Steel and other steel manufacturing sites, namely Sumitomo Metals Japan, has shown that radiant tube failure is a problem for all steel manufacturing sites. The service conditions, temperatures, and failures noted were all comparable. Of interest was the decision of two manufacturing sites to invest in design modifications to prolong tube life.

Chapter 5 discusses the in-service temperatures a radiant tube experiences at CAPL, Port Talbot, which was accomplished with the fitment of thermocouples to a tube installed in one of the highest failure rate zones. Temperature data for various furnace scenarios was collated and analysed to provide an accurate picture of the tube temperature profile during different operating conditions. This information is

necessary in determining the correct material specification for tube manufacture and estimating the tube life potential at known stress values.

Building on the 'Port Talbot Furnace History' discussed in Chapter 3, a comprehensive metallurgical analysis of failed radiant tube samples was conducted and explained in Chapter 6, with the aim of determining the type of failure experienced in radiant tubes at CAPL. Understanding how the material fails in service, provides a structure for future development work to tackle areas that affect tube life.

The accumulation of temperature data obtained in Chapter 5 and detailed radiant tube designs in Chapter 3, enabled accurate models to be built in a finite element software to model the stress generated in the various tube designs at different temperature profiles, Chapter 7. A comparison between different support designs was drawn and the adoption of expansion bellows, with the aim of reducing stress, was modelled.

Interestingly, expansion bellows, which is being adopted by other annealing furnaces (highlighted in Chapter 4), introduced a massive stress reduction in the firing leg, which resulted in a doubling of tube life before rupture. This coupled with increasing the material specification for the radiant tube, can provide significant increases in tube longevity.

Chapter 8 discusses the design and manufacture of a temperature cycling rig capable of heating and cooling heat resistant material (as used for radiant tube manufacture) in an oxidising environment. Different experiments were conducted to investigate the effect of temperature cycling, up to temperatures of 1000ºC, on the microstructure of the material. It was concluded that longer experimentation time was required to see any significant effects on microstructure, but the onset of spalling was witnessed when samples were held at elevated temperatures for prolonged periods of time.

Finally, Chapter 9 gathers the overall conclusions of the research and describes future work recommended as a result of this investigation.

2 Background and Literature Review

2.1 Radiant Tubes

2.1.1 Introduction

A radiant tube is a method of transferring heat indirectly to a load, i.e. without the load becoming exposed to the source of heat.

The radiant tube can be utilised in one of two ways; the heat source is contained within the radiant tube while the load is traversed in close proximity to the outside of the tube, such as in an annealing furnace, Figure 2-1. For example, a natural gas burner can be situated in one half of the radiant tube and a plug-in recuperator in the exhaust leg, preheating combustion air from hot exhaust gases to maximise efficiency. The burner heats the inside of the tube and heat energy is transferred to the load via the external surfaces, thus providing the radiant heat source to anneal the strip steel.

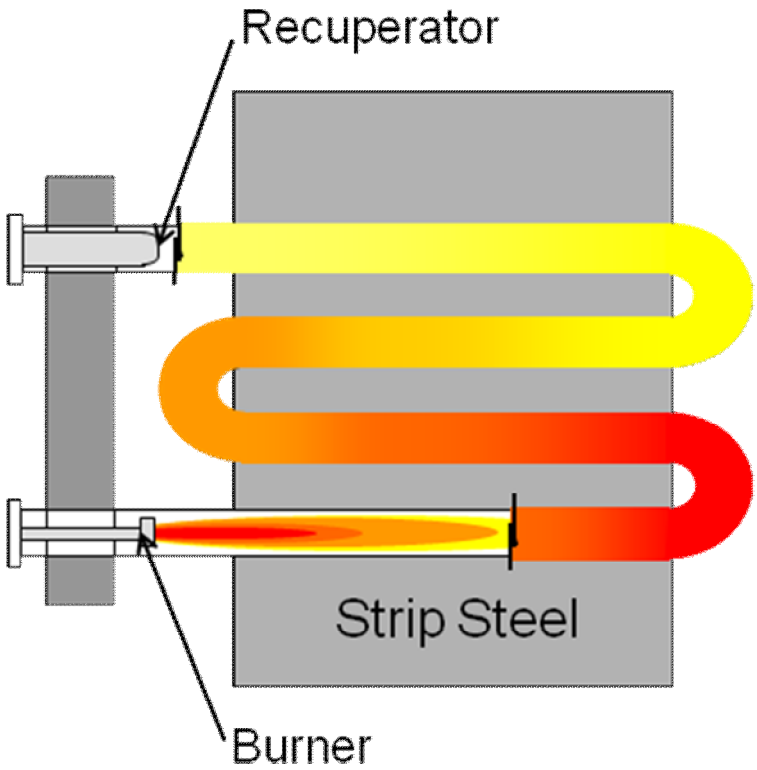

Figure 2-1 - Schematic showing a radiant tube being used to anneal strip steel

Alternatively, the product that requires to be heated is on the inside of the radiant tube, for example, in the petrochemical industry, radiant tubes are used in a cracking furnace where hydrocarbon fluids flow on the inside of the tubes, which are heated indirectly on the outside by floor/roof mounted burners[14].

2.1.2 Combustion

Combustion relies on three elements to be present; fuel, oxygen and a source of ignition.

$$\textbf{Fuel + Oxygen} \xrightarrow{\textbf{(Source of ignition)}} \textbf{Heat + By-products} \quad (1)$$

The chemical reactions between the fuel and oxygen releases heat energy, some reactions release more energy than others and some react more readily. For continuous combustion to occur, the heat released needs to be sufficient to overcome the losses. In a controlled manner, continuous combustion can be achieved easily and is a reliable source of heat energy. In uncontrolled sources, the potential for severe explosion is great.

2.1.2.1 Stoichiometric Volume

During combustion of hydrocarbons, the combustion is said to be complete when the only oxide of carbon present is CO_2 and no elemental carbon remains[15]. This occurs when there is sufficient oxygen available to react with the fuel.

Too little oxygen and the combustion is incomplete, CO is formed and requires more oxygen to react fully. Too much oxygen and the adiabatic flame temperature decreases, due to unused cold reactants entering the combustion volume. The correct volume of oxygen for a given amount of fuel is known as the stoichiomteric volume.

Predominantly, industrial fuels are natural gas, of which the main component is methane. Normally, the combustion of fuels occurs in air, which contains 20.9% oxygen, but as pure oxygen is expensive to purchase most processes use air, but larger volumes of air is required to provide the necessary oxygen.

To provide the equivalent of 1 volume of oxygen, approximately 5 volumes of air are required for complete combustion. Therefore, 1 volume of fuel requires 2 volumes of oxygen which is the equivalent of 10 volumes of air, a ratio of 10:1 of air to fuel. The correct ratio is 9.57:1 which is known as the stoichiometric ratio for the combustion of methane.

Thus:

$$\mathbf{CH_4 + 2O_2 + 7.52N_2 \rightarrow CO_2 + 2H_2O + 7.52N_2 + Trace\ Species} \quad (2)$$

2.1.2.2 Combustion Considerations

If a combustion process is set up with the correct ratio of fuel to air, it doesn't necessarily mean that the combustion will be complete. For an efficient combustion process, the design of the burner system is critical to ensure that the fuel and air mixes effectively to ensure complete combustion.

It is difficult to ensure that all available oxygen reacts with the fuel; therefore, most combustion processes operate with air rich ratios or excess air, to ensure that the fuel achieves complete combustion.

Excess air is defined as the amount of air required over and above the minimum required for complete combustion as highlighted in equation 3, i.e. in excess of the stoichiometric air requirement[15].

$$Excess\ Air\% = \frac{total\ air - \ stoichiometric\ \ air}{stoichiometric\ \ air} \times 100 \quad (3)$$

The amount of excess air required is a balance between having enough to ensure complete combustion is achieved and not too much to make the process inefficient, Figure 2-2.

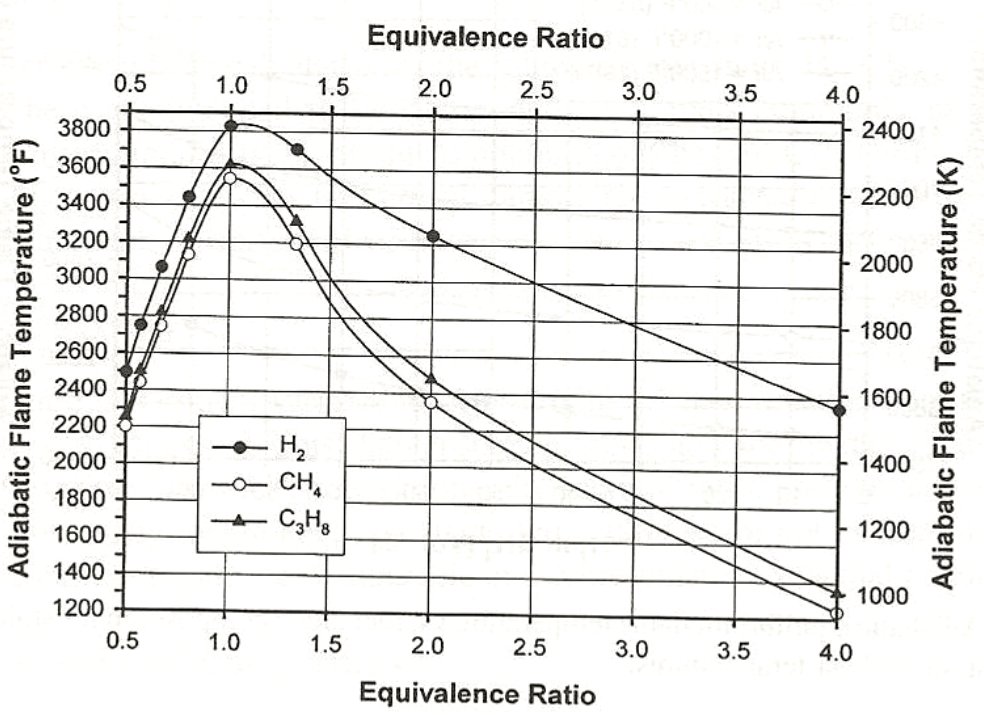

Figure 2-2 - The change in adiabatic flame temperature with equivalence ratio[16]

Where, the equivalence ratio[17], Φ:

$$\Phi = \frac{Stoichiometric\ volumetric\ ratio\ of\ \ oxygen : fuel}{Actual\ volumetric\ ratio\ of\ \ oxygen : fuel} \tag{4}$$

The problem with having too much excess air is that the free oxygen present in the exhaust gas can form with the nitrogen at the very high temperatures to form NO_x (termed Thermal NO_x). NO_x is an undesirable gas, which contributes to the ground level ozone and can be problematic to certain portions of the population (e.g. asthmatics, diminished lung capacity, etc.)[18].

Thermal NO_x is the oxidation of diatomic nitrogen at very high temperatures and the formation rate is a function of temperature. With increasing excess air, the volume of reactants increases, but the formation of thermal NO_x reduces, because the unused reactants decrease flame temperature.

Typically, in industrial applications, combustion systems are operated with approximately 2 to 4% excess oxygen (approximately 10 to 20% excess air). This is

sufficient to ensure complete combustion whilst not reducing the available flame temperature greatly. Operating with very low excess air levels or sub-stoichiometric conditions can be dangerous, as the combustion could potentially be incomplete, thus producing carbon monoxide in the exhaust gases.

If furnace combustion systems exhaust into workshop bays or operating areas, the formation of carbon monoxide can potentially kill persons/operators in the vicinity through carbon monoxide poisoning. Also, carbon monoxide is an unstable gas and is also combustible, therefore pockets of exhaust gases with quantities of carbon monoxide has the potential for a dangerous explosion.

2.1.2.3 Recuperators and Regenerators

Recuperators are often used to preheat combustion air up to approximately 400ºC. The recuperator is positioned in the exhaust leg of the radiant tube and heat transfer is aided through fins positioned on the external diameter of the tube.

Hot exhaust gases are forced past the external fins and transfer energy through convection to the recuperator material. The heated recuperator material transfers energy via conduction to the inside surface, which in turn transfers energy to the incoming combustion air, Figure 2-3.

Figure 2-3 - Recuperator heat exchanger recovering heat energy from the hot exhaust gases and transferring them to the incoming combustion air

A report by Hekkens et al[19] was produced in order to compare recuperator with regenerative burners. Experimental results from Hekkens et al[19], showed that maximum radiant tube peak temperature, with a recuperator burner, were mostly between 950 - 1000ºC. Tube temperature profile was not very uniform with a difference between maximum and average temperatures of 107ºC (at medium heat extraction level).

A further study by Hekkens[20] investigated the potential benefits of using regenerative burners. Results showed that a regenerative system led to better temperature uniformity, resulting in much lower thermal stresses in the tubes and an increase in tube life-time[20]. Figure 2-4 displays the comparison between the radiant tube temperature of a regenerative and a recuperative system and supports the results mentioned by Hekkens[20]. Maximum tube temperatures were lower in a regenerative system, practical experiences showed this was a contributing factor in increasing tube life[21,22].

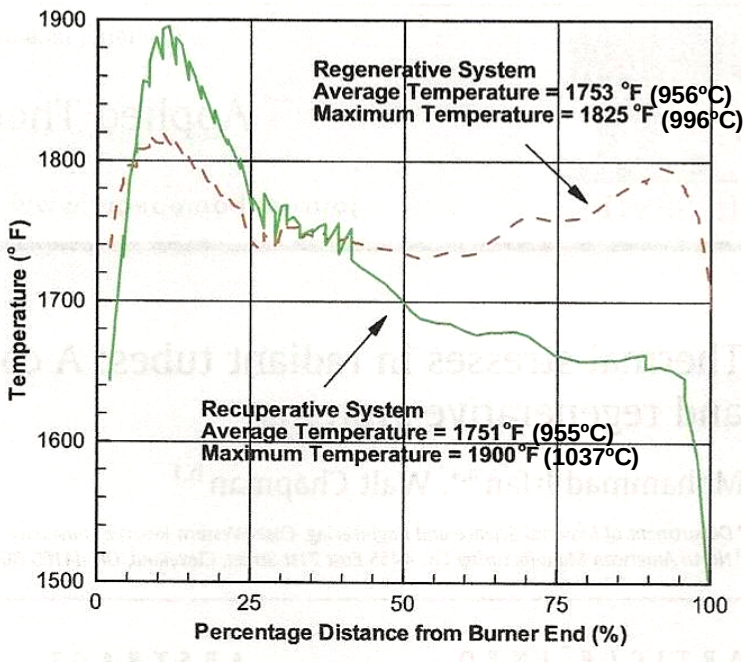

Figure 2-4 - Temperature profile comparison of a radiant tube with regenerative and recuperative systems[21]

A regenerative burner setup uses a pair of burners to alternatively combust fuel or recover heat from the exhaust gases. In operation, one burner burns the fuel with combustion air that is preheated from heat stored in the burner's refractory media. The other burner recovers heat from the exhaust gases and stores it in its' separate refractory media. When fully heated, the burners swap duty.

Although regenerative burners provide some advantages over recuperative systems in terms of temperature differences and improved efficiencies, one would have to consider the greater costs associated with regenerative systems when installing a new furnace as they have burners and heat exchangers situated in both legs of a 'W' type radiant tube, Figure 2-5. As well as doubling up on equipment, the control philosophy is more complex as the burners fire in off/high fire mode in alternating pairs.

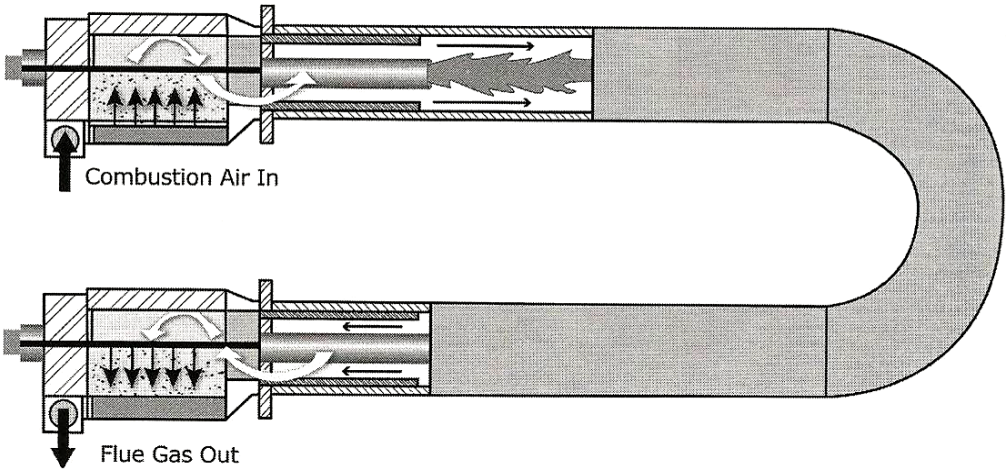

Figure 2-5 - Regenerative burners being utilised in a radiant tube application[23]

2.1.2.4 Radiant Tube Burners

For the application of non re-circulated radiant tubes, the burner flame is required to be long to distribute heat along the length of the tube and to minimise the potential for hot spots[18]. To enable the slow release of heat energy from the flame the fuel and air need to be mixed progressively.

The design of some radiant tube burners Figure 2-6, is such that the fuel is combusted initially with a primary air flow directed towards the base of flame and then with a secondary air flow which is directed along the inner diameter of the tube wall. This allows for a long flame, where the fuel is combusted initially in a region of insufficient oxygen and the secondary air ensuring complete combustion but with a lower maximum flame temperature through a longer diffused flame.

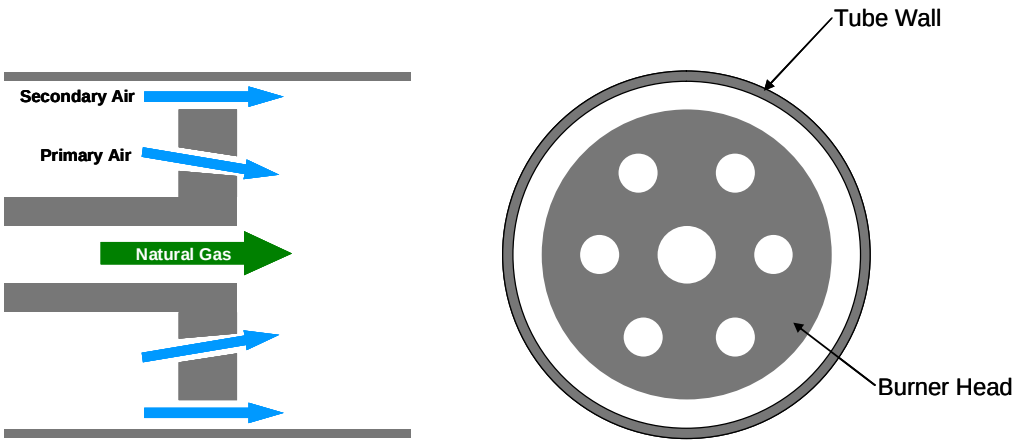

Figure 2-6 - Schematic displaying the design of a burner head

Recent advancements in burner technology[24-27] have shown to improve temperature uniformity whilst also reducing NO_x formation. As discussed by Quinn[24], an ideal radiant tube should have consistent heat flux along the length of the tube from perfect temperature uniformity, therefore, resulting in reduced stresses and a long service life.

Quinn[24] suggests using a compact regenerative burner system over a re-circulating tube design due to the extra costs associated with replacing the existing radiant tube. In contrast Wuenning et al[25,26] suggest using a self regenerative burner in a re-circulating tube design which will give optimum temperature uniformity, high combustion efficiency and low NO_x production.

Conventional regenerative systems employ two burner systems working in pairs, whereas a self regenerative system is a single unit installed into a re-circulating radiant tube. The single unit is capable of switching between heat recovery and combustion in numerous burner ports. While half the ports are recovering heat energy from exhausting gases, the preheated ports are heating incoming combustion air for the reaction with fuel, Figure 2-7.

This self regenerative unit is also capable of operating in flameless combustion mode, where no flame front is visible. Flameless combustion is possible due to very high flue gas re-circulation within the tube and as a result maximum temperatures are reduced which have a positive effect on NO_x formation.

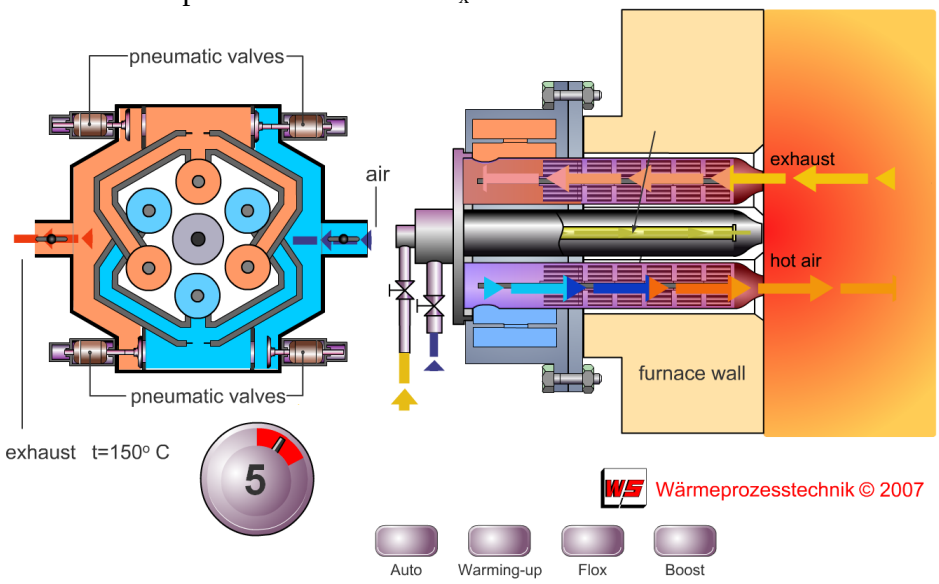

Figure 2-7 - WS self regenerative burner for radiant tube applications[28]

2.1.3 Heat Transfer Considerations

Having discussed the combustion in a radiant tube burner, it is necessary to understand the heat transfer from the combustibles inside the radiant tube to heating the load at a certain distance from the outside of the tube wall.

2.1.3.1 Available Energy from Combustion

Assuming the combustion of methane gas, then the amount of energy released is as follows:

The complete oxidation of carbon[29]:

$$\mathbf{C + O_2 \rightarrow CO_2 - 394\ kJ\ mol^{-1}} \qquad (5)$$

Note:

- The above would occur if there is sufficient oxygen present in the mixture
- Negative value denotes an exothermic reaction

The complete oxidation of hydrogen:

$$\mathbf{2H_2 + O_2 \rightarrow 2H_2O +} \begin{cases} \mathbf{- 572\ kJ\ mol^{-1}\ (HHV)} \\ \mathbf{- 484\ kJ\ mol^{-1}\ (LHV)} \end{cases} \qquad (6)$$

Where:

HHV - Higher Heating Value
All products of combustion are returned to pre combustion temperature

LHV - Lower Heating Value
Water is in vapour state at the end of the reaction

2.1.3.1.1 Combustion Air Preheating

To increase the combustion efficiency, the combustion air is preheated before the combustion, through heat transfer via the recuperator situated in the exhaust leg. Figure 2-8 displays a typical recuperator heat exchanger, where the combustion air on the inside of the recuperator is heated by hot exhaust gases flowing on the outside.

Thermal energy is transferred from the exhaust gases to the combustion air through conduction through the recuperator material.

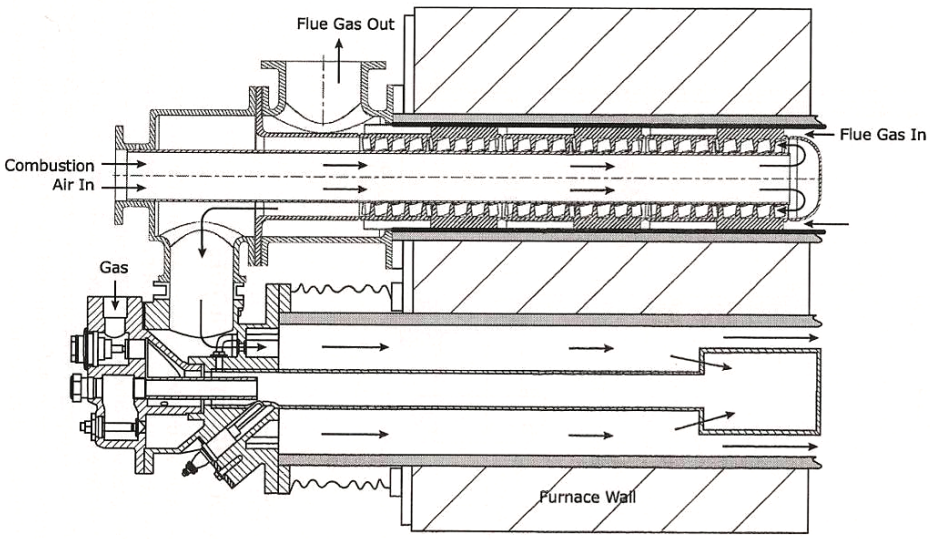

Figure 2-8 - Example of a plug-in recuperator used in a radiant tube application[18]

2.1.3.2 Effect of Preheating Combustion Air

Preheating the combustion air through heat transfer from the exhaust gases is a simple method of increasing the temperature of combustion, as well as reducing the heat losses from the exhaust gas. Figure 2-9 depicts how increasing the air preheat temperature increases the adiabatic flame temperature.

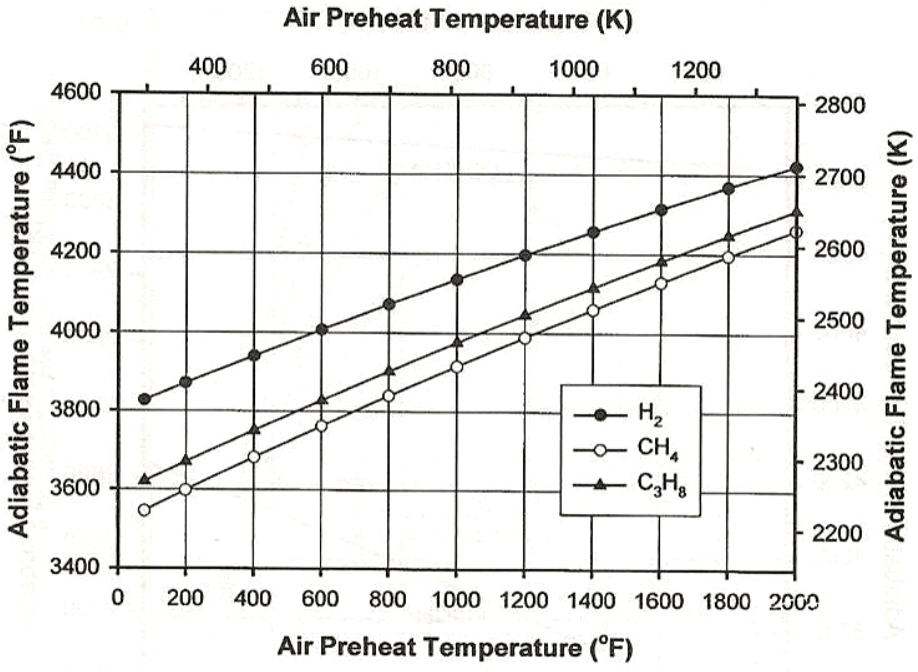

Figure 2-9 - Figure displaying the effect of preheating the combustion air on adiabatic flame temperature[30]

Fuel preheating can also be achieved; but has much less of an impact than preheating the combustion air. This is due to the much greater volumes of air required for the combustion reaction than fuel[30].

2.1.3.3 Heat Transfer within the Firing Leg

As discussed by Baukal[18]; Optimisation of a radiant tube involves balancing the heat transfer from the flame and products of combustion to the inner surface of the tube, its conduction through the tube wall, and the emission from the outer surface of the tube, while respecting the tube material limits. Neglecting this balance can result in premature tube failure from thermally induced stresses and material creep.[18]

The heat generated by the combustion releases its heat energy through radiation and convection along the length of the radiant tube. The energy is used to heat up the inside of the radiant tube wall, which then transfers this heat via conduction to the outside tube surface.

2.1.3.4 Heat Transfer to the Load

The primary heat transfer mode between the tube outer wall and the load (in this case strip steel) is radiation, but there is some, albeit low, heat transfer from other sources within the furnace. The radiant tubes not only heat the load, but also the furnace walls and the protective atmosphere gas.

In steady state conditions, the load will always be at a lower temperature than the radiant tubes, furnace walls and atmosphere gases. The furnace walls are continuously heated by the radiant tubes, some of this heat will be lost through conduction through the wall to the outer face of the furnace. The atmosphere within the furnace is also heated and will transfer heat back to the colder incoming strip by convection, Figure 2-10.

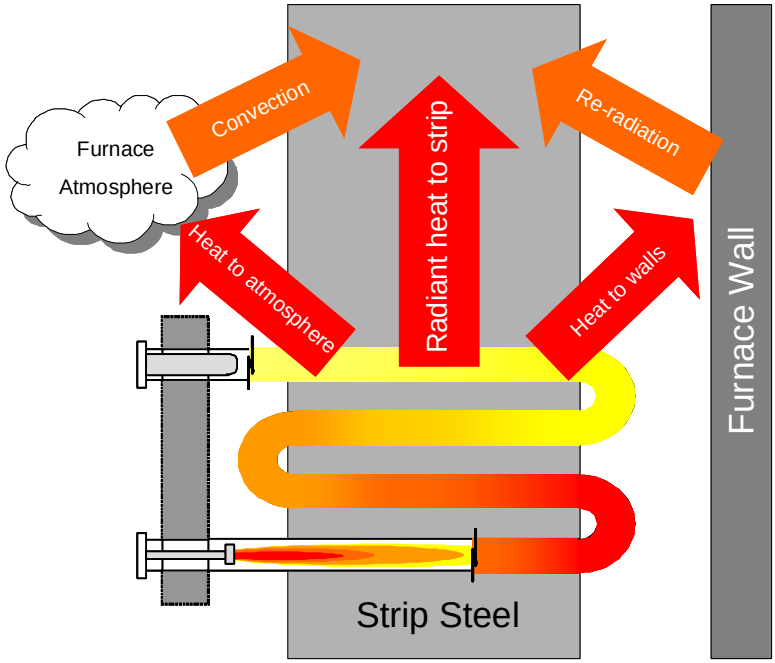

Figure 2-10 - Heat transfer within a typical radiant tube furnace

2.1.4 The Manufacture of Radiant Tube Heating Elements

Radiant tubes can be manufactured from 2 processes, these being:

1. Fabricated from sheet material
2. Cast tubes, where the tube body is horizontally spun-cast and bends statically cast

2.1.4.1 Cast Tubes

A cast radiant tube is manufactured from two common elements, a cylindrical tube and a return bend. The tube is spun-cast in a mould rotated on rollers as shown in Figure 2-11, while the bends are statically cast in sand moulds. After solidification and sufficient cooling the mating ends of the tubes and bends are chamfered as part of the weld preparation and then welded to form the main radiant tube structure. Subsequent quality control measures at the foundry ensure gas tightness and weld quality.

Figure 2-11 - Image showing a spin-casting machine able to produce cast tubes. Note different size moulds in background to produce various diameters of tubes

The advantages of cast tubes are numerous. Complex chemical compositions can be made to suit each and every application, while intricate designs and shapes can be statically cast, although expensive for one-off manufacture, through the manufacture of various sand moulds. Creep strengths are generally higher than fabricated steels due to the higher carbon content and the manufacturing costs associated with casting is lower, therefore lower purchase costs.

2.1.4.2 Fabricated Tubes

Fabricated tubes are generally smaller in diameter, lighter in mass and are manufactured from freely available stainless steel grades such as Inconel. A typical fabricated W tube is shown in Figure 2-12. Rolled sheets are welded to form tubes and bends, which is a more time consuming manufacturing process due to the high man hours associated with welding.

Although fabricated tubes are more expensive to buy, they are widely used in annealing and galvanising furnaces. Tube wall thicknesses are greatly reduced in

comparison to spun-cast tubes (Approx 3mm in comparison to 8mm cast tubes) and as a result, a furnace fitted with fabricated tubes would have a significantly less thermal mass. Therefore, faster response times when heating and cooling, ideal for furnaces with constantly varying strip parameters, and less energy required to heat the furnace from shutdown periods.

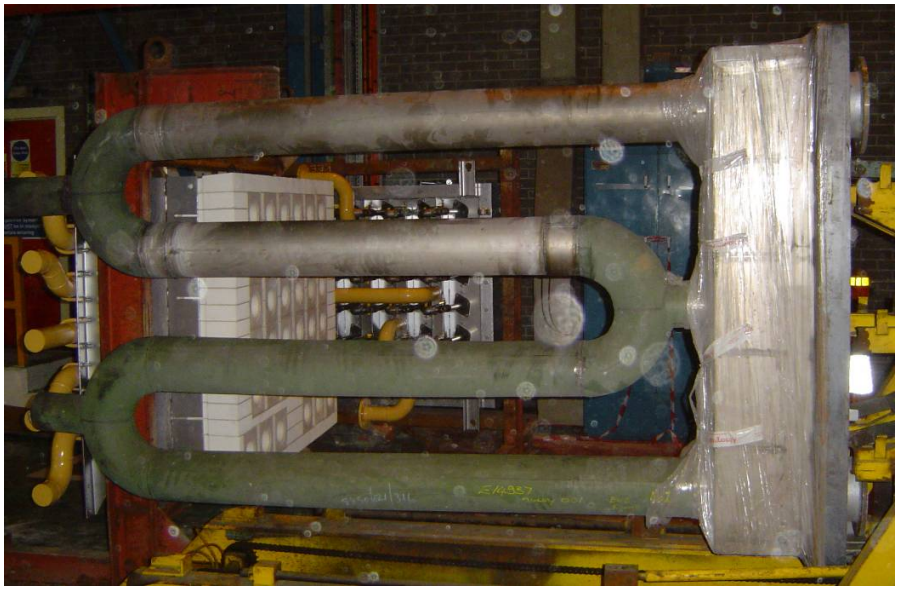

Figure 2-12 - Image of a 'W' shaped fabricated tube used in the galvanizing line at Tata Steel, Llanwern

2.1.5 Material Choice

Radiant tubes are manufactured from a family of materials known as the heat resistant alloys. A material is classed as heat resistant if they are capable of sustained operation when exposed either continuously or intermittently, to operating temperatures that create metal temperatures in excess of 1200 F (648ºC)[31]. Common grades in the heat resistant family primarily contain Fe, Cr and Ni. Grades for use at slightly higher temperatures and high stresses, for example turbine blades, are either nickel or cobalt based.

The desired properties required from a heat resisting steel grade are[32]:

- Resistance to high temperature corrosion
- Sufficient strength at operating temperature
- Need to maintain dimensional stability at operating temperature

- Resistance to creep under load
- Resistance to degradation under cyclic heating and cooling regimes

2.1.5.1 Role of each Element

As mentioned, the three primary elements in heat resistant alloys are iron, nickel and chromium, in varying quantities. Generally, iron is the dominant element by quantity and depending on grade; chromium and nickel are of comparable quantities. Iron is the base element with chromium providing high temperature corrosion resistance and nickel providing stability to the material phase structure, Figure 2-13.

The quantities of both nickel and chromium are important, as sufficient quantities are required to provide the necessary protection/strength. To be classed as stainless steel chromium quantity of greater than 11% is required to provide a continuous protective oxide layer on the surface of the material[44]. Greater quantities are used in high temperature steels to provide greater protection against corrosion at the higher service temperatures.

Nickel is a very important element as it is very resistant to oxidation due to its relatively low reactivity[33]. It also stabilises the phase structure of the material ensuring that it remains in an austenite phase, which provides excellent strength even at high service temperatures and has been shown to increase resistance to cyclic oxidation[34]. Another factor that increases the creep strength of the material is the ability of the chromium to form carbides at high temperatures.

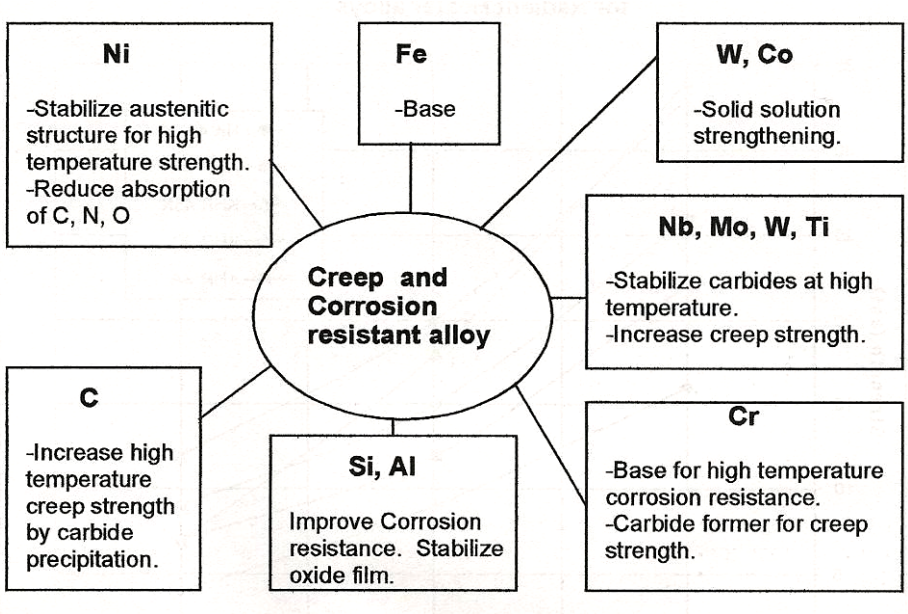

Figure 2-13 - The role of each major element in a heat resistant alloy material[46]

Other elements that are added in small quantities are niobium, molybdenum, tungsten and titanium. These are added to improve creep strength through the stabilisation of carbides at high temperatures. Silicon and aluminium are sometimes added to improve the formation of a protective oxide layer and cobalt can be added up to quantities of 5%, again to improve high temperature strength.

2.1.5.2 Heat Resistant Grades

Heat resistant stainless steel comes in various grades to provide the correct material for any high temperature application. Experience of failures in service and developments in processes has developed the need for improved performance from materials; as a result the number of various grades has also increased.

Figure 2-14 displays the more common grades of heat resistant stainless steel castings. Grade designations HA to HD are known as the ‘straight chromium alloys’, which contain 10 to 30% chromium and small quantities or no nickel at all. Primarily, these grades are used for their oxidation resistance and due to their low nickel content however; do not possess good strength at high service temperatures.

Grades HE to HL are known as the 'Fe-Cr-Ni alloys' (element symbols in order of descending quantity). Nickel content is always lower than chromium, but these grades are used in oxidising and reducing environments. Increasing the levels of nickel provides a higher material strength at elevated temperatures. Commonly, radiant tube castings were of the grade HK, which provide sustained strength properties at elevated temperatures.

Finally, grades HN to HX are known as the 'Fe-Ni-Cr alloys' and always contain nickel levels of 25% or higher. The relatively high nickel content provides excellent resistance to carburisation and nitridation. Also, due to the higher additions of nickel, material strength is increased and provides excellent life in fluctuating service temperatures[31].

Designations				Composition(a)			
ACI	AISI(b)	SAE	ASTM(c)	C	Cr	Ni	Si (max)
HA	...	.....	A217, A199, A200	0.20 max	8 to 10	....	1.00
HB	...	.....	....	0.30 max	18 to 22	2 max	2.00
HC	446	70446	A297	0.50 max	26 to 30	4 max	2.00
HD	327	70327	....	0.50 max	26 to 30	4 to 7	2.00
HE	312	70312	A297	0.20 to 0.50	26 to 30	8 to 11	2.00
HF	302B	70308	A297	0.20 to 0.40	19 to 23	9 to 12	2.00
HH	309	70309	A297, B190	0.20 to 0.50	24 to 28	11 to 14	2.00
HI	...	.....	A297	0.20 to 0.50	26 to 30	14 to 18	2.00
HK(d)	310	70310	A297	0.20 to 0.60	24 to 28	18 to 22	2.00
HL	...	70310A	....	0.20 to 0.60	28 to 32	18 to 22	2.00
HN	...	.....	....	0.20 to 0.50	19 to 23	23 to 27	2.00
HT	330	70330	A297, B207	0.35 to 0.75	13 to 17	33 to 37	2.50
HU	...	70331	A297	0.35 to 0.75	17 to 21	37 to 41	2.50
HW	...	70334	A297	0.35 to 0.75	10 to 14	58 to 62	2.50
HX	...	70335	A297	0.35 to 0.75	15 to 19	64 to 68	2.50

(a) Manganese is 0.35 to 0.65% for HA, 1% for HC, 1.5% for HD and 2% for the other alloys. Phosphorus and sulfur are 0.04% max. Molybdenum is not intentionally added except in type HA, which has 0.90 to 1.20% Mo; maximum for other alloys is set at 0.5% Mo. Type HH also contains 0.2% max N. (b) Wrought alloy designation. All others are cast alloy designations. These are listed for identification only. Castings should be ordered under cast alloy designation. (c) ASTM specification numbers; alloy designations are the same as ACI. (d) AMS 5365.

Figure 2-14 - Designation and composition of heat resistant alloys[31]

Casting companies have developed many new grades based on these original compositions. Material grades have been fine tuned, dependent upon application, due to customers requiring longer service life and producers are vying for larger market shares[34].

2.1.5.3 Material Properties

The factors that make heat resistant alloys suitable materials in high temperature service is their excellent properties such as creep strength, oxidation resistance and corrosion resistance from attack via carburisation, sulphidation and nitridation.

2.1.5.3.1 Creep Strength

Creep is an undesirable failure when materials are subjected to stresses in conditions of elevated temperatures, such as radiant tubes and turbine blades. Creep is the permanent deformation of a material when subjected to elevated temperatures (above 40% of the melting temperature for metals) under constant load or stress[35].

A more common example of creep is the sagging of lead pipes used for water pipes in older houses. Sagging would occur due to creep and it was invariably found that the hot water pipes sagged more than the cold. Cracks would eventually form resulting in burst pipes[36].

Radiant tubes are one application where the material operates at temperatures above $0.4T_m$ (where T_m is absolute melting temperature in K) for prolonged periods of time. Coupled with this are static loads from the weight of the tube and thermal stresses induced in the material from differences in material expansion. All are factors which promote deformation due to creep failure.

Thermal stress is governed by the formula[35]:

$$\sigma = \alpha_l E \Delta T \tag{7}$$

Where:

σ = thermal stress

α_l = coefficient of thermal expansion

E = modulus of elasticity

ΔT = difference in temperature

The influence of stress and temperature on the creep behaviour of a material can be seen in Figure 2-15. At temperatures of below $0.4T_m$, some strain is evident but does

not increase with time and does not result in failure. At temperatures above $0.4T_m$, increases in stress or temperature reduces the time taken to failure and also increases the steady-state creep rate.

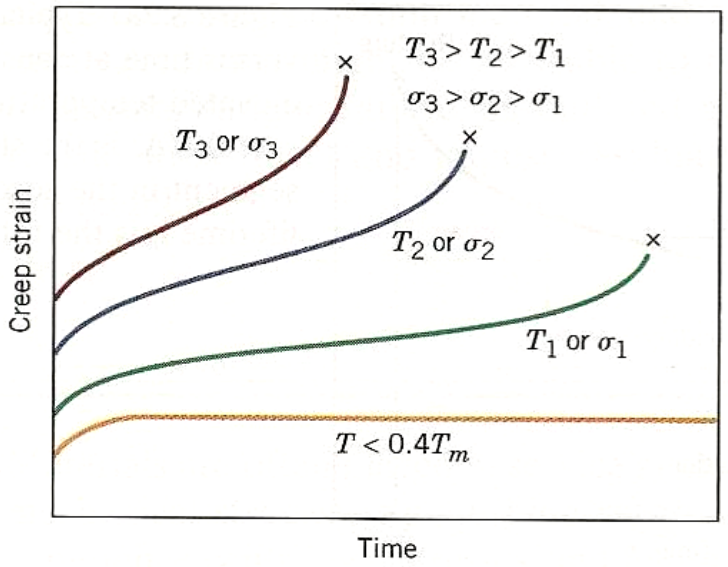

Figure 2-15 - Influence of stress and temperature on creep behaviour[35]

Creep rupture testing on various materials is widely documented as engineering designers need information on the service life of components. There are two commonly used methods for presenting creep data, these being Figure 2-16, where the logarithm of stress is plotted against the logarithm of rupture lifetime at various temperatures and Figure 2-17, where the logarithm of stress is plotted against the logarithm of steady state creep rate.

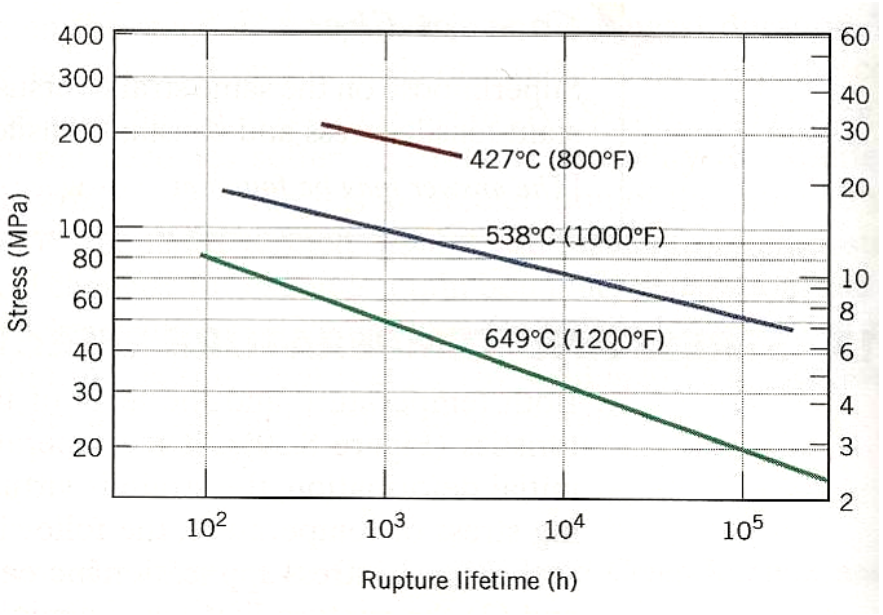

Figure 2-16 - Stress versus rupture lifetime for a particular material at three different temperatures[35]

The most common plot used is the time to rupture, Figure 2-16, as it provides an indication to the serviceable lifetime of a component operating in a certain temperature range and under a particular stress. Less commonly used is the steady state creep rate, which is governed by the formulas[35]:

$$\varepsilon_s = K_1 \sigma^n \tag{8}$$

Where:

ε_s = steady state creep rate

K_1 = material constant

σ = stress

n = material constant

When the influence of temperature is included:

$$\varepsilon_s = K_2 \sigma^n e^{\left(-\frac{Q}{RT}\right)} \tag{9}$$

Where:

K_2 = material constant

Q_c = activation energy for creep

R = universal gas constant

T = temperature

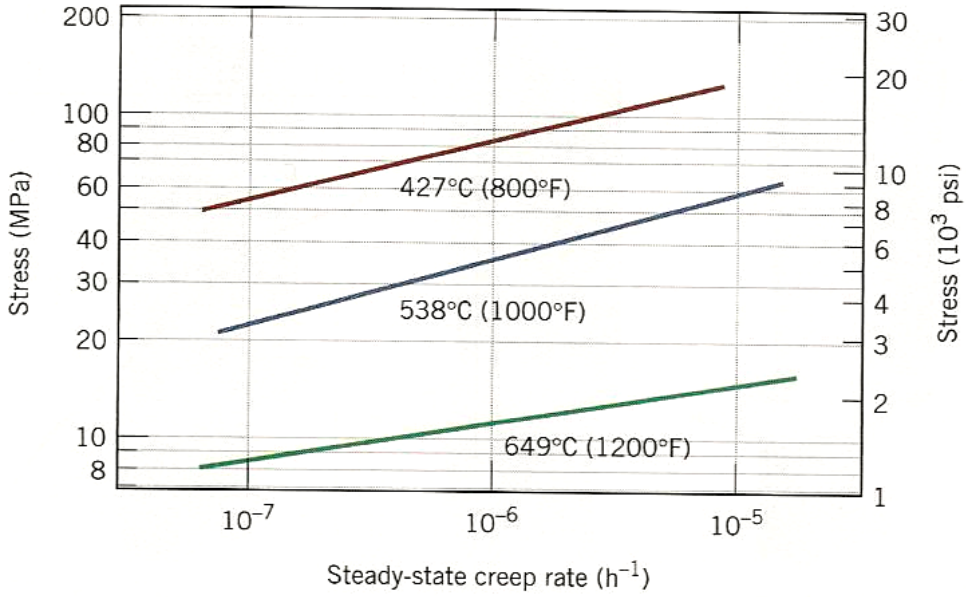

Figure 2-17 - Stress versus steady state creep rate at three different temperatures[35]

Therefore, using documented material data, a good understanding of the behaviour of any particular material under creep conditions can be had, which can aid with the design and selection of materials for components in high temperature service.

2.1.5.3.2 Oxidation Resistance

The high levels of chromium provide a stable, passive oxide layer which protects the base metal to further oxidation as schematically shown in Figure 2-18. Sufficient quantity of chromium is needed (>12%) to sufficiently cover and stabilise the iron and passivate the combined alloy. When an alloy is said to be passivated, it resists further oxidation[33].

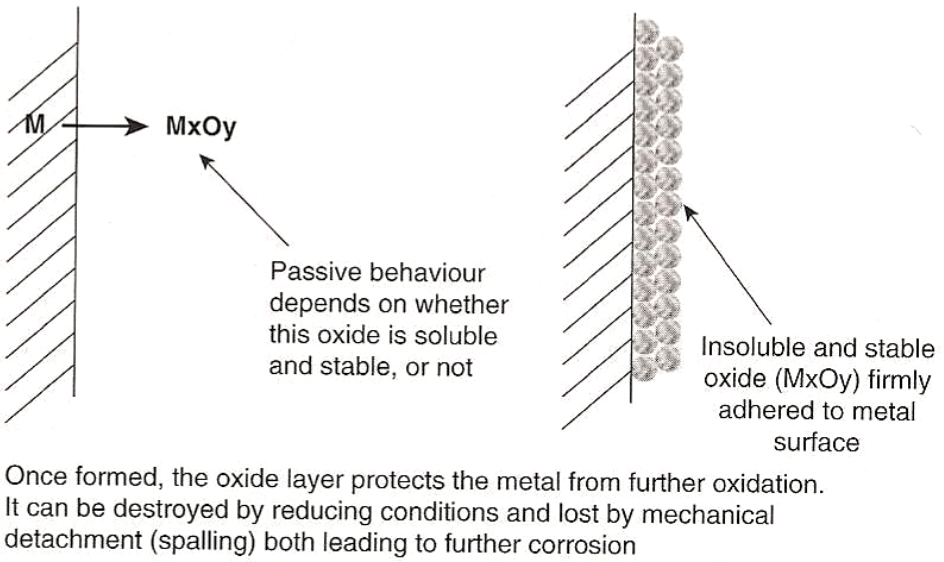

Figure 2-18 - Oxide layer formation which protects the base metal[33]

To provide and maintain a passive oxide film at temperatures of 980°C, it has been found that chromium levels of 25% and above is needed[34]. This is one reason why HK grade has been so popular for the manufacture of radiant tubes in annealing furnaces.

2.1.5.3.3 Resistance to Spalling

As mentioned by Mullinger et al[37], intermittent duty is far more arduous than continuous demand due to the constant heating and cooling of the material. The passive oxide layer, which forms on the surface and protects the material, detaches from the base metal, reducing its serviceable life. This is known as spalling.

Spalling is the mechanisms of the oxide layer breaking away from the base metal due to stress generation in the oxide layer, Figure 2-19. As well as applied loads on the material, additional stresses can be generated from the oxidation process. These can be growth stresses, which develop from the formation of the scale and thermal stresses, which develop from differences in thermal expansion between the substrate and oxide scale[38].

The stresses in oxide layers on most engineering alloys tend to be in compression, which is developed when the oxide layer is formed. When the alloy is cooled from

elevated temperatures the compressive stresses increase, due to the differences in thermal expansion between the oxide layer and the base metal[38].

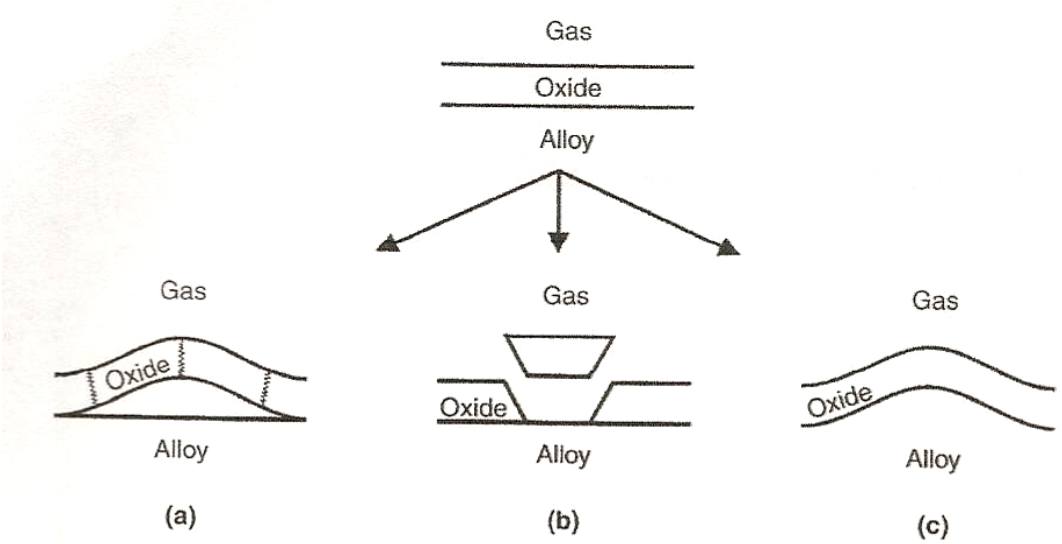

Figure 2-19 - The mechanism of spalling as identified by the schematic diagram above. This is the response of the oxide when loaded in compression: (a) Buckling of the oxide (b) Shear cracking of the oxide, and (c) plastic deformation of the oxide and alloy[38]

2.1.5.3.4 Resistance to Corrosive Environments

Heat resistant stainless steels are used in many applications and are subjected to many environments, some of which are corrosive, which can lead to metal loss, embrittlement and distortion. Mainly, corrosive gases can contain carbon, nitrogen and sulphur which can attack the material at elevated temperatures.

Carburisation is an attack due to the penetration of carbon into the base metal which can lead to embrittlement due to growth and coalescence of carbides. This type of attack can be localised or over a wide area and results in the loss of mechanical strength due to the low ductility of the carbides and they induce internal stresses due to their large volume uptake.

Sulphidation is an attack from sulphur bearing fuels and gases. The sulphur reacts with the nickel to form nickel rich sulphides that have a low melting point. The slag formation penetrates the oxide layer and leads to breakaway oxidation.

Nitridation is where the material absorbs nitrogen from the gas which leads to Fe or Cr nitride particles. This leads to volume expansion and internal stresses which can cause embrittlement and distortion.

To combat these corrosive environments, additions of aluminium and silicon can be employed to improve the formation of oxide layer to resist penetration, and also higher nickel contents have been used to resist nitrogen pick up. But, additions such as silicon can have a detrimental effect on creep strength; therefore careful quality control is needed where a balance of oxidation and creep strength is required[34].

2.1.6 Radiant Tube Designs

A common radiant tube design (as depicted earlier in this chapter) are of the 'W' shape, containing two ports, where in one a burner is positioned and in the other a recuperator to preheat the incoming combustion air. There are of course many different designs to be had, which range from straight tubes, to 'U' shaped, to 'Double-P' designs.

2.1.6.1 Non Re-circulating Radiant Tubes

The simplest form of radiant tube is the straight version, which can be either open ended or return annulus. Open-ended tubes have a burner on one end and the exhaust gases are taken off the other side of the furnace, while the return annulus has the burner and exhaust outlet on the same side, see Figure 2-20.

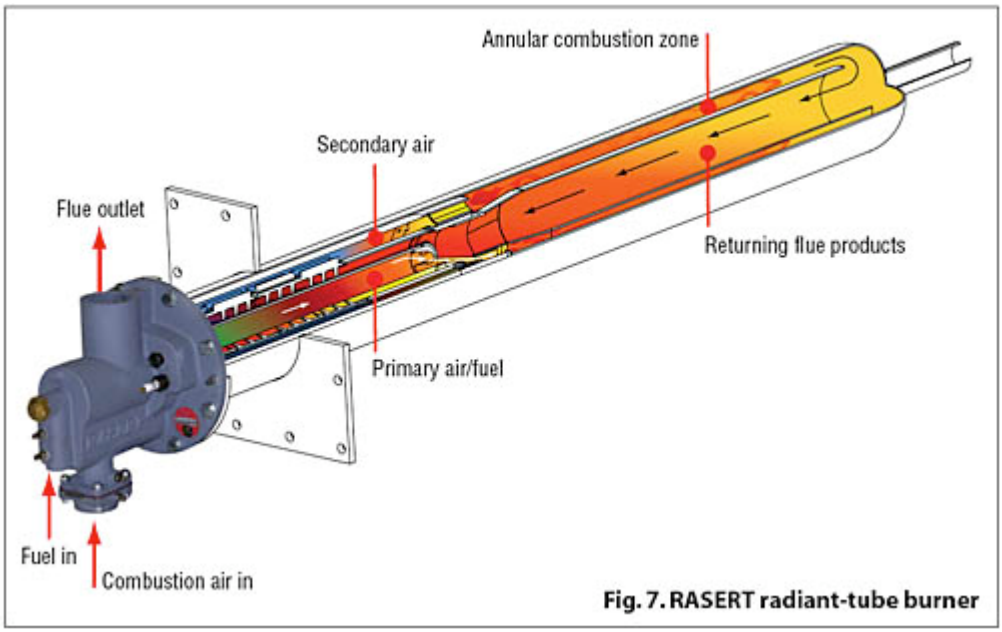

Figure 2-20 - A single ended radiant tube with a reverse annulus flow for the exhaust gases.[29]

Non re-circulation in radiant tubes means that the design of the tube doesn't inherit the exhaust gases to be re-circulated within the tube and therefore only pass the once through the tube. In comparison, re-circulating tube designs use high-velocity burners to entrain combustion products from the exhaust leg and entrain the fresh and re-circulated products of combustion through the firing leg[39].

The other non re-circulating alternatives are the 'U' and 'W' type tubes. These have a higher surface area for greater transfer of heat energy and operate from the same side of the furnace. The non re-circulating types can and usually operate with a heat exchanger unit, termed recuperator, to preheat the incoming combustion air to improve emission levels and to increase efficiency. Recent developments have adopted regenerative burners at either end of the tube to further improve efficiencies and to lower the temperature differential.

2.1.6.2 Re-circulating Radiant Tubes

Recent developments in radiant tube technology[24-26,39,40] have generated various new designs and burner technology, Figure 2-21. The improvements have focused on re-circulating the exhaust gases to achieve very low NO_X/SO_X levels whilst still improving energy efficiencies. Another advantage of the re-circulating types is that

temperature distribution across the length of the radiant tube is very even due to reduced peak temperatures and as a result low stress levels due to differences in thermal expansion.

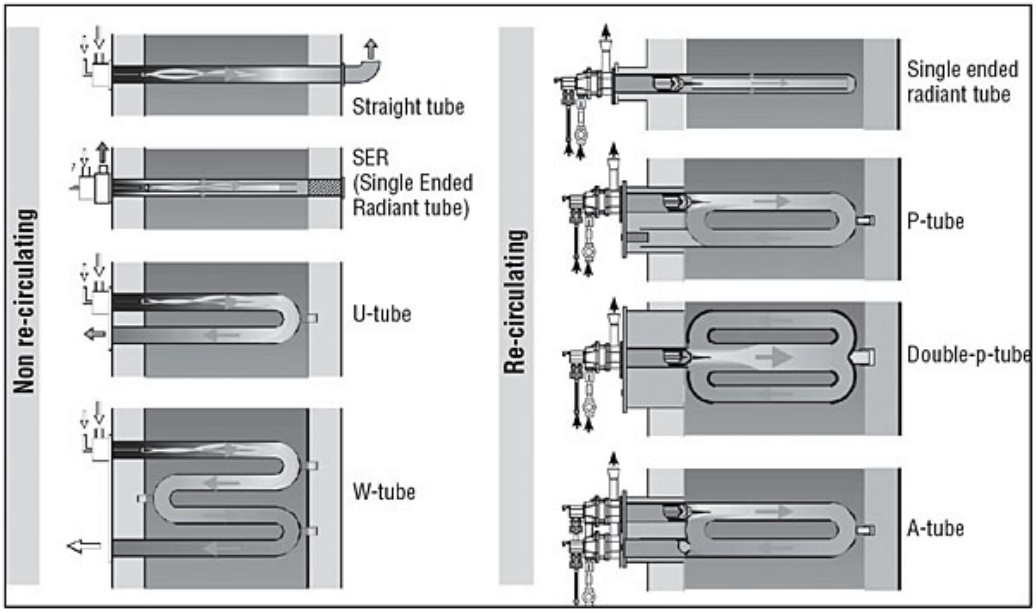

Figure 2-21 - The various radiant tube designs and types that are available and used in furnaces today[41]

Practical experiences with a re-circulating double-P tube annealing furnaces are reported by Beck et al[42]. After five years of service, no visual signs of deformation or cracks were reported. Also, as the double-P radiant tube is manufactured from wrought grades of heat resistant stainless steel resulting in a greatly reduced furnace thermal mass, which aids flexibility when producing varied steel grades.

2.1.7 Fuels

Radiant tubes rely on the combustion of a gas to provide the heat energy required to transfer to the load. This fuel is primarily natural gas, but as some annealing lines are situated in an integrated steel works, other available fuels such as Coke Oven Gas (COG), Blast Furnace Gas (BFG) or Basic Oxygen Gas (BOS) can be used.

2.1.7.1 Calorific Values

Outlined in a study by Lewis et al[43], calorific value of the fuel used for combustion could attribute to radiant tube lifetime through the intensity of the flame produced.

Gross calorific values of fuels used in combustion for various continuous lines are outlined below, from Lewis[43]:

- Natural Gas (North Sea) – 38MJ/Nm^3
- Continental Natural Gas – 34.5MJ/Nm^3
- Coke Oven Gas – 18MJ/Nm^3
- Blast Furnace Gas – 3.6MJ/Nm^3
- Basic Oxygen Furnace Gas – 8MJ/Nm^3

While there are advantages in using coke oven gas and blast furnace gases in an integrated steel works, due to their abundance as a by product from other processes, one must consider the implications of doing so. Natural gas is considered a clean gas, in comparison coke oven gas and blast furnace gases can be very dirty, in the sense that they can contain particulate matter. Careful attention must also be paid towards the combustion of these process gases, as they can contain large amounts of inert substances that do not oxidise.

2.2 Radiant Tube Annealing Furnaces

A radiant tube is a method of transferring heat energy indirectly to a load, i.e. without the load becoming exposed to the source of heat energy. This is particularly useful in the application of annealing strip steel. At the high temperatures required for annealing steel, an open flame combustion would oxidise the surface of the steel even with a shortage of combustion air; a clear disadvantage when an excellent surface finish is required at the end application in the steel industry for example.

2.2.1 The Requirement for Annealing

Annealing is a heat treatment process, which restores the mechanical properties of a metal, for example cold rolled strip steel. The process of 'cold reduction' in the steel making process plastically deforms and hardens the steel strip below the recrystallisation temperature (~0.4Tm). In this process, the gauge of the strip is reduced through stress, which is applied by force from the work rolls, and tension through the difference in speed between work stands.

2.2.1.1 Slip

The polycrystalline structure of the steel deforms plastically through the process of slip, which involves the motions of dislocations, Figure 2-22. These atomic distortions move along the slip plane when stress is applied, due to bonds breaking and reforming with atoms further along the slip plane. When stress is removed they do not return to their original positions[44].

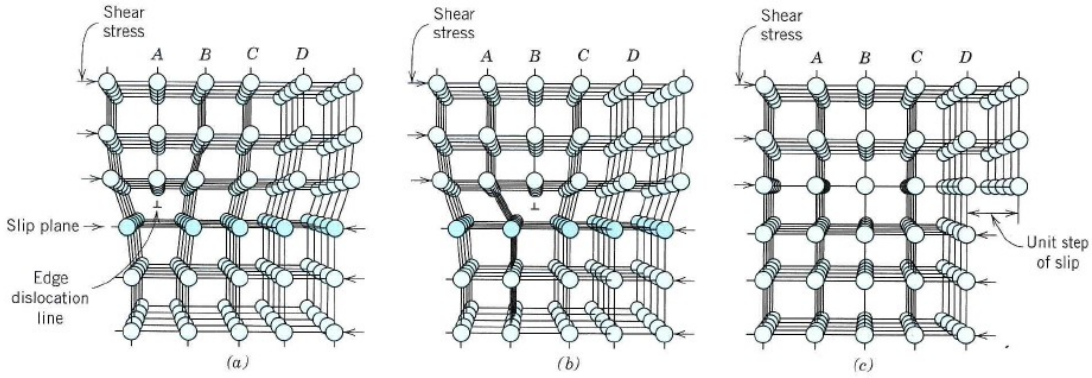

Figure 2-22 - Dislocation movement along slip plane due to applied stress[44]

2.2.1.2 Strain Hardening

As the strip steel is plastically deformed it becomes strain/work hardened. This is due to the increase in dislocation density, from multiplication and formation of new dislocations. On average, dislocation-dislocation strain interactions are repulsive. Therefore, the progression of dislocations is made more difficult with the increasing presence of other dislocations. As a result higher stresses are needed to continue dislocation movement[44].

The large amount of deformation incurred on the strip steel during cold rolling produces elongated grains with a high dislocation density and high strain energy. Thus, the steel is high in strength but has poor ductility, resulting in undesired mechanical properties. Therefore, the strip is subsequently heat treated by an annealing treatment. Ordinarily, annealing is carried out to (1) relieve stress; (2) increase softness, ductility and toughness; and/or (3) produce a specific microstructure[44].

The annealing process generally consists of 3 processes, from Callister[44]:

- Heating to the desired temperature
- Holding or 'soaking' at that temperature
- Cooling, usually to room temperature

The elevated temperatures experienced during annealing initiate restoration processes of *Recovery* and *Recrystallisation*, which may be followed by *Grain Growth*, depending on heating cycle.

2.2.1.3 Recovery

During the recovery period, some of the strain energy in the lattice is reduced due to dislocation motion, as a result of enhanced atomic diffusion at the elevated temperature[44]. Therefore, the number of dislocations decrease and some arrange in configurations where strain is low.

2.2.1.4 Recrystallisation

By annealing the steel above 600ºC recrystallisation occurs, where new, stress free, equiaxed grains grow at the expense of the deformed original grains. The new grains have low dislocation densities and are similar to pre-worked grains. Also, the mechanical properties are restored to pre-worked values.

The small, strain-free grains form initially along the original grain boundaries, where they grow by absorbing the highly deformed grains. The recrystallisation process is

complete when the distorted grain structure is completely replaced by equiaxed strain-free grains[45].

2.2.1.5 Grain Growth

If the recrystallised strip is held at the annealing temperature, the grains will grow (grain growth). The driving force for grain growth is the potential energy, which is stored in the atoms that are near the boundaries. As the grains increase in size, the total boundary area decreases. Thus, the potential energy is relieved.

Figure 2-23, displays the migration of grain boundary, where the atoms move from the strained crystals to the unstrained grains. Both recrystallisation and grain growth occur by grain boundary movement.

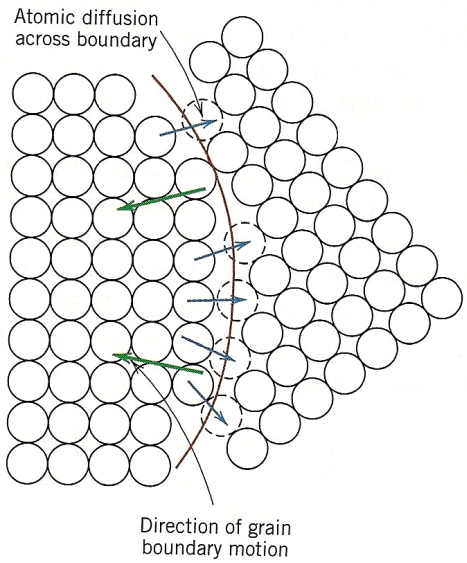

Figure 2-23 - Grain boundary migration during recrystallisation and grain growth[44]

2.2.2 Continuous Annealing

Radiant tube furnaces are predominantly employed in continuous annealing process lines, which involves uncoiling and welding the strip to the end of the previous coil. The continuous strip is then processed in a single layer through a heating furnace and then divided and recoiled. The continuous lines, in a matter of minutes, provide a treatment that takes days with batch annealing[46].

Pioneered by the Japanese in the 1970's[47], continuous lines provide a treatment that exposes the strip to a constant heating cycle. Therefore, the coil is uniform throughout in terms of mechanical properties. The strip is heated in a reducing atmosphere generally containing approximately 95% nitrogen and 5% hydrogen, which mitigates the possibility of the strip surface oxidising at high temperatures.

The process is continuous, through the inclusion of two strip accumulators at either end of the furnace section. When the coils are welded together or divided apart, the accumulators fill up/empty, allowing a continuous feed of strip into the furnace. Thus, allowing the strip to travel at a continuous speed and be exposed to the same heat treatment cycle.

2.2.3 Radiant Tube Furnaces

The construction of a Radiant Tube Furnace (RTF) lends itself well to the design of a continuous annealing process line; the strip steel enters the furnace at ambient temperature and traverses either side of a number of radiant tube columns increasing in temperature to the required annealing temperature before exiting the furnace, Figure 2-24.

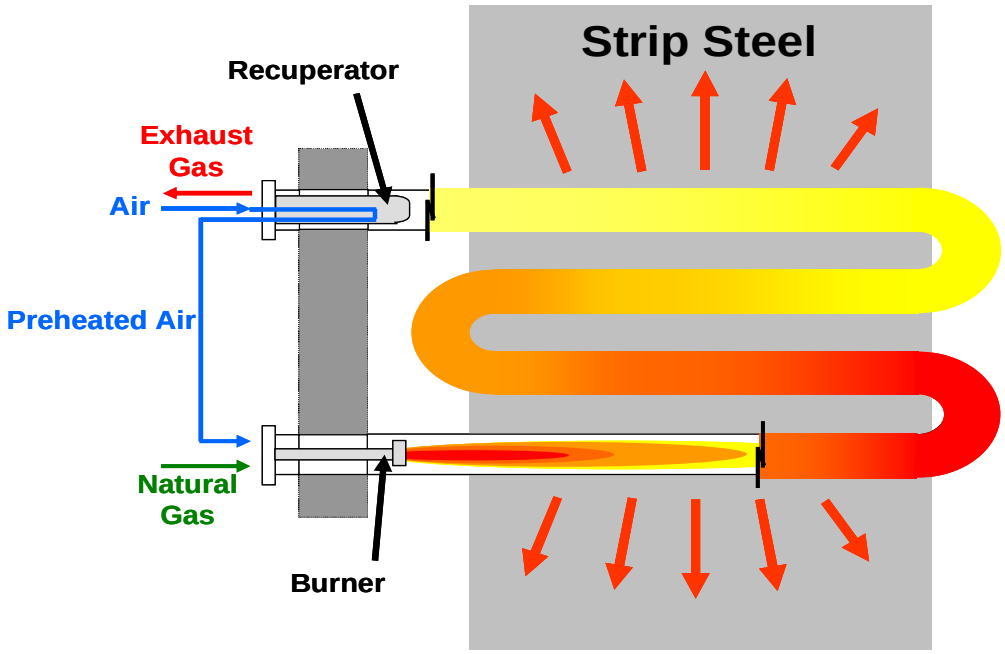

Figure 2-24 - Schematic displaying the operation of a W shaped radiant tube in a typical vertical annealing furnace to provide the necessary heat treatment to the steel

In a radiant tube furnace the load is heated indirectly by the heat source. The heat energy produced is then transferred through the tube wall and furnace atmosphere to the surface of the strip steel.

Tube furnaces generally contain reducing atmospheres, which is primarily nitrogen and a small percentage of hydrogen. This prevents the strip from oxidising at the high temperatures within the furnace, ensuring an excellent strip surface finish.

Natural gas is the most common fuel used for combustion, although in some cases coke oven gas is used. Burners are used with an excess of air to ensure complete combustion and energy recovery is attained through the heating of the combustion air via the exhaust gases through recuperative or regenerative means.

Over recent years, developments in burner designs have produced reductions in emissions and increases in fuel economy. The main process improvement programmes in industrial annealing lines currently, is to increase radiant tube longevity and increase the thermal efficiencies of the furnace.

2.3 Summary

Radiant tubes are a popular method of heating a particular load indirectly, with the most common tube design being the 'W' shape, which offers greater thermal efficiencies over other non re-circulating designs.

In continuous annealing applications, for the processing of strip steel, radiant tube furnaces are predominantly the chosen heating method, especially when excellent surface quality is required. In operation, deterioration of the tubes occurs, ultimately leading to tube failure. Consequently, process costs increase as a result of renewing and replacing radiant tubes. Chapter 3 outlines a case study site, where the failure of radiant tubes in its continuous annealing line has led to increasing maintenance costs.

3 Case Study Site: Port Talbot Works, Continuous Annealing Process Line

3.1 Introduction

This chapter provides an overview of Port Talbot integrated works, the annealing furnace and a background to the project. The furnace history was investigated and the failure rate and tube life for each furnace zone was determined. Also highlighted, are the various failures observed throughout the service life of the furnace and the different radiant tube designs used.

Port Talbot Works is an integrated steel manufacturing site capable of transforming iron ore to steel in coil form. During the transformation from raw materials to finished coil, the material undergoes many processes to hone chemical composition and shape. During the forming processes, undesired mechanical properties are produced in the material; therefore require an annealing treatment to restore properties that are required by the end application/market of the steel. Thus the works is the case study site for this research programme.

The Port Talbot Continuous Annealing Process Line (CAPL), is designed to anneal work hardened, cold rolled strip steel, at speeds of up to 350m/min in a reducing atmosphere (nominally 5% hydrogen in nitrogen) to temperatures up to 810°C. The high annealing temperatures are achieved via a Radiant Tube Furnace, as discussed in Chapter 2, and this is true for numerous other Tata Steel sites.

3.2 Tata Steel Port Talbot Works

Tata Steel Europe, is a division of Tata Steel which produces strip steel metal for use in various applications.

Port Talbot is the only Tata Steel site in the UK that can produce steel in coil form from raw materials. Llanwern is run as additional flexible capacity where slabs are rolled to finished coil. Together they produce hot-rolled steel, cold-rolled steel and hot-dip galvanized steel.

3.2.1 Raw Materials to Steel Making

Iron ore, limestone and coke are the main constituents needed to produce liquid iron with low sulphur content. The molten iron is tapped from the bottom of the blast furnace and transported to the steel making plant, where oxygen stirring reduces carbon content, Figure 3-1.

Alloy additions are added, if required, in a secondary steel making process to alter the chemical composition. Once correct, the liquid steel is transported to the continuous casting process to form solid slabs of steel. The slabs are cut to length and then transported to the rolling mills to be reduced in thickness to the desired gauge.

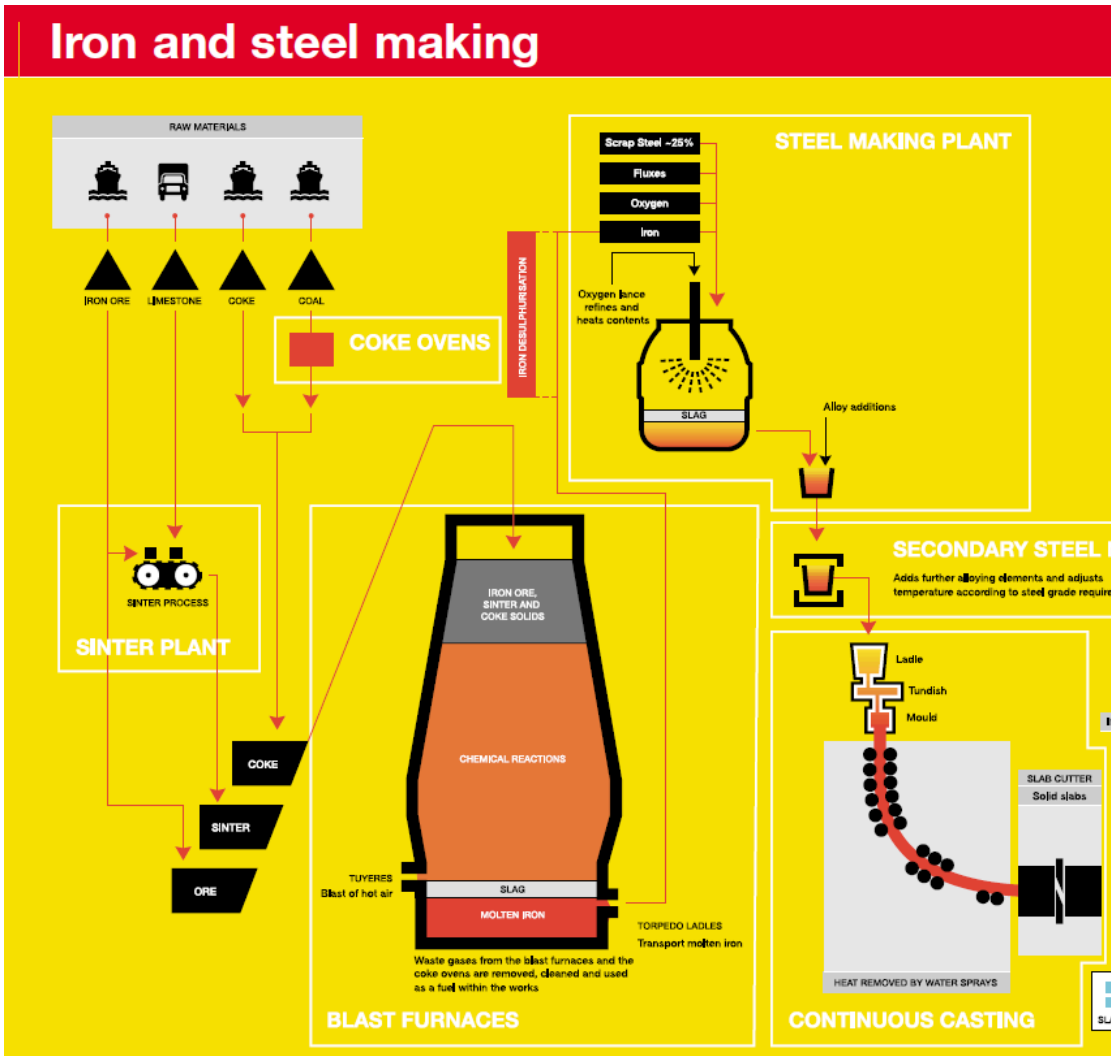

Figure 3-1 - Heavy end process route for the manufacture of steel slabs from raw materials at Port Talbot Works[48]

3.2.2 Hot Rolling

Hot rolling is the main process for rolling slab steel into strip form, which is subsequently coiled, Figure 3-2. Hot rolling is undertaken in both Port Talbot and Llanwern sites, where the slabs are heated in a reheat furnace before being subjected to a sequence of operations, namely:

- Scale breaking
- Roughing mill
- Finishing mill
- Run out table
- Coiler

Figure 3-2 - Hot rolling mill at Llanwern Integrated Steel Works

Hot coiled steel can have a final gauge of between 1.5 to 10mm and is sold to other Tata sites for further processing or transported to the cold rolling mill for further reduction.

3.2.3 Cold Rolling

Cold rolling is a secondary rolling process to further reduce the thickness of the steel to suit required applications. The cold reduction mill is a part of a sequence of operations, which include the following:

- Pickling
- Cold Rolling Mill
- Annealing
- Post-Annealing Processes – Temper Mill and Levelling

Pickling is a continuous process, which involves passing the strip through baths of dilute hydrochloric acid. Pickling removes the oxide layer, which forms on the surface of the strip during the process of hot rolling.

The cold rolling mill is usually a multi-stand close-coupled mill, where the strip is reduced to a thickness of approximately between 0.5 – 3.0mm. Cold rolling is undertaken at temperatures below $0.4T_m$ (melting temperature), thus, ferrite grains are deformed but recrystallisation does not occur. Also, tensile strength increases and ductility falls due to strain hardening.

3.2.4 Annealing

Annealing is a heat treatment process, which restores the mechanical properties which are lost during cold rolling. The strip is heated and cooled according to a specific heating cycle, depending on grade, in a large process line as seen in Figure 3-3. The net result is a steel strip that is ductile with a high quality finish. Post annealing processes such as temper rolling and levelling apply the final surface and mechanical properties to the steel.

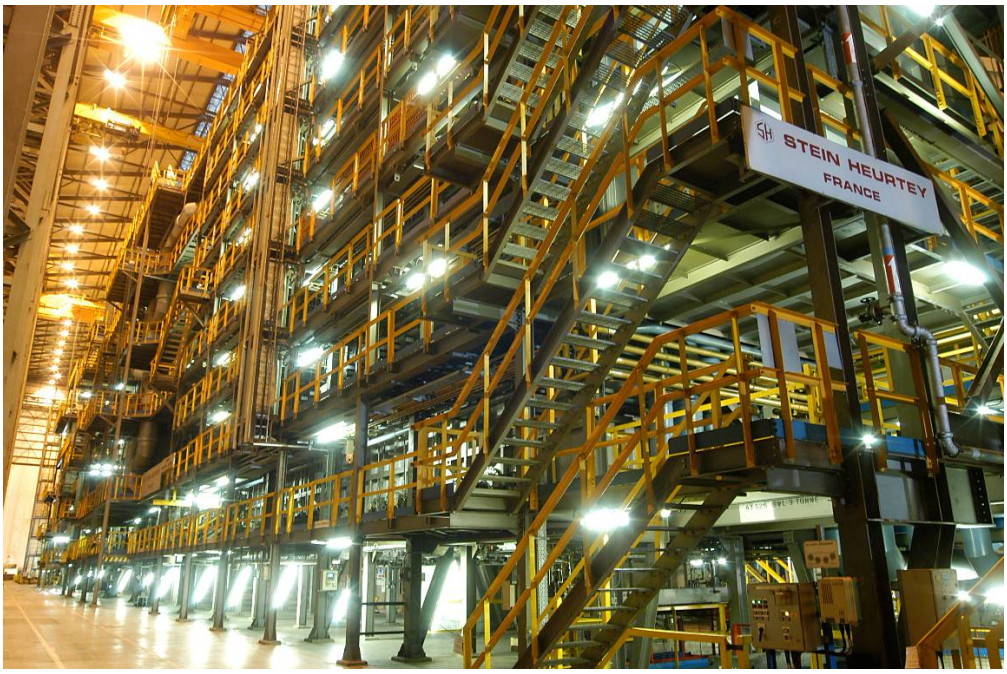

Figure 3-3 - The Continuous Annealing Process Line (CAPL) at Port Talbot Integrated Steel Works

3.3 The Continuous Annealing Process Line

3.3.1 Process Sections

CAPL can be split into 3 sections; Entry, Furnace and Exit section, as shown in Figure 3-4. The three sections are responsible for a particular procedure and are separated by vertical strip accumulators, which balance the speed of strip in each section allowing the process to be continuous.

3.3.1.1 Entry Section

The entry section prepares the strip ready for the annealing cycle. The strip is uncoiled from one of the two payoff reels and fed into the welding section, where the front edge of the coil is prepared and seam lap welded against the trailing edge of the previous coil. The strip is then fed through the cleaning section where it is washed in an electrolytic cleaning solution to remove all traces of oil and deposits.

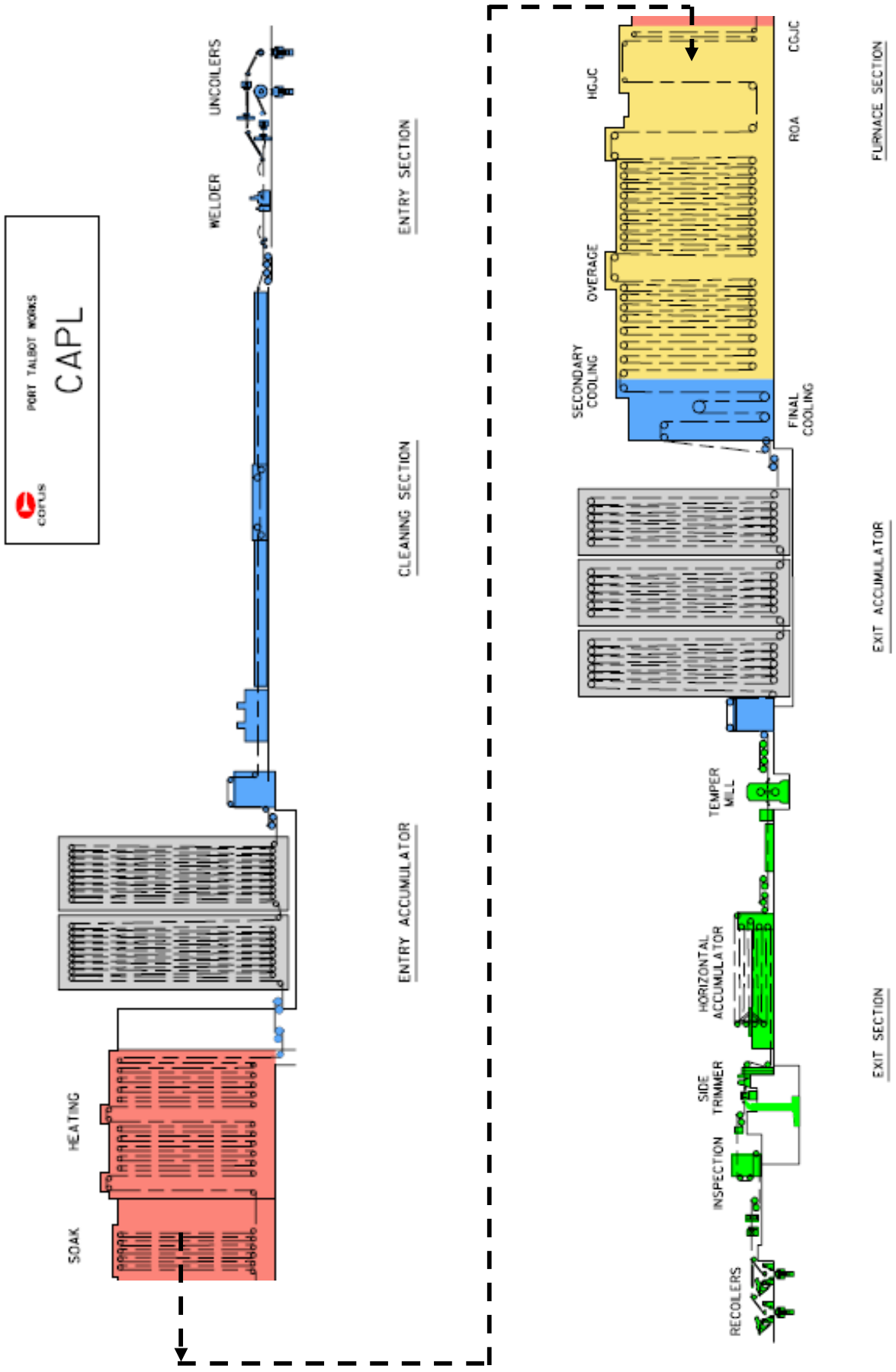

Figure 3-4 - Schematic depicting the CAPL (Port Talbot) sections[49]

3.3.1.2 Radiant Tube Furnace - RTF

The furnace section is where the strip undergoes a complex heating cycle. Figure 3-5, shows the heating cycles for the various grades processed through the CAPL. First, the strip enters the Radiant Tube Furnace (RTF), where the strip is heated from ambient temperature up to a minimum of 730°C and a maximum of 850°C, depending on the heating cycle. The RTF is an insulated chamber containing an atmosphere of 95% nitrogen and 5% of hydrogen. This reducing atmosphere mitigates the possibility of the strip surface oxidizing under intense heat.

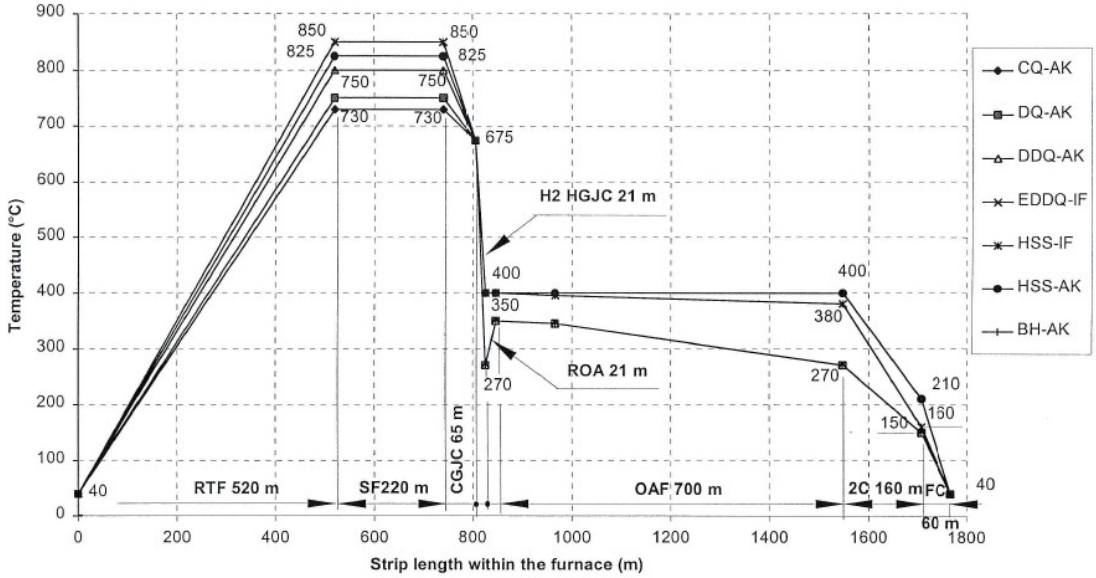

Figure 3-5 - Steel grade heating cycles[50]

The furnace is sectioned into 8 zones, each running vertically from level 1 to level 7. There are a total of 338 radiant tubes in the furnace, mounted in equal numbers on the operator side and motor side. The tubes are located in the zones in the following numbers as highlighted in Figure 3-6:

Zone 1 – 36 Radiant tubes (18 per side)
Zone 2 to 7 – 42 Radiant tubes
Zone 8 – 50 Radiant tubes

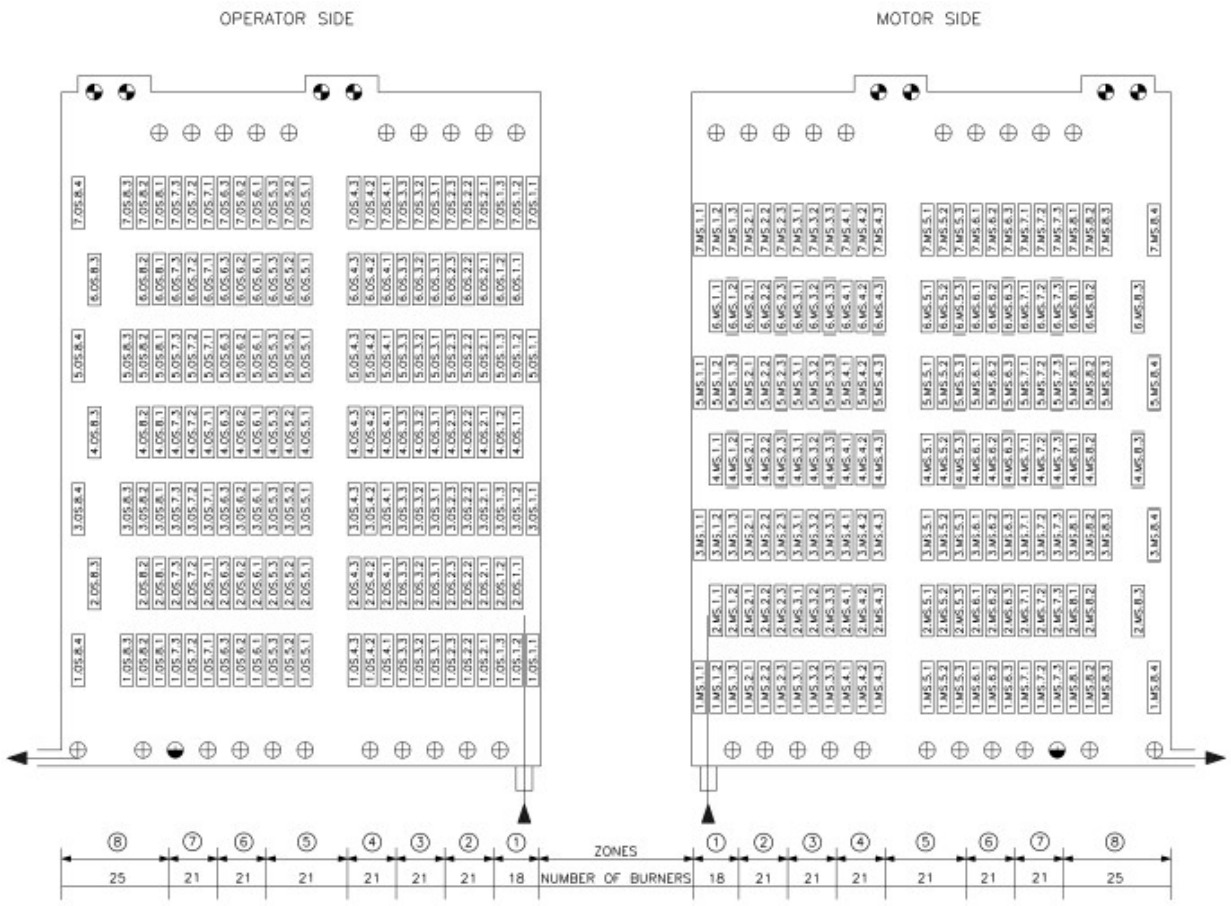

Figure 3-6 - Drawing showing the radiant tube location within the furnace[50]

The main heating section characteristics of the annealing furnace is described as[50]:

- Number of strip passes 24
- Strip length inside furnace approx. 525m
- Distance between roller axis 20.5m
- Heated strip length per pass 17.5m
- Installed heat input max. 216MWh
- Number of radiant tubes 338
- Number of control zones 8
- Max. Strip speed (for whole furnace) 350m/min

3.3.1.3 Soaking

Assuming maximum speed of 350m/min, the strip is heated for approximately 90 seconds in the RTF before entering the soaking section. Here, the strip temperature is

maintained at the same level in accordance with the required heating cycle for approximately 38 seconds. The heat input is supplied by 12 electrical ribbon heaters, which are mounted on ceramic pegs protruding from the furnace walls.

3.3.1.4 Conventional Gas Jet Cooling - CGJC

The strip from the soaking section enters the Conventional Gas Jet Cooling section (CGJC), where the strip is cooled to 675°C for every heating cycle. This section contains four cooling areas and two heating areas. The cooling section contains one conventional gas jet cooler and 6 electrical radiant tubes, while the heating area has 3 electrical radiant tubes.

The 5% hydrogen atmosphere is blown onto the strip through blowing boxes on each side of the strip. The electrical radiant tubes are used to maintain the required strip temperature reduction if the line speed is low or strip in danger of over-cooling.

3.3.1.5 High Gas Jet Cooling - HGJC

Further cooling is performed in the following High Gas Jet Cooling section (HGJC), where the strip is cooled from 675°C, to between 400°C and 270°C, depending on the heating cycle. The HGJC uses 50% hydrogen atmosphere rather than 5% because of its excellent thermal conductivity properties. Also included in this section are electrical radiant tube heaters, which again are used to heat the strip if needed.

3.3.1.6 Reheat Over-Aging - ROA

For certain grades of steel the Reheat Over-Aging section (ROA) is used to reheat the strip from 270°C up to 350°C. For all other grades, it maintains the strip temperature at 400°C. The ROA is split into two zones. In the first zone, there are 3 electrical radiant tubes and in the second there are four 900kW induction heaters.

3.3.1.7 Two Sectioned Over-Aging

Following the ROA are two more Over-Age sections (OA1 and OA2). Here the strip is either cooled from 400°C to 380°C or 350°C to 270°C. OA1 and OA2 both contain electrical heating elements, which are identical in construction and in operation to the elements in the soaking section. The latter zones of OA1 and zones in OA2 are equipped with gas jet coolers. Together with the electrical heaters they provide a controlled cooling capability.

3.3.1.8 Secondary Cooling

Further controlled cooling is performed in the secondary cooling section. Conventional gas jet coolers are used to cool the strip down to a temperature of 210°C, 160°C or 150°C, depending on heating cycle. Final cooling and quenching follows to cool the strip down to 40°C before it enters the accumulator and exit section.

3.3.1.9 Exit Section

The exit section is the finishing end of the line, where the strip is trimmed, inspected and oiled ready for coiling. The temper mill is used to induce a very low strain ‘skin pass’, which eliminates discontinuous yielding and can modify surface roughness. The two vertical strip accumulators allow a continuous feed of strip into the furnace section, so that the strip is uniformly heated

3.4 Port Talbot Furnace History

3.4.1 Introduction

Since the installation of the CAPL in 1998, a Microsoft Excel database has been kept listing all radiant tube changes that have occurred. Each radiant tube has an individual burner code, which is displayed on the database. After each maintenance stop, the replaced tubes are recorded with a replacement date positioned under the correct code. Also, records have been kept of when a radiant tube has been blanked off or been cut out (due to distortion).

Although basic, the record had enough information to determine the performance of the furnace and its individual zones in terms of tube replacement rate, and expected tube life. The results and figures produced in this chapter is a result of the manipulation of the database records by the author.

3.4.2 Failure History

Since the commissioning of CAPL there has been 299 tubes replaced and various designs used (Correct to 31/12/2009). The vast majority of these changes have been in the hotter zones (Zones 5 – 8) with the exception of 21 tubes, which have been replaced in zone 4 and 2. The first tubes were changed during 2001 and since, there has been on average, 33 radiant tubes changed each year.

Figure 3-7 displays the number of tube changes per year. 2001 was the first year radiant tubes were replaced in the annealing furnace, which had been in operation since 1998. From 2002 to 2004 the amount of tubes replaced is on par with average. In 2005, 55 tubes were replaced as the general condition of the furnace was reported to be poor, in 2006 a further 48 tubes were replaced. In subsequent years, the replacement rate has varied drastically.

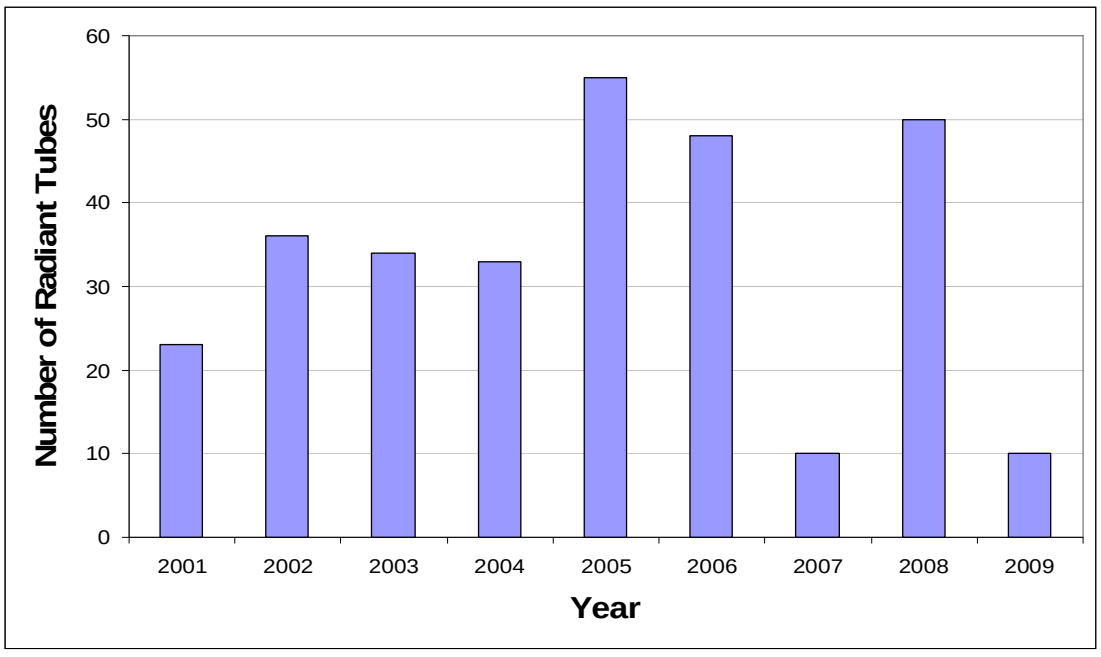

Figure 3-7 - Number of radiant tubes changed per year at the continuous annealing line, Port Talbot

What Figure 3-7 shows, is that the yearly replacement rate is variable and that any design changes undertaken to prolong tube life have not worked due to the greater replacement rate from 2005 onwards. Therefore, the reason for tube failures is not fully understood. Also, it could suggest that early design changes could have resulted in poorer tube lives.

To further understand where the radiant tubes were replaced, the furnace was divided up into its 8 control zones. Each zone is independently controlled to the others; therefore it provides an interesting insight into if how the zone is controlled has any affect on tube life.

Figure 3-8 displays the amount of radiant tubes changed per zone during the period between 2001 and 2009. It is easy to see that there is a definite trend between tube failure and furnace zones. Zone 8, the last zone of the furnace, has the highest tube replacement rate of all zones at 110 tubes, while zone 7 has had 75 replaced and zone 6, 64 respectively.

The replacement rate reduces from the final furnace zone, zone 8, to the entry of the furnace, zone 1. There have been no replacement tubes in zones 1 and 3; and only 2 tubes in zone 2. Therefore, by a simple manipulation of data, it is easy to see that the last half of the furnace, zones 5 to 8, has the highest failure rate.

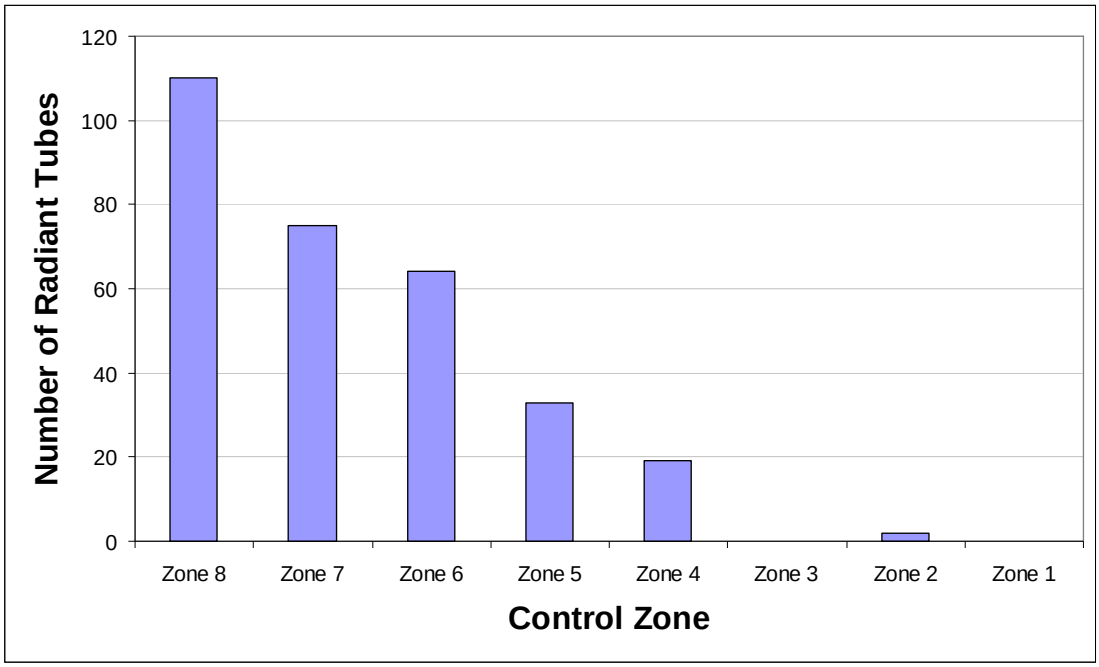

Figure 3-8 - Number of radiant tubes changed per furnace zone

To clarify the failure rate discussed earlier, by studying the installation and replacement date of each failed tube, the average time until replacement of each zone could be determined. Figure 3-9, displays the average age of radiant tube when replaced from each furnace zone.

As expected, the trend was the inverse of that seen in Figure 3-8. Zone 8 had the highest failure rate and as a result the shortest tube life of approximately 200 weeks. Zone 6 and 7 did not fare much better at 235 and 226 weeks respectively. This shows that the tubes in the final parts of the furnace require changing between 4 and 4.5 years. This equates to a significant amount of radiant tubes as these 3 zones contain a total of 134 radiant tubes.

In contrast, zone 5 had an average tube life of approximately 6 years, while zone 4 had a tube life of approximately 8.5 years. Zones 1 and 3 have not had a tube replaced and as such they have been in operation since commissioning in 1998, which equates to 11 years. Zone 2 has had 2 tubes replaced in 2009, while this is not a significant number, it could be a sign that tubes are beginning to fail in the first zones of the furnace, which could need replacing in the next few years.

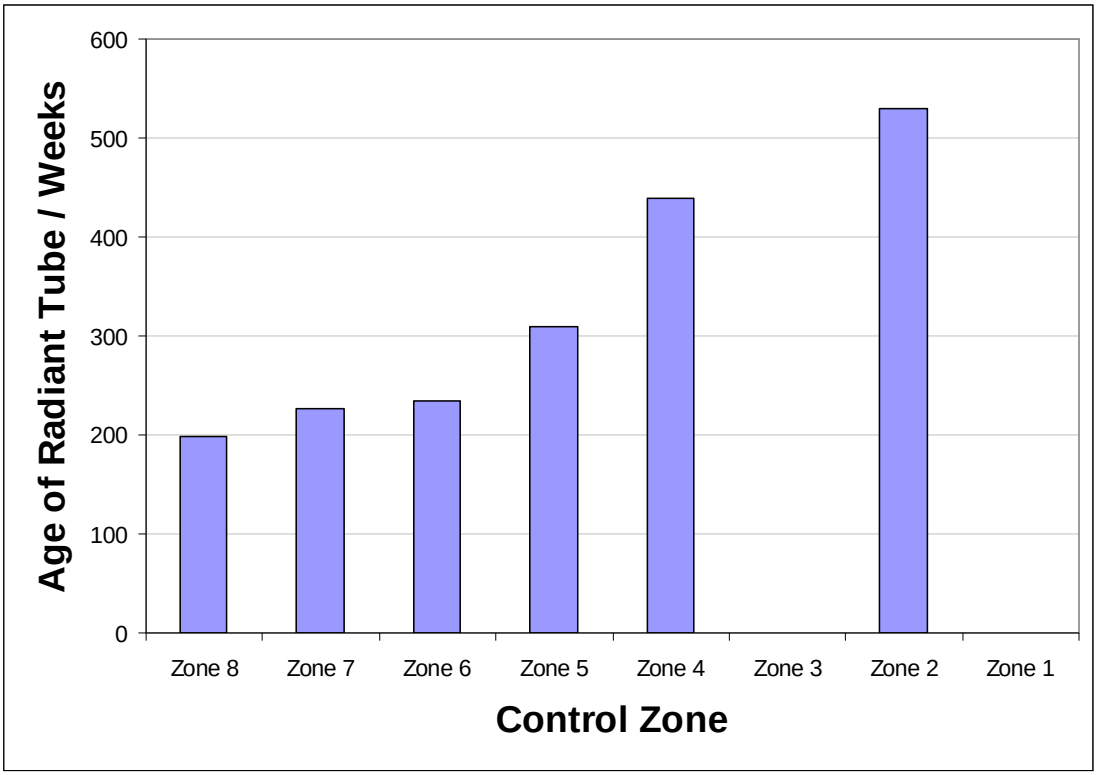

Figure 3-9 - Average age of failed radiant tube when replaced per furnace zone

While failure rates of tubes according to furnace location have been compared, the method of failure will be discussed in section 3.4.5 once an understanding of the varying designs is discussed.

3.4.3 Radiant Tube Designs

It is important to understand the various designs and supports used for radiant tube manufacture and the experience gained from their failure. This chapter discusses the various support options used at CAPL, which will also provide the basis for finite element modelling undertaken and discussed in section 7, where the stress in the firing leg has been compared for each support design.

There have been a number of companies manufacturing radiant tubes for Port Talbot CAPL since commissioning, these being Stein Heurtey, Almorgroup, Thermocast and currently FAI. Although the main design has remained the same since the installation (essentially a ‘W’ shaped tube), there have been many small design modifications, mainly to supports.

Stein Heurtey manufactured all the initial tubes required for the furnace (338 tubes), in addition, they provided 35 spare tubes. The design was as per Figure 3-10. But the two important sections are the outer tube support and central bend saddle (highlighted below). The outer tube support is a critical element of the design because it is the only support for the firing leg. The saddle meanwhile, provides support for the central legs and bend. But, this weight is transferred onto the firing leg near the bung.

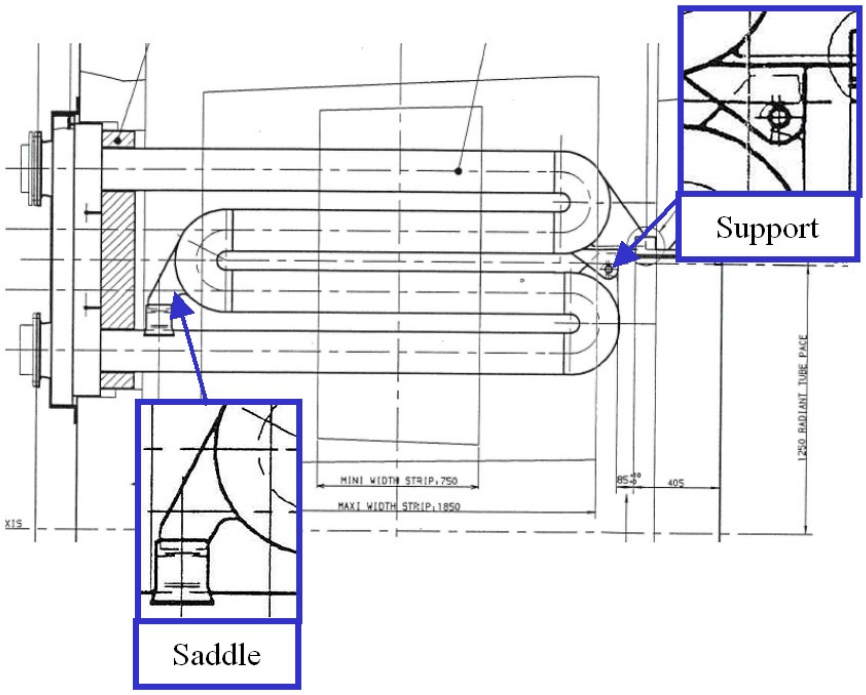

Figure 3-10 - Stein Heurtey original radiant tube design with 'Hook and Eye' support

Almorgroup were approached in late 2001 to manufacture replacement radiant tubes, and have continued to supply Port Talbot CAPL until late 2006. During this period, Almorgroup introduced many modifications, mainly to the support and saddle. Material specification was also changed for the bottom two legs, from the original 35Ni/25Cr to 37Ni/18Cr heat resistant alloy castings.

The design below, Figure 3-11, was the first radiant tube manufactured by Almorgroup, in 2001. The overall design was similar, but had changes made to the outer tube support and saddle. As nearly all Stein Heurtey tubes failed through the detachment of the 'hook and pin' support, Almorgroup introduced an enclosed two-

pin link, Figure 3-11. They had previously used the same link design on radiant tubes supplied to continuous annealing lines at Trostre and Ebbw Vale.

The saddle was also changed to a simpler slide bracket arrangement. Brackets were welded to tube legs 1 and 2, and were free to slide within each other but not along the tube leg. Thus, allowing natural movement but also retains some sideward hold within the channel slide, unlike the original design (Stein Heurtey).

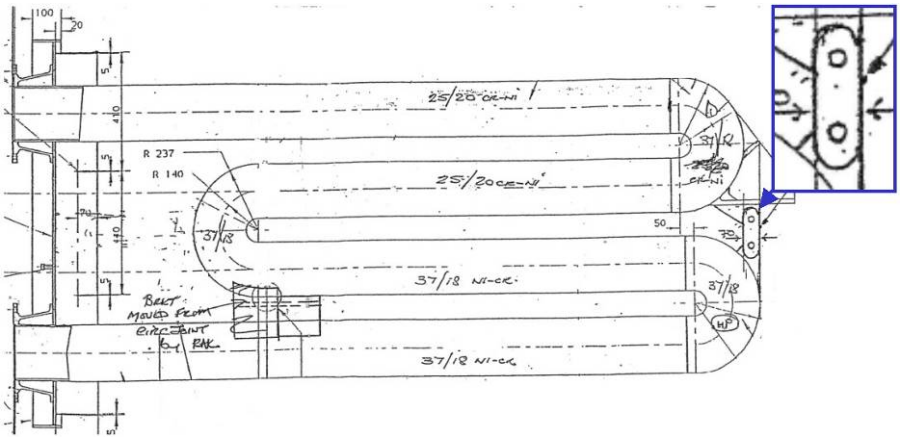

Figure 3-11 - First radiant tube design proposed by Almorgroup

Due to the rise in radiant tube failure rate, a survey by Veld[51], was performed to compare the inter-tube support with systems used at the annealing lines of Tata Steel-Ijmuiden and a review to evaluate the different radiant tube material.

The survey concentrated mainly on the inter-tube support, as it was believed to be the root cause for the premature failure of the tubes. The major defects have been associated with the dislodging of the connection between the lower and upper legs of the tubes[51].

Concluding from the comparisons it was recommended that the inter-tube construction would be modified to resemble the inter-tube link used on DVL-1 galvanizing line in Tata Steel-Ijmuiden, see Figure 3-12. The advantage of such a link was it would provide a flexible construction and in principle under all normal circumstances a secure, closed connection[51].

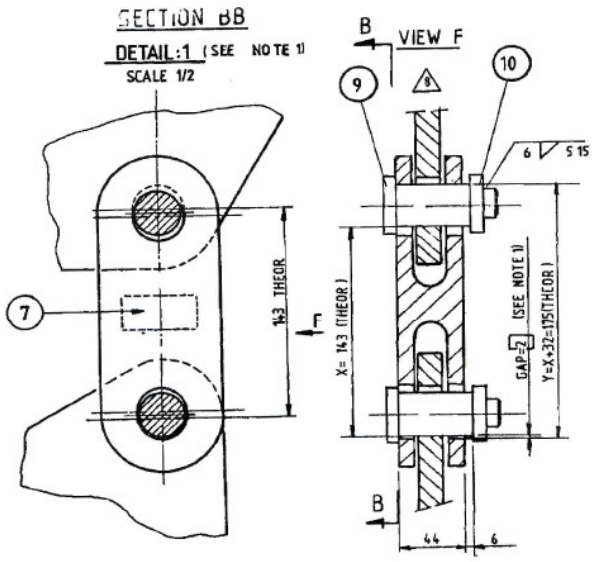

Figure 3-12 - Inter tube link used on DVL-1 galvanising line in Ijmuiden[51]

The proposed design, Figure 3-13, had a modified upper hole. The normal circular hole in the upper tube connector is modified in a slot hole of approximately 25 to 40 mm depending on the expected creep and the applied heat resistant steel. The built in position of the pin and brace is on the right side of the slot hole. It allows more horizontal movement (caused by creep) and it is in principle under all normal circumstances a fixed and closed connection[51].

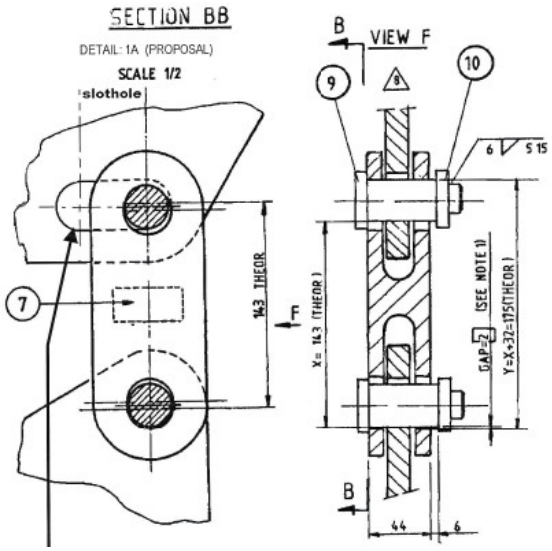

Figure 3-13 - Proposed inter tube design for use on Port Talbot CAPL radiant tubes[51]

The review into the material specification for the radiant tubes resulted in the preference towards the initial material specification employed by Stein Heurtey. The materials used in Port Talbot CAPL, with Gx40CrNiSi35.20 for the hotter sections and Gx40CrNiSi25.20 for the cooler sections.

Figure 3-14, shows the modification made to the outer tube attachment. Due to the concerns with the enclosed link, the design was modified to allow linear expansion. The new design though, did not resemble the proposed design from the survey. But, still being a closed couple to prevent the opening of the tube legs. Unfortunately, no documentation can be found to identify when this change was proposed.

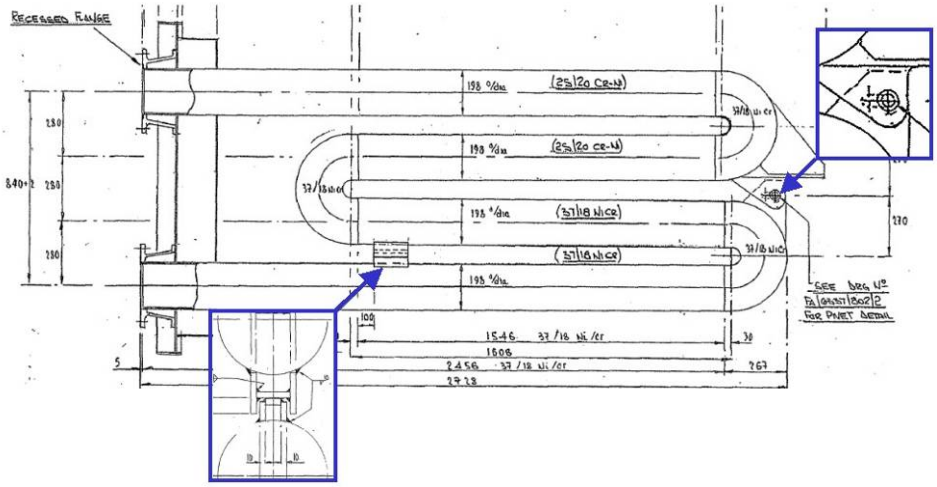

Figure 3-14 - Modified Almorgroup radiant tube

The final modifications Almorgroup introduced were during 2005, after a discussion with CAPL team members. Concerns were had with the design of the saddle. Therefore, it was agreed to reinstate a design that resembled the Stein Heurtey saddle, as it was considered to be of superior design. The outer tube link was also changed from a rectangular slot to a triangular hole. Thus, allowing limited expansion in a linear and vertical plane. See Figure 3-15.

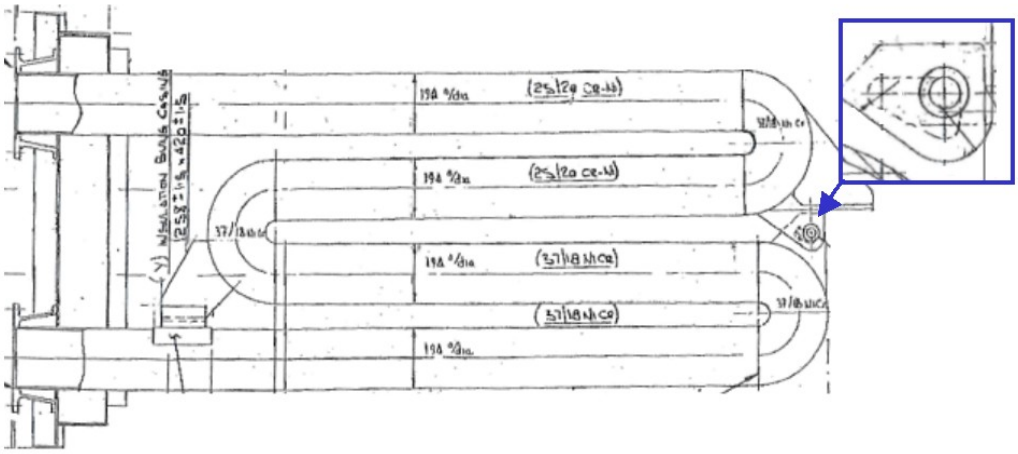

Figure 3-15 - Final radiant tube design proposed by Almorgroup

As a result of a breakdown in the relationship between Tata Steel and Almorgroup, due to poor quality control and unexpected short tube lives, Thermocast were contracted to supply radiant tubes from 2006. The design had now reverted back to original with a saddle and 'hook and eye' support. This was due to a high number of tube cracking failures experienced with the Almorgroup design changes.

The decision to revert back to original design was made by the furnace operators. Experience showed that this design generally failed due to the detachment of the outer tube support, which allowed the lower half of the tube to deform under its own weight. Although this was a concern, and in severe deformed cases caused surface issues, the tube was still in an operable condition and could provide heat energy into the furnace.

The later design modifications made by Almorgroup resulted in tube cracking failures. This was considered as more problematic as a high number of cracked tubes in the furnace caused major issues in maintaining reducing atmosphere pressure. In severe cases, shutdown was forced, emergency inspection was undertaken and the suspected cracked tubes were taken out of service. Resulting in reducing atmosphere pressure being maintained, but furnace heating capacity was affected.

From 2008, FAI has been manufacturing radiant tubes for CAPL Port Talbot. Changes were made to the design as a result of suggestions made as part of this project. These changes are shown in Figure 3-16.

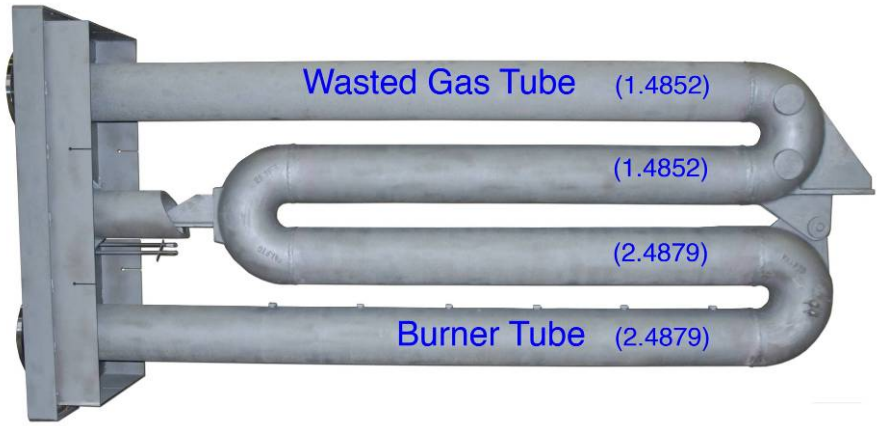

Figure 3-16 - FAI manufactured radiant tube for Port Talbot CAPL

The saddle support, which previously had relied on the firing leg, has now been abolished. The support for the central two legs now comes from the bung, a non-critical region of the tube structure; this ensures that no extra force is applied to the firing leg. Other changes have been to the material specification, where the content of nickel and chromium has increased to promote greater creep strength at the high temperatures in the latter zones of the furnace.

3.4.3.1 Radiant Tube Developments at other Steelwork Sites

The Japanese pioneered continuous annealing in the 1970's and therefore, have vast experience with regards to radiant tube and burner developments. Nakagawa et al[52], investigated the reduced life expectancy of radiant tubes and development techniques when operating at high temperatures (1000ºC).

Nakagawa[52] discusses that the life of a radiant tube is determined by the occurrence of deformation and cracking rather than the deterioration of the material from which it is made, which results from oxidation at high temperatures. In preventing these deformations and cracking, the authors consider the heat resistance of the radiant tube, which can be evaluated in terms of the high temperature strength characteristics of the

material, the difference between the highest temperature and the average temperature of the radiant tube (referred to as ΔT) and the value of the stress, which affects the creep rate, that is produced in the radiant tube, as shown in Figure 3-17.

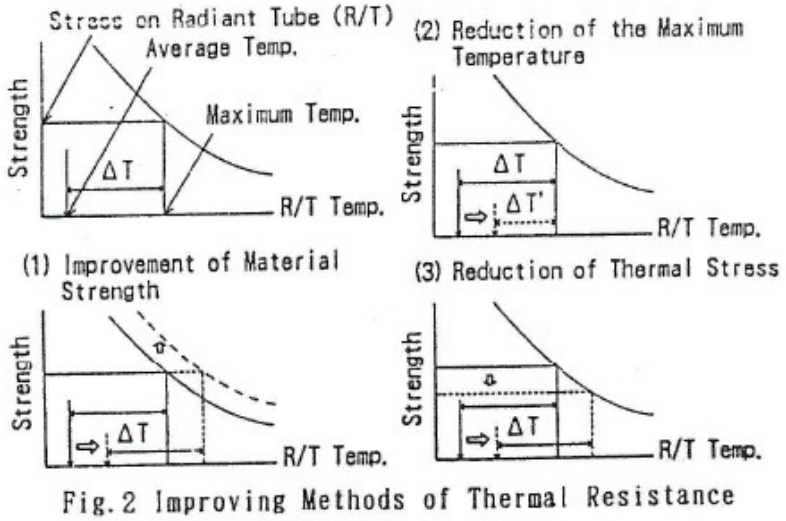

Figure 3-17 - Improving methods of thermal resistance[52]

Therefore, to improve the heat resistance the following factors were considered[52]:

- Increasing the high temperature strength of the radiant tube material
- Reducing ΔT
- Reducing the stress which is produced in the radiant tube

The developments made focused on the optimisation of the radiant tube construction and the design of the burner. The study found that reducing the temperature distribution in the radiant tube was of importance for increasing its heat resistance. Also, increasing the diameter of the high temperature parts (firing legs) and increasing the number of support points were effective for preventing deformation of the radiant tube, see Figure 3-18.

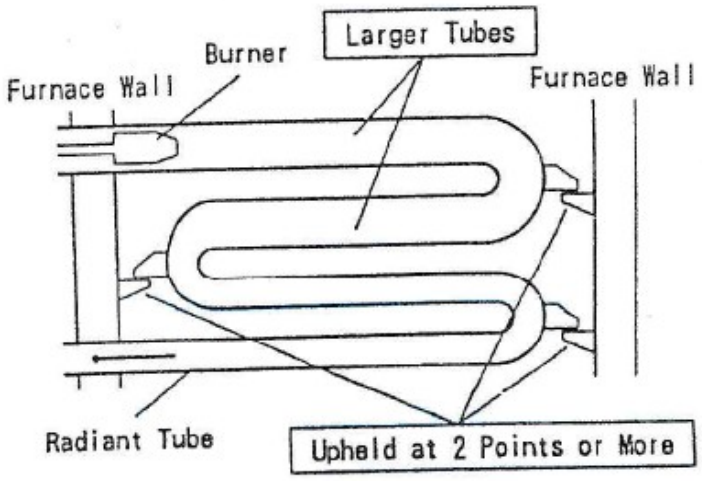

Figure 3-18 - Radiant tube design for high temperature and high combustion load[52]

Modifications made to the burner unit resulted in ΔT measurements being half those of a conventional burner. Also, the temperature of the combustion tube with the developed burner was about 100ºC lower. The development to the radiant tube and burner were thought to have a life expectancy of at least 5 years at a furnace temperature of 1000ºC[52].

3.4.4 Material Specifications

Due to the nature of the radiant tube design, the combusted products travel through the tube and dissipate heat energy. Therefore, the tube nearer the firing leg operates at higher temperatures than the exhaust leg. This allowed financial savings to be made when selecting material, as the exhaust leg didn't require the higher mechanical property specification of the firing leg.

There have been three different material specifications for the radiant tubes since the commissioning of CAPL. One introduced by Stein Heurtey since the installation, second introduced by Almorgroup in August 2001 and finally another in 2008.

Stein Heurtey chose 35Ni/25Cr nickel alloy castings for the 1st and 2nd tube (firing leg) and the 1st bend. While the other tubes and bends were 25Cr/20Ni grade. See appendix A for the material composition.

Almorgroup opted for a slightly lower nickel alloy grade (in terms of creep resistance) for the lower half of the radiant tube and for all the bends. A nickel alloy grade of 37Ni/18Cr was chosen, which has a lower creep resistance up to 1050°C, when compared to 35Ni/25Cr. The upper tubes remained at grade 25Ni/20Cr, while the bends were all cast from the same grade to reduce manufacturing costs.

Since 2008 the material spec has been 48Ni/28Cr/5W for the bottom to legs, wile the upper two have been to a specification of 35Ni/25Cr. The 1st bend has been to the higher spec, while the 2nd and 3rd bend manufactured to the lower 35Ni/25Cr.

3.4.4.1 Trial Tubes

There are currently two radiant tubes, which are of 'trial' material specification installed in the CAPL furnace. The tubes are from two different manufacturers, Almorgroup and Thermocast.

The two tubes were installed during maintenance stop week 34, 2005. The Almorgroup tube was requested to have a higher specification material on the 1st leg (firing leg), 2nd leg and 1st bend "as a means of increasing creep resistance"[51]. Consequently, material was upgraded to Cronite 48Ni/28Cr Nickel alloy casting (see appendix A for composition). The tube was installed into the furnace in location 5 O.S. 7.2 (Level **5**, **O**perator **S**ide, Zone **7**, Radiant Tube **2**) and on the last visual inspection in March 2011; there were no visual defects reported and no signs of deformation.

Thermocast supplied a similar specification tube, with the 1st leg, 2nd leg and 1st bend manufactured from Cronite 48Ni/28Cr Nickel alloy casting. The design of the tube was similar to the Almorgroup tube, albeit with one difference. The inner bore of the firing leg was machined smooth. This was done to remove the layer of slag and inclusions which form on the inner bore of the tube during spin casting. During operation, the inclusions could oxidise, affecting thermal conductivity and could deflect flame travel. The tube was installed into the furnace in location 5 O.S. 8.4 (Level **5**, **O**perator **S**ide, Zone **8**, Radiant Tube **4**) and on the last visual inspection in March 2011; there were no visual defects reported and no signs of deformation.

3.4.5 Failure Types

The radiant tubes installed into the furnace have all failed as a result of one (sometimes more) of five different failure types. Two of which can be put down to quality control issues regarding Almorgroup during manufacturing, the other three could be due to poor design or the result of operational influences.

All but two (187 tubes) of Stein Heurtey designed tubes, failed due to the detachment of the 'hook and pin' retaining linkage, which resulted in the lower combustion legs separating from the upper exhaust legs (see Figure 3-19 below). The hotter leg then drops down under its own weight, or to the side, and becoming a potential strip marking/break risk. The two exceptions failed due to a crack occurring just before the weld between the firing leg and first bend.

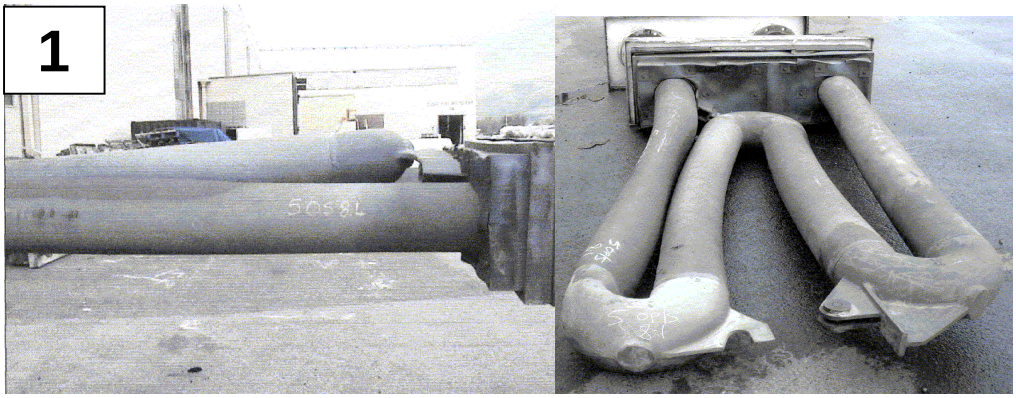

(A) (B)

Figure 3-19 – Failure type of the Stein Heurtey radiant tube (Failure type 1)

Due to the high percentage of Stein Heurtey tubes failing through the 'detaching' method, it can be assumed that it was a result of a poor outer tube support design.

To solve the detaching failure, Almorgroup proposed an outer tube link. This meant that the tube legs could no longer detach and open in the manner they did previously. But, this modification, along with the new saddle and material specification, introduced new failure types. Thus, determining the cause of failure is difficult.

Below are pictures of the two new failure types that occurred with tubes supplied from Almorgroup. Figure 3-20 (A), displays the catastrophic deformation of the entire

firing leg. While Figure 3-20 (B), displays the deformation of the tube due to the inferior saddle design.

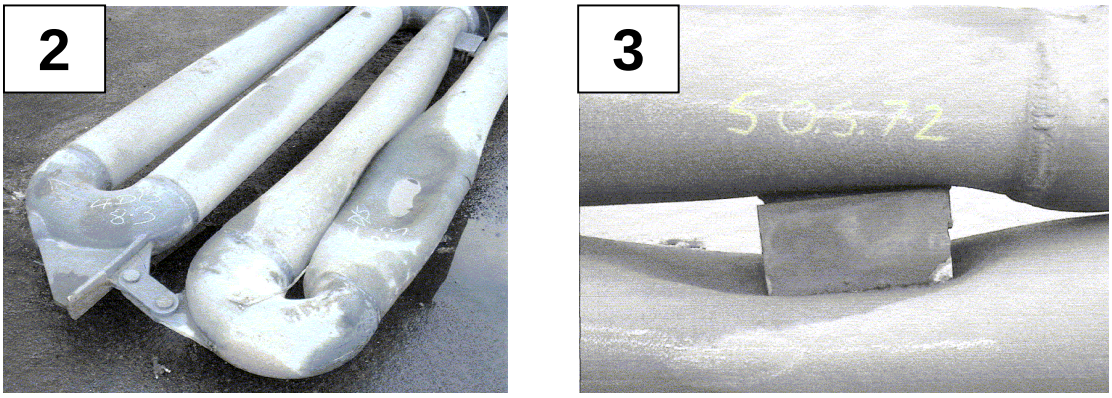

(A) (B)

Figure 3-20 - Failure types of Almorgroup radiant tubes (Failure type 2 & 3)

The narrow base design of the saddle generated large forces acting down on the firing leg. When operating at high temperatures, the creep resistance of the tube material decreases drastically. Therefore, the base of the saddle forces the tube to deform inwards.

Concerns were also expressed about the closed outer tube attachment. The differential expansion between the upper and lower tubes allow for a bending moment in the first return bend. The force produced in this area results in an area of tension across the welded join, resulting in a crack failure along the weld path.

The two failure types displayed below, were identified as being the result of poor manufacturing quality control on behalf of Almorgroup. Inferior bend castings, Figure 3-21 (A), and cracked welds between the firing leg and first bend, Figure 3-21 (B), resulted in substantial amounts of tubes failing prematurely.

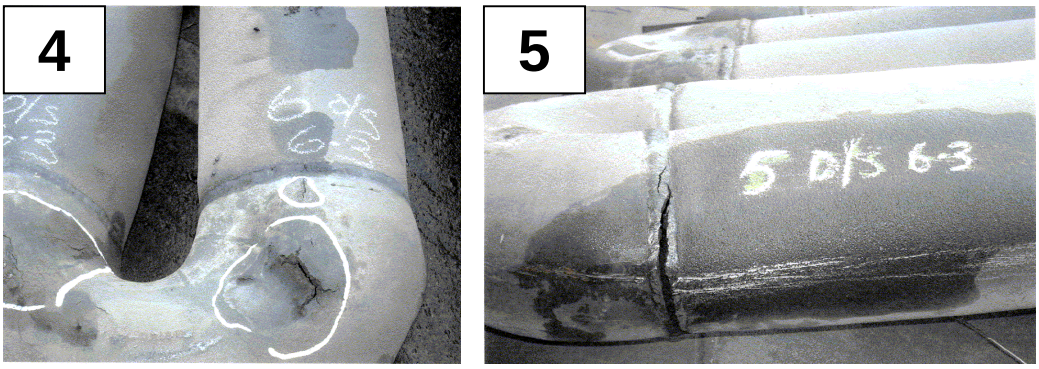

(A) (B)

Figure 3-21 - Failure types resulted from poor quality control at Almorgroup

(Failure type 4 & 5)

3.4.6 Radiant Tube Failures at Other Sites

3.4.6.1.1 Failure of Radiant Tubes in a Continuous Galvanising Furnace

A paper by Chakrabarti et al[53] in 2003 discusses the nature and the possible causes of tube failure, which were frequently observed in a continuous furnace for galvanising steel strip. The furnace contained 24 'U' shaped radiant tube burners, which were used in a heating and soaking section, placed alternately on top and bottom of the strips and maintained in a reducing atmosphere of nitrogen and hydrogen[35].

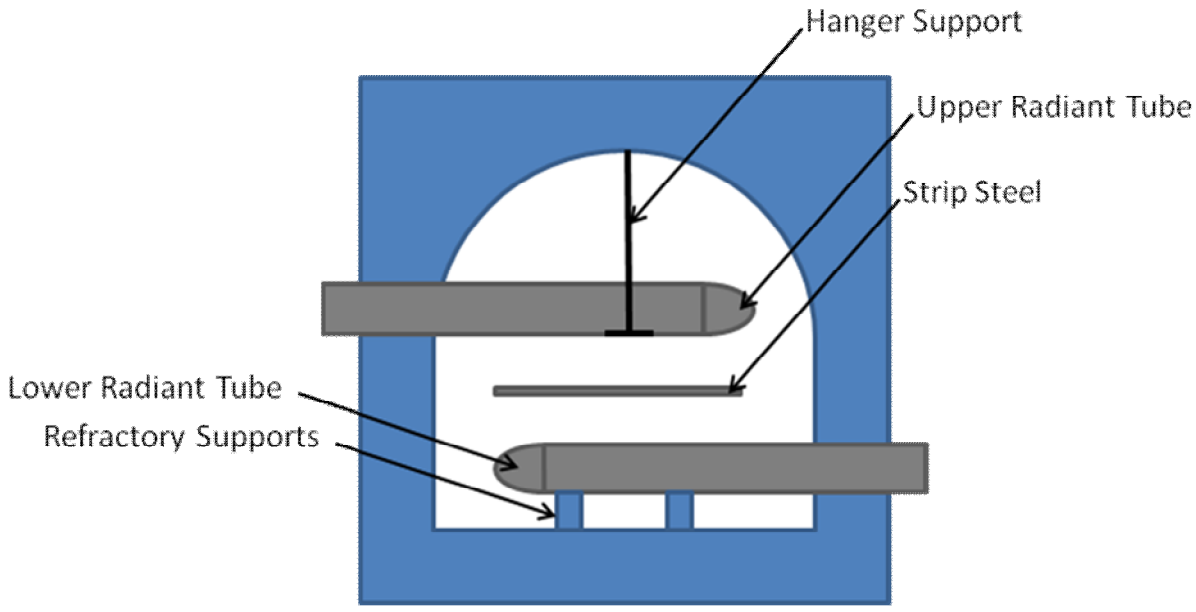

Figure 3-22 - Drawing displaying the layout of the galvanising heating/soaking section

It was found during a routine major shut down, a year after its commission, that 9 radiant tubes had ruptured, some quite severely. All failed tubes exhibited star shaped cracks, which were all positioned on the lower half of the tubes. Most of the failures also occurred very close to the point of maximum temperature on the radiant tube, at approximately 1090ºC[53].

The following investigations were undertaken to determine the cause of failure:

- Analysis of tube material
- Fluctuations in calorific value of combustion fuel (in this case Coke Oven Gas)
- Non-destructive testing of radiant tube walls (used and new tubes)
- Operating parameters of air-fuel ratio and set-point temperatures
- Investigate the possibility of localised overheating
- Cause of star-shaped cracks in tubes

A micro-structural analysis was undertaken to determine levels of oxidation on inner surfaces of the tube. Clusters of oxidation product were revealed at locations along the cracks. Under higher magnification, extensive grain boundary oxidation and voids were observed, an indication of excess oxygen in the combustion regime. Under X-ray mapping the voids and oxidations revealed that the chromium was oxidising while the iron was unaffected.

Micro-structural analysis showed that the protective chromium oxide film succumbed to heat, forming unstable oxide and voids at triple points and in chromium rich areas. These voids at the triple points gradually coalesced to weaken the matrix leading to failure. High temperature and high oxygen in the combustion regime resulted in the failure of the tubes[53].

The material used (MORE-1 – a proprietary alloy of high nickel, high chromium steel, stabilised with niobium and tungsten) was decided to be suitable for use at

temperatures around 1000ºC. But, the presence of a refractory brick support generated localised hot spots, which aggravated the failure through high temperature oxidation.

3.4.6.1.2 Oxidation Failure of Radiant Heater Tubes

Yoon et al[54] performed a failure analysis on a radiant tube heater, which was used for heat treatment in a hot rolling process of an iron foundry. The radiant tube was of a 'U' design, which was fabricated by centrifugal casting. The material used is either HK or HP steel (same as the material grades used at Port Talbot CAPL), which have a high content of Ni or Cr and in the process discussed the tubes usually endure constant high temperatures of approximately 900 - 1000ºC.

Failure analysis of the tube was performed by careful inspection of tube cracks, metallographic observation of the near crack region and the chemical analysis of tube metal and oxide scales.

The main cause of failure was through the formation of cracks, which were frequently reported near the location of a supporting hanger close to the burner. Cracking direction was random and not related to the principal stress direction. As a result, Yoon et al[54] argued that the formation of cracks was not caused primarily by internal pressure or thermal gradients. Therefore, a metallographic investigation was performed.

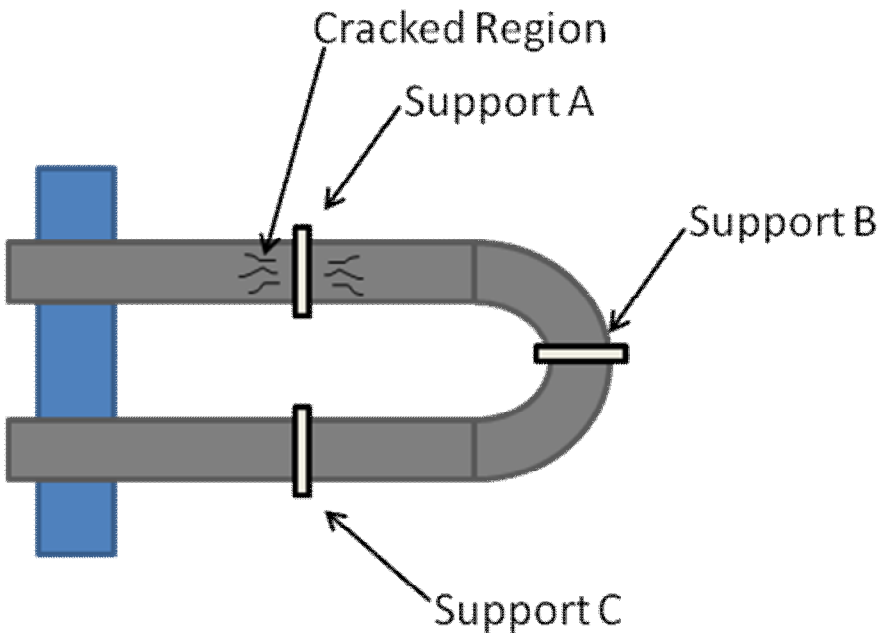

Figure 3-23 - Schematic view of radiant tube and support mechanisms[54]

From a visual inspection it was shown that the tube walls had suffered from thinning, which was fairly localised and irregular. Erosion was therefore excluded as the possible form of failure. It was found that these locally thinned areas had formed as a result of excessive oxidation.

HK steels can be used without problems when running at operational temperatures of less than 1000ºC. This is because a stable protective Cr_2O_3 oxide layer forms. It was shown from the microstructure of the failed specimen that the radiant tube had operated at temperatures of between 1090 - 1230ºC. At temperatures above 1090ºC, the Cr_2O_3 layer transforms into volatile CrO_3, losing its protective properties. Abnormal and rapid oxidation occurred leading to excessive tube wall thinning.

Some oxide pits were filled with oxide scales formed by rapid oxidation. The thick oxide scale was usually cracked due to the difference in between the thermal expansion coefficients of the scale and the tube metal. The cracked scale led to fresh tube metal beneath the scale, which was prone to repeated oxidation leading to small cracks and eventually tube failure.

3.4.6.2 Radiant Tube Failures in the Petrochemical Industry

3.4.6.2.1 Introduction

Indirect heating via radiant tubes are employed in other industries such as petrochemical, where the radiant heat is transferred into the tube from an external heat source to process the gas within the tube.

3.4.6.2.2 Analysis of Failed Ethylene Cracking Tubes

High chromium and nickel cast steel, HP grade (35Ni/25Cr), is used in ethylene cracking tubes where operational temperatures range between 700 - 900ºC. A report by Guan et al[14] was produced discussing the analysis of failed tubes, which had failed after only one year of service.

Cracks and bulges occurred in a number of tubes, which was thought to be as a result of overheating or low material strength. An investigation was performed, which included a tensile test, optical microscopy, scanning electron microscopy, energy dispersive spectroscopy and X-ray diffraction analysis.

Results showed that the tubes had failed due to exposure to high temperatures over long periods of time. The outer surface of the tubes had reached temperatures of 1200ºC (measured), which is greater than the material limit of 1060ºC. The overheating was the significant factor in degrading the mechanical properties and microstructure in the failed portion of the tubes[14].

3.4.6.2.3 Failure Analysis of Furnace Radiant Tubes Exposed to Excessive Temperature

Radiant tubes constructed from HP 45 heat-resistant steel are also used in petrochemical plants in applications such as ethane pyrolysis furnaces. A failure analysis by Ul-Hamid et al[6] discussed how radiant tubes had failed after a fraction of the service life.

As part of the investigation, samples of tubes were analysed using a scanning electron microscopy and X-ray spectroscopy to characterize the microstructure and chemical composition. Micro-hardness testing was used to evaluate the mechanical strength while structural analysis was conducted in an X-ray diffractometer[6].

Results concluded that the tubes had failed due to creep damage and carburization attack due to overheating during decoking. If temperatures were continuously exceeding 900ºC it was recommended that tube material should be upgraded to a HP + W grade, which should have better performance against creep and carburization attack[6].

3.5 Summary

Radiant tube failure at CAPL, Port Talbot is a major attribute of the annual manufacturing costs. With increasing pressures to reduce the annual expenditure, focus is put on improving tube life. Chapter 4 aims to compare the tube replacement at CAPL with other radiant tube furnaces within Tata Steel and other companies.

4 Analysis of Existing Radiant Tube Furnaces

4.1 Introduction

To determine the performance of Port Talbot CAPL radiant tubes, a comparison of service conditions, design, material specification and failures of other radiant tube furnaces was required. A comprehensive benchmarking study was conducted, internally within the Tata Steel group and at other steel manufacturing sites, namely Sumitomo Metals, Japan.

4.2 Radiant Tube Furnaces within Tata

Tata Steel has a number of annealing and galvanising facilities that contain radiant tube furnaces. This chapter aims to highlight and compare the pertinent features of the tube design, operation and failure types of these process lines.

4.2.1 Tata Packaging, Trostre

Tata have a site situated in Trostre, Llanelli, which manufactures tin plate primarily for the packaging market. They have two continuous annealing lines named “CAPL” and “CAL”, which have replaced the majority of their batch-annealing units.

4.2.1.1 Continuous Annealing Process Line (CAPL)

Stein Atkinson Stordy installed the latest continuous annealing line at Trostre in 1989. The design is similar to the CAPL situated at Port Talbot, although it’s designed to anneal narrower and thinner gauge steel. The radiant tube furnace (RTF) has a total of 144 ‘W’ shaped radiant tubes. The furnace has 5 zones, with each zone having the following number of tubes:

- Zone 1: 18 tubes
- Zone 2 to 4: 36 tubes each
- Zone 5: 18 tubes

The furnace atmosphere is made up of 93% Nitrogen and 7% Hydrogen and is run at temperatures of between 620ºC to 670ºC. Stein Atkinson Stordy originally manufactured the tubes using a centrifugally cast HK40 alloy material (25Cr/20Ni). Almorgroup now manufactures and repairs the radiant tubes using Inconel 601 (wrought heat resistant material of composition 61%Ni, 23%Cr) and T64 (cast heat resistant material of composition 35%Ni, 25%Cr, 1%Nb) as the material for the radiant tube legs.

The tube design is similar to that used at Port Talbot, albeit slightly smaller. The main difference is that the burner is situated in the top leg (outer left leg in Figure 4-1). This firing leg is supported by a bracket from the furnace wall with the lower half of the tube being supported by a 2-pin link from the upper bend and also a small sliding saddle between the 3rd and 4th legs. The concept of the 2-pin link support adopted by Port Talbot was sourced from this design utilised by Trostre.

Figure 4-1 - Radiant tube design used at the CAPL at Trostre Works

Trostre works change approximately 14 to 22 radiant tubes annually on CAPL, depending on the condition. Tubes fail primarily by cracks occurring mostly on the

firing leg and the first bend, Figure 4-2. Other failures that occur are distortion, twisting and collapse.

(A) (B)

Figure 4-2 - Pictures indicating the common failures of tubes at Trostre; (A) cracking of the firing leg and (B) of the weld region of the 1st return bend

A basic failure log is maintained indicating where and when each radiant tube has been replaced. Figure 4-3 depicts the number of radiant tubes replaced each year since the line was commissioned, until 2006. As shown, 64 tubes were changed in 1993, this equates to approximately 44% of the total number of tubes in the furnace. In 1994, a further 32 tubes were replaced resulting in over 90% of the tubes within the furnace having being either replaced or refurbished at this point in time[43].

This high failure rate was associated with a low material grade specified for the firing leg, which resulted in either premature or catastrophic failures[55]. The material specification was subsequently increased for the firing and second leg since 1993 onwards resulting in reduced tube replacements.

It is important to note from Figure 4-3, that material choice for a radiant tube application is very important and requires careful consideration of the operating parameters, particularly temperature. Choosing an unsuitable or too low a grade results in premature tube lives and increased maintenance costs. Equally, choosing an unsuitably ‘exotic’ material grade at the furnace installation phase increases the project cost.

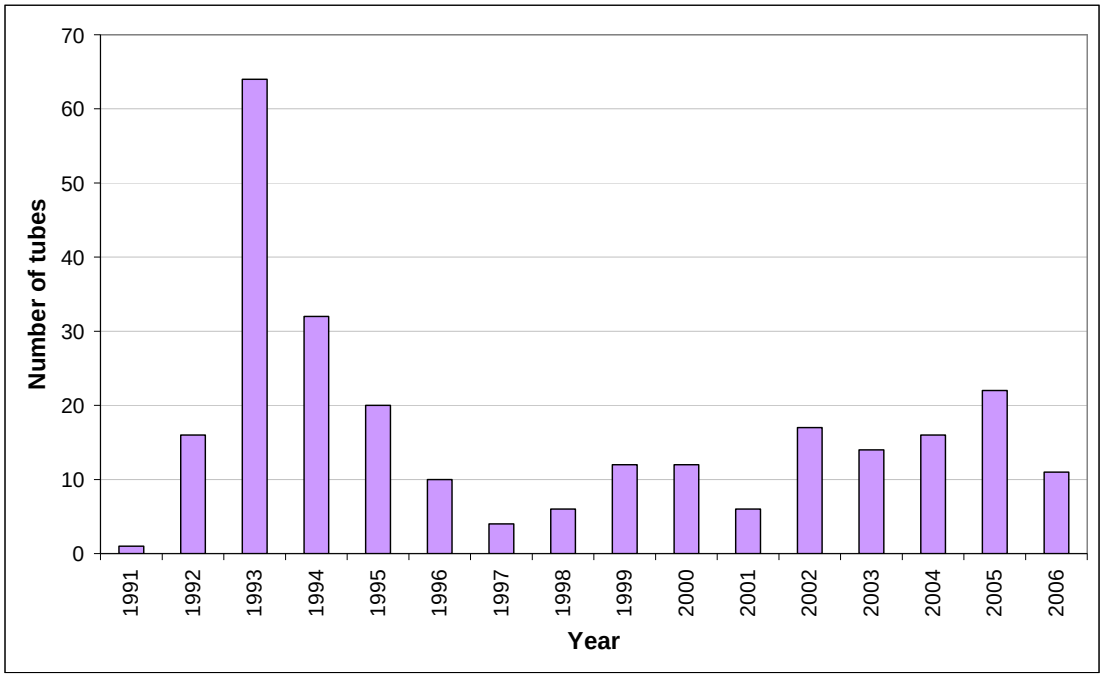

Figure 4-3 - The number of radiant tubes replaced each year since CAPL was commissioned until 2006

Figure 4-4 displays the number of tubes changed in each zone of the RTF at Trostre. The worst performing zones are numbers 2, 3 and 4, where the temperatures are reportedly higher as these are the main heating zones. Again, this shows that radiant tube life is dependent on temperature.

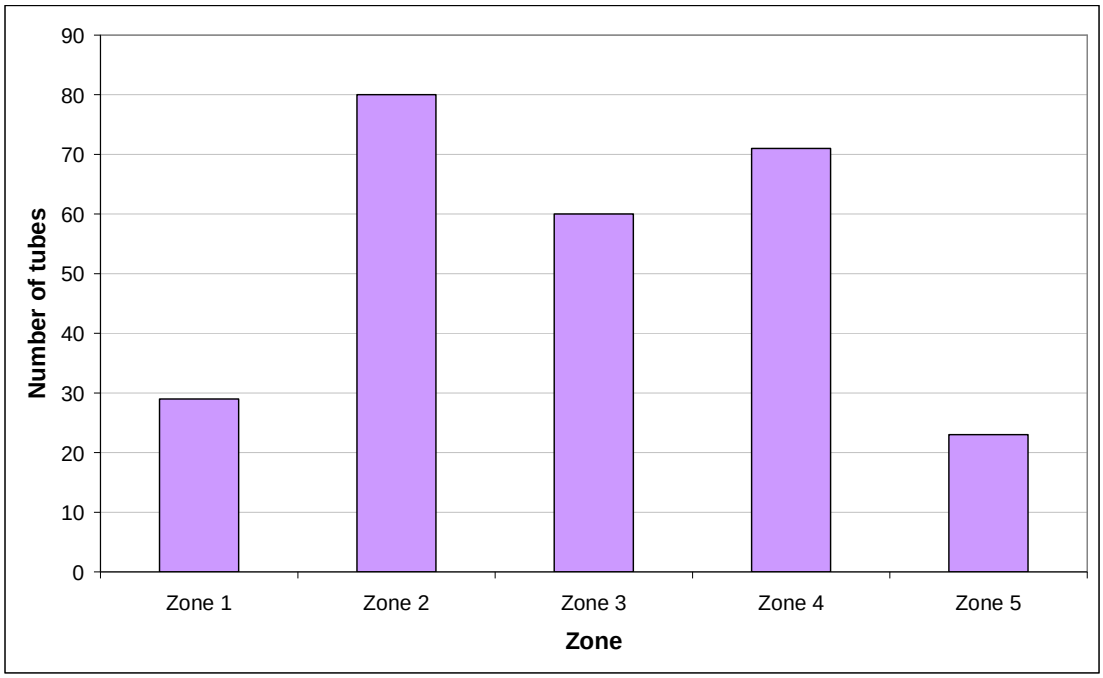

Figure 4-4 - The number of radiant tubes changed per zone

4.2.1.2 Trostre Furnace Tube Life

The continuous annealing line at Trostre works suffered from low tube life in the first few years after commissioning in 1988. As a result, a number of research projects have focused on the failures and process parameters in order to rectify the problem and prolong tube life. Below are the main findings and observations from the published technical reports resulting form the research work.

A failure analysis report by Lewis et al[55] was produced 3 years after commissioning, discussing the examination of failed radiant tubes. It was discovered that a large number of radiant tubes in the hottest zone (Zone 4) had grown and bowed excessively leading to cracks and severe distortion.

An examination of the internal bore of the tubes discovered large deposit build-up. An x-ray diffraction analysis showed that the deposit contained oxides of the alloying element and the element themselves namely chromium, nickel, haematite, chromite and bunsenite.

The analysis showed that the top of the tube had suffered excessive scaling, which had fallen to the bottom of the tube. The deposit then acting as a thermal and oxygen barrier. This process of degradation is a function of cooling from the operating temperature of the inner surface of the tube[55].

It was also noted that a year prior to the investigation, the furnace operation had changed. The rate of cooling had been increased, and as a result a greater rate of cold air was forced through the tubes during the cooling cycle. This was contributed to the type of failure and as a result the forced cooling was discontinued. Also, a recommendation was made to consider increasing the material grade from HK40 to a grade higher in nickel content, as this would enable the material to resist the deteriorating effect of spalling.

Due to further unacceptable radiant tube life experienced at Trostre CAPL, an investigation by Lewis et al[43] was undertaken to determine those factors, which affect

tube life and whether incorrect combustion was a major factor as claimed by the radiant tube manufacturer Stein Heurtey Ltd.

Since its commissioning in 1988, the CAPL furnace has experienced unacceptably low radiant tube lives, with over 90% of the original set of tubes now having been replaced or reconditioned (by 1994)[43].

Known and alleged factors influencing tube deterioration were[43]:

- Radiant tube material of construction
- Burner design
- Furnace (thermal) cycling
- Combustion stoichiometry outside specifications

The original radiant tube material for the firing leg, as specified by Stein Heurtey, was HK-40 (see appendix A). But due to the unacceptable failure rate, the specification was upgraded to Inconel 601, which was believed to reduce spalling rates[43]. The HK-40 material grade was susceptible to spalling degradation, as substantial deposits of chrome oxide particles were found at approximately 0.5m from the burner crown. A further study Lewis et al[55] showed that the changeover to different Inconel grade for firing leg was successful in reducing the effect of spalling, thus extending tube life expectancies and reducing maintenance costs.

The findings from these studies prompted Trostre to trial two new material grades for the firing and second leg of their radiant tubes. These two grades were a spun-cast heat resistant T64 grade (35%Ni, 25%Cr, 1%Nb) and a wrought Inconel grade of I-601 (61%Ni, 23%Cr). After furnace service of approximately 2 years, tubes were examined for evidence of spalling. The T-64 grade showed signs of the onset of spalling while the I-601 grade was in very good condition. In comparison, the HK40 grade used previously would have deposits of approximately 2.5kg on the onset of failure at just over 3 years[55].

With this comparison, the investigation concluded that the T-64 grade should have a service life of approximately 5.5 years, while the I-601 should last in the region of 8

years. Although, the feasibility of using I-601 would have to be calculated as the cost is greater than the spun-cast T-64.

As Lewis[55] reported before the manufacture of the CAPL for Port Talbot, it states that the expensive mistake of taking Stein Atkinson Stordy advice on radiant tube design should not be repeated on future lines i.e. CAPL (Port Talbot) – The situation on the CAPL (Port Talbot) line is that the tube firing rates will be consistently higher than CAPL (Trostre) and correctly specified radiant tubes will be essential. As a result the firing legs for the Port Talbot CAPL were upgraded to 35Ni/25Cr nickel alloy casting.

The claims of incorrect combustion, made by Stein Heurtey, attributing to increased radiant tube failure rates was deemed questionable, as no correlation could be made[43]. Over 60% of the failed radiant tubes that occurred had operated throughout their lives within the acceptable tolerance levels outlined by Stein Heurtey specifications.

The second Continuous Annealing Line (CAL) at Trostre was subjected to a furnace improvement programme in 1995. During a furnace inspection, it was found that 2 tubes had burst and 8 had suffered from cracks. The investigation by Lewis et al[56], states: 'No discernable pattern was evident from the location of these failures and no evidence could be drawn to suggest that failure was attributable to incorrect firing rate or stoichiometry[56']'.

4.2.1.3 Continuous Annealing Line (CAL)

The CAL (Continuous Annealing Line) was installed at Trostre Works, then part of 'The Steel Company of Wales', in 1962. At the time it was the highest speed line in Europe[57]. The design of the line is similar to the newer continuous lines (CAPL) installed at Trostre and Port Talbot, albeit being smaller and slower. The line is divided into three sections; entry, furnace and exit.

The entry section contains two pay off reels, shear, welder and an electrolytic cleaning tank. The purpose of the entry section is to weld subsequent coils together and to remove all contamination from the strip[57]. The two looping towers allow each section to be operated independently.

The furnace consists of five sections:

- Heating chamber
- Holding chamber
- Retard cooling chamber
- High speed jet cooling chamber
- Air blast cooling chamber

The strip is protected from oxidation by a hydrogen-nitrogen atmosphere gas (Approx. 94%N and 6%H) during the first four sections[57].

The heating chamber, now more commonly known as a radiant tube furnace, contains 108 'W' shaped radiant tubes. These are arranged in 9 vertical columns of 12 tubes, divided equally between the operator and drive side to allow equal strip heating. The furnace is divided into 6 zones to allow for flexible temperature control. Each zone has the following amount of tubes:

- Zone 1, 2 and 6: 12 tubes
- Zones 3 to 5: 24 tubes

From a discussion with the annealing engineer at Trostre, it was found that the radiant tube material specification is the same as CAPL, where Inconel 601 or T64 grade material is used for the whole tube construction. When the CAL was run at full load, tube replacements were of the magnitude of 12 – 14 per year. But during the last two years CAL has only been operating on a start stop basis for only 5 days a week. Therefore, the number of tubes replaced has fell to 5 – 7 tubes per year.

In both cases, the highest failure rate occurred in the hotter region on the furnace, which is towards the exit of the furnace. Failure types varied from split tubes (at the end of the firing leg) to tube distortion and collapsing.

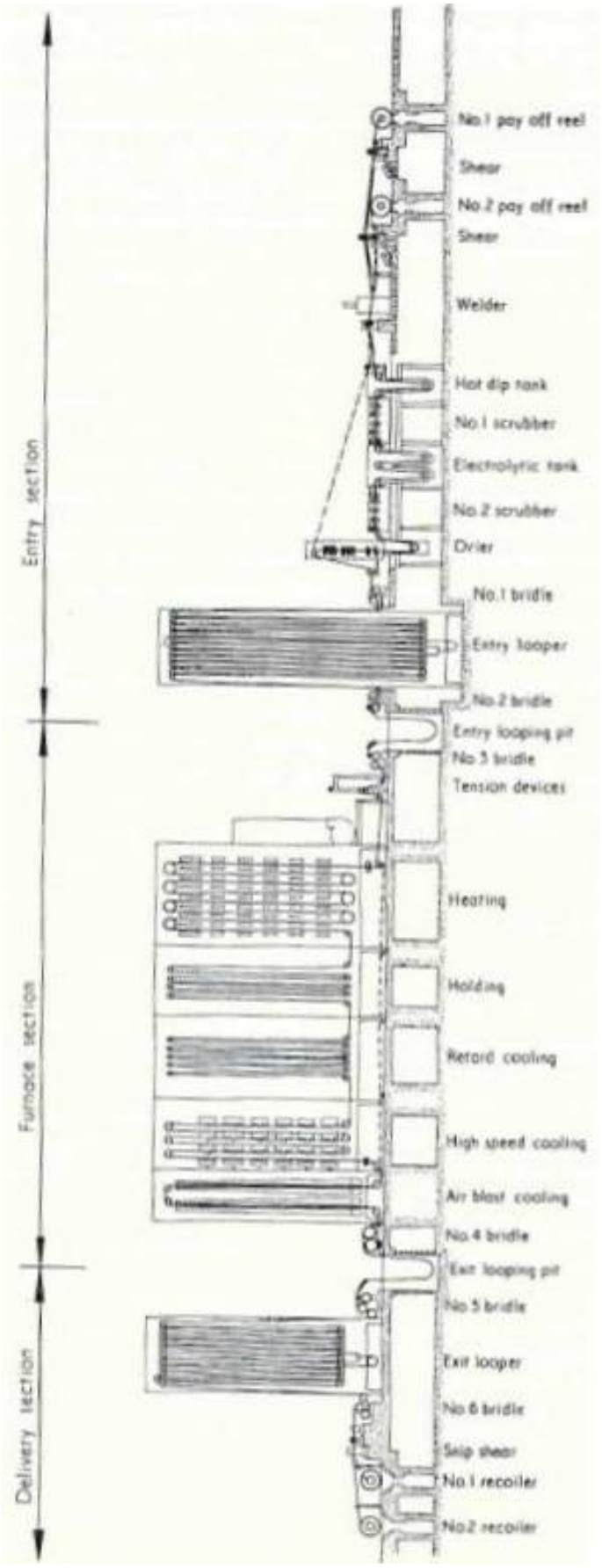

Figure 4-5 - Schematic displaying CAL layout at Tata Packaging, Trostre[57]

4.2.2 Tata Steel, Llanwern – “Zodiac”

Zodiac is a galvanising line situated at Llanwern Steel Works, Newport, which was designed and constructed by Selas in 1990. Its annealing furnace is a direct fired furnace followed by a radiant tube section containing 44 radiant tubes of ‘W’ and ‘U’ shape.

The radiant tubes are manufactured form Inconel 601 grade, which is a wrought grade of heat resistant stainless steel allowing for thinner tubes to be manufactured. For example, a typical ‘W’ shaped tube manufactured from wrought material can be as thin as 3mm, where a cast tube in comparison can be up to 8mm in thickness.

The natural gas burners are situated in the top leg and exits through the lower exhaust leg where a recuperator is situated to preheat the combustion air. The ‘W’ shaped tubes have a support for each return bend in the form of a cylindrical tube. These cylindrical supports fit into larger cylindrical tubes situated in the furnace wall and allow movement in one plane to compensate for thermal expansion. The central bend is supported in similar fashion from the bung manufactured with the radiant tube assembly, Figure 4-6.

Figure 4-6 - A deformed firing leg in location inside furnace

Tube temperatures are reported to achieve between 850 and 950ºC, with primary failures observed in the upper firing leg due to ‘implosion’, which means the tube has collapsed inwards, Figure 4-7. Other failures arise from strip breaks, where the steel strip breaks and hits the radiant tubes causing damage.

Figure 4-7 - A typical failure of Zodiac radiant tube. Deformation of firing leg, which in location, inside furnace, is the uppermost leg

Generally, the tubes are expected to last greater than 5 years, with approximately 5 tubes changed every year. Depending on condition, the tubes can be replaced by a complete new ‘W’ tube or the damaged/failed sections can be cut out and replaced by new items, Figure 4-8.

Figure 4-8 - A refurbished fabricated radiant tube used in the furnace of Zodiac, Llanwern. Note: Green colour on tubes/bends indicate old part of radiant tube

4.2.3 Segal, Liege, Belgium – Galvanising Line

As part of the benchmarking process for this project, a visit was arranged to a Tata galvanising line, Segal, situated in Liege, Belgium, where a radiant tube furnace is in operation as part of a Hot Dip Galvanising (HDG) process line. The aim of the visit was to focus on tube design and modifications, material specification, inspection and operational conditions.

4.2.3.1 Furnace Details

The furnace was manufactured by Drever in 1989 and contained originally 152 'W' shape radiant tubes until year 2000, where a further 35 tubes were installed into the furnace to increase thermal capacity. An improvement strategy was undertaken following the high number of failures experienced, as nearly half of the original 152 tubes required replacement within 5 years of operation[58]. During 1994 and 1999 the following revisions were made respectively:

- 1994
    - Bellows fitted to burner leg
    - Revised material specification
- 1999

- Support design – Rod support between outer bends
- Tube design – 2 Double-P tubes fitted as trial

4.2.3.2 Bellows

During 1994 bellows were fitted to the firing leg flange (top leg), highlighted in Figure 4-9, as part of a Drever recommendation, although no explanation was given as to why they were fitted. It is unclear from Segal's failure database whether bellows actually extend tube life.

Figure 4-9 - Bellows fitted to the firing leg of the Segal radiant tube allowing expansion along the length of the tube

The reliability of the expansion bellows was questioned as they are generally constructed from thinner material and lower grade steels. Segal has not reported any failures in expansion bellows, which have been specified on their radiant tube design since 1994.

4.2.3.3 Material Specification

In 1994 the tube material specification was changed. The firing leg and first return bend were changed from 25Cr/35Ni to a 'super-alloy' grade 25Cr/45Ni/5W/4Co, the second leg changed from 25Cr/20Ni to 25Cr/35Ni and the remainder as per original

specification (25Cr/20Ni). Again, this was a recommendation from Drever as operational temperature in the furnace was higher than designed.

Although no zone/tube temperature data was supplied, discussions with furnace operators highlighted that maximum tube temperatures did rise to approximately 1000ºC (similar to CAPL). Comparisons in creep properties, Figure 4-10, between Segal and CAPL firing leg material identifies that there is no significant benefits in using the higher 'super-alloy' grade at the high operational temperatures[58].

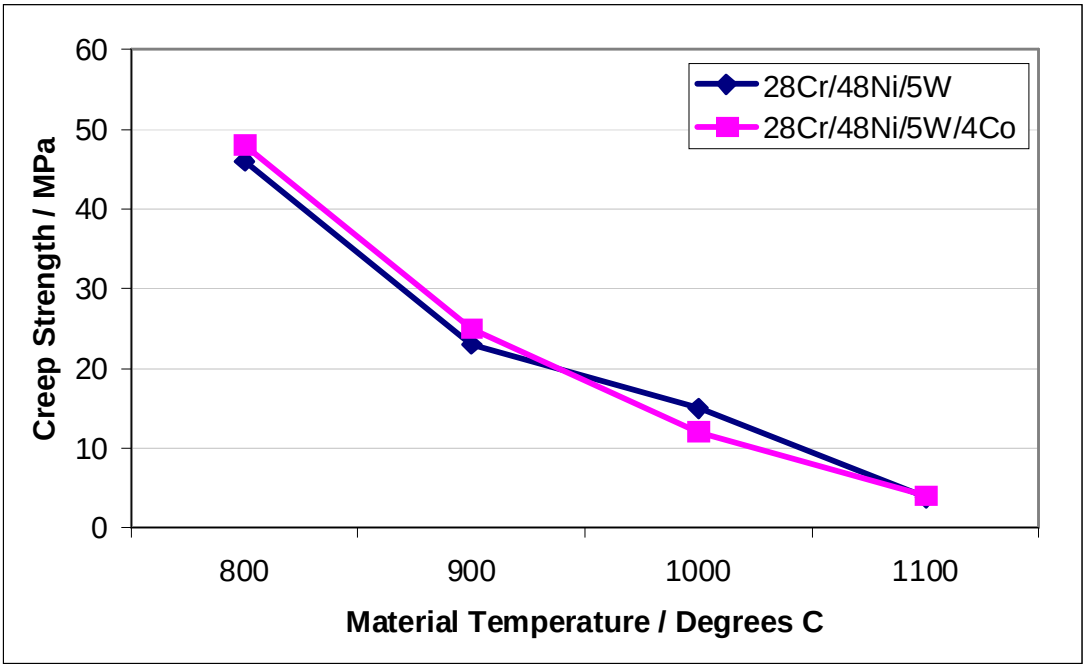

Figure 4-10 - Creep strength comparison of firing leg materials[58]

4.2.3.4 Support Design

Comparisons between the original tube design and the revised design (circa 1999) can be seen in Figure 4-13 and Figure 4-14. The only difference is the firing (top) leg support, which has changed from a saddle support (i.e. the weight of the firing leg supported on the exhaust leg) to a link between the two return bends, highlighted in Figure 4-11. The central bend has been supported from the bung since conception; a feature now adopted by CAPL, which is seen as a benefit as it does not rely on another part of the tube for support.

Figure 4-11 - New support design adopted by Segal, where the top return bend is supported by the lower support via a tubular link/rod

4.2.3.5 Failure Database Analysis – Segal

Similar to Port Talbot, Segal records all tube replacements in a Microsoft Excel failure database. Figure 4-12 displays the number of tubes replaced each year, which clearly shows that modifications mentioned previously were undertaken during periods where a high proportion of tubes were replaced. Taking an overall average, approximately 13 tubes are replaced each year, which based on the original total of 152 within the furnace equates to ~8.5% failure rate per annum.

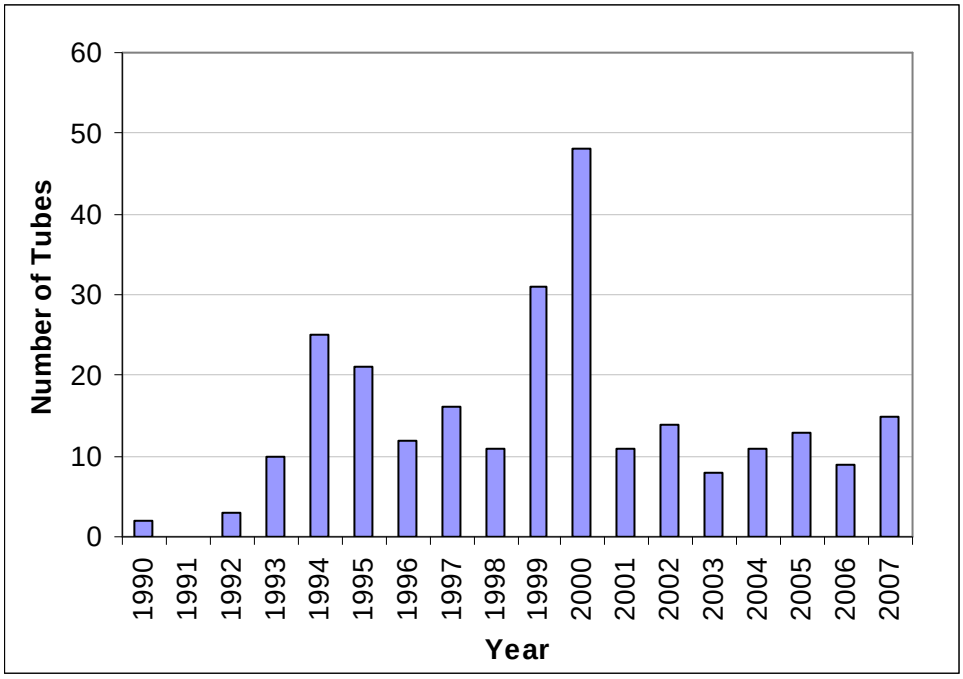

Figure 4-12 - Number of radiant tubes replaced per year - Segal Furnace

Unfortunately, the database does not contain all the information required to determine how all radiant tubes (RT) failed. Rather, the database contains information on the last failure type of each burner position. Clearly, the most predominant failure type is bending of the top 2 tubes, with other failure types being deformation/collapse of the firing leg and cracking.

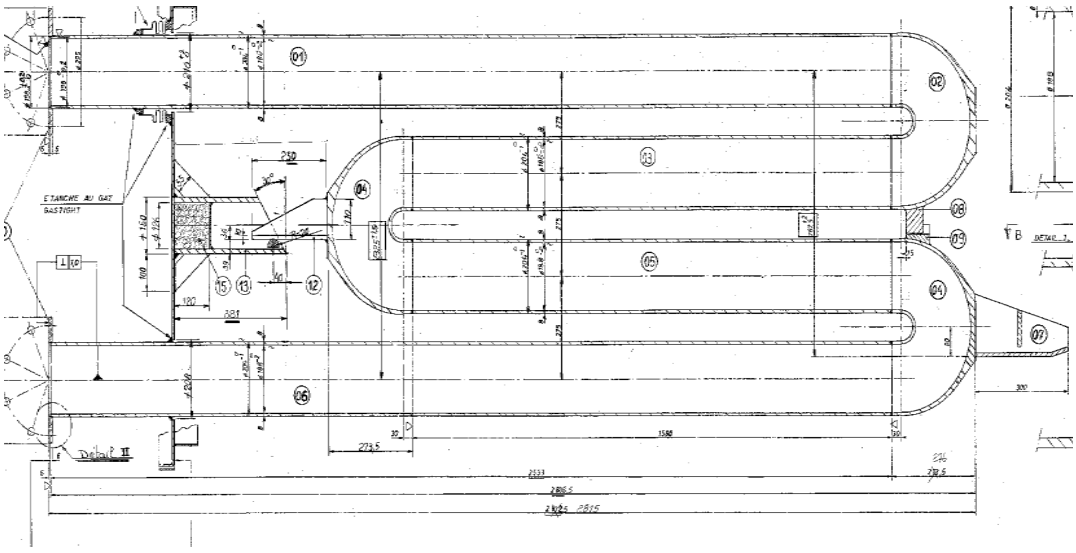

Figure 4-13 - Original Radiant tube design employed by the Drever furnace at Segal Works, Liege, Belgium

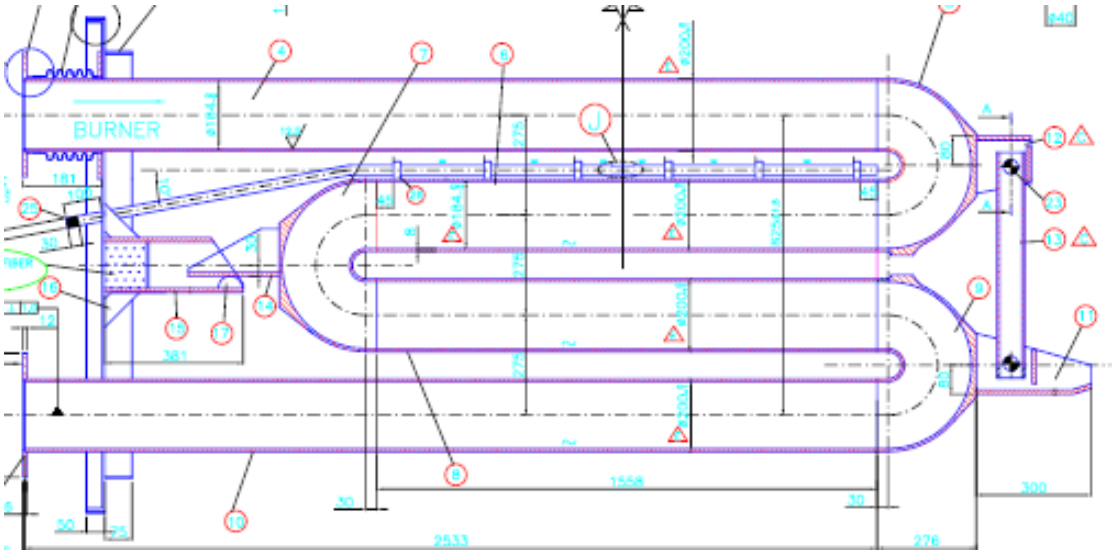

Figure 4-14 - Revised radiant tube design currently used by Segal. Note the expansion bellows on burner flange and elongated rod which provides support for the upper bend

4.3 Sumitomo Metals Ltd., Kashima Works, Japan

During a visit to Sumitomo Metals in Kashima City, Japan, in 2010, an analysis study of the Kashima Works was undertaken. Kashima Works is Sumitomo's main integrated steel works, based on the coastal region of Kashima in the Ibaraki Prefecture, approximately 40 miles East of Tokyo. The works was founded in 1968 and is capable of producing 8M tones of steel into coil, plate or sheet (strip) form. Approximately 60% of the output is rolled into coil form, primarily for the automotive market, of which 50% is sold to automotive manufacturers in Japan, with the remaining amount being sold to markets in China and Korea.

Kashima Works is an integrated steel works comprising the following (Figure 4-15):

- Coke Ovens
- Sinter Plant
- Blast furnaces (Currently only 2 operating)
- Steel Making Plants
- Continuous Casting Plant
- Pipe Mills
- Plate Mill
- Hot Strip Mill

- Cold Strip Mill
- Pickling Lines
- Continuous Annealing Lines
- Galvanising Lines

Figure 4-15 - Plant Layout of Kashima Steel Works

4.3.1 Continuous Annealing Line

The Continuous Annealing Line (CAL), Figure 4-16, was constructed in May 1992 and is capable of processing strip widths of between 600 - 1850mm wide and thickness of between 0.4 - 2 mm. It receives cold reduced strip steel and provides a heat treatment to restore mechanical properties that were lost during the cold reduction process.

The process line can be split into three sections:

- **Entry**
    - The coils are unwound and joined together to form a continuous strip

- Strip is subjected to a pre-cleaning process where it is scrubbed in a Caustic-Soda solution

- **Furnace**
  - This is where the strip undergoes a predetermined heating cycle to restore mechanical properties
  - The strip is preheated by the combustion gases from the Direct Fired Furnace (DFF) and then subjected to rapid heating via open flame burners directed towards the strip in the DFF zone
  - Final annealing temperature is obtained in the Radiant Tube Furnace (RTF) where the strip is heated to temperatures of 900°C
  - Soaking section contains radiant tube heaters which maintain high strip temperature over a period of time to promote grain growth
  - Cooling is performed in two stages; initially slow and then cooling rate is increased in the accelerated cooling section
  - Overaging and final cooling completes the furnace section

- **Exit**
  - In the exit section the strip is subjected to a skin pass reduction in the temper mill and then inspected for defects and dimension quality

Coil accumulators situated between the entry-furnace section and furnace-exit section allow a constant strip speed to travel through the furnace section; to ensure homogenous heating throughout the coil length and to facilitate the joining and separating of coils at entry and exit section respectively. Thus, allowing the process line to be continuous.

Figure 4-16 - Continuous Annealing Line No.2 at Kashima Works

4.3.2 No.2 Continuous Galvanising Line

The No.2 Continuous Galvanising Line (CGL) was commissioned in January 1992 and in respect is very similar to the CAL process mentioned above. The main differences being the galvanising lines provide a coating at the end of the furnace section for corrosion protection, which is now widely used in the automotive sector. The differences between a CAL and a CGL are the following:

- Zinc-Pot
    - The zinc-pot is situated directly after the furnace, where the strip is submerged into a hot bath/pot containing primarily zinc to provide a protective coating to the base metal
- Galv-annealing Furnace
    - Depending on the grade and coating required, a moveable open burner furnace can be positioned “on-line” or “off-line” within minutes. The inclusion of the furnace heats the strip sufficiently (approx 550°C) to alloy the zinc coating with the iron in the steel substrate. Thus, providing an excellent surface for paint adherence and good welding performance

- Air-Cooling
    - To ensure the coating has solidified before further treatment, an air-cooling section cools the strip temperature quickly

4.3.3 No.3 Continuous Galvanising Line

Number 3 CGL was manufactured in 2006, adjacent to No. 2 CGL and No. 2 CAL. The design and layout are identical to No. 2 CGL, albeit the only differences is that No.3 is a narrower manufacturing line (i.e. only capable of manufacturing narrower widths of coils) and capable of processing lighter gauges of strip, also the furnace section is a full radiant tube section and does not include a direct fired furnace. The reason for this was to reduce the cost of construction. Now, they have two facilities capable of producing the same grades of steel with the balance of throughput based on the coil dimensions required.

A comparison of the capabilities of the CGL process lines are outlined in Table 4-1:

Table 4-1 - Process Line Capability

Process Line	Strip Thickness (mm)	Strip Width (mm)	Max Line Speed (mpm)
No. 2 CGL	0.35 – 2.3	600 - 1830	180
No. 3 CGL	0.4 – 1.6	600 - 1650	160

4.3.4 Radiant Tube Discussions at Kashima Works

The main purpose of the visit was to benchmark the design, operation and performance of the radiant tube furnaces based at Kashima Works against the continuous annealing line at Tata Steel, Port Talbot. The visit would allow the assessment and comparison between the two sites/production lines and information sharing of best technologies/best practices.

Having numerous continuous annealing and galvanising lines situated at Kashima Works, radiant tubes furnaces are utilised greatly to increase the temperature of the strip steel. Some are reliant entirely on radiant tubes, while others have a Direct Fired

Furnace (DFF) before the tube section. The table below outlines the process lines and the number of tubes installed.

Table 4-2 - Description of Radiant Tube Installed

Process Line	1 CGL	2CGL	3CGL	2CAL
No. of Radiant Tubes	88	75	145	195
Type	U	W	W	W
DFF Section	No	Yes	No	Yes

All W shaped radiant tubes are based on the design shown in Figure 4-17. They are manufactured from a heat resistant cast stainless steel grade containing 35% nickel and 25% chromium and have supports on each return bend. The burner is situated in the top leg and an external recuperator pre-heats the combustion air prior to combustion.

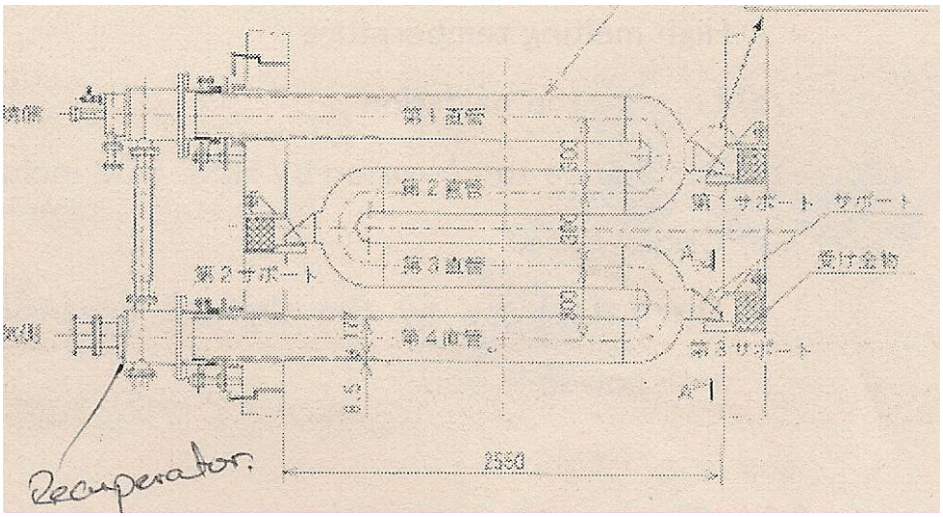

Figure 4-17 - Radiant tube design used at Kashima Works

Tube life in all 3 lines incorporating W shaped tubes is comparative and can be between 3 - 7 years. The tube furnaces at Kashima Works are divided into a heating section and soaking section. As the name suggests, the heating section raises the strip temperature up to the required annealing temperature (between 750 - 850°C) while

the soaking section maintains the high strip temperature ensuring sufficient residence time. As a result there is less demand on the tubes located in the soaking section. Thus, resulting in longer tube lives of up to 7 years. In contrast, tube lives in the hardest fired heating zones can result in tube lives of only 3 years.
The predominant failure is severe deformation due to creep. Process lines 2 CGL and 2 CAL are the eldest lines and suffer from distortion in the firing leg and second leg, while in the newer 3 CGL the tubes deform in the second and third legs. Tube cracking does occur, but generally in small numbers.

Cracks generally occur due to one of possible three scenarios. Firstly, cracks have occurred in welded joints between the first bend and firing/second leg. This is generally seen as a result of severe distortion, creating large tension across the joint, Figure 4-18. Secondly, the firing leg can fail due to the build of carbonaceous deposits inside the firing leg, which acts as a thermal mass creating a 'hotspot' and degrades the material faster resulting in a crack. Finally, iron oxide particulate accumulate inside the firing leg, again acting as a thermal mass, resulting in a cracking failure further down the length of the tube.

Figure 4-18 - Cracked radiant tube where weld are has failed

The accumulation of particulate and carbonaceous deposits inside the firing leg is a result of using Coke Oven Gas (COG) as a fuel. COG is notoriously known to be a dirty fuel, which has its disadvantages in use, as mentioned above. But, as Sumitomo is an integrated steel works with 2 fully operational coke oven plants, COG is an abundant by-product and is a great advantage in reducing the cost of manufacturing strip steel.

Figure 4-19 depicts the amount of deformation experienced in failed tubes at Kashima Works. Engineers counteract this deformation, due to creep, by rotating the tubes once a year once signs of deformation begin. The tubes can be rotated up to four times in total until the deformation is considered too severe.

Figure 4-19 - Failed radiant tubes showing signs of deformation in the firing and second leg

As the radiant tube is manufactured entirely from the same heat resistant grade, the creep strengths are the same throughout. Therefore, there is no difference in material properties and as a result the exhaust leg can deal with the high temperatures experienced in the firing leg after rotation.

Kashima works have developed an innovative solution to inspect the condition of their radiant tubes. They have manufactured a suspended gantry; Figure 4-20, which includes two sets of lights and cameras that can be operated independently and remotely to film live pictures from inside the furnace to monitors on the shop floor. This is not only a safer procedure, but is also far quicker and efficient.

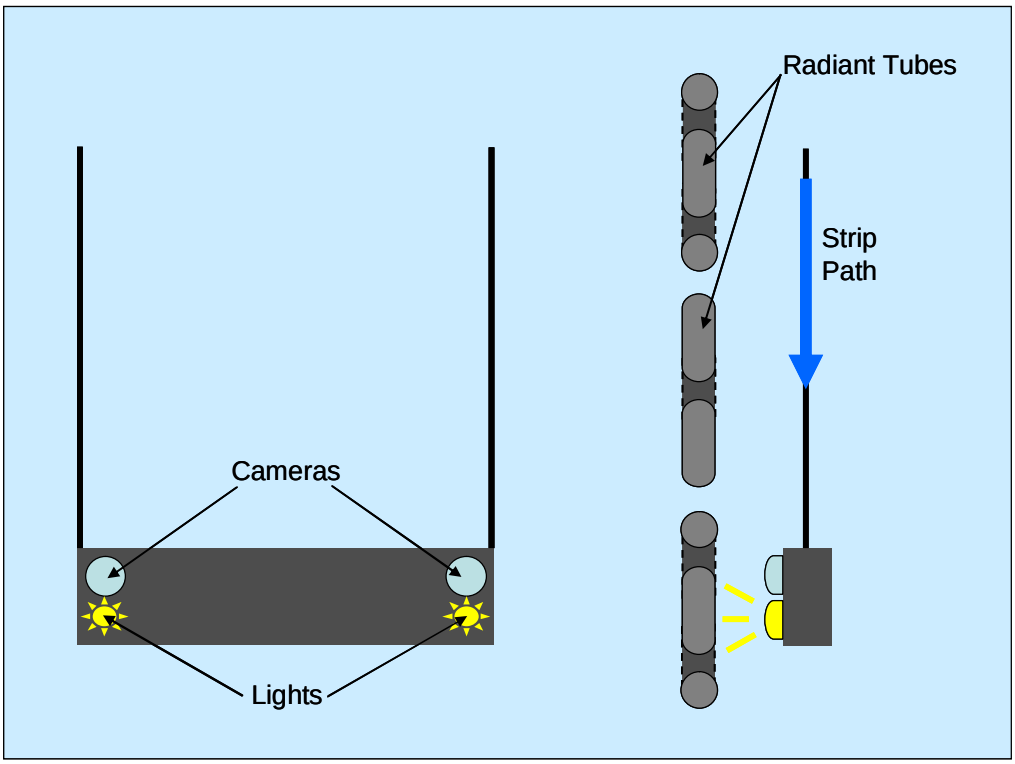

Figure 4-20 - Schematic showing the operation of the inspection camera

The gantry is suspended, down from the top of the furnace, along the direction of the strip travel. The removal of the furnace covers (both top and bottom) is required for inspection. But, once this is completed, each vertical column of tubes is then inspected in turn, which is easily facilitated through the movement of the crane.

4.3.5 Radiant Tube Improvements

Engineers at Kashima Works have developed the design and material specification of their radiant tubes to prolong life and improve efficiency. The following steps have been taken:

- **Change in material specification**

The material specification has changed from HK40 (25%Cr – 20%Ni) to KHR35H (25%Cr – 35%Ni). This was done to increase the melting temperature of the steel, increase the oxidation resistance and increase the creep strength of the material.

- **Change in support design**

The previous support design was believed to increase the bending rate of the tube once a certain level of deformation had been achieved. The new design (Figure 4-21) is believed to lower the stress in the tube and as a result the rate of deformation is reduced resulting in longer tube lives.

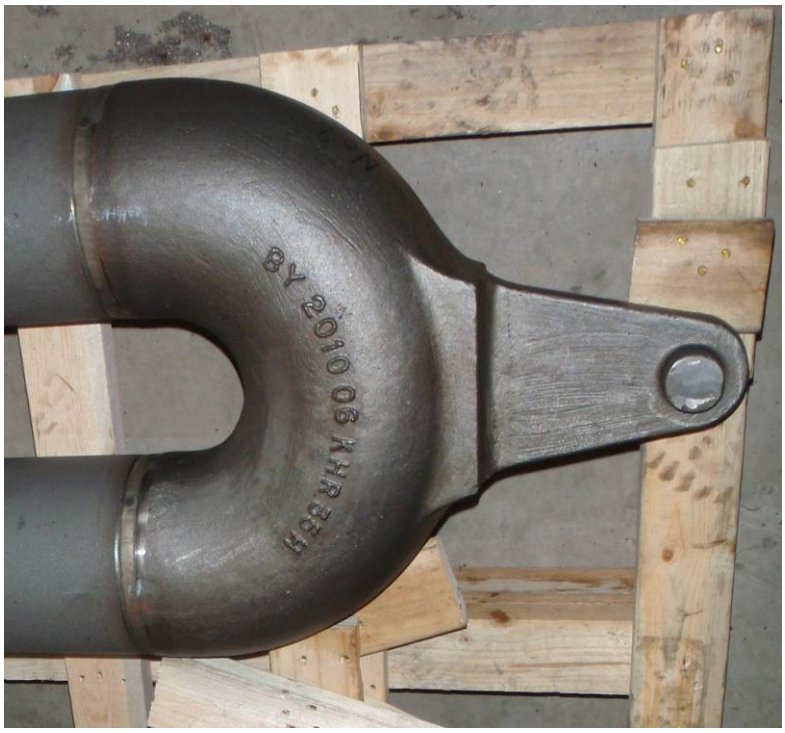

Figure 4-21 - New bend support design aimed at reducing the bending force in the tube

- **Internal boring**

The internal diameter/bore of the tubes is machined to provide a smooth surface. This has shown to reduce the rate of oxidation of the tube and thus minimising the deterioration of material.

- **Ceramic inserts**

Sumitomo have undertaken off-line experimental analysis of using ceramic inserts in their radiant tubes. The inserts are installed in the exhaust leg and increase the rate of heat transfer from this leg, therefore increasing the combustion efficiency. The off-line trials have shown that exhaust tube temperatures have increased 10-15°C. Kashima are now conducting on-line trials.

4.4 Summary of Findings

As the CAPL at Trostre is an older line, lessons can be learned from the problems and results, which have been experienced. Similar problems were seen, with premature failures on radiant tubes and subsequently have changed the material grade. Improvements in tube lives are apparent, identifiable by the reduction of replaced tubes during maintenance, Figure 4-3. Therefore, questions need to be answered on the performance of the new material specification:

- Has the change in material grade resulted in longer tube lives?
- Has there been a dormant period before year 2000 where there were no failures as predicted in a study by Lewis[43]?
- Has the furnace parameters changed resulting in longer tube lives?

It is also interesting to note how other authors have approached the process of failure analysis. Similar techniques can be utilised during the analysis of failed tubes at CAPL, Port Talbot.

Many comparisons can be drawn against Segal, as there are many similarities in operational temperatures, material specification and firing capacities. However, it is unclear from the failure database as to whether the Segal tubes would be superior to Port Talbot in terms of operational life.

The material specification used is near identical to that used in new tubes for CAPL, although the slightly higher cost of Segal's inclusion of cobalt for the firing leg seems unnecessary when comparing material creep strength. In terms of design, CAPL now

use the central bend support that facilitates the bung, which is seen as a benefit, while the inter-tube support employed by Segal cannot be replicated due to the support being on the lower leg rather than the top (Note: Segal fire through top leg).

What can be replicated is the use of the expansion bellows between the flange and the bung. The bellows allow a limited amount of movement to reduce thermally induced stresses along the length of the tube. While Segal adopts the bellows on the top firing leg, Port Talbot CAPL could fit a similar system to the lower leg, or possibly to both flanges. The advantages, if any, of using one or two bellows needs to be determined.

While the majority of annealing furnaces utilise cast radiant tubes, wrought stainless steel is used in a small number of furnaces. The wrought material can operate at similar temperatures as their cast counterparts, but are far lighter in weight, with wall thicknesses of approximately 3mm in comparison to 8 or 9mm wall thicknesses in cast tubes. This has a significant effect on the thermal mass of the furnace and reduces the effect of creep failure from reduced stresses due to weight reduction.

Radiant tubes manufactured from wrought materials are much greater in cost to purchase due to the higher material costs and greater fabrication requirements. What needs to be determined is if the greater purchase costs are justified and offset by the tube lives.

The visit to Sumitomo Metals in Japan provided an insight into another company's perspective into radiant tube lives. What's interesting to note is that Sumitomo were working along similar routes and ideology in trying to improve tube life. While Sumitomo had different supports for their tubes, tube life was comparable, with lives ranging from 3 years in the hardest fired zones to 7 years in the cooler regions of the furnace.

The identical support on each return bend, and same material grade throughout, allows Sumitomo the opportunity to rotate their tubes during shutdown periods to counteract the effect of creep once deformation is identified.

Other measures taken to prolong tube life are machining the inner bore of the radiant tubes and increasing the tube material grade. These measures have been shown to reduce creep deformation through choosing a higher creep strength material and reducing the effect of surface oxidation by having a higher oxidation resistance in the material and having a smooth surface on the inside of the tube.

The benchmarking process identified that radiant tube failure is an issue for all steel manufacturers. Tube longevity is a balance between furnace operation, tube design and material specification.

Most furnaces employ cast radiant tubes and provide a support for each return bend via the furnace walls. At Sumitomo, the design of the tube supports allowed the rotation of the tube structure to counteract deformation from creep.

HK40 (25%Cr/20%Ni) and HP (25%Cr/35%Ni) are the most popular choices of material grade for cast tubes, but Segal were using a higher specification containing 28%Chromium, 48%Nickel, 5%Tungsten and 4%Cobalt for the hottest radiant tube regions, while also adopting an expansion bellows on the firing leg flange. Interestingly, Segal on average replaces the least amount of radiant tubes per year.

Sumitomo use HP grade throughout the whole tube, because they rotate their tubes. But they also specify that all tubes must have a machined inner bore, which produces a smooth surface on the inside and removes all slag that is formed on the inner surface during the process of centrifugal casting. They argue that this helps prolong tube life through reducing the rate of oxidation, which results in tube failure.

These are all interesting points, which need to be investigated further to determine the effect and result of each one on tube longevity. In summary, Table 4-3 provides a comparison of the pertinent points of the parameters of each furnace.

The benchmarking process identified that radiant tube failure is an issue for all steel manufacturers. Tube longevity is a balance between furnace operation, tube design and material specification.

Table 4-3 - A summary of the various radiant tube parameters discussed:

	Tata Steel					Sumitomo Metals		
	CAPL - Port Talbot	**Zodiac - Llanwern**	**Segal - Liege**	**CAL - Trostre**	**CAPL - Trostre**	**2CAL**	**2CGL**	**3CGL**
Number of Tubes	338	44	182	108	144	195	75	145
Design	W Tubes	W and U Tubes	W Tubes	W Tubes	W Tubes	W Tubes	W Tubes	W Tubes
Material Specification	Exhaust Leg: 25Cr/20Ni Firing Leg: 35Ni/25Cr & 37Ni/18Cr	Inconol 601	Firing leg : 25Cr 45Ni 5 W 3Co Second leg : 25Cr 35Ni Exhaust leg : 25Cr 20Ni	Inconel I601 or T64 (35Ni/25Cr) for whole tube	Inconel I601 or T64 (35Ni/25Cr) for firing leg. HK40 for exhaust leg	35Ni/25Cr for all tubes	35Ni/25Cr for all tubes	35Ni/25Cr for all tubes
Cast or Fabricated?	Cast	Fabricated	Cast	Cast	Cast	Cast	Cast	Cast
Reasons for Change	Catastrophic failure of locating hook, strip breaks, collapse, inferior bends/welds	Implosion, strip breaks	Bending, Deformation, First tube breakage	Split tubes, distortion and cracking	Cracks in firing leg or at weld region between firing leg and first return bend	Tube deformation. Cracking in firing leg and weld region of first return bend	Tube deformation. Cracking in firing leg and weld region of first return bend	Tube deformation. Cracking in firing leg and weld region of first return bend
Frequency of Change	35/year	Change by inspection 5 tubes per year	Change by inspection 13 tubes per year	12 to 14 tubes per year	14 to 22 tubes per year	20 to 22 tubes per year	8 to 10 tubes per year	15 tubes per year
Operating Position	Vertical Furnace. Burner on bottom leg	Vertical Furnace. Burner on top leg	Vertical Furnace. Burner on Top Leg	Vertical furnace. Burner on top leg	Vertical furnace. Burner on top leg	Vertical furnace. Burner on top leg	Vertical furnace. Burner on top leg	Vertical furnace. Burner on top leg
Tube Temperature	750 to 1000°C	850-950°C	Max 950°C	Max 900°C	Max 950°C	Max 950°C	Max 950°C	Max 950°C
Life Expectancy	Dependant on zone, ~4yrs in hotter zones	5 years +	12 years 5 years for some positions	8 years	5.5 to 8 years	3 to 7 years	3 to 7 years	3 to 7 years
Type of Recuperate	Cast recuperator in exhaust leg to heat up incoming combustion air	Recuperator on exhaust	Stage 1 : Cast recuperator for heating the incoming air Stage 2 : Gas to Gas heat exchanger for heating the preheating section Stage 3 : Water to gas exchanger	Cast recuperator in exhaust leg to heat up incoming combustion air	Cast recuperator in exhaust leg to heat up incoming combustion air	Cast recuperator in exhaust leg to heat up incoming combustion air	Cast recuperator in exhaust leg to heat up incoming combustion air	Cast recuperator in exhaust leg to heat up incoming combustion air
Type of Fuel	Natural Gas	Natural Gas	Natural Gas	Natural Gas	Natural Gas	Coke Oven Gas	Coke Oven Gas	Coke Oven Gas

5 Radiant Tube Temperature Analysis

5.1 Introduction

This chapter outlines the use of thermocouples to analyse the temperature profile of a radiant tube, enabling a further understanding of in-service exposure and subsequent analysis of temperature data.

High temperature and especially over-temperature operation (or over-firing) have been reported to have a detrimental effect on radiant tube life[4,6,14]. Temperature affects the creep strength; material expansion and subsequent stresses generated in the tube legs.

In order to fully appreciate the behaviour of a radiant tube under operating conditions within the furnace, measurements are required of furnace parameters, especially temperature. As well as being useful information to determine the correct material specification for subsequent replacements, the data obtained from a multi thermocouple tube installed can also be used as parameters for future finite element analysis modelling. The purpose of such modelling would be to fast track design suggestions and to gain a better understanding of its stress behaviour under varying furnace loading.

5.1.1 Multi Thermocouple Radiant Tube

Temperature monitoring within the furnace was very limited with only 24 radiant tubes being monitored out of a total of 338. Each zone has a type ‘K’ thermocouple attached to the first return bend of 3 tubes, at levels 4, 5 and 6 of the furnace drive side respectively.

Due to the limited temperature monitoring and no detailed knowledge of the temperature distribution across the length of the radiant tube, a multi-thermocouple tube, Figure 5-1, was designed by the author from the concept of using thermocouples for over-temperature safety monitoring in each zone.

A radiant tube was modified to allow the fitment of extra thermocouples and installed into the furnace during a major maintenance in January 2008. The tube was installed into burner position 5 O.S. 7.1, (5 O.S. 7.1 denotes landing 5, Operator Side, Zone 7, Tube 1) which was decided as an ideal location due to its central position in Zone 7, one of the highest failing zones of the furnace.

Figure 5-1 – Image displaying the radiant tube fitted with 20 thermocouples installed into zone 7 of the furnace for data acquisition

The radiant tube was supplied by Thermocast with a 'hook and eye' outer tube support and the central bend being supported from the bung. Material specification had been increased on the firing leg and second leg to 48Ni/28Cr/5W, while the exhaust leg remained at HK40 (25Cr/20Ni).

Twenty thermocouple clamps were welded to the tube outer surface and attached with type 'K' thermocouples. CAPL use this grade of thermocouple throughout the furnace for safety over-temperature monitoring and have an operating range up to 1350ºC.

The thermocouples were calibrated according to the zone safety thermocouples and were positioned in the following manner:

- Sixteen thermocouples (T/C 1 to 16) were attached along the length of the tube at 50cm spacing to obtain a measurement for the temperature profile.

- Thermocouples 17 and 18 (T/C 17 and 18) were positioned on the side and bottom of the firing leg respectively (same distance from burner as T/C 3), to identify any changes in temperature across the circumference of the tube.
- T/C 19 was positioned on the end of the firing leg (on the return bend) to measure if flame length has any effect on the return bend, i.e. generating a 'hot spot'.
- T/C 20 was located in the standard thermocouple position as used for all zone safety thermocouples. The reading obtained from this thermocouple can be compared against the other safety thermocouples within the zone. The thermocouple positions are highlighted in Figure 5-2.

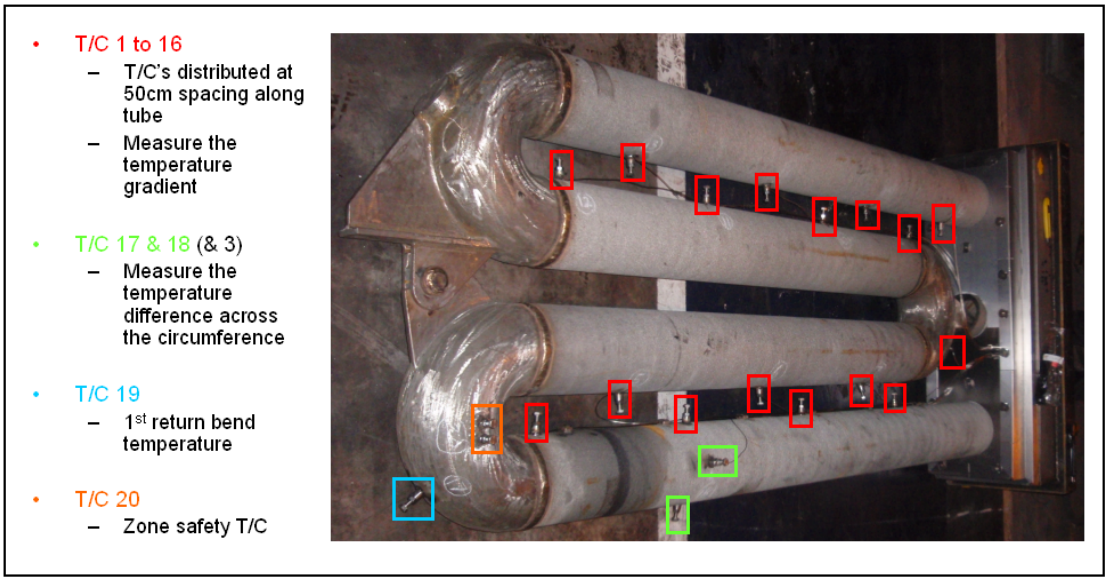

Figure 5-2 - Image displaying the location and purpose of each thermocouple

5.1.2 Data Acquisition

Temperature readings from the thermocouples were fed into a main process control computer and were continuously logged. The data obtained from the multi thermocouple tube was inputted into two visual illustrations. The first was a schematic of the tube with the temperatures of all 20 thermocouples displaying in their relevant positions. The second was a continuous log of all 20 temperature readings (sampling rate of 5sec) displayed in a graphical format. In this form the data

for temperature was able to be compared with other information obtained from the process such as strip width, strip gauge, line speed, etc.

5.1.3 Data Presentation

The temperature data obtained from the multi thermocouple tube was displayed in two ways. Figure 5-3 displays a schematic of the tube with the location, thermocouple number and live temperature reading from each thermocouple. Other useful data includes zone power demand, gas and combustion airflow rates, and the temperature readings from the other zone safety thermocouples. All data collated was logged for future analysis.

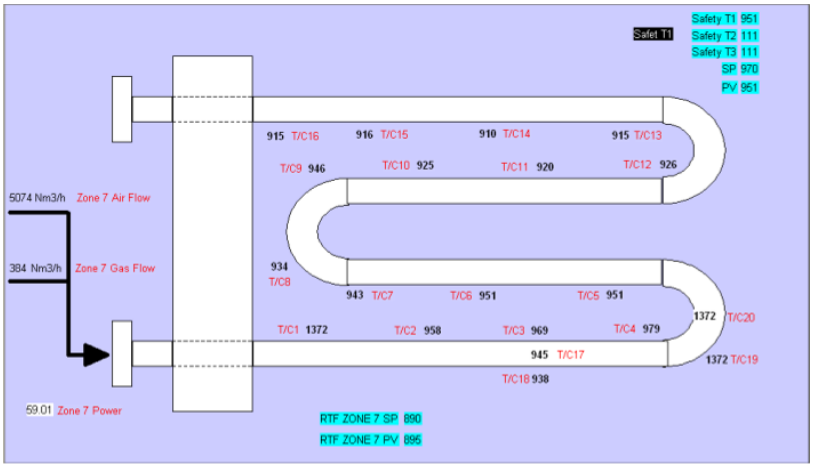

Figure 5-3 – Pi ProcessBook image displaying radiant tube schematic and live thermocouple readings

Figure 5-4 displays a continuous log of the temperature readings taken from each thermocouple. This information is stored and can be manipulated using Microsoft Excel. The temperature readings can also be compared against other process line parameters using this software.

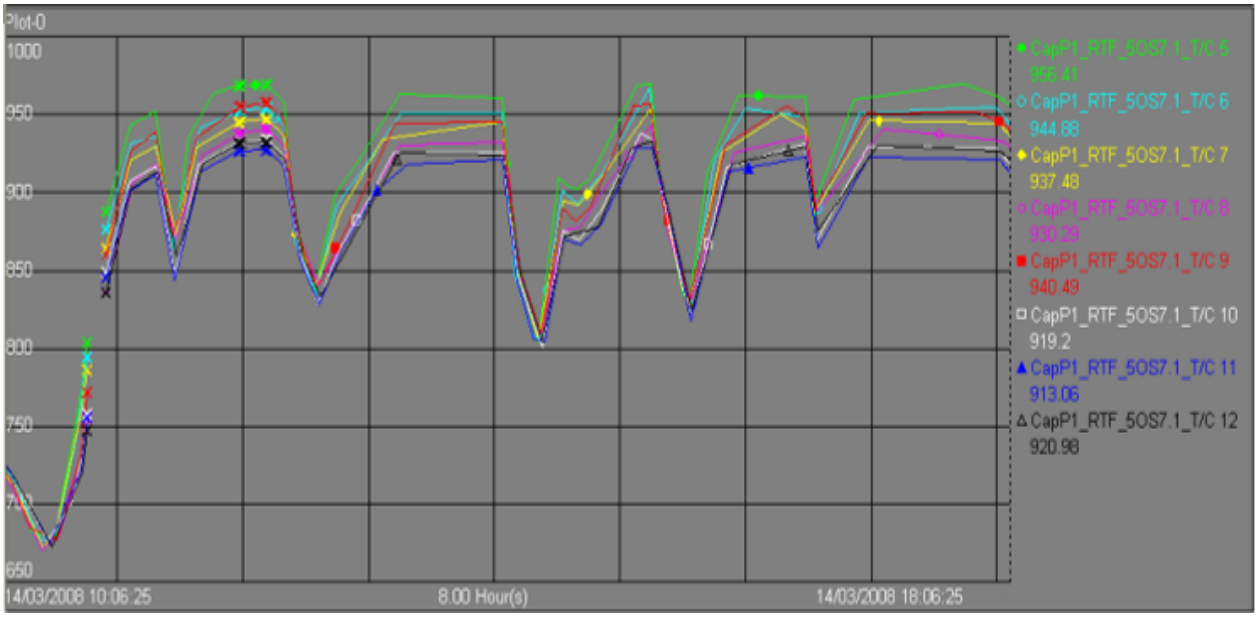

Figure 5-4 – Pi ProcessBook image displaying continuous log of thermocouple readings

5.2 Areas of Investigation

The installation of the multi thermocouple tube was executed to highlight the following:

- Maximum Temperature – The maximum tube temperature was required to determine if the furnace was operating at or near to maximum material limits.
- Temperature gradient – Thermocouples numbered 1 to 16 recorded the temperature gradient along the length of the tube. In doing so maximum, minimum and average temperature readings could be determined and compared against manufacturer recommendations. This data also formed boundary conditions for future computational modelling.
- Zone temperature comparison – Data from thermocouple number 20 can be used to compare temperature readings from other safety thermocouples within the same zone.
- Process analysis – The continuous monitoring of data can be used in the future to analyse how the process line is operated and its effect on tube temperature under different scenarios. For example, steady state operation, furnace heating, cooling/fast cool, processing of heavy gauge/narrow strip.

5.3 Temperature Analysis and Results

5.3.1 Introduction

The information from the process-logging computer was exported and manipulated in Microsoft Excel Spreadsheet. For ease of use and to reduce the volume of data, the information was sampled at every hour, on the hour from 24th Jan 08:00hrs to 30th Nov 23:00hrs. Where a more detailed analysis was required, the information was sampled at 15-minute intervals.

Thermocouple number 1 provided inconsistent readings due to electrical faults. As a result, data from this thermocouple has not been included in the final analysis. Also, from regular scrutiny, it was found that thermocouple 6 provided irregular readings at various time periods. It was found that a short circuit was temporarily occurring, resulting in spurious temperature readings (usually 1372ºC – indicating maximum voltage). Filters were implemented in Excel to minimise this affect on the overall analysis, but some anomalies remain.

5.3.2 Maximum Temperatures

The maximum temperature of the radiant tube and its location along the length of the tube was determined easily by manipulating the data for each thermocouple. Figure 5-5 shows the maximum thermocouple reading for each month. The maximum temperature recorded was 1022ºC at thermocouple 4 during the month of February.

Neglecting T/C 1 and T/C 6, the figure clearly shows that the maximum temperature profile is consistent throughout the year and that the maximum temperature predominantly occurs at T/C 4 (near end of firing leg). This indicates that maximum temperatures are experienced under normal operating conditions and not a feature of bad practice or problems encountered within the furnace.

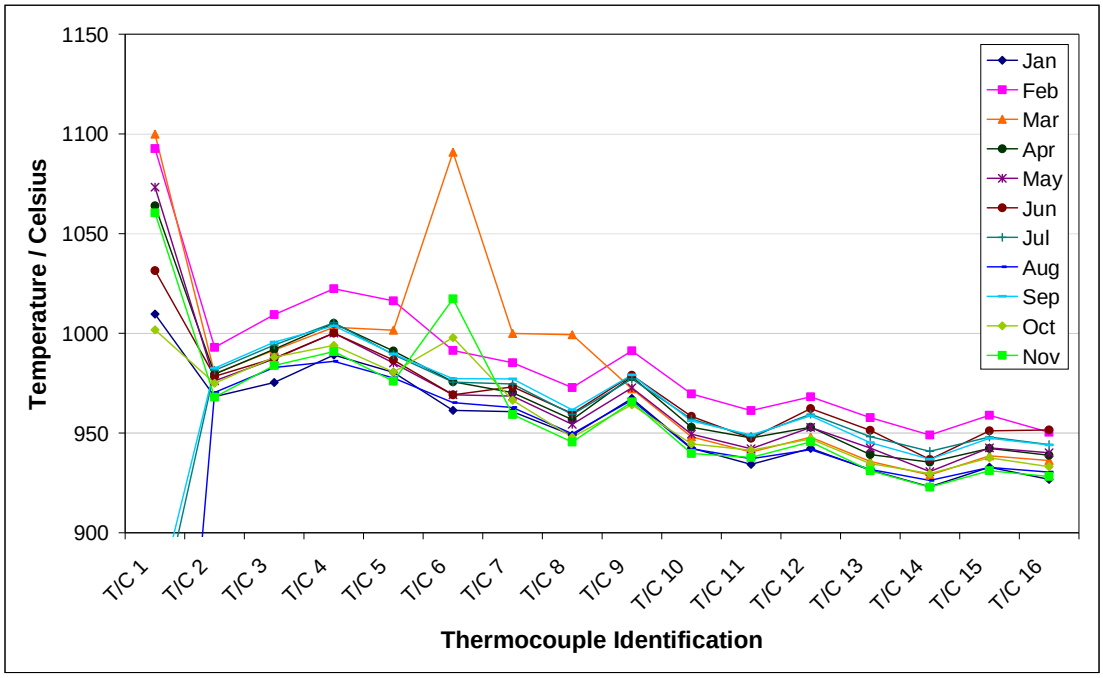

Figure 5-5 – Figure displaying the maximum thermocouple temperatures recorded for each month

5.3.3 Average Temperature Profile

Figure 5-6 displays the average temperature profile of the tube for each month. The values were calculated from the sampled data, whether the line was operational or down for maintenance. The only exception to the rule was that corrupt signals from electrical faults were not taken into consideration. See appendix B for average calculation.

The shapes of the temperature profiles are again consistent for each month, with the exception of thermocouple 1 (and on occasion 6) due to electrical faults. The difference in temperature for each individual thermocouple is approximately 400ºC. This result is greatly affected by the low average readings taken in March, October and November respectively and is a consequence of increased downtime during these months. This indicates that furnace operation is not constant and the radiant tubes are subject to variations in operating temperature, which will affect the rate of deformation and subsequent tube life.

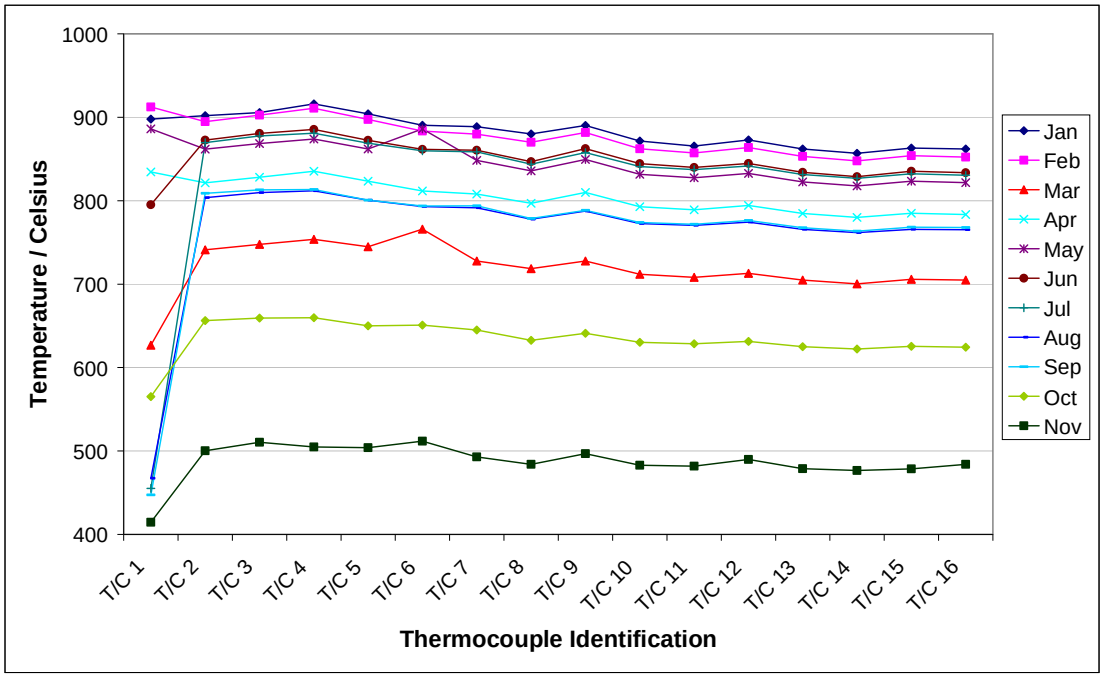

Figure 5-6 – Figure displaying the average thermocouple temperature for each month

5.3.4 Weekly Analysis

As downtime had a great influence on the average results, it was decided to compare a continuous operational week from each month, which would hopefully show a better representation of the furnace operation. Shown in Figure 5-7, is the data for an operational week in June compared against the whole month's data, which contains downtime. While the shape of the profile is very similar, the temperatures have been increased by approximately 70ºC across the length of the tube.

In summary, by analysing a week (without downtime) provides a better working profile for the tube, but the difference in temperatures between month and week are dependent on the amount of downtime experienced during the month in question.

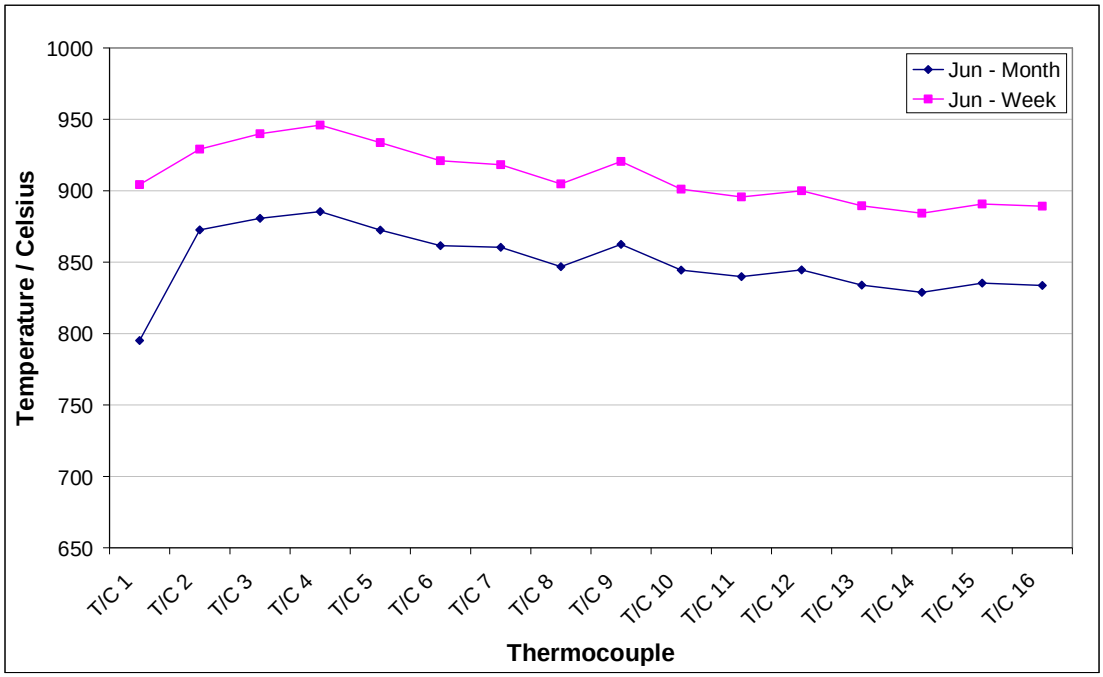

Figure 5-7 - Average thermocouple temperature for June (Month and Week)

Figure 5-8 shows that the average temperatures for a continuous week are consistently high. Excluding the month of November, the firing leg (Thermocouples 1 to 4) predominantly operates at temperatures greater than 900ºC, nearer 940ºC towards the end of the firing leg.

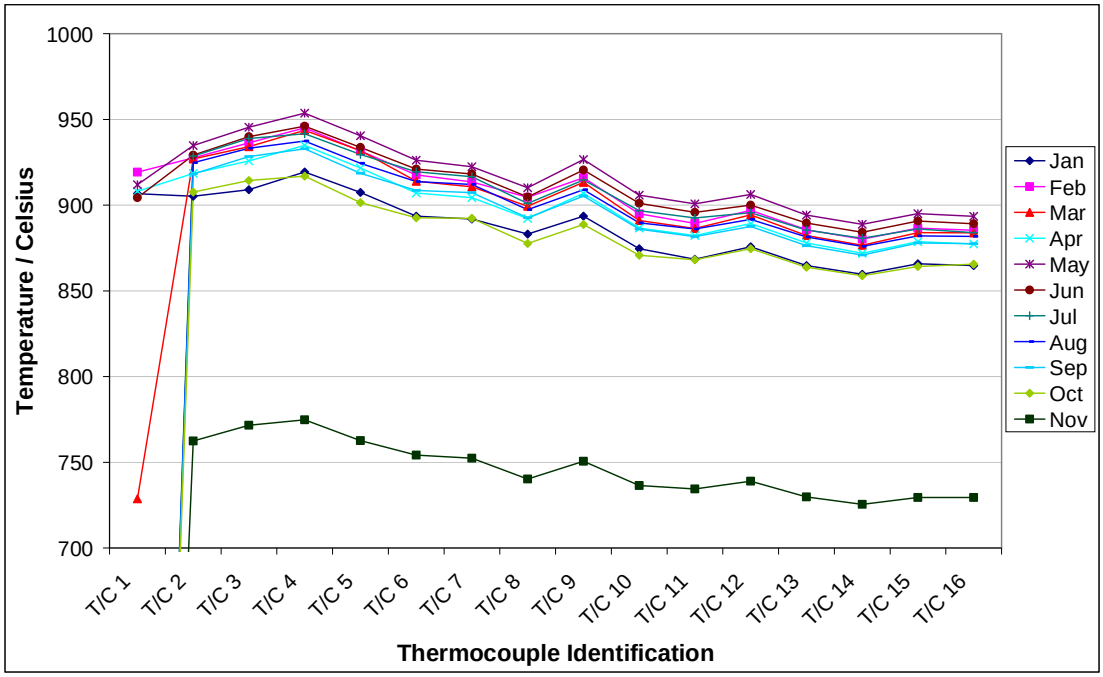

Figure 5-8 - Radiant tube average temperature profile for continuous week in each month

By excluding the downtime the results provide a better representation of the temperatures during furnace operation. Also, it shows how the demand of the furnace can be very onerous, with temperature varying greatly.

5.3.5 Temperature Differential

Figure 5-9 is the tube temperature differential, which highlights the difference between the maximum and minimum temperatures, recorded in any of the 16 thermocouples (T/C 1 to 16) at any given time. Typically the average difference in temperature was approximately 60 to 65ºC for both month and continuous operational week, while the maximum peak temperature difference on the other hand varies massively.

For the analysis of a continuous week, the maximum temperature differential varies between 75 and 90ºC typically, with two instances where the difference was approximately 112 and 120ºC respectively. For the month analysis, the differential temperature results are much higher, with values typically above 120ºC and peaks as high as 200ºC.

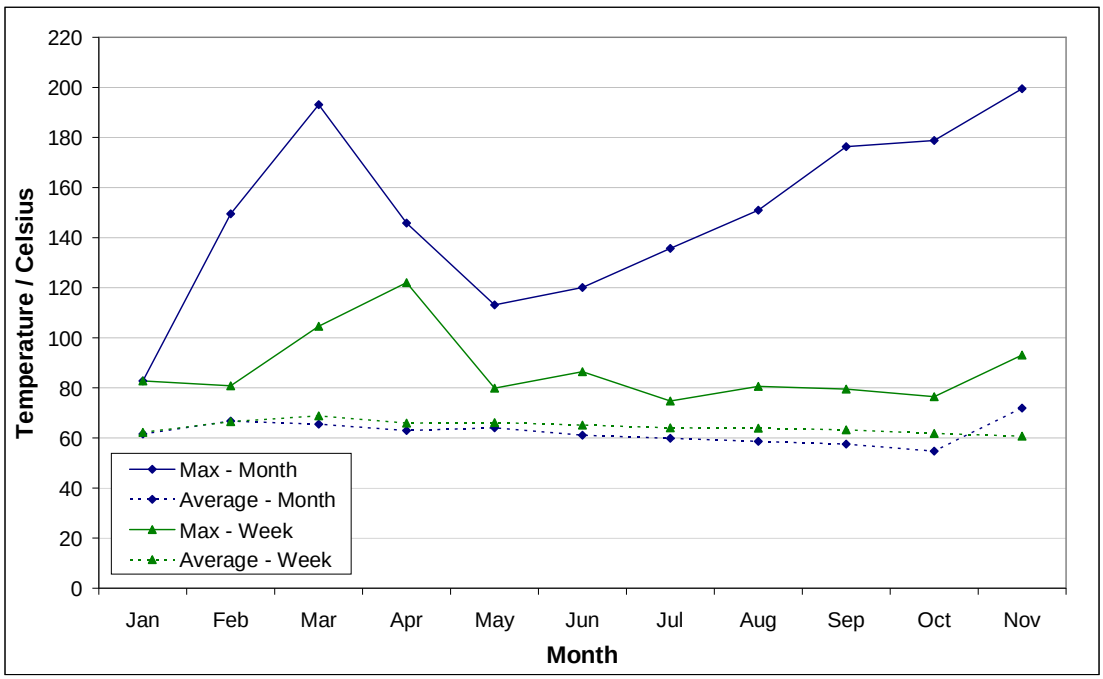

Figure 5-9 – Figure displaying the maximum and average radiant tube temperature differential for each month and continuous operational week

With further analysis, it was found that the large temperature gradients occur during furnace cooling or heating (for a period of downtime), while under processing conditions the difference in tube temperature varies from 50 - 70ºC. This is worth noting as large gradients in temperature in the tube assembly can generate large stresses as the material growth along the tube varies and is dependent on temperature.

5.3.6 Temperature Differential during Periods of Downtime

As large temperature differentials were seen during periods of furnace downtime, further analysis was undertaken to determine whether the large difference occurred during furnace cooling, heating or it was a factor of both.

Firstly, periods of downtime were recognised from the data, simply when the furnace was cooled to ambient temperature. In doing so, three instances were found according to Table 5-1.

Table 5-1 - Periods of Downtime

	Month										
	Jan	Feb	Mar	Apr	May	Jun	Jul	Aug	Sep	Oct	Nov
No. of downtime periods	0	0	2	1	0	0	0	0	0	0	0

In analysing the downtime periods, the sampling rates were increased to 15-minute intervals. This allowed a greater detail of representation of the cooling and heating procedure. Of the three periods, two were chosen at random for analysis.

Figure 5-10 displays the zone temperature, maximum tube temperature and the differential in tube temperature respectively for a period of downtime during the 11th to the 14th of March 2008. During 0 to 300 minutes the furnace was at operational temperature with maximum tube temperature of about 960ºC. During this period, the difference in tube temperature (Note: read right axis) is on average 75ºC.

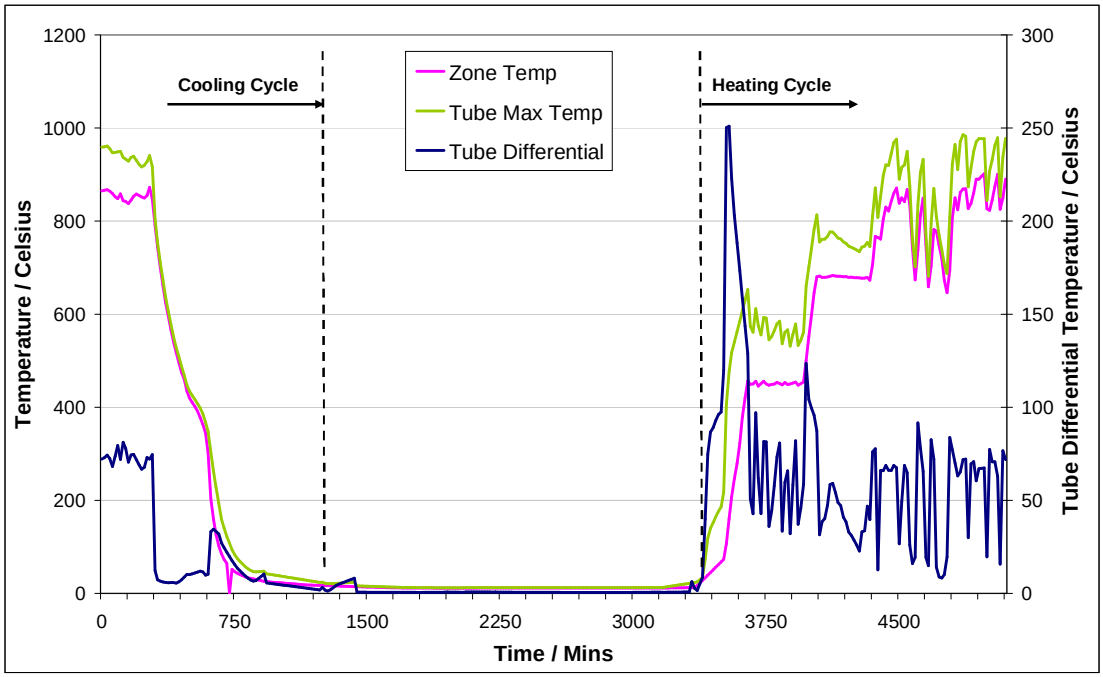

Figure 5-10 – Figure displaying the behaviour of the radiant tube during furnace cooling and heating, for the period 11th – 14th March 2008

During 300 to 750 minutes, the furnace is cooled from 875ºC to 50ºC. While the furnace is cooling, the tube temperature differential drops to as low as 10ºC and remain low for the duration. But, by looking at the heating period, from 3400 minutes onwards, the tube temperature differential increases suddenly to a maximum of 250ºC and remains over 100ºC for duration of approximately 150 minutes.

Figure 5-11 shows the furnace conditions during a downtime period during 26th – 31st October in 2008. Between 0 and 600 minutes the furnace is operational and the difference in tube temperature is approximately 65ºC. During furnace cooling, the difference in tube temperature, although fluctuates, remains low and is predominantly below 40ºC. Once again, on the onset of furnace heating period, the tube temperature differential increases rapidly to 130ºC and remains above 100ºC for approximately 90 minutes.

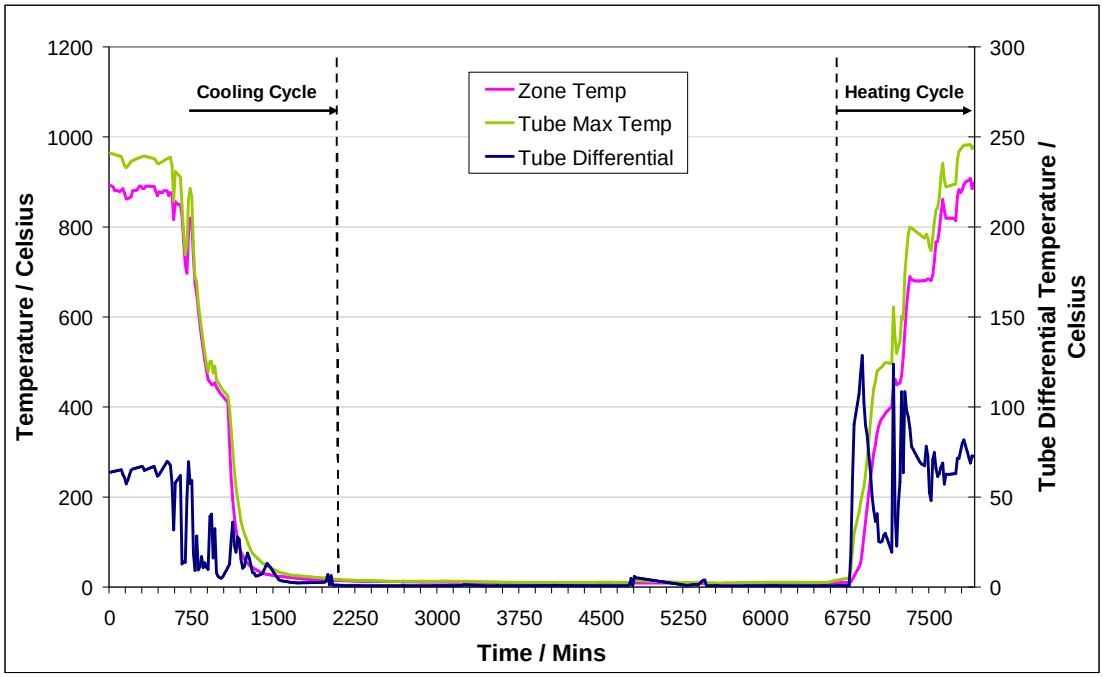

Figure 5-11 - Radiant tube behaviour during furnace cooling and heating, for the period 26th – 31st October 2008

It can be drawn from these two examples that the initial furnace heating cycle has potentially a greater effect on tube life than any other period. It was evident that the cooling cycle reduces the heat input from the radiant tube and as a result the difference in temperature across the length of the tube reduces.

In contrast, during the heating cycle the burners input heat energy and as a result the tube heats up, firstly in the lower leg, then second and so forth. Thus, creating a large temperature differential across the total length of the tube. It would be beneficial to calculate the stresses generated in the tubes during this period and discover the area and magnitude of high stresses.

5.3.7 Furnace Heating and Cooling

As the temperature differential study identified that the radiant tube was subjected to very large gradients during furnace heating and cooling, further analysis was undertaken to determine the heating/cooling rates of the furnace and the coinciding tube temperature profile.

5.3.7.1 Furnace Cooling

Examining the three cooling cycles together, as highlighted in Figure 5-12, it is evident that there are definite cooling rates at various stages of the cycle. Firstly the primary cooling rate, which takes the zone temperature to approximately 450ºC, then a slower secondary cooling rate. Depending on available time, this secondary cooling rate is utilised until the furnace covers are removed, where the zone temperature drops quickly and is easily distinguishable.

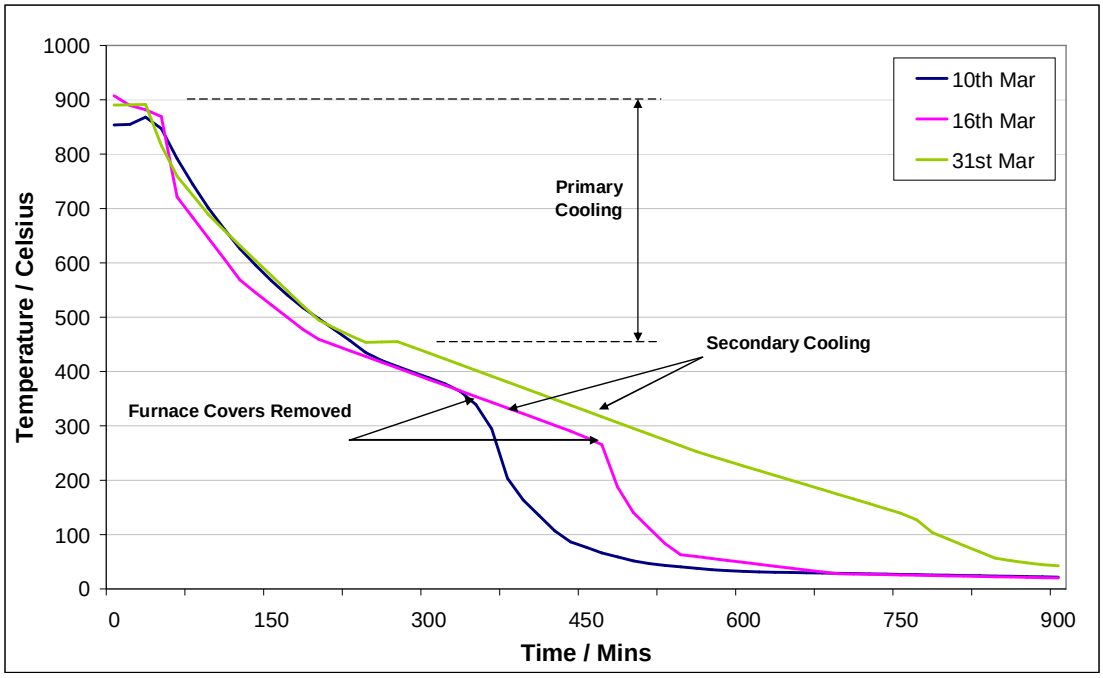

Figure 5-12 – The figure displays zone 7 temperature during three separate furnace cool down cycles

During the primary cooling rate the furnace operators use the 'Fast Cool' procedure, which reduces the furnace temperature by approximately 120ºC per hour. The

secondary cooling rate, where 'Fast Cool' is not utilised, reduces the temperature by approximately 50ºC per hour. Removing the furnace covers cools the furnace at a rate of 4.6ºC per minute (276ºC/hr) initially and then settles out to 1.3ºC per minute (78ºC/hr). The calculations for cooling rates are shown in appendix C and agree with furnace technical literature.

As discussed earlier, the temperature differential of the radiant tube during furnace cooling is very even and low. Figure 5-13 shows this clearly for the furnace cooling during the 11th March 2008. Initially the tube is at operating temperature, where the firing leg is hottest and a 'typical' operating profile is seen. Then, furnace cooling is initiated and the furnace undergoes the primary cooling phase down to a temperature of 450ºC and then a relatively quick secondary cooling.

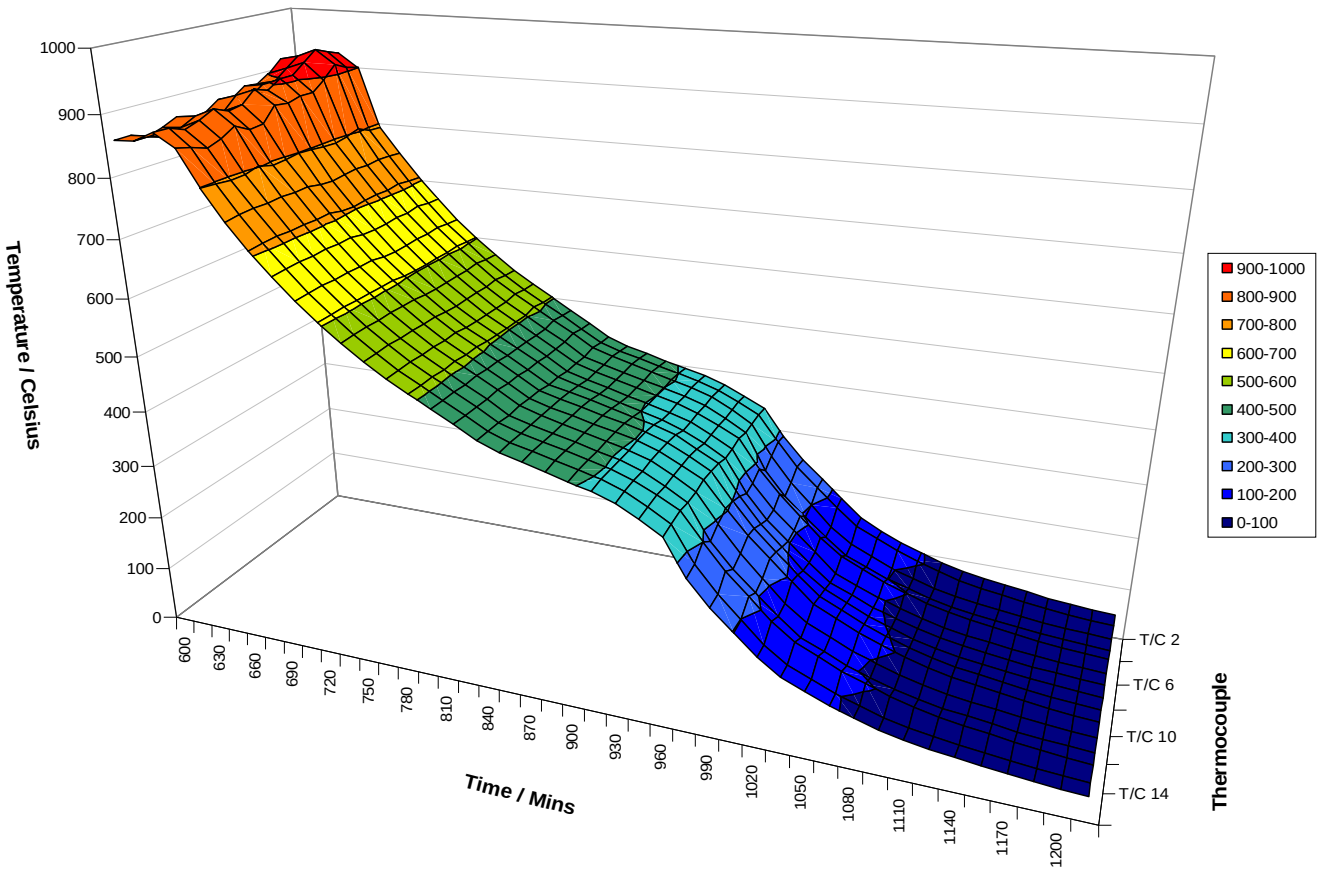

Figure 5-13 – The figure displays the tube temperature profile during a typical furnace cool down cycle

5.3.7.2 Furnace Heating

By combining the three heating cycles together, Figure 5-14, it is evident that the cycles are varied in the time taken and the number of heating phases (due to operator influence), but there are definitive heating rates. Each zone has an individual 'heat up' set temperature, a value of 670ºC for zone 7. In achieving this pre-defined temperature, there is a set heating rate in built in the control system, which is at 200ºC per hour. Once the zone has reached the set point the control limitations are removed and the heating rate is then variable. Calculations using collated data agree with this (Appendix D).

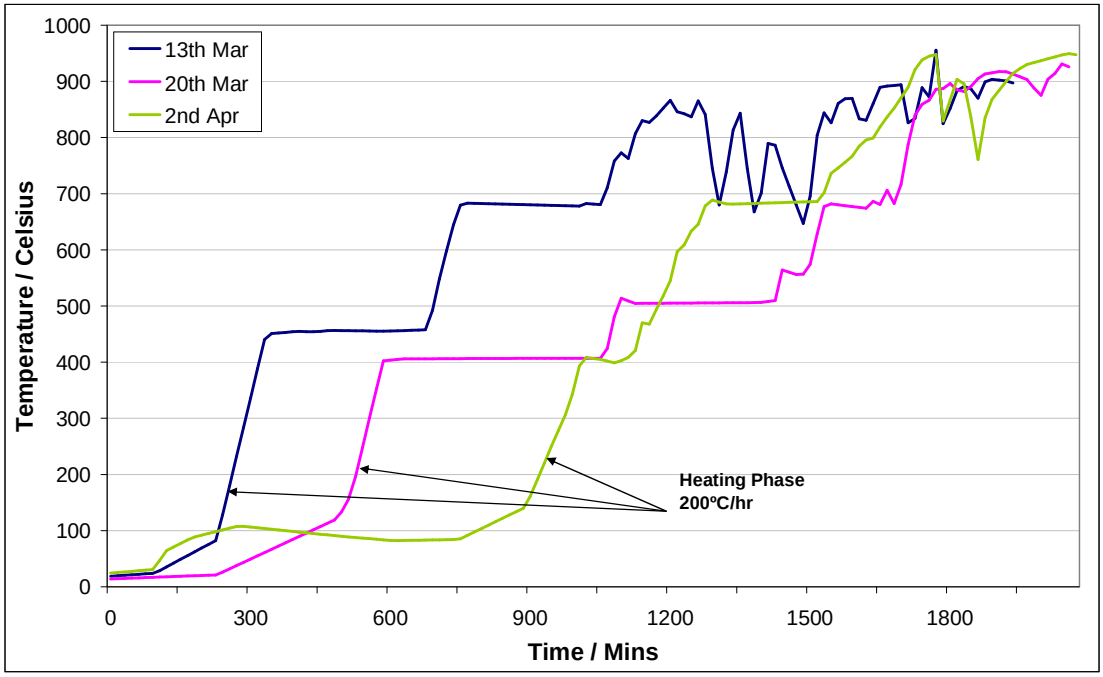

Figure 5-14 – The temperature of zone 7 during three separate furnace heating cycles

By focusing on one heating cycle, as identified in Figure 5-15, and comparing it to tube temperature differential and tube average temperature, the behaviour of the tube to a heat input can be shown. This reinforces what was discussed earlier and clarifies that during furnace heating, the tube temperature differential varies wildly, but during the heating phases the temperature differential increases severely, to a maximum of 250ºC.

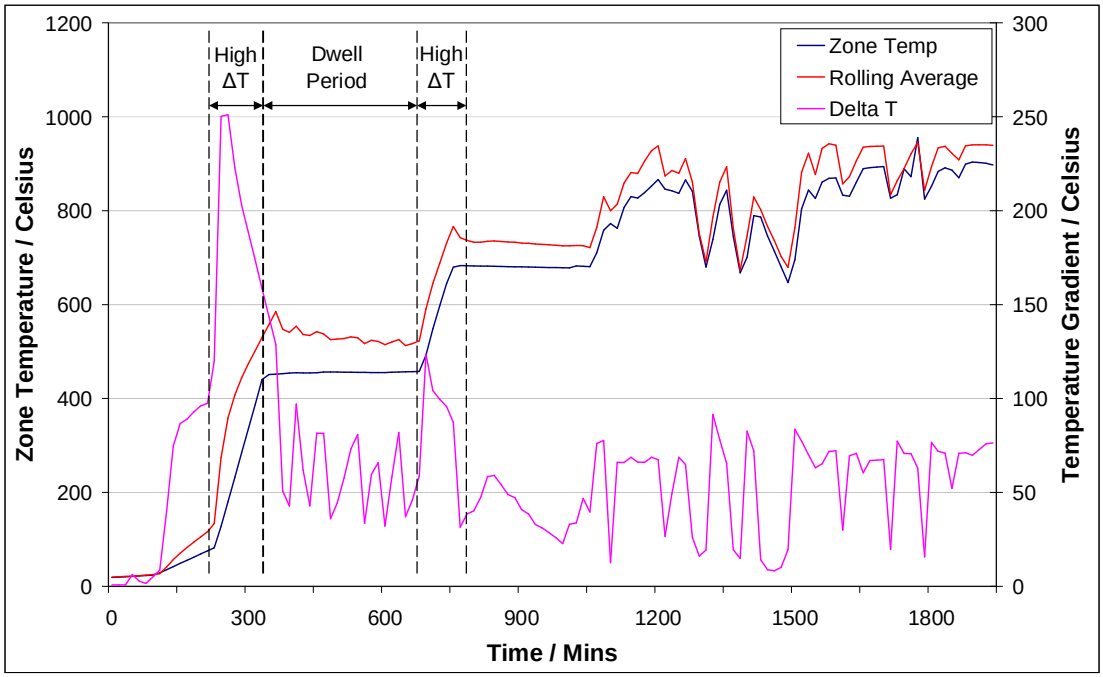

Figure 5-15 – Figure displaying the response of the radiant tube during a furnace heating cycle

For clarity, Figure 5-16 shows the temperature profile of the radiant tube for the heating procedure during the 13th March 2008. It clearly shows that the firing leg and second leg undergo severe temperature cycling during the 'dwell' periods, while the latter end of the tube remains quite even in terms of temperature. It also clearly shows the difference in temperature along the length of tube, which is quite severe during the two 'ramp-up' or heating phases.

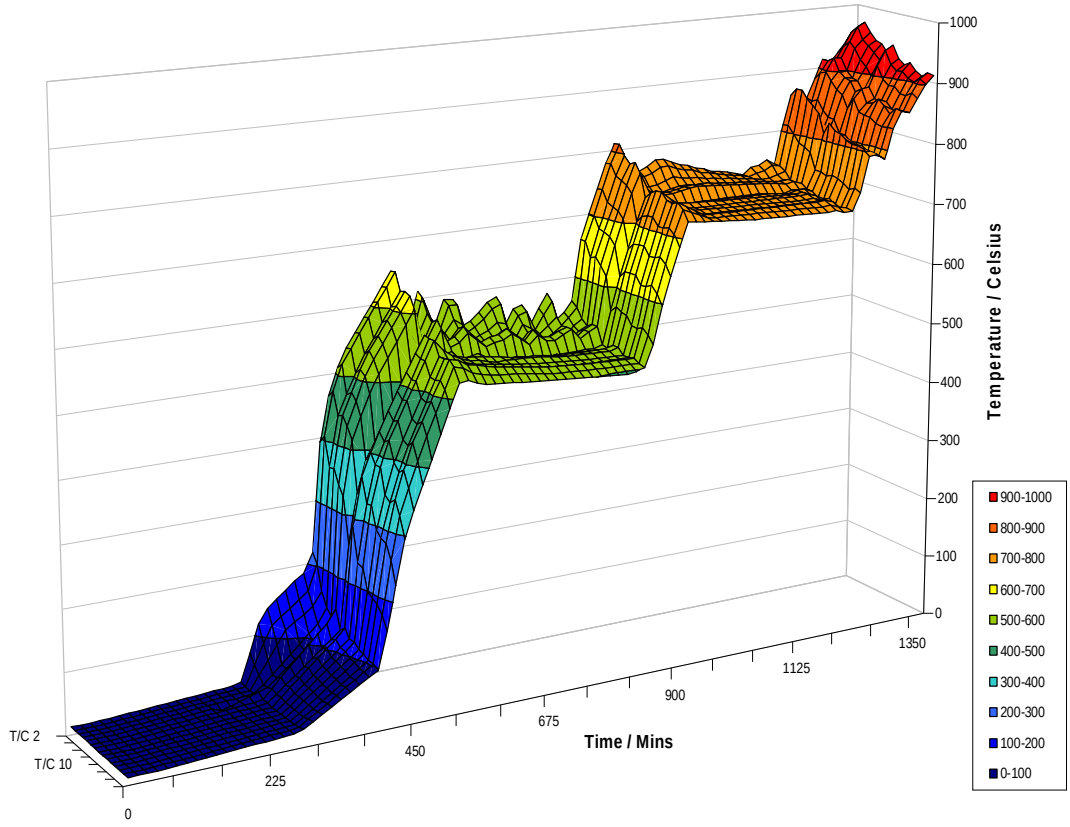

Figure 5-16 – The figure displays the tube temperature profile with time during a typical furnace heating cycle

5.3.8 Tube Temperature Profile

To gain a better representation of the tube temperature profile, the data was analysed for different strip grades that required different heating scenarios. It was decided that the two best options for analysis were steel grades that required a high zone thermal demand (1815mm wide strip) and a low zone thermal demand (1071mm wide strip). The benefit of looking at these two strip dimensions is that they are run in batches periodically, which provides relatively steady state furnace conditions.

5.3.8.1 High Thermal Demand

A strip grade that requires a high thermal demand from zone 7 is the 1815mm wide x 1.15mm gauge strip of annealing grade CQ-AK, which requires the strip to be heated to 700ºC by the end of the furnace. This grade is run periodically in large batches and

utilises the furnace for periods between 9 to 30 hours. Therefore, the furnace operates at near steady state conditions.

Figure 5-17 illustrates the furnace conditions during a total period of 230 hours, accumulated during the eleven-month period of scrutiny, for heating the aforementioned strip grade. Zone thermal demand is generally high (95% of zone total installed input), but averages out to 83% demand; maximum tube temperature is predominantly above 960ºC, while the tube temperature difference is very even at an average of 65ºC. Zone power demand is measured in % and is a measure of the output of the zone, i.e. 100% demand would imply that the zone is operating at its maximum thermal power capability.

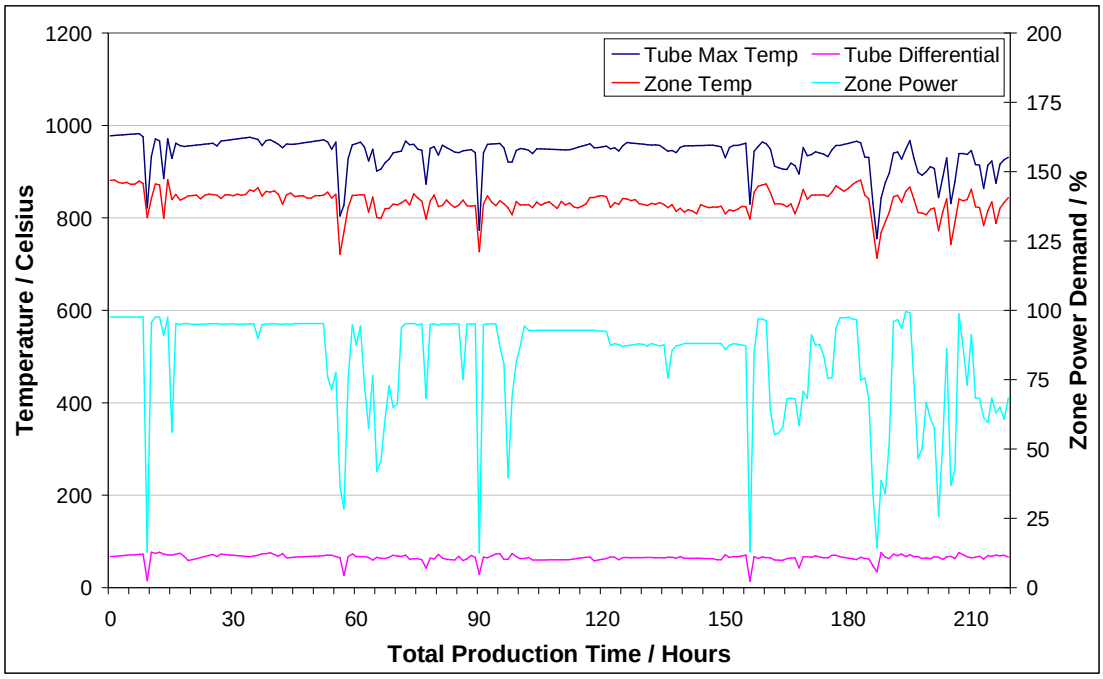

Figure 5-17 – Showing the zone 7 and radiant tube temperature and demand during the production of 1815mm wide x 1.15mm gauge strip. (Zone Power Demand of 100% indicates that all installed thermal power is utilised).

5.3.8.2 Low Thermal Demand

For the analysis of low thermal demand in zone 7, an annealing grade of CQ-AK was chosen with the following dimensions: 1071mm wide x 0.4mm gauge. This grade is

scheduled periodically in batches that utilises the furnace for periods of 3 to 9 hours and requires to be heated to a temperature of 700ºC by the end of the tube furnace.

Figure 5-18 illustrates the zone conditions during a low thermal demand. The zone demand average for the total of 107 hours equates to 52%, while the maximum tube temperature averages to 894ºC. The temperature difference along the length of the tube is again very even at an average of 65ºC.

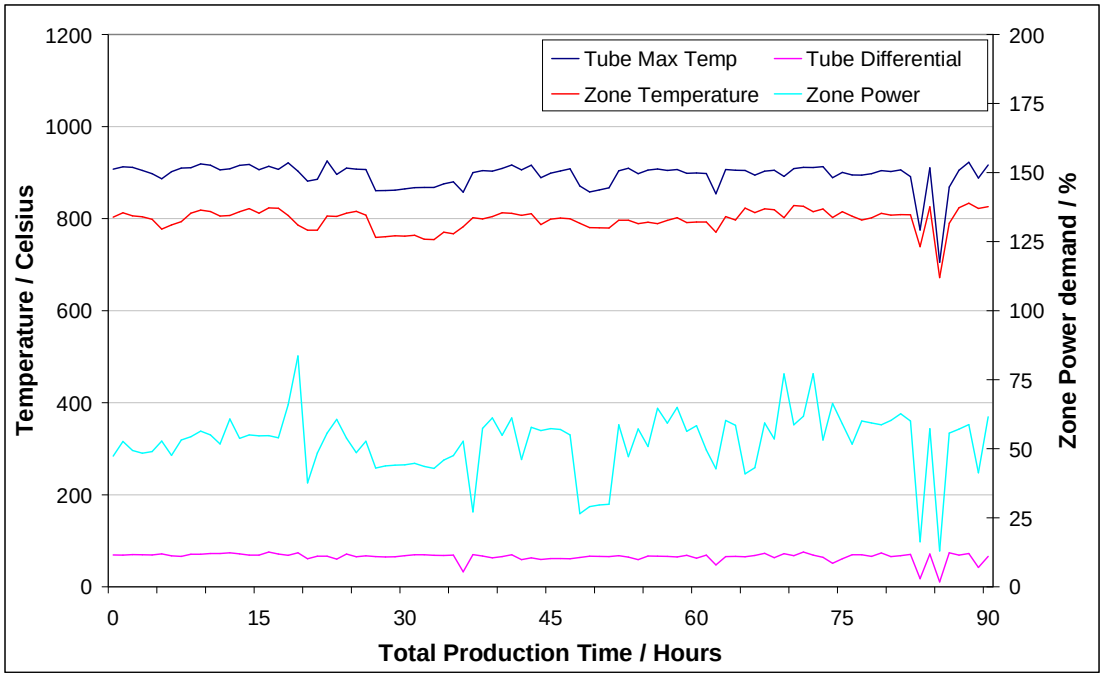

Figure 5-18 – Figure displays the zone 7 and radiant tube temperature and demand for the annealing of the 1071mm wide strip (Low power demand). (Zone Power Demand of 100% indicates that all installed thermal power is utilised).

5.3.8.3 Temperature Profile Comparison

Figure 5-19 illustrates the temperature profile for the radiant tube situated in zone 7 under high and low firing scenarios. Shown are the average and maximum profiles for the operating hours displayed in Figure 5-17 and Figure 5-18 respectively. Thermocouple 1 results have been omitted due to the incorrect values obtained from electrical faults.

All four profiles are similar in shape albeit for the temperature distribution along the firing leg (T/C 2 to T/C 5) and the increase in temperature at thermocouple 12 for the low fire profiles. By comparing the high fire profiles, the maximum temperature is achieved towards the end of the firing leg on the average profile; while the higher temperatures are achieved towards the first return bend on the maximum profile. Apart from this, both are near identical with approximately 30ºC differences between the average and maximum results for each thermocouple.

By comparing the low fire profiles, both are near identical in shape, with the maximum temperature occurring at the end of the firing leg (T/C 4). There are also two temperature peaks visible at thermocouples 9 and 12 respectively, which coincide with the second and third return bend.

There is approximately 50ºC difference between the two maximum profiles and between the two average profiles and typically thermocouple 4 is the location of the maximum temperatures. Only under certain high firing conditions does the first return bend get hotter than the end of the firing leg tube. Worth noting is the increase in temperature at the location of thermocouple 9 in all instances, which is in the vicinity of the central return bend. Also, there is a peak in temperature at thermocouple 12, but only under low firing conditions. These effects have been shown on the radiant tube test facility at Tata RD&T by Hekkens[19].

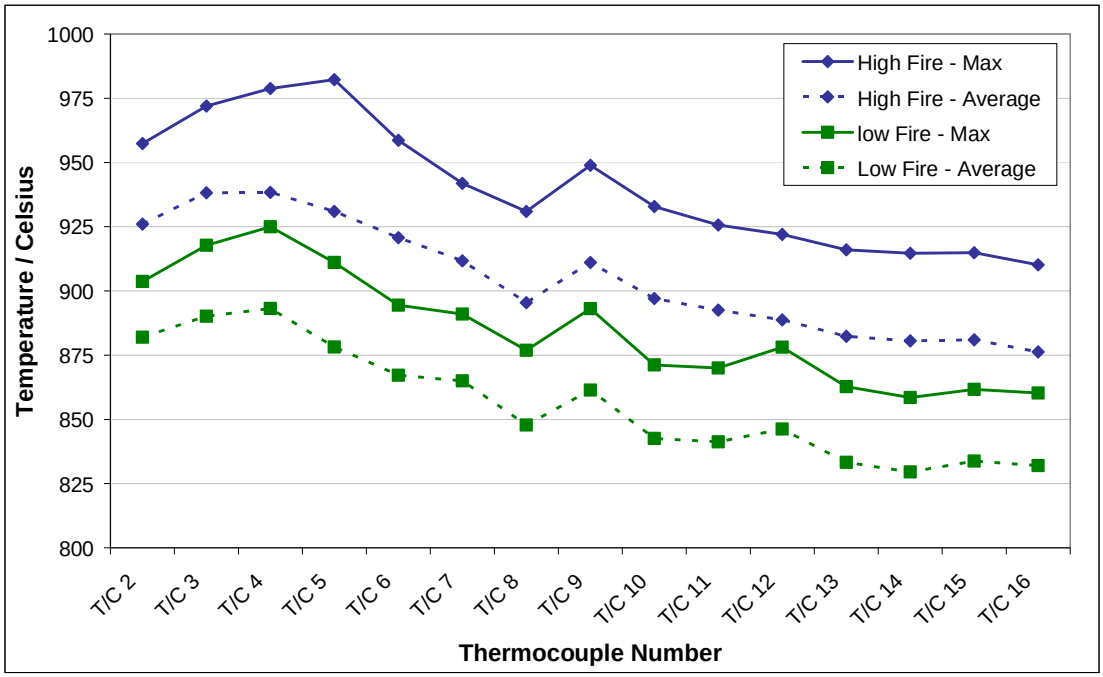

Figure 5-19 – The figure shows the radiant tube temperature profile during high and low firing scenarios

In summary Figure 5-19 highlights the influence temperature has on tube failures and tube life. CAPL radiant tube temperature is always at its highest towards the end of the firing leg and the first return bend, under all furnace demand, an area where all reported tube failures have occurred (Chapter 3). This indicates that temperature has an effect on tube failures and tube ultimately tube life.

5.3.9 Furnace Temperature

The multi thermocouple radiant tube was situated in zone 7, which has one of the highest failure rates of the whole furnace. In comparison, failure rates towards the entry of the furnace are very low, with some zones having no radiant tubes replaced since the commissioning of the line. As the furnace is controlled via zone thermocouples, which send an error signal back to the control loop, a simple comparison could be made between the furnace zone temperatures.

Figure 5-20 displays the comparison in zone temperature as the furnace is heated from ambient temperature after a maintenance period to production temperature. During the initial heating phase, A, the zone heating rates varies slightly and in B, the zone

temperatures vary by approximately 80°C. These two initial phases are dependent on operator choice and differ greatly between different shift teams.

The important phase in heating the furnace is segment D on Figure 5-20. The furnace operating procedure requires each zone to reach its set point prior to increasing furnace temperatures further. Set point temperatures increase from zone 1 to zone 8 in approximately 30°C increments.

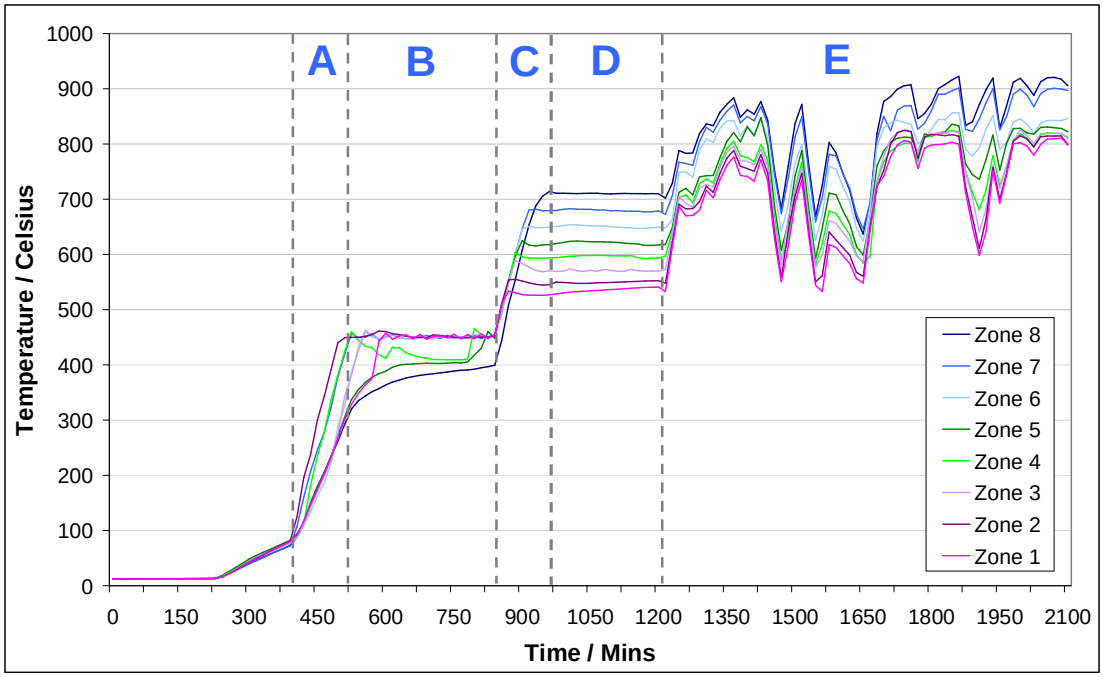

Figure 5-20 - A comparison of furnace zone temperatures from heating from ambient to production temperatures

Once the set points have been achieved and the furnace has reached thermal balance, the control system allows the operator to increase the temperatures to the desired operating temperatures. As can be seen from Figure 5-20, there is a large difference in zone temperatures. Zone 8 has the highest temperatures and can reach operating temperatures of above 900°C. In comparison, zone 1 temperatures are approximately 800°C during the same time period.

In summary, the operating philosophy of the furnace governs the zone temperatures and as a result, the zones towards the exit of the furnace are operated at higher temperatures than zones towards the entry. High zone temperatures of approximately 900°C can result in maximum radiant tube temperatures of above 1000°C, which

when compared to average tube life in Chapter 3 clearly has a detrimental effect on tube life.

5.3.10 Frequency of Temperature Variation

The data accumulated from the monitored radiant tube was subsequently sorted into a frequency chart. This allowed the data to be manipulated into one figure, which is easily understandable, while outlining many aspects of operation of the furnace radiant tubes.

Each temperature value, from every thermocouple was manipulated into 'frequency bins' of predetermined range. The bin range is dependant on the level of detail required to analyse the results, initially, each bin size was 25°C. For example, a temperature value of 936°C would be counted in the frequency bin 925 to 949°C, 10°C in bin 0 to 24°C, and so forth.

5.3.10.1 Results

Figure 5-21 shows the temperature data accumulated from all thermocouples over the 11 month period. It can be seen that there is a definite trend visible between 850 and 1000°C and with all the months peaking at 940°C, where the radiant tube spends most of the time. This range is where the radiant tube is at its operating temperature.

The frequency chart can identify noise from short circuits in the electrical equipment as seen from the three small peaks near 1400°C. When the thermocouples passed a maximum voltage the potential difference equated to 1372°C in temperature. As a result, the histogram filters this noise out from useable data.

What the figure can also show is when the furnace has been at low temperatures for prolonged periods of time. The large area under the figure for months March, October and November identify that the furnace has either been off for maintenance or reduced in temperature due to faults or problems.

Disregarding the temperature readings due to noise, the figure clearly shows that maximum temperature readings of over 1000°C are experienced throughout the year. Accuracy of the readings is dependent on the 'bin' size. Therefore, with relatively large bin sizes it is difficult to accurately state what the maximum temperature was, but in Figure 5-21, maximum temperatures of approximately 1050ºC were experienced.

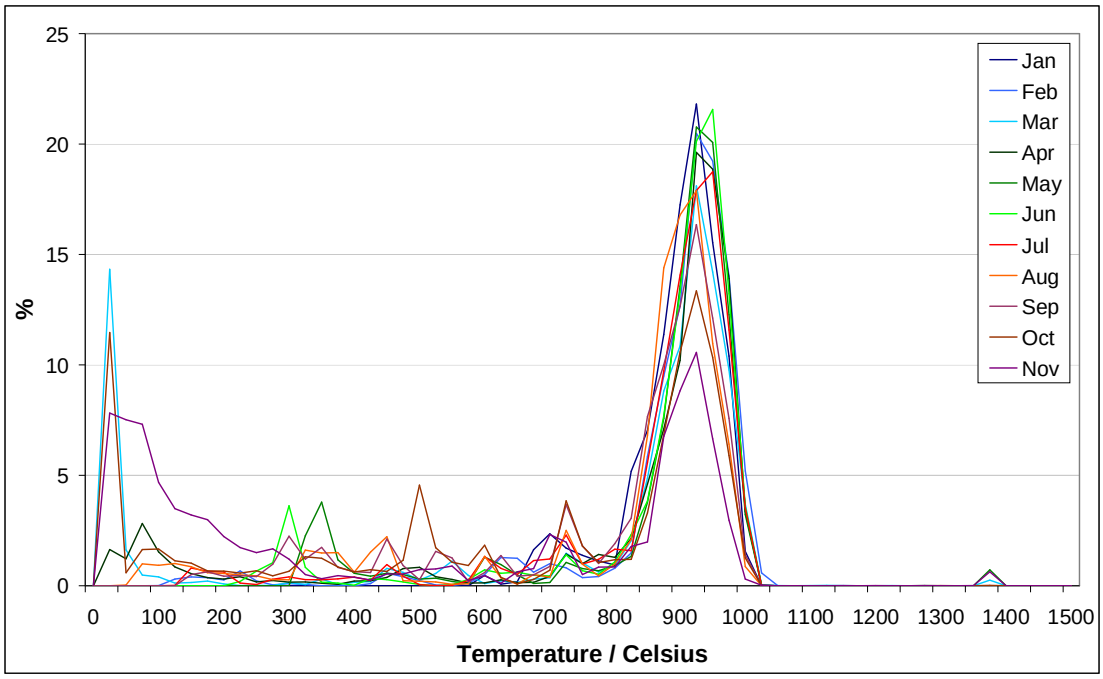

Figure 5-21 – Frequency of temperature variation for the 11 months of operation

To identify the differences in temperature between the four tubes of the radiant tube, the data was manipulated to show the frequency of temperature variation for each leg, Figure 5-22. What is interesting to note is that the time at temperature for each tube is nearly identical in shape but at the operating temperature range of 850 to 1000°C, the distribution varies 20°C between each tube and a maximum of 80°C between the firing leg and the exhaust leg. This correlates with the measurements made for the ΔT earlier in the chapter.

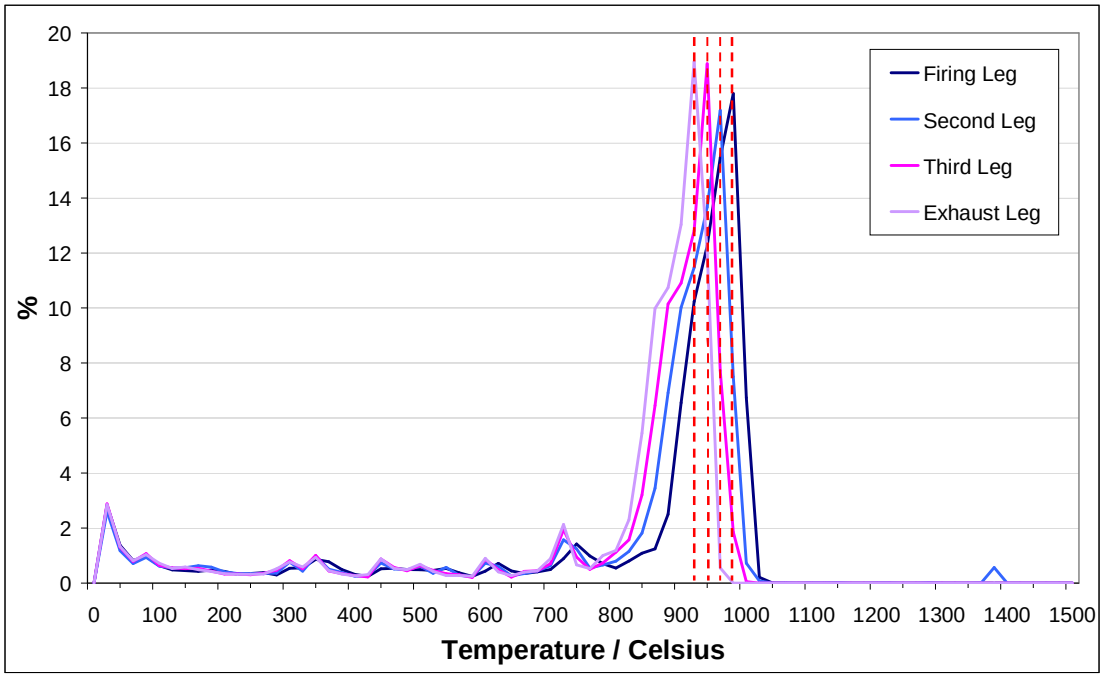

Figure 5-22 - Histogram of temperature data for each radiant tube leg

5.3.11 Heating Rate Trial

As a result of the findings from the temperature gradient analysis, a trial was undertaken to measure the effect of reducing the furnace heating-rate on the temperature response of a radiant tube.

The current furnace heating-rate is set at 200ºC/hr, which is fixed until the zone temperature reaches 670ºC (Zone 7 set-point temperature). The results have shown that during the heating phase, temperature gradients of up to 250ºC were seen between the firing leg and the exhaust leg. This severe difference in temperature has a large effect on the differences in thermal expansion and as a result generating large thermal stresses.

It was agreed to trial a reduced heating rate of 100ºC/hr across the entire furnace, after a maintenance period, where furnace temperature had been reduced to ambient. As the furnace is automatically controlled during this period, the step change in heating rate could be applied by simply entering a new value in the closed loop control system via the furnace control pulpit.

5.3.11.1 Trial Results

The trial was completed after a planned maintenance period on the 29th April 2010. Data was collated for the 16 thermocouples that monitor the temperature along the length of the radiant tube. The results were exported to Microsoft Excel and sampled at 5-minute intervals. Thermocouple 1 was reported to be not functioning, therefore has been excluded from the results. All other thermocouples were working without errors.

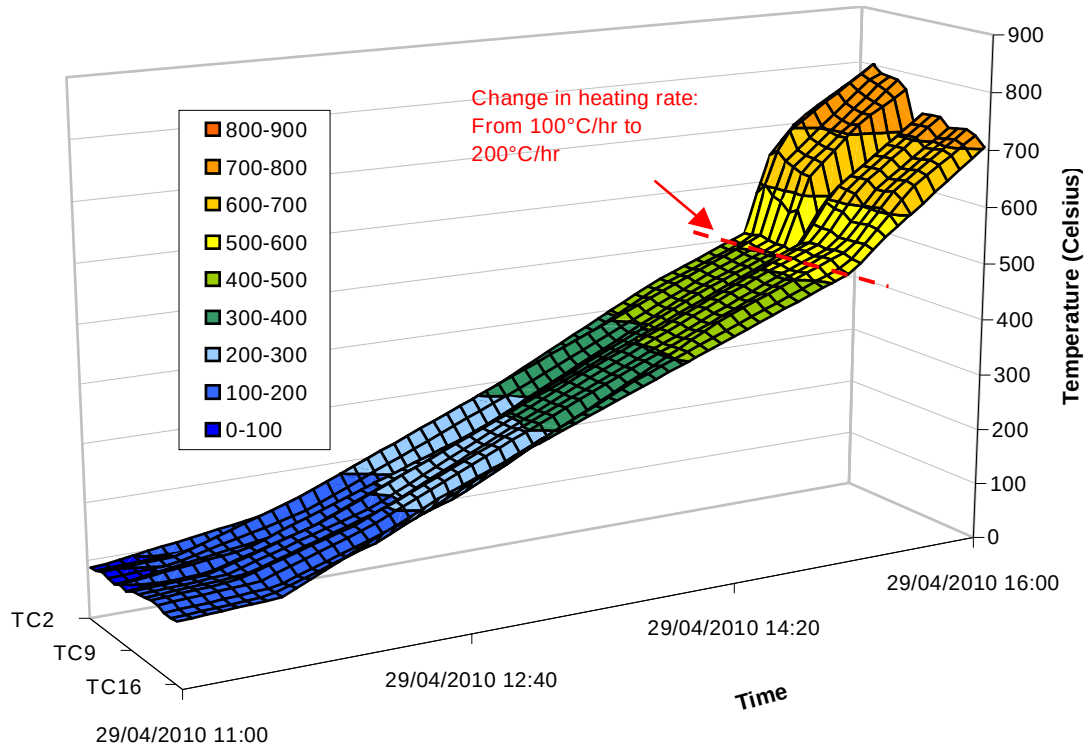

Figure 5-23 - Temperature data for radiant tube profile from reduced heating rate trial

Figure 5-23 displays the temperature profile for the monitored radiant tube during the reduced heating rate trial of 100ºC/hr. The control feedback was modified during the maintenance period and furnace operators were told to reheat the furnace as per normal procedure.

As can be seen from the figure, the profile of the radiant tube is smooth and relatively linear between 11:00hrs and 15:00hrs. The whole length of the tube increases in temperature uniformly, which reduces differences in thermal expansion and resultant stresses. The temperature increases linearly to 500ºC; where the heating rate is

changed back to the default of 200ºC/hr and immediately, large variances in temperature occur once again.

By further manipulation of temperature data during the trial, a comparison could be made between the two different heating rates. Figure 5-24, displays the maximum, average and ΔT (difference between maximum and minimum temperatures) respectively.

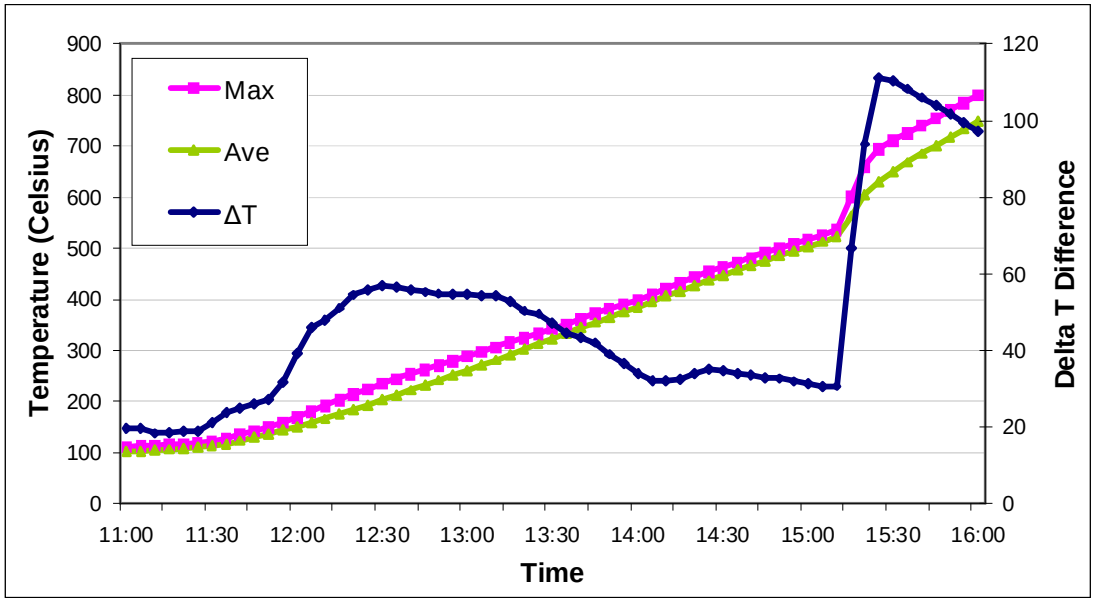

Figure 5-24 - Comparison of temperature parameters during heating trial

During the reduced heating rate of 100ºC/hr (between 11:00 and 15:10hrs), the difference between the maximum and average tube temperature is very small and as a result ΔT remains low, below 60ºC for the whole duration. Once the heating rate is altered back to default setting of 200ºC/hr, it is visible that the difference between maximum and average tube temperature increases and as a result ΔT increases dramatically to over 115ºC.

In conclusion, reducing the heating rate of the furnace from 200ºC/hr to 100ºC/hr, during the initial heating phase from ambient temperature, minimises the difference in temperature along the length of the radiant tube. As a result, the thermal expansion of the tube is more uniform and should have a resultant reducing effect on the stresses generated.

5.4 Discussion

The installation of a multi thermocouple radiant tube in the annealing furnace has provided an insight into how the radiant tube behaves under varying furnace loading/scenarios. Maximum tube temperatures of 1022ºC have been recorded at the end of the firing leg at thermocouple number 4, a position that regularly operates at, and sometimes over, temperatures of 1000ºC. Under consistent operation the firing leg temperatures averages at over 900ºC and an average of 940ºC for thermocouple 4.

The temperature differential along the length of the tube remained relatively low and constant at an average of between 65 and 75ºC during operating conditions. But during periods of furnace cooling and heating, to/from ambient temperature, resulted in differences of up to 250ºC along the 8.5m length of tube.

Heating and cooling rates were calculated and were found to be 120ºC per hour for cooling under 'Fast Cool' conditions and 200ºC per hour during heating. Faster cooling rates of up to 270ºC were obtainable by removing the furnace covers, although this procedure is only allowed under temperatures of 450ºC.

During furnace cooling, the temperature across the radiant tube length stabilises and reduces uniformly. In contrast, during heating, the firing leg and second leg experience much higher temperatures than the exhaust legs. During some scenarios, the temperature in the firing leg cycles back and forth, while the remainder of the radiant tube operates at even temperature. This occurs when the burners operate under high fire conditions over short periods of time to maintain a constant furnace zone temperature.

When analysing the radiant tube temperatures during periods of high fire demand, the average tube temperature was approximately 900ºC, with the end of the firing leg operating at an average of 940ºC. While, this is not extremely high, the radiant tube has to increase in temperature periodically to increase the zone temperatures to the required level. This is when the radiant tube temperatures achieve the maximums above 1000ºC.

When comparing furnace temperatures, zones 7 and 8 predominantly operated with the highest zone temperatures and as a result the highest radiant tubes temperatures. In comparison, zones 1, 2 and 3 were the coolest, with zone temperature of up to 100ºC lower.

The reduced heating rate trial, during furnace heating from ambient, provided interesting results. The tube temperature profile was uniform through the heating phase with a heating rate of 100ºC per hour. When the trial terminated and heating rate reverted back to 200ºC per hour, the temperature differential across the length of the tube increased drastically to 110ºC.

The disadvantage of operating with a reduced heating rate is that the furnace takes twice as long to reach operating temperatures, but at the benefit of temperature uniformity in the radiant tube. Further work on this topic could experiment with a heating rate of 150ºC per hour and observe the differences.

5.5 Summary of Investigation

The following conclusions can be drawn, from the analysis of the radiant tube temperature under varying furnace scenarios:

- Maximum tube temperature from the sampled data was 1022ºC situated at thermocouple 4 (end of firing leg). The maximum temperature occurs at this point consistently under operating conditions, while the first return bend can experience the highest temperatures during periods of high fire to reach zone temperatures quickly
- Average temperature profiles, when looking at a continuous operational week are high. The first and second legs average temperatures are consistently over 900ºC with the end of the firing leg operating at approximately 940ºC for all months
- Tube temperature differential at operational temperature is steady at an average of between 65 and 75ºC. Maximums of above 150ºC have been identified and occur during periods when the furnace is heated
- By analysing the furnace heating procedure from ambient temperature in greater detail, the temperature differential was found to increase dramatically during the heating periods. Maximum difference in temperature was approximately 250ºC in one instance and remained above 100ºC for a period of 150 minutes
- Reducing the heating rate from 200 to 100ºC resulted in the tube temperature being uniform throughout the heating phase
- Heating and cooling rates were calculated from the data and agreed with technical guidelines supplied by process line manufacturer
- Tube temperature profiles have been acquired for the length of the tube under varying furnace scenarios, which will be used in future finite element modelling
- Zones 7 and 8 are the highest temperature zones within the furnace. Operating at temperatures of approximately 100ºC higher than zones 1, 2 and 3

6 Radiant Tube Metallurgical Failure Analysis

6.1 Introduction

This chapter outlines the failure analysis study undertaken to inspect and assess the scale of material degradation and to determine the various types of failure observed in failed tubes.

As described in chapter 2, the continuous annealing of strip steel is performed in a radiant tube furnace, which is responsible for heating the steel from ambient temperature to the desired annealing temperature of between 750ºC to 850ºC. The strip travels across the furnace in a vertical position in between columns of radiant tubes, which transfer radiant heat energy to the steel. The outside surface of the radiant tubes are exposed to a reducing atmosphere containing 95% nitrogen and 5% hydrogen, which prevents the steel from oxidising at the high annealing temperatures.

Radiant tubes continuously operate at very high temperatures and as a result the tube material is subjected to degradation. Despite changes to the design of supports, catastrophic failure still occurs. Severe deformation of tube legs can result in contact with the strip and mark the surface, while cracking of the tube can allow the reducing atmosphere to be sucked into the exhaust stack causing furnace pressure problems, which is costly to replenish and can also affect strip surface quality.

As the radiant tube material is expected to operate at temperatures above 900ºC for prolonged periods of time, material selection is limited to the heat resistant stainless steel family. This material can either be cast to the desired shape or fabricated from wrought product. In the case of this failure analysis, the material was cast to standard alloy contents to thicknesses of approximately 8mm.

6.2 Background

The radiant tube furnace at the case study site contains 338 ‘W’ shaped radiant tubes separated into 8 control zones. The process line was commissioned in 1998 and the

first radiant tubes were replaced in 2001. In total, 299 tubes have been replaced due to failure in various ways.

Radiant tubes are mounted in vertical columns, which allow the steel to traverse either side, maximising the potential energy transferred to the strip. The natural gas burner is installed in the lower of the four legs (termed the firing leg) and predominantly operates at the highest temperatures, averaging at 950ºC and sometimes exceeding 1000ºC. The hot tube material then transfers heat energy to the steel strip predominantly via radiation.

The tube structure is manufactured from two different material grades, originally HP and HK40 grades. The higher material grade, HP, was used for the firing leg and second leg, while the lower HK40 grade was used for the upper exhaust legs. During a change in suppliers, the HP grade was changed to a HU grade, which was argued would give better creep strength. The compositions of these grades were highlighted previously in chapter 2

Support designs have also changed from original design with the main intention of prolonging tube life. In reality, no effect has been made on tube life but new failure types have been generated. The majority of failures are seen in the latter, hotter zones of the furnace where tube life is approximately 4 years.

6.3 Experimental

6.3.1 Sample Selection

Eight samples were taken from failed radiant tubes replaced during a 2-week maintenance period in January 2008. The sample matrix comprised examples of two dominant failure types seen in the furnace at the time of research. The first set contained tubes that had cracked at the weld region between the firing leg and the first bend, Figure 6-1, while the second set, Figure 6-2, had samples of tube that had deformed and cracked along the firing leg.

Figure 6-1 - Example of failure at weld region between firing leg and the first return bend

Figure 6-2 - Example of deformed firing leg, which has resulted in a crack

Large sections of approximately 0.5m in length were cut from the tubes by a rotating disc cutter, for ease of transportation to the laboratory, where the material was subjected to metallographic, chemical and mechanical analysis. Photographic evidence and burner position of each sample was taken for completeness. The position of each failed tube; time in service and failure type, etc. is noted in Table 6-1.

Table 6-1 - General information regarding failed samples taken for further analysis

Burner Code*	Time in Service (Hrs)	Type of Failure	Tube Manufacturer	Support Design+
5 OS 6.1	38,976	Weld failure	Almorgroup	Mk2
6 MS 8.1	26,376	Weld failure	Almorgroup	Mk2
3 OS 8.2	26,376	Weld failure	Almorgroup	Mk2
7 MS 8.4	38,976	Weld failure	Almorgroup	Mk2
6 MS 6.3	30,240	Deformed and cracked	Almorgroup	Mk2
3 MS 4.3	80,976	Deformed and cracked	Stein Heurtey	Hook and Eye
3 OS 8.4	38,976	Deformed and cracked	Almorgroup	Mk2
5 MS 6.3	26,376	Deformed and cracked	Almorgroup	Mk2

* - OS denotes Operator Side. MS denotes Motor Side
+ - Refer to chapter 3 for diagram representation of various support design

6.3.2 Sample Preparation

Each long tube section was cut into smaller samples from near-crack regions. Transverse and longitudinal samples were cut to approximately 20mm x 20mm coupon size for further metallographic analysis. Each coupon was mounted in conductive Bakelite using an automatic press (PrimoPress 3000) and carefully ground, according to ASM Metals Handbook[59], by using increasingly finer grades of silicon carbide paper. Final polishing was done on a polishing machine (Struers Knuth Rotor 3) using 6µm and 1µm diamond paste until the desired finish was achieved.

Samples were etched using a glyceregia (10ml HNO_3, 50ml HCl, 30ml glycerol) delineating etchant to show contrast and reveal general structure. Some samples

remained un-etched for reference and also new as-cast material of HP grade was acquired to provide a base reference.

6.3.3 Sample Analysis

All samples in this study were subject to detailed analysis in the 'as received' condition and in polished and etched conditions by light optical microscope (Reichart-Jung Polyvar) and Scanning Electron Microscope (SEM). The chemical composition of the samples were checked in accordance with standards using a Inductively Coupled Plasma – Optical Emission Spectography (ICP-OES)

By conducting the analysis in this manner, results can be compared and similarities can be drawn with available literatures, where similar analysis on heat resistant stainless steel castings has been conducted.

6.3.3.1 ICP-OES Sample Preparation

For a successful analysis the ICP-OES requires a nearly solid free solution. Firstly, small filings were ground from each sample and stored in a 50ml sample bottle. 0.1g of each sample was then heated for 10 minutes in 10mL of phosphoric and sulphuric acid (1:2 concentrations) in a conical flask, until only carbon remained in a yellow solution. Nitric acid was then added until all carbon was gone and heated further for 2 minutes. De-ionised water was then added and solution was diluted 20 times prior to analysis.

The ICP spectrometer was calibrated with pure elements for the composition analysis of Nickel, Chromium and Manganese in each radiant tube sample.

6.3.4 Visual and Dimensional Examination

All samples, Figure 6-3, underwent visual and dimensional examination prior to sample cutting. This procedure provides a good general overview of the failure and condition of the sample and could potentially highlight features that could be missed by looking in detail through a microscope.

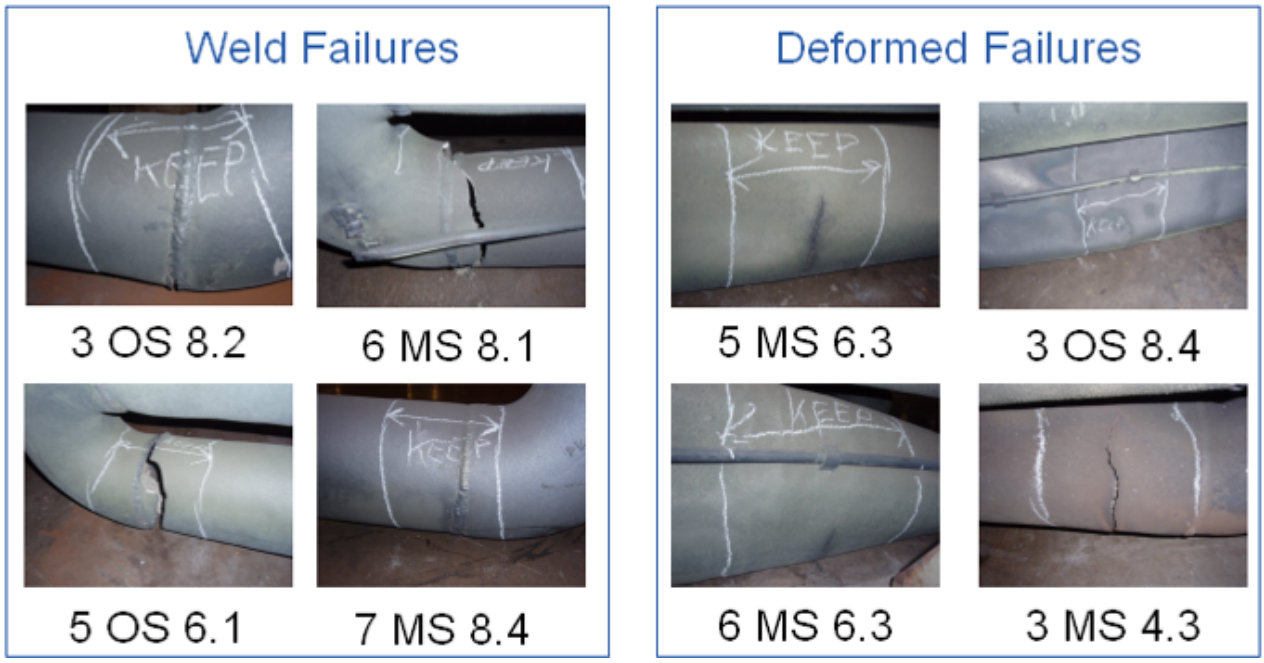

Figure 6-3 - Pictorial representation of failures at the respective burner positions

6.4 Results

6.4.1 Weld Failures

All weld failure samples were visibly in good condition with low levels of corrosion and outside surface similar to as-cast condition. Deformation was very low, with only a slight oval to be seen in tube circumference, Figure 6-4. All four samples had cracks of various severities in the weld region between the firing leg and first return bend.

Figure 6-4 - Very low levels of deformation visible in weld failure samples

All four samples were taken from radiant tubes of the same design (Almor mk2). Two tubes had crack propagation from the bottom surface of the tube; along the weld bead on both sides and finish approximately at mid point. The other two tubes exhibited cracks which had sheared the firing leg completely away from the first return bend. All cracks were transverse to the direction of principle stress.

Cracks in radiant tubes, of any nature, determine the end of the tube life as they cause major problems to the pressure control of the furnace. Slight deformation in a radiant tube is tolerable as long as the structure is intact. Cracks in contrast, allow the reducing atmosphere to escape through the tube and exhausted to atmosphere. Problems are encountered in maintaining furnace reducing atmosphere when large numbers of tubes have failed due to cracks.

On inspection of the inside surface, there was a notable difference in colour. Tubes 3 OS 8.2 and 5 OS 6.1 had a very dark brown colour on the inside surface, while tubes 7 MS 8.4 and 6 MS 8.1 displayed a vivid dark green colour, Figure 6-5. The dark green colour could be due to what is termed as ‘green rot’. This green colour occurs

when chromium carbides oxidise, which is a common form of attack in nickel-chromium-iron alloys[60].

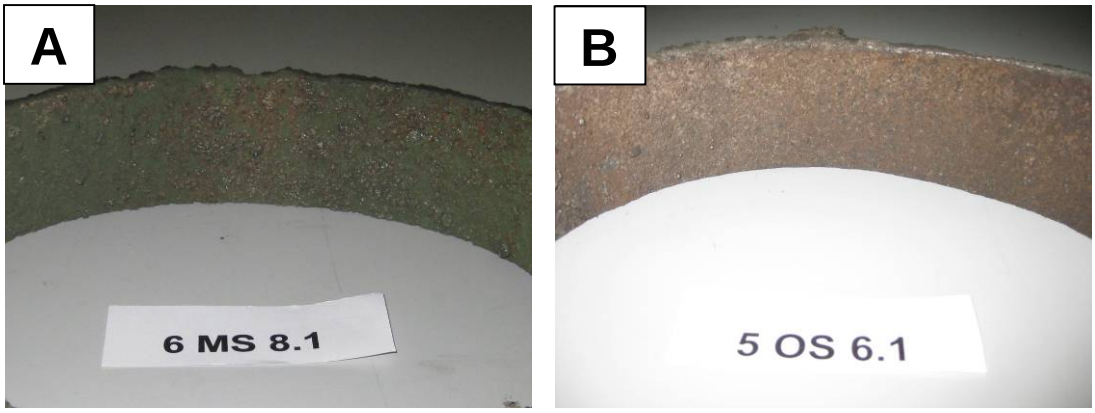

Figure 6-5 - Colour difference visible on inside surface

Visible signs of corrosion were evident on all weld failure samples, although in relative to the deformed samples, the level of corrosion was low. Sample 7 MS 8.4 was generally in a good condition with low amount of pitting on the inside surface. Samples 5 OS 6.1 and 3 OS 8.2 had greater levels of pitting, where the inside surface layer had started to 'scale' and break away from the base metal. Some of the scale on 3 OS 8.2 had started to crack allowing base metal to be exposed and subjected to further attack.

Sample 6 MS 8.1 showed visible signs of corrosion which were quite severe, primarily on the lower inside surface. The surface showed signs of scale, as if the metal had blistered and then cracked, Figure 6-6. The agglomeration of metal/oxide scale was easily removed from the base metal, leaving a pit of exposed metal underneath.

Similar blistering and cracks in the oxide layer are mentioned by Yoon et al[61], which formed due to the differences in thermal expansion between the oxide layer and the base metal.

Figure 6-6 – Scale layer on inside surface of tube 6 MS 8.1

6.4.2 Deformed Failures

In comparison to the weld failures, the general condition of the deformed and cracked radiant tubes was very poor with visible signs of extensive corrosive attack. Severe deformation was evident along both the firing leg and second leg leading to cracking through the thickness of the wall in various places, Figure 6-7.

Figure 6-7 - Severe deformation of firing leg leading to cracking (not shown)

Positioning of all cracks was always on the underside of the firing leg at transverse position to the direction of principle stress direction. Crack position on the Stein Heurtey designed tube was approximately 15cm from the weld region between firing

leg and first return bend. Cracks on the other three tubes (Almor mk2 design) were approximately between 30cm and 60 cm from the end of the firing leg.

On inspection of the internal surfaces, all four samples showed severe corrosion with material flaring and scabbing, leaving crevices and pits that recessed deep into the wall thickness. Most of the deformed samples had regions on the lowest part of the internal surface which were relatively smooth compared with other regions, Figure 6-8. In these smooth regions, pits and crevices were still evident, but they had been filled with what could be described as a green coloured oxide material.

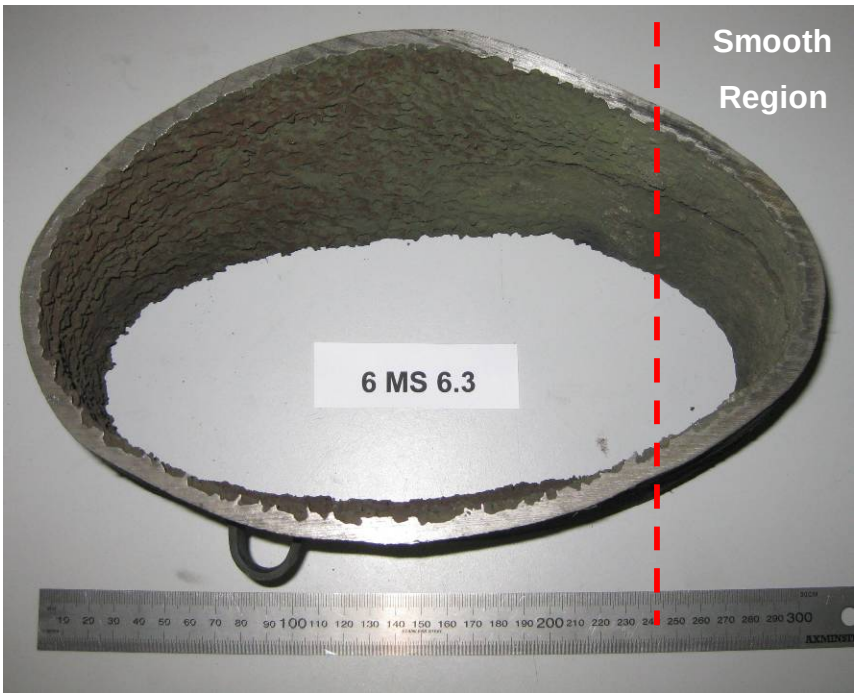

Figure 6-8 - Internal surface defects of a deformed radiant tube. Visible signs of wall thinning through deep crevices and pits

6.4.3 Dimensional Analysis

To quantify the deformation and wall thinning in the failed samples, a dimensional analysis was undertaken. All eight samples were measured at the crack position to determine the severity of failures and a comparison between the two failure types.

A single circumference measurement was made at the location of failure using a flexible tape. Several wall thickness measurements were taken using callipers at the

worst deteriorated area surrounding the crack. The lowest thickness measurement taken was recorded for comparison against other samples.

Figure 6-9 displays the measurements of tube circumferences. It is interesting to see that there is a significant difference between the weld failures and the deformed failures. As reported, the condition of the weld failures was relatively good and as a result the growth around the circumference is minimal, with only 20mm enlargement over original measurement. In comparison, the deformed failures had enlarged between 60 and 100mm over the original circumference.

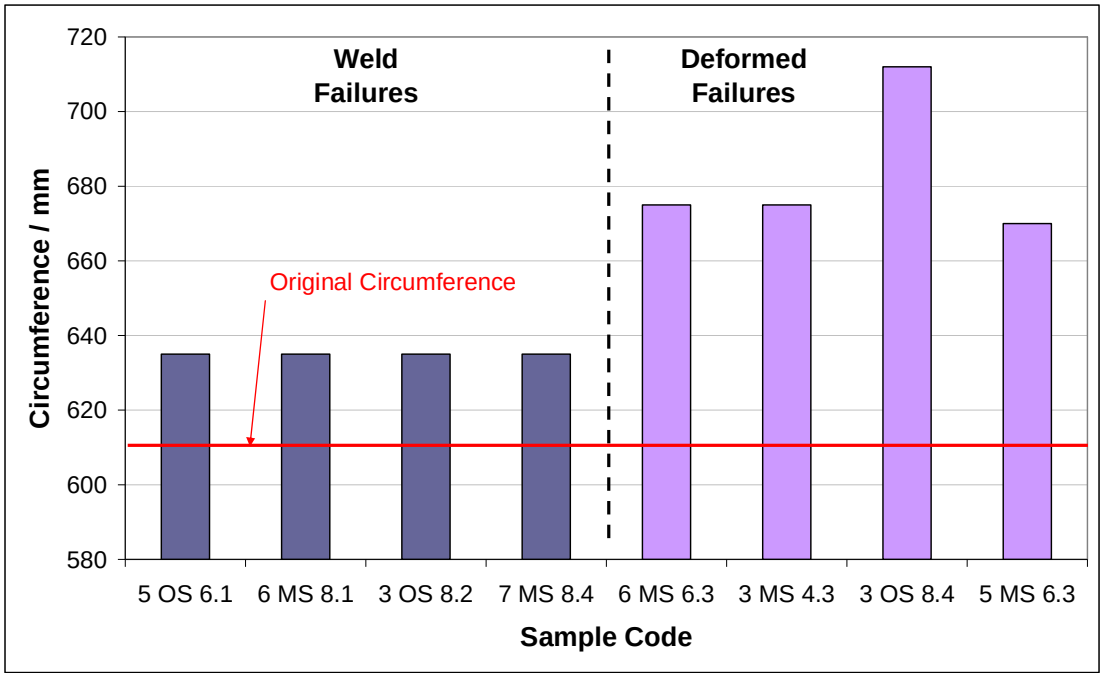

Figure 6-9 - Circumference of failed tubes in as received condition

Wall thicknesses were measured to indicate the severity of the corrosive attack and to show how much sound wall thickness was remaining in each sample. Again, due to the non degraded condition of the weld failures, the wall thicknesses were close too or within casting tolerances, Figure 6-10. The designed tube wall thickness is 8mm with a tolerance of +/- 0.5mm. The thinnest regions recorded on the weld failures were 6.5mm.

The deformed failures in comparison, recorded very low wall thicknesses. All three Almor tubes (grade HU) showed severe attack and wall thicknesses surrounding the failed area were nearly half the original value at 4.5mm. The Stein Heurtey tube (grade HP), which had been in service for over double the life of others, had a minimum wall thickness of 5.5mm. The concern with wall thinning is that tube metal thickness deteriorates with time, due to oxidation and therefore with constant load, stresses within the tube increase as the available cross sectional area reduces.

With wall thicknesses corroded to approximately half the original value in the deformed failures, it is no surprise that the firing legs have all deformed badly, resulting in failure. The resultant stresses on the firing leg increase with diminishing wall thickness, which has a detrimental effect on creep strength.

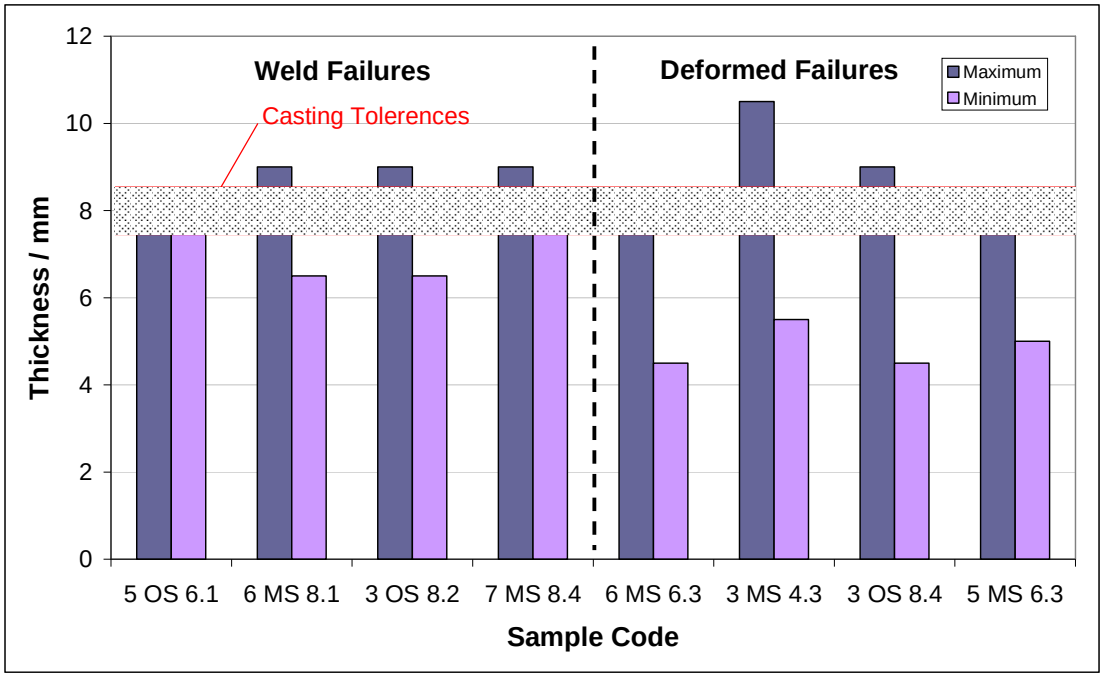

Figure 6-10 - Maximum and minimum tube wall thickness of each sample

6.4.4 Compositional Check

To check the composition of each sample, fine metal filings of each sample were sent for ICP-OES[62,63] analysis at Cardiff University. All samples, apart from 3 MS 4.3, had been manufactured from heat resistant stainless steel grade HU, 3 MS 4.3 was manufactured from HP. The composition for each grade is listed in Table 6-2. Figure

6-11, displays the results for chromium and nickel content in all Almor designed radiant tubes.

As-cast compositions were unattainable for all failed radiant tube samples, but all results were compared against material grade standards for heat resistant castings as outlined by BS EN 10295:2002[64]. For clarity, 3 MS 4.3 has been omitted from this figure as it was of a different grade, but element levels recorded were within material standards.

Table 6-2 - Table of composition of heat resistant stainless steel grades used at CAPL Port Talbot

Grade	Composition (%)					
	C	Mn (Max)	Si (Max)	Cr	Ni	Fe
HP	0.3 to 0.75	2.00	2.50	24 to 28	34 to 38	Rem
HU	0.35 to 0.75	2.00	2.50	17 to 21	37 to 41	Rem

The desired quantity of nickel and chromium for grade HU is 38% and 18% respectively. Allowable tolerances for these elements are 37-41% for nickel and 17-21% for chromium, which is highlighted in Figure 6-11.

Nickel levels of all samples fall within this tolerance band, although most are at the highest level of 41%. Chromium on the other hand, in most samples falls below or is at the minimum allowable level. Although not a significant amount, the low readings for chromium could be explained by the attack of the internal surface layer of the tube.

Chromium forms a protective, passive oxide layer, which protects the base metal from further oxidation. All samples have shown varying levels of attack and as a result the chromium rich oxide layer has degraded and possibly broken away from the sound metal due to spalling. Repeated scale attack could lower the chromium concentration at the alloy surface and allow the base metal vulnerable to further attack[65]. This could explain the low measurements observed in Figure 6-11.

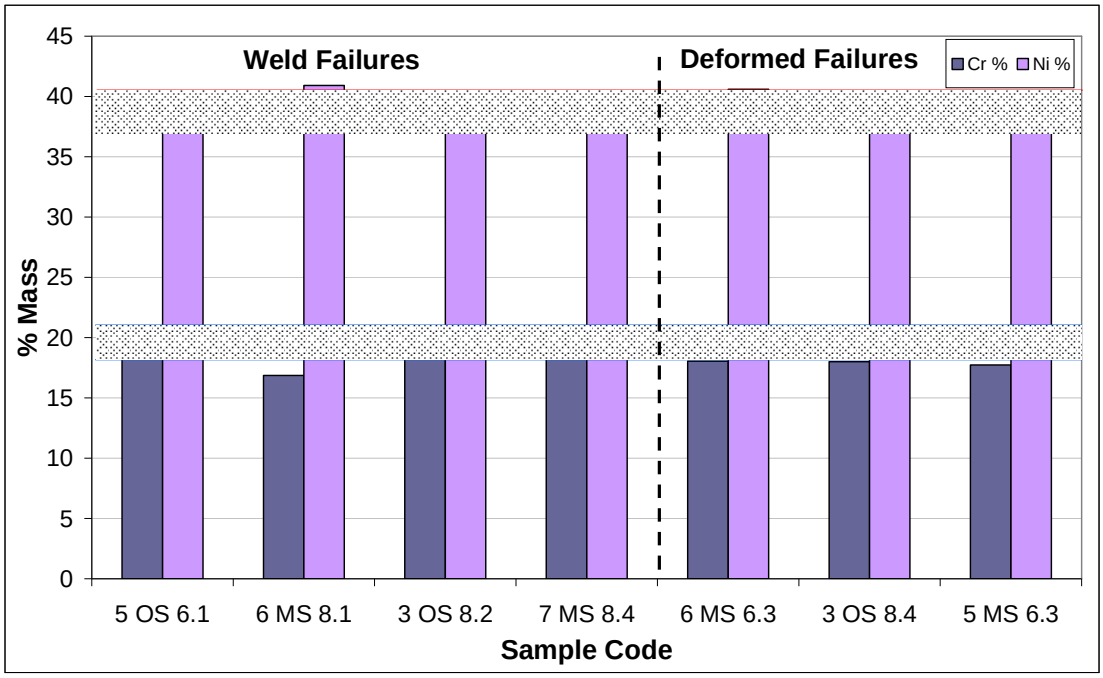

Figure 6-11 - Nickel and chromium content of each sample

6.4.5 Mechanical Testing

Hardness testing was undertaken to determine if the sample showed signs of variation in mechanical properties across the width of the tube wall. Tests were undertaken, according to BS EN ISO 6507[66], on surface polished samples mounted in Bakelite. A test force of 196N was used to allow a number of readings to be taken across the thickness.

A selection of samples were analysed and results are displayed in Figure 6-12. The first test was taken at 1mm distance from the outside surface of the tube wall, successive tests were at 0.6mm distances towards the inside surface.

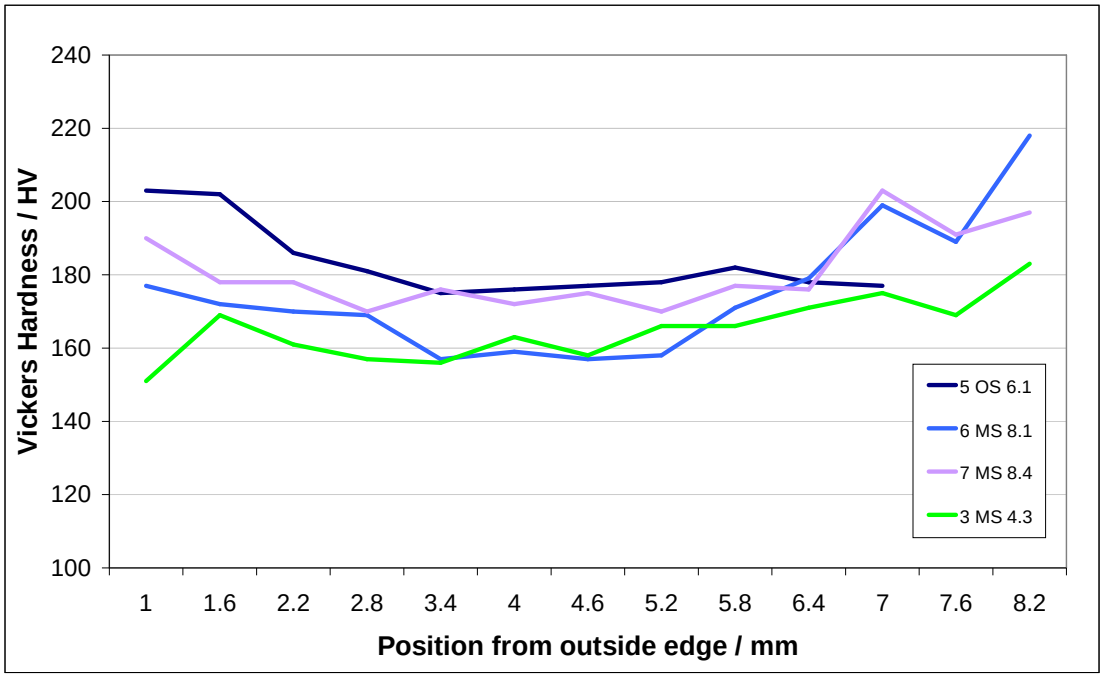

Figure 6-12 - Vickers hardness values across the tube wall thickness

It can be seen that the hardness increases in most samples towards the inner and outer surfaces by approximately a magnitude of 20HV. The only exceptions are samples 5OS6.1 towards the inner edge, where the hardness level has remained low at approximately 180HV and sample 3MS4.3 towards the outer edge, where the measured value was 152HV.

In comparison a new as-cast specimen was subsequently analysed and the results displayed in Figure 6-13. The hardness results for the new sample were very even across the width at approximately 180HV.

In most samples this identifies that there is some case hardening affect on aged samples at the internal and external surfaces. This could be due to carburisation, which is the diffusion of atomic carbon into the alloy forming a harder surface layer, due to the growth and coalescence of carbides (Chapter 2.1.5.3.4).

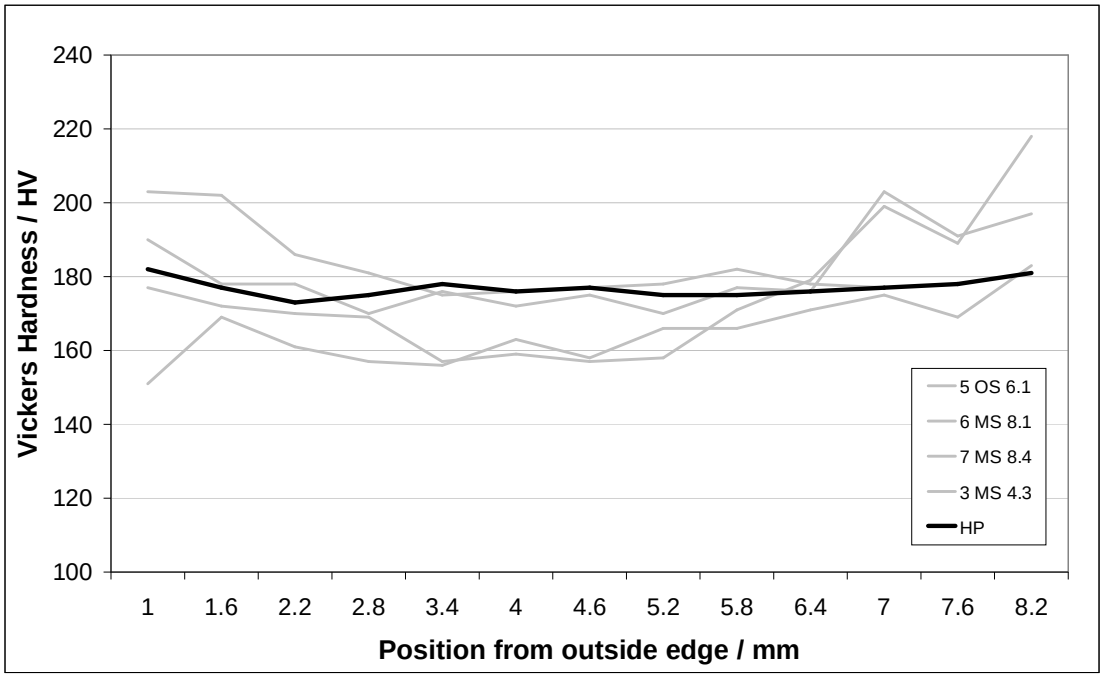

Figure 6-13 - Vickers hardness comparison of new as cast samples versus failed samples

6.4.6 Microstructure Analysis

6.4.6.1 Light Optical Microscopy

Samples of as-cast (new) material of HP grade was cut and polished to provide a benchmark for comparison. Light micrographs of the as-cast material are displayed in Figure 6-14 A and B. As shown, the material consists of equiaxed grains with chromium carbides in a lamellar formation at the grain boundaries; this structure is common for cast heat resistant stainless steels[3,6,67-69]. No voids could be detected in the grain structure, which is an inherent problem with centrifugally casted products at the bore surface[6].

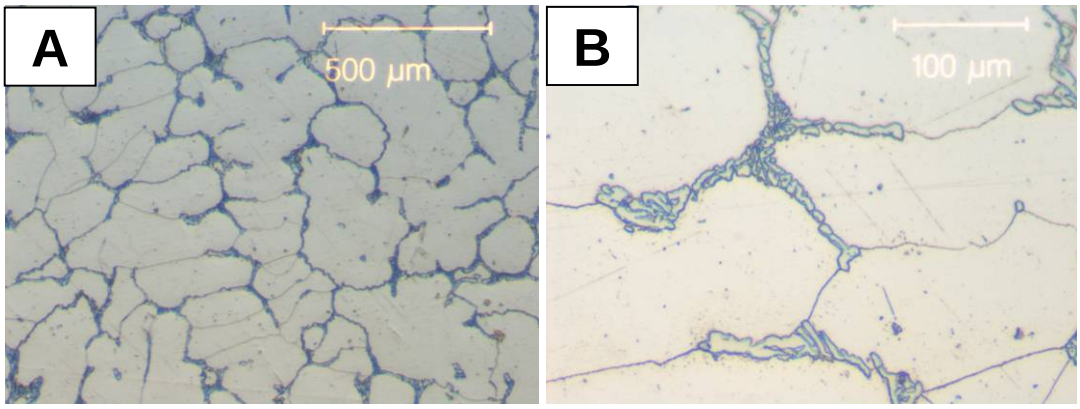

Figure 6-14 - Light optical micrograph of the general structure of as-cast HP grade material

Heat resistant stainless steels in cast form consist of an austenitic matrix with carbide precipitates. Such steels have excellent creep strengths at high temperatures provided the carbides are properly distributed throughout the matrix[6]. The effect of these carbides is to make the movement of dislocations more difficult, i.e. precipitation hardened. With a certain tempering time and temperature, the precipitation reaches a maximum. Further tempering time and a process of over-aging begins, this simply means the precipitate become larger and less numerous. When this occurs, the strength of the material decreases as dislocations can move more freely within the matrix[70].

6.4.6.2 Weld Failures

Low magnification optical micrographs of each sample were taken to outline the attack on the internal and external surfaces. Figure 6-15 shows the cross section of sample 5 OS 6.1, indicating regions near the internal surface, A, and the external surface, B. Evident in A is the protective oxide layer breaking away from the base metal. In doing so, it is exposing the base metal to further attack resulting in a crack of approximately 3mm in length, propagating towards the external surface. In contrast, the external surface B is in very good condition, with a very thin oxide layer which is in good condition.

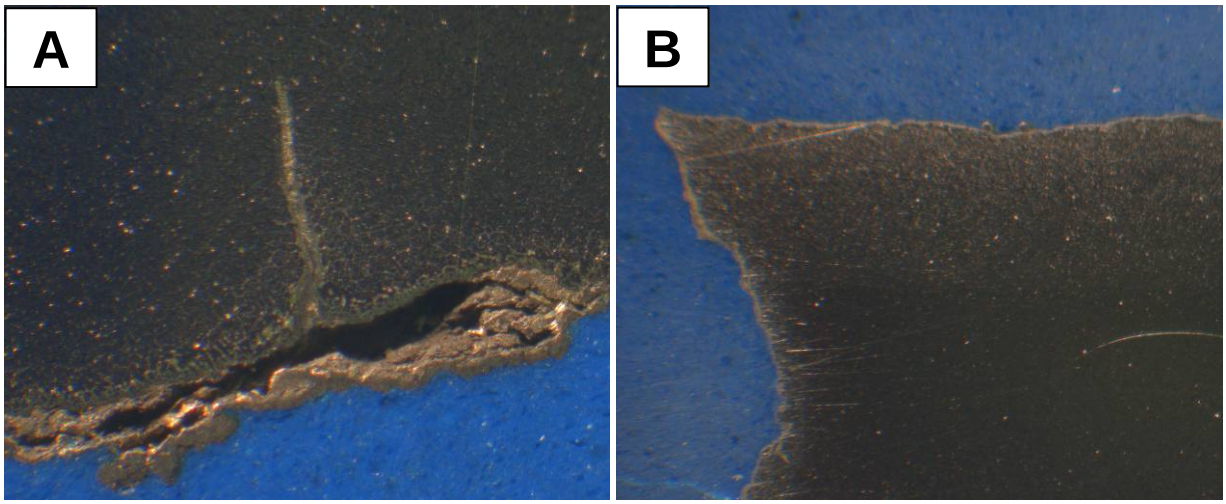

Figure 6-15 - Low magnification micrographs of sample 5 OS 6.1, indicating (a) internal oxide layer breaking away from base metal (b) external surface of radiant tube which is exposed to reducing atmosphere

Figure 6-16 shows how the oxide layer breaks up and cracks, eventually breaking off from the base metal and allowing fresh metal underneath to become exposed to further oxidation attack. Similar experiences have been detailed in Yoon[61], where repeated oxidation eventually led to wall thinning and fracture.

General oxidation, or scaling, is a major problem in elevated temperature operations and is particularly true in repetitive heating and cooling cycles. A thin layer of oxide, termed scale, forms on the surface of the metal due to exposure to air at high temperatures. This oxide layer breaks off when the metal cools due to differences in thermal expansion coefficients between the scale and the base metal[60,71].

Figure 6-16 - Example of how the oxide layer breaks up and cracks and eventually breaking off exposing fresh metal underneath to further oxidation

On closer inspection of the crack in Figure 6-15 A, it is possible to see that the surfaces of the crack have oxidised and areas of de-carburisation are visible surrounding the crack, highlighted in Figure 6-17. Towards the internal surface, there is evidence of sub surface oxidation which have resulted in voids below the surface. Surrounding these voids is an area of de-carburisation to a depth of approximately 300µm.

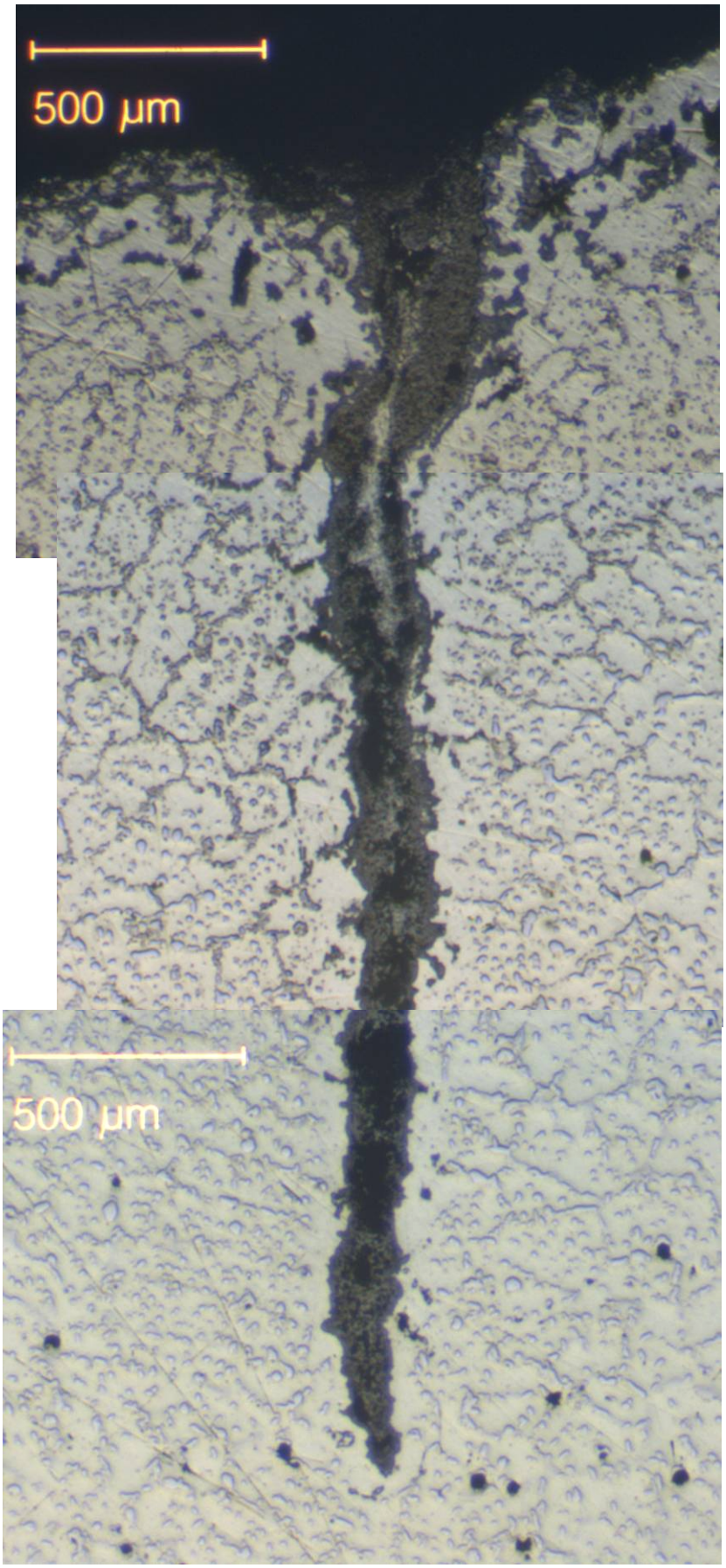

Figure 6-17 - High magnification micrograph of crack displayed in sample 5 OS 6.1 in Figure 6-14 (a)

The microstructure of the sample changes with depth from the internal surface. Below the carbide-free zone there is an area where the chromium carbides form a continuous network along the grain boundaries, which continues for approximately a depth of 2mm below the internal surface. Below this, towards the tip of the crack, the chromium carbides are more dispersed within the matrix but are beginning to agglomerate and spherodise. Similar evolutions in material structure across the thickness have been reported by Alvino et al[72]. Also present in this region along the crack tip, are voids, which seem to be determining the path of crack propagation.

To promote good creep strength, the carbides need to be in a fine dispersion within the austenite matrix. This can be achieved with relatively low temperature. But, when the service temperature is increased, the carbides become coarse and agglomerate and lose their effectiveness as a source of strength. Prolonged periods at elevated temperatures, enable the precipitation of carbides at the grain boundaries, which are undesirable as they embrittle the alloy and promote intergranular cracking[6].

The sub surface oxidation voids seem to have formed in areas occupied by the chromium carbides. Therefore, oxidation of the metal is preferentially along the grain boundaries (intergranular corrosion). This form of attack is also present at the surfaces of the crack.

The failure of the oxide layer and generation of a carbide free region below the surface is explained by Petkovic-Luton[67]. As a result of thermal fluctuations and erosion effects, the oxide scales tend to spall off, exposing fresh alloy surface to the process environment. The periodic spalling and regeneration of the chromium oxide layer causes the matrix beneath the surface to lose chromium at an enhanced rate. This results in the formation of a chromium carbide free zone due to the reduction in the activity of chromium in the solution. The thickness of the chromium-depleted zone is controlled by matrix diffusion and can reach a maximum value of 300μm.

Figure 6-18 displays the backscattered electron image of the area near the inner surface of sample 5 OS 6.1. (Result of the semi-quantitative microanalysis is included in appendix E). The effect of the spalling and oxide layer regeneration mentioned by Petkovic-Luton is visible in the outer layers of the sample. Region 10 is the

Iron/Nickel-Oxide phase breaking away from the base metal, with the passive chromium oxide layer (Region 9) regenerating beneath to provide further protection. The diffusion of chromium to the surface layer then produces the chromium carbide free zone beneath.

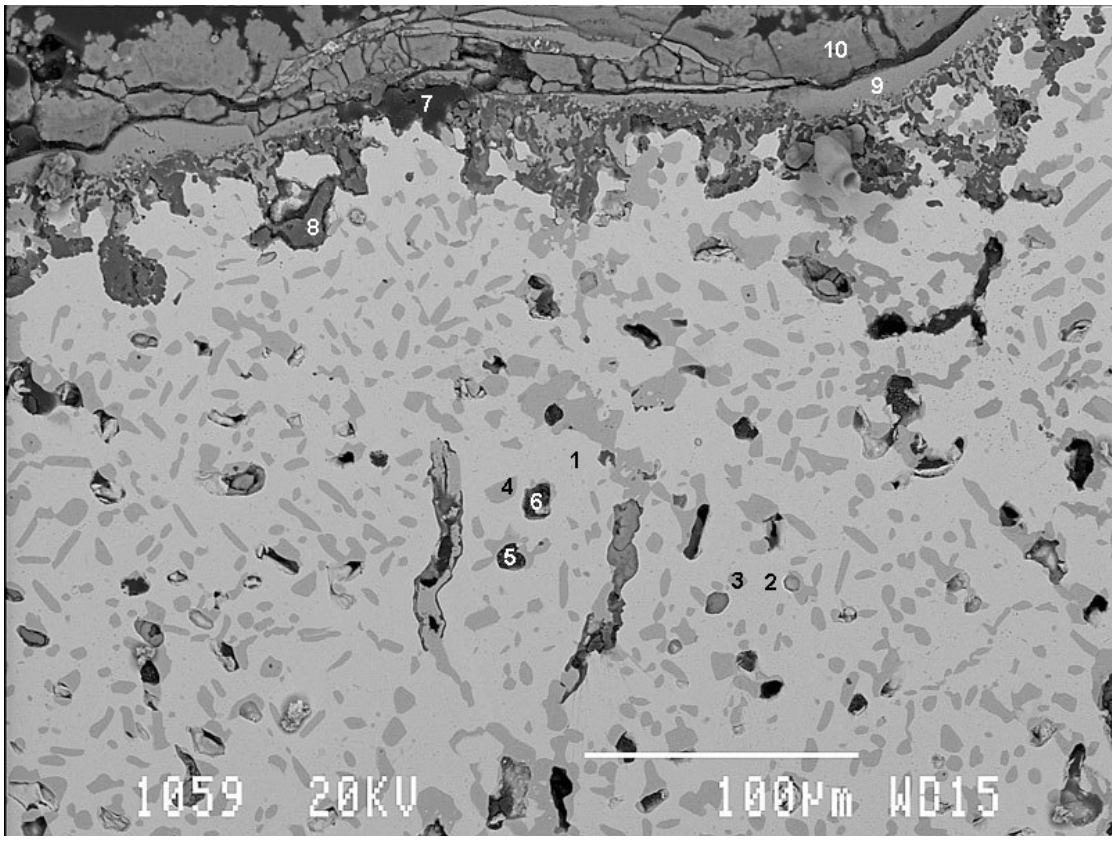

Figure 6-18 - Backscattered electron image of area near the inner surface of sample 5 OS 6.1.

Figure 6-19 displays a micrograph of the root of the weld where it is joined to the tube metal. The low magnification image, shows a region of deep oxidation in the tube metal and weld filler. On closer inspection, in the region of the weld fusion there is an area of aligned voids, which could potentially provide a path for crack propagation[73]. Indeed, the failure surface visible to the left of the weld bead could have potentially started due to aligned voids formed in the weld filler.

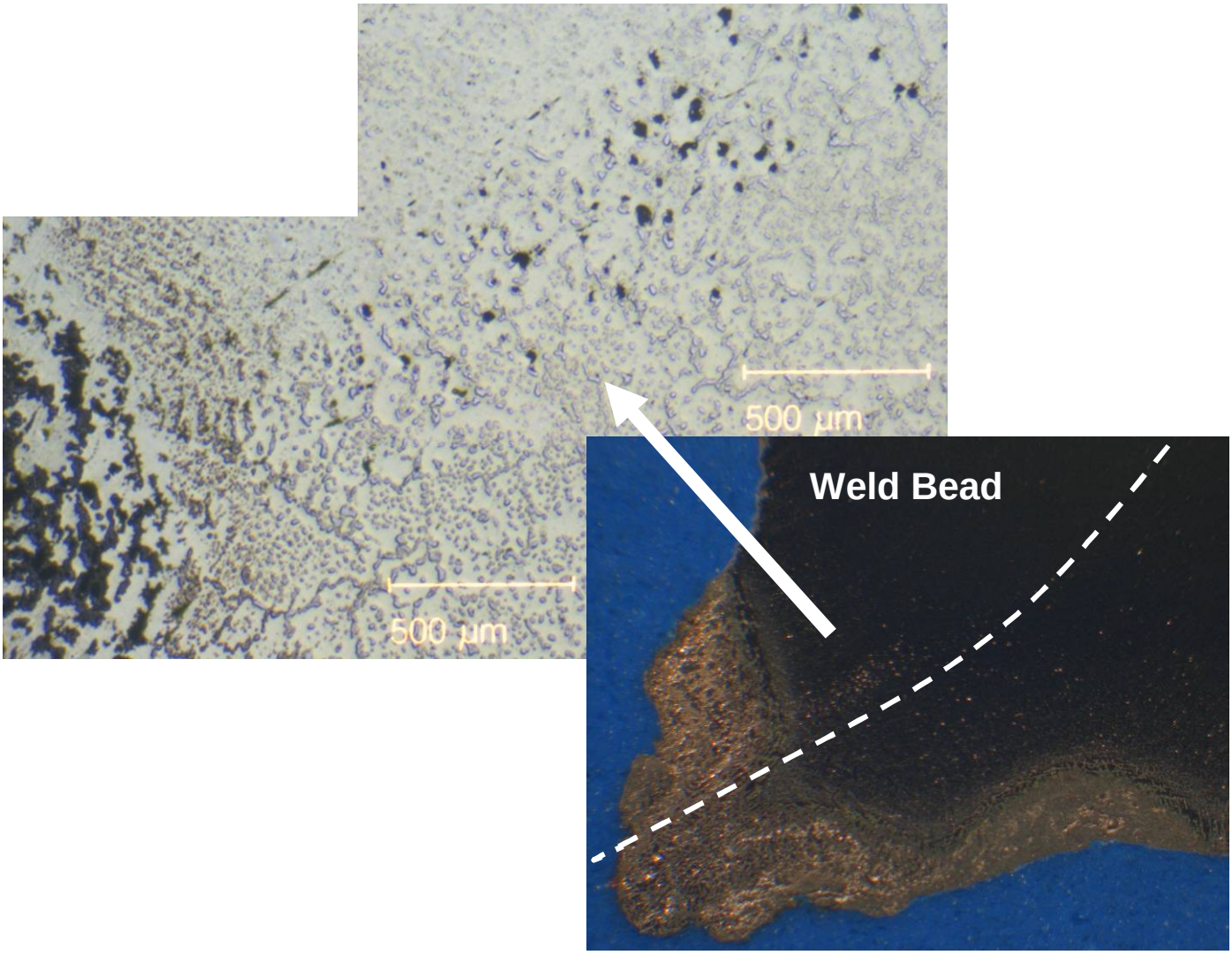

Figure 6-19 - Region of aligned voids at the weld fusion line in sample 5 OS 6.1

Interestingly, in sample 3 OS 8.2, similar results were found between the weld filler and tube metal, Figure 6-20. The figure shows that a crack had formed and propagated along the boundary at the weld fusion boundary. Furthermore, it is worth noting that the weld filler has not penetrated through to the inside surface of the tube. This indicates that the weld is unsatisfactory and a step has arisen between the tube leg and first return bend, thus creating a stress concentration factor. Indeed, weld penetration was evidently poor on all weld failure samples.

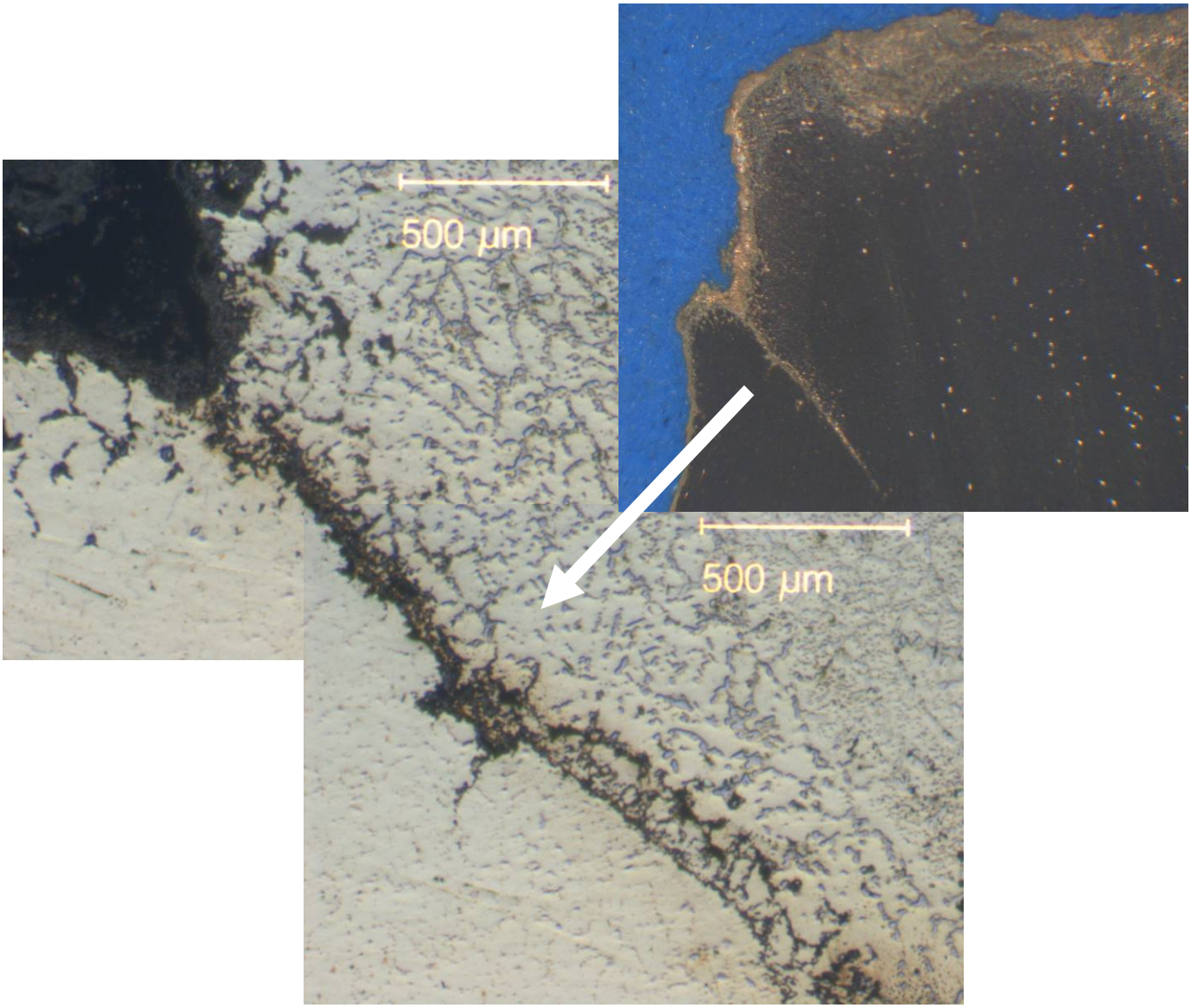

Figure 6-20 - Micrographs of sample 3 OS 8.2 displaying the formation of a crack between the weld filler and tube metal.

The increase in stress along at the highest temperature region of the radiant tube could have accelerated creep failure. Indeed, this radiant tube did have a short service life of just 3 years. What is also prevalent in this sample is the build up of a thick scale layer along the internal surface, which is cracked and porous, Figure 6-21.

This scale does not contribute to the strength of the base metal and fails to protect the substrate from further oxidation. This is evident as sub surface attack is present in the form of oxidation along the carbide rich grain boundaries. Below the surface is an

area of de-carburisation to a depth of approximately 250µm, followed by a continuous network of carbides situated at the grain boundaries.

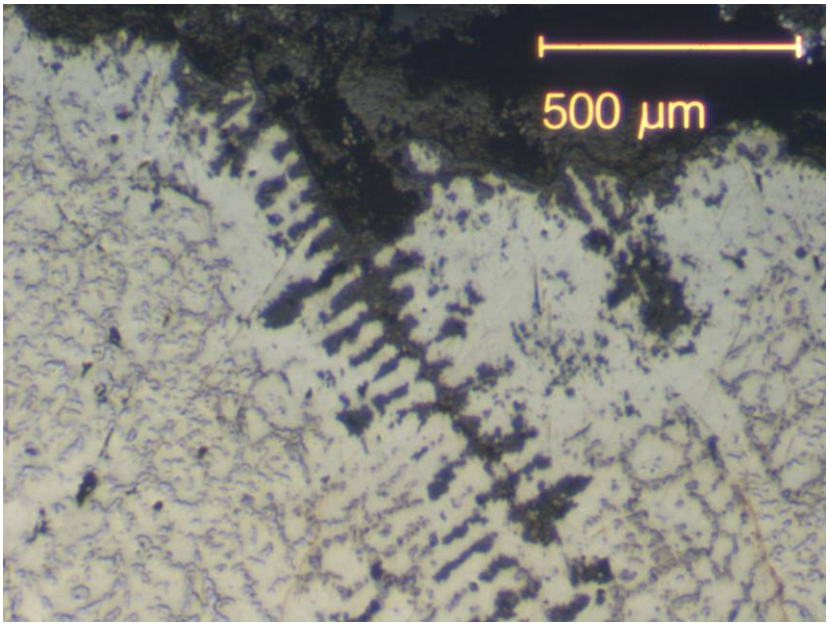

Figure 6-21 - Preferential oxidation along the grain boundaries resulting in metal loss in sample 3 OS 8.2

Not only are there surface defects, but from closer inspection of the interior, presence of voids were visible, which were congregated at the grain boundaries, Figure 6-22.

Figure 6-22 A, C and E display increasingly higher magnification of the interior of sample 7 MS 8.4. Visible in these images are the formation and agglomeration of carbides in a surrounding of relatively fine secondary precipitated carbides. Highlighted by 'black specs' are the formations of voids within the grain boundaries. To highlight the amount of voids present in these figures clearly, images A, C and E have been converted to black and white images, B, D and F respectively.

Similar voids throughout a Ni-Cr rich structure have been reported by Yoon[61], which suggest that the voids are formed when the material has been exposed to service temperatures of between 1090 to 1230°C. Temperatures of approximately 1050°C have been recorded on the external surface of a radiant tube in CAPL furnace.

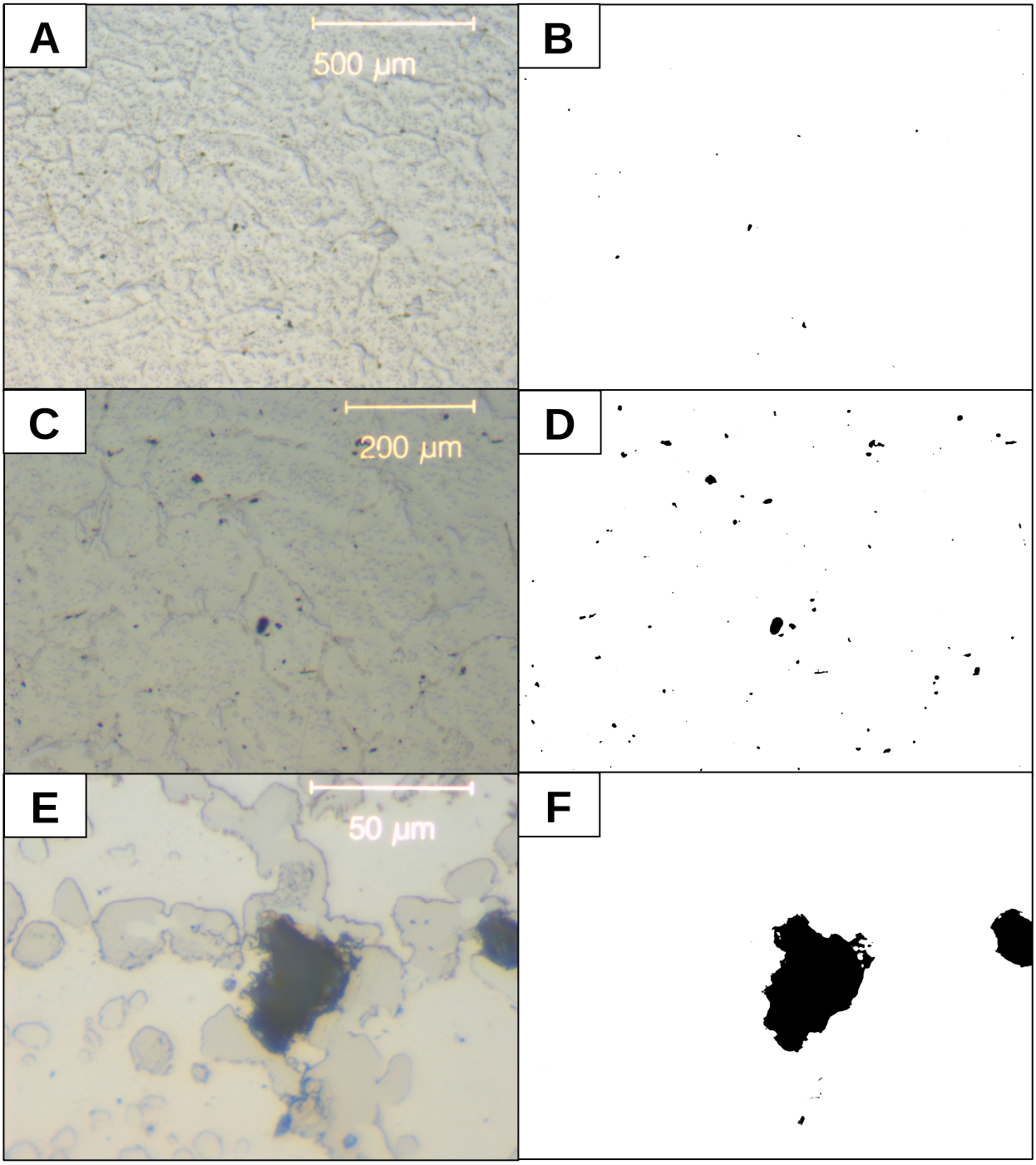

Figure 6-22 - High magnification micrographs of sample 7 MS 8.4 interior displaying the presence of voids at grain boundaries

6.4.6.3 Deformed Failures

As was seen from the visual inspection, the attack on the internal surfaces of the deformed radiant tubes was extensive and so was the deformation. The firing legs in all cases had lost structural strength and deformed due to exerted loads. Cracks had

formed in areas of deformation; therefore one theory could suggest that deformation occurred first and the cracking or fracture of the tube was secondary.

Considerable scaling was evident on the internal surface of all samples, which had broken up and detached from the base metal. As recorded earlier in the weld failures, the porous scale layer allowed the base metal susceptible to further attack. As a result, areas of de-carburisation were visible beneath the scale layer surrounding voids of sub surface oxidation, as highlighted in Figure 6-23.

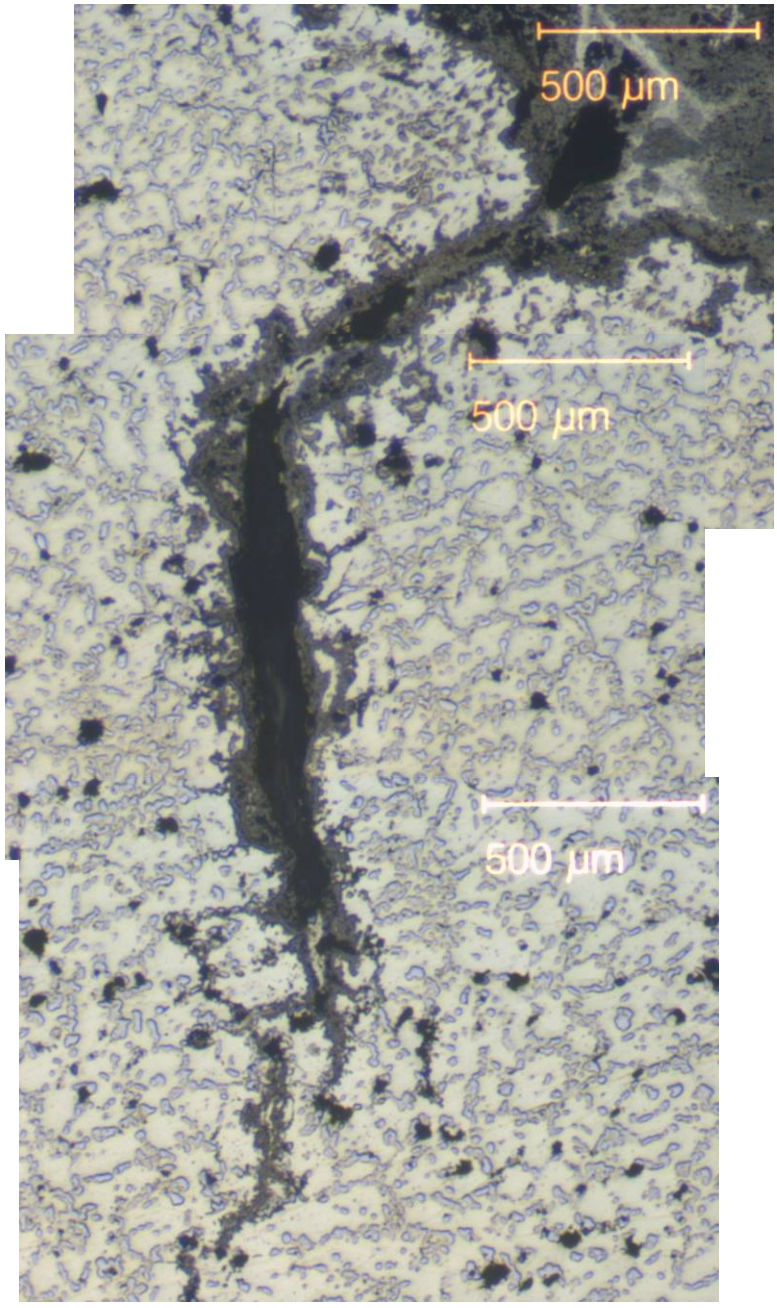

Figure 6-23 - Crack in sample 3 MS 3.4 which is propagating along the network of voids

Voids were present in all deformed samples, none more so than sample 3 MS 3.4, Figure 6-23 and Figure 6-25. The voids were confirmed through higher magnification optical microscopy, Figure 6-24, and proved not to be pullout marks through surface polishing.

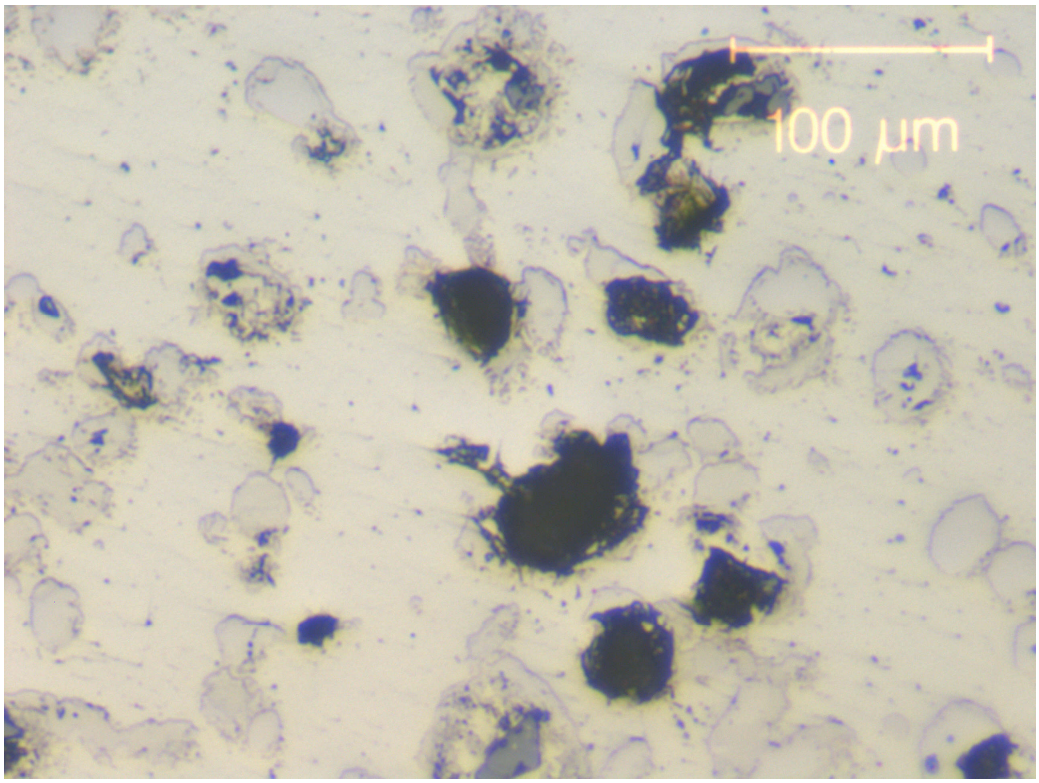

Figure 6-24 - Higher magnification inspection of void formation in interior of sample

Considerable amount of voids were present throughout the sample, which could be due to the deformation in the firing leg, age of the tube or high service temperature. 3 MS 3.4 had been in service for over 9 years and in this time the carbides have agglomerated and spherodised leading to losses in structural strength.

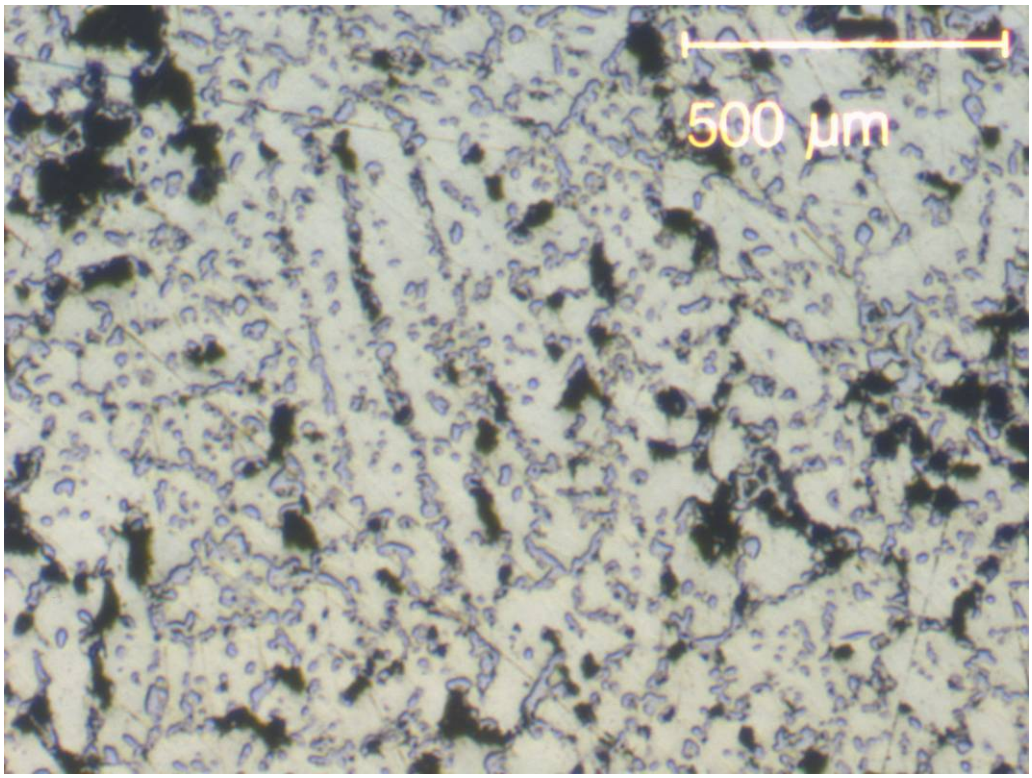

Figure 6-25 - Interior structure of sample 3 MS 3.4. Evidence of considerable void formation through sample

Similar structures were seen in samples 3 OS 8.4 and 5 MS 6.3, Figure 6-26 A and B respectively, which also had deformed very badly. May et al[74] report that for the formation of structures seen in Figure 6-26, the material has been exposed to temperatures above 900°C.

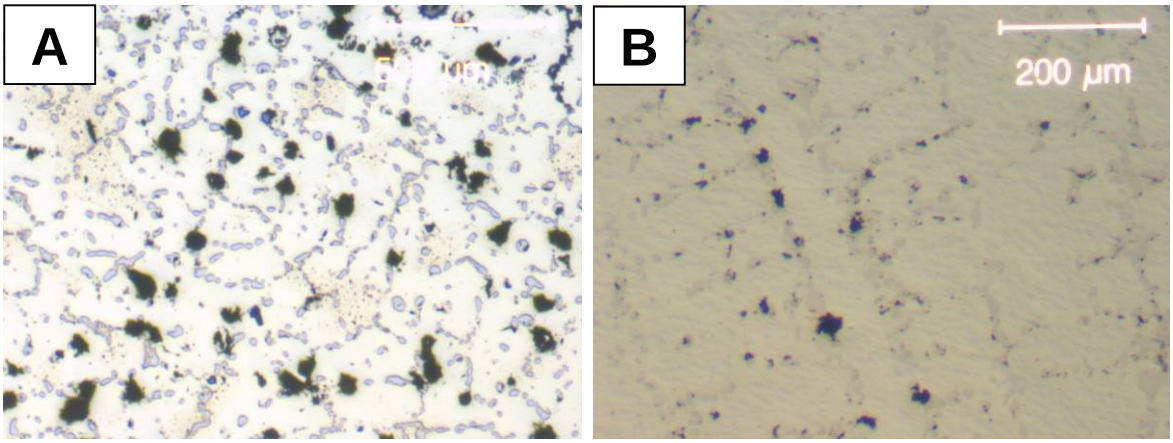

Figure 6-26 - Interior structure of 3 OS 8.4 (A) and 5 MS 6.3 (B) with large amounts of voids present

Micrographs of sample 6 MS 6.3 in Figure 6-27, correlates with what was identified in Figure 6-23. The failure of the oxide layer at the internal surface subjects the substrate to further oxidation. Due to the continuous network of carbides formed at the grain boundaries, from exposure to excessive temperature[4], the oxidation attacks the carbides (intergranular corrosion) and initially propagates along the boundaries.

Voids formed within the structure, possibly through creep[14] or thermal cycling[6,67] (due to differences in thermal expansion of carbides to austenite), provide a path for the crack to follow. Eventually, the crack progresses through the thickness of the material at the grain boundaries and fractures the external surface.

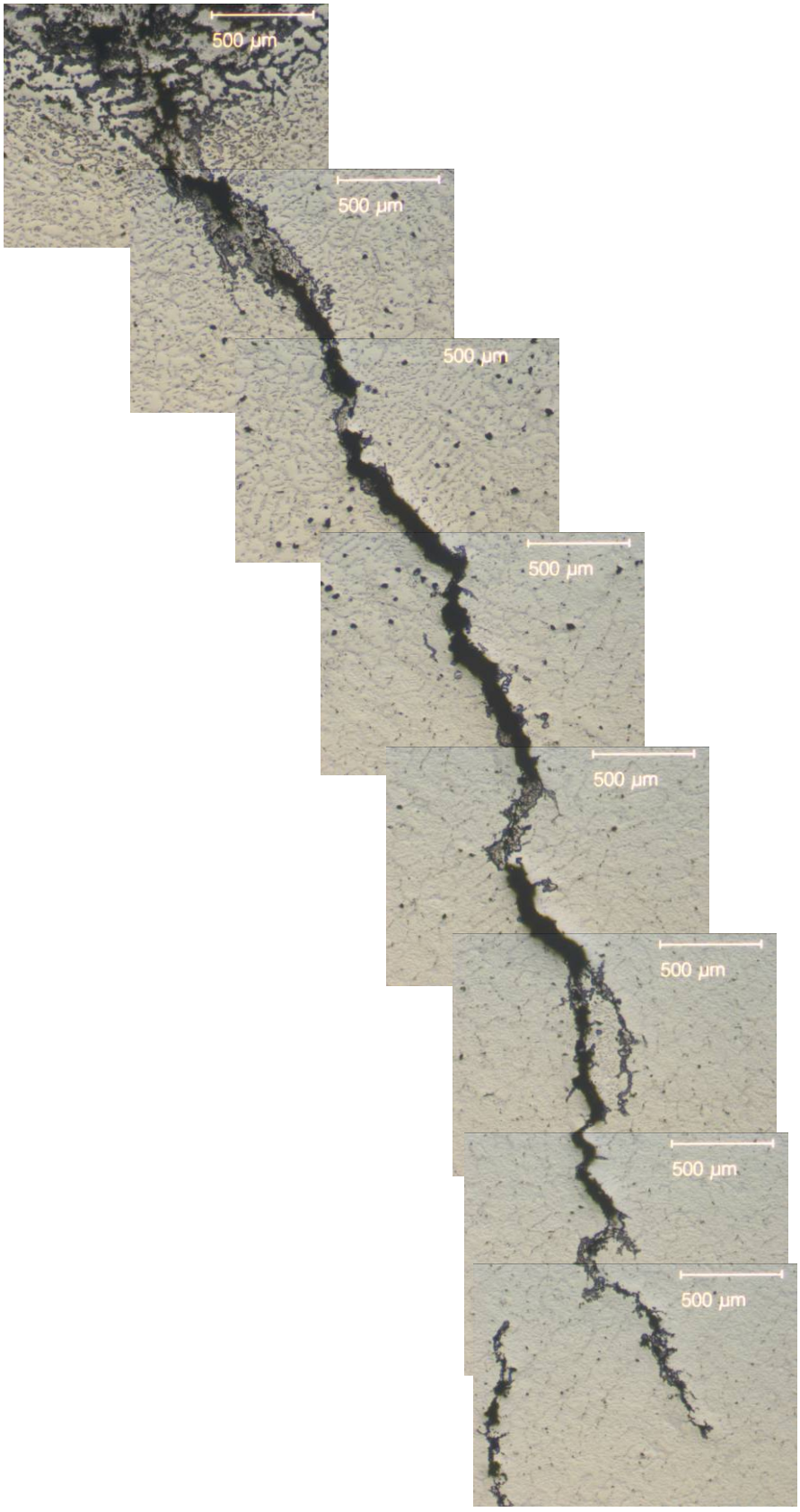

Figure 6-27 - Deep crack in sample 6 MS 6.3, initiated due to a failure in the oxide layer and progresses along the grain boundaries following voids which have developed in the structure due to creep deformation

6.4.7 Scanning Electron Microscope (SEM) Analysis

6.4.7.1 Weld Failures

A selection of samples was analysed by SEM to provide a detailed image of the fracture faces. Figure 6-28 shows the weld root of sample 3 OS 8.2 and the exposed surfaces subjected to oxidation. The region between the weld root and the inside surface is the step discovered between the firing leg and first return bend. This step exists due to the failure of the welding process, either through lack of preparation prior to welding or poor welding practices.

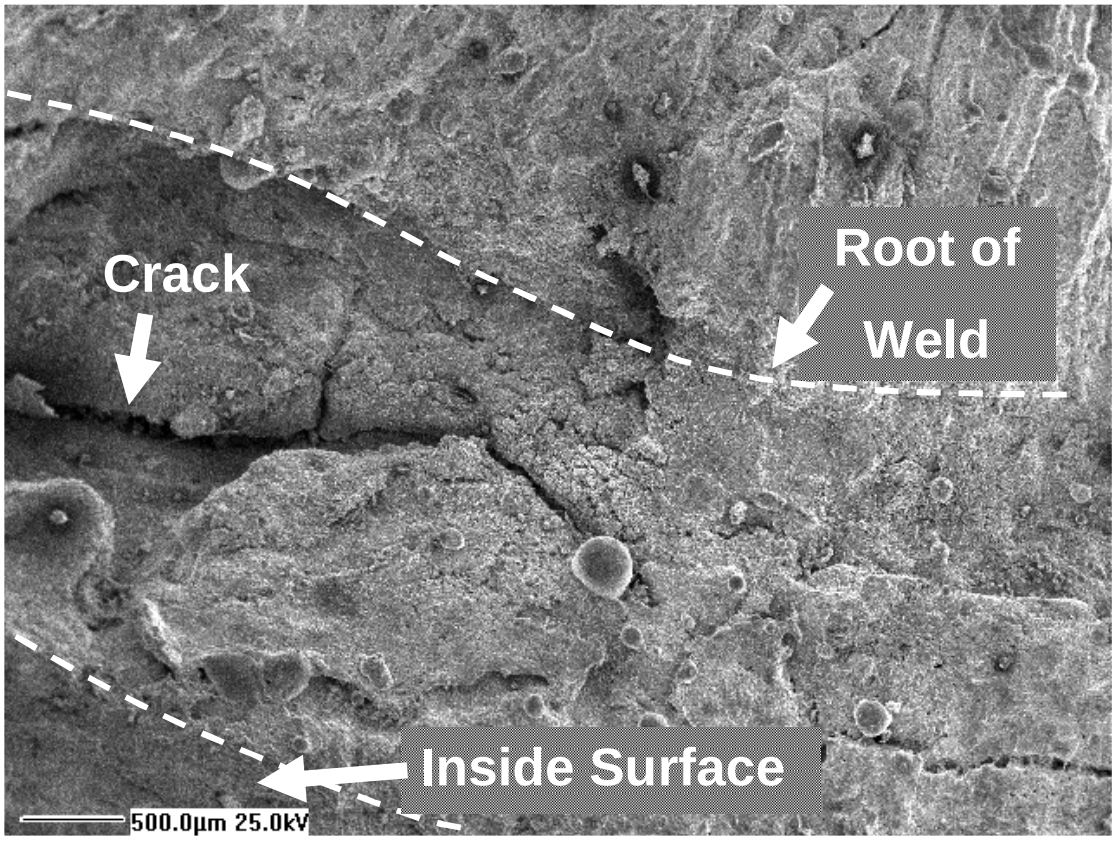

Figure 6-28 - SEM image of sample 3 OS 8.2 at the weld root showing the lack of weld penetration and cracks at the weld root

Not only does the step create a stress concentration factor within the tube, but it allows the metal at the base of the weld to be attacked through oxidation. Highlighted in Figure 6-28 is a crack, which initiates at the weld root and propagates along the fusion line (as discussed earlier in the chapter) potentially creating a mode of failure.

There is a high possibility that the failure caused in this radiant tube was due to a similar scenario.

Figure 6-29 is another image at the base of a weld region in sample 6 MS 8.1. Again, similar characteristics are seen here, with a step generated due to a sub standard weld bead. The images focus closely on the scale build up at the weld base to highlight the large number of cracks in the oxide layer. Figure 6-29 B and C in particular show how porous and granular the oxide layer is.

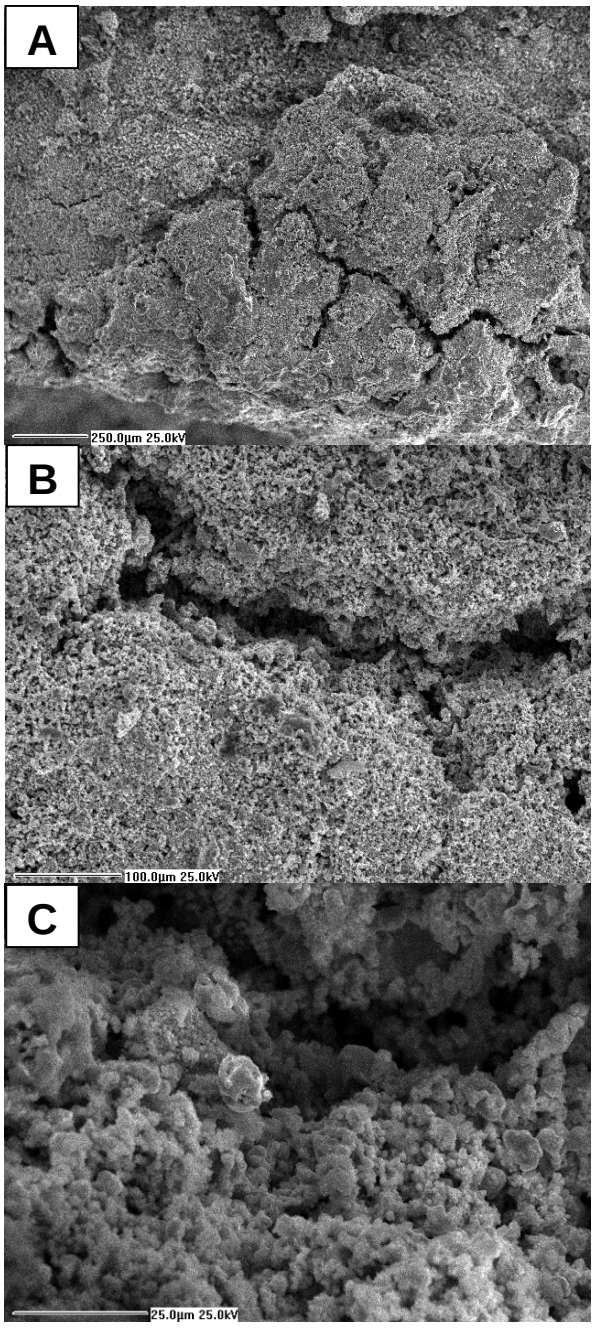

Figure 6-29 - SEM images of cracks formed in the scale at the base of a weld (A), Close up of crack (B) and highly porous oxide layer (C)

6.4.7.2 Deformed Failures

Samples 5 MS 6.3 and 6 MS 6.3 were analysed by SEM to provide a detailed view of the fracture surfaces. Figure 6-30 shows the fracture surface for sample 5 MS 6.3, which clearly identifies significant cracking throughout the tube wall thickness. These images suggest that the sample has failed from creep cracking[14,75], which is supported by the evidence viewed from the light optical microscope analysis that suggested the cracks were following a path of creep formed voids within the matrix.

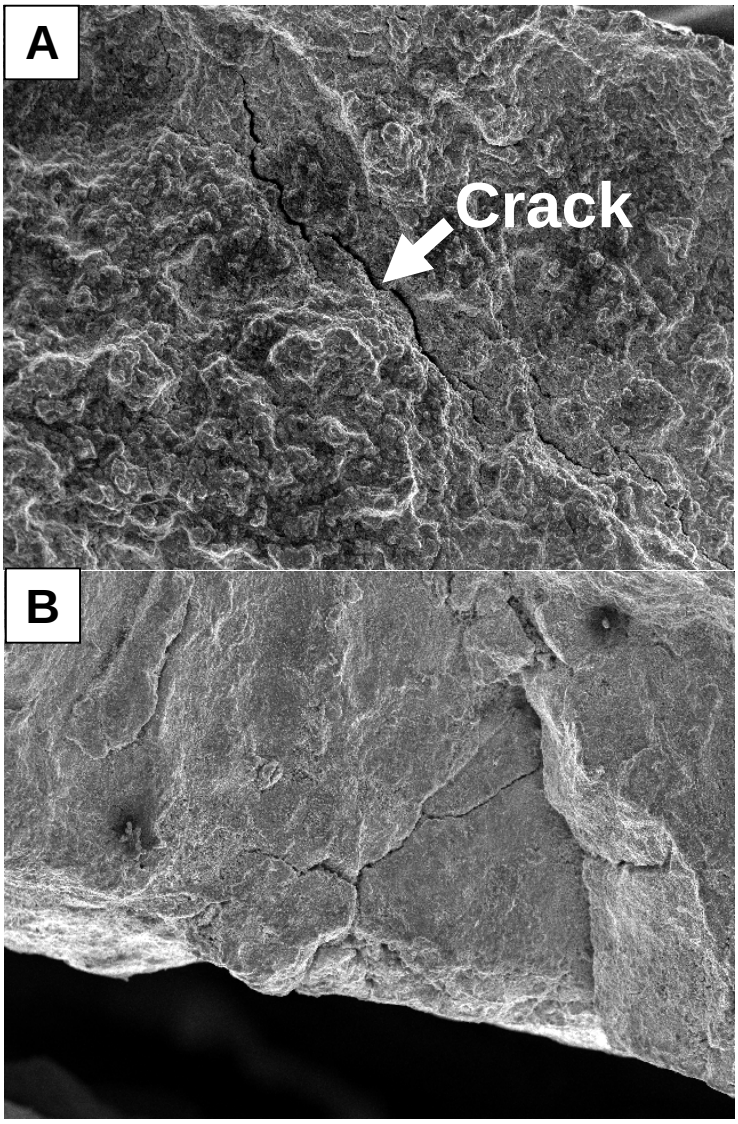

Figure 6-30 - Cracks highlighted in fracture surface of sample 5 MS 6.3

Similar cracks are seen in Figure 6-31, which strengthens the case for failure by creep cracking. The cracks are similar to intergranular fracture[75] which propagate from the internal surface through the material structure to the external face and causes eventual fracture.

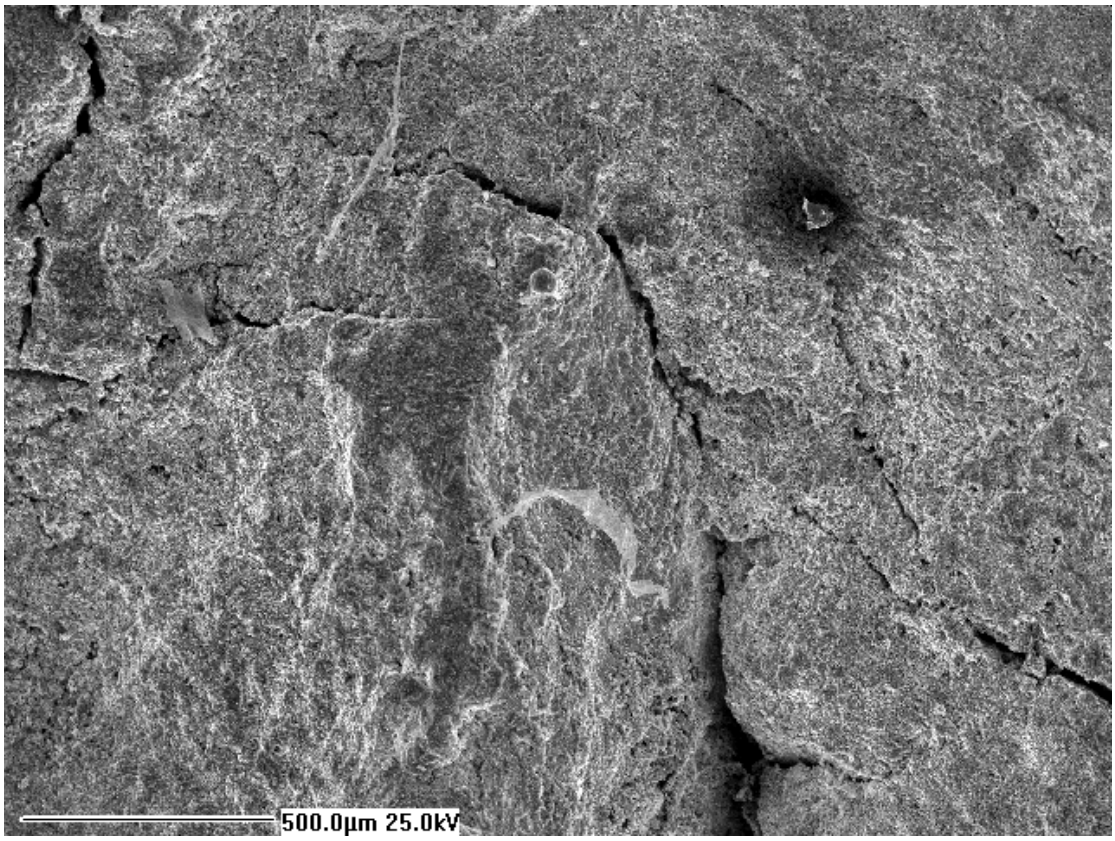

Figure 6-31 - Cracking propagating from the inner surface towards the external face in sample 6 MS 6.3

6.5 Discussion

At the case study site, radiant tubes fail predominantly due to cracking and deformation. Weld failures were associated with the second generation radiant tubes designed by Almor, while deformation is a failure generally seen across all tube designs.

It was found that the weld failures were due to poor weld penetration during the fabrication of the radiant tubes, which resulted in a stress concentration factor being introduced in the join between the firing leg and the first return bend. Under

mechanical and thermal stresses, during normal operation, this stress increase resulted in premature failure of the weld region.

In all weld failures, the general condition of the radiant tube was relatively good compared to the deformed failures. Deformation and internal surface attack was low, but visual signs of oxidation, creep void formation and intergranular corrosion were still present.

All deformed samples showed signs of severe attack through oxidation and spalling. The extent of attack was so great that approximately half the wall thickness had corroded away. This combined with a cumulative detrimental affect from creep void formation leading to cracks propagating along the grain boundaries following paths of voids.

Failures in heat resistant casting material are very well documented as they are widely used in the steel making and petrochemical industries. Material failure due to cracking and deformation is the prevalent factor, which is predominantly due to excessive service temperatures[4,6,14,61,69,72-74]. From the temperature analysis conducted on a radiant tube at the case study site, high temperatures of approximately 1050°C were recorded at the end of the firing leg, the location for all failures experienced at CAPL.

Figure 6-32 displays the oxidation process for heat resistant alloys in oxygen-carbon containing environments[67]. The microstructural degradation can be highlighted in five stages, which are:

1. Initial oxide scale formation
2. Oxidation in a carbon-containing environment
3. Internal redistribution of chromium and carbon
4. Inward carbon diffusion
5. Oxidation of carbides

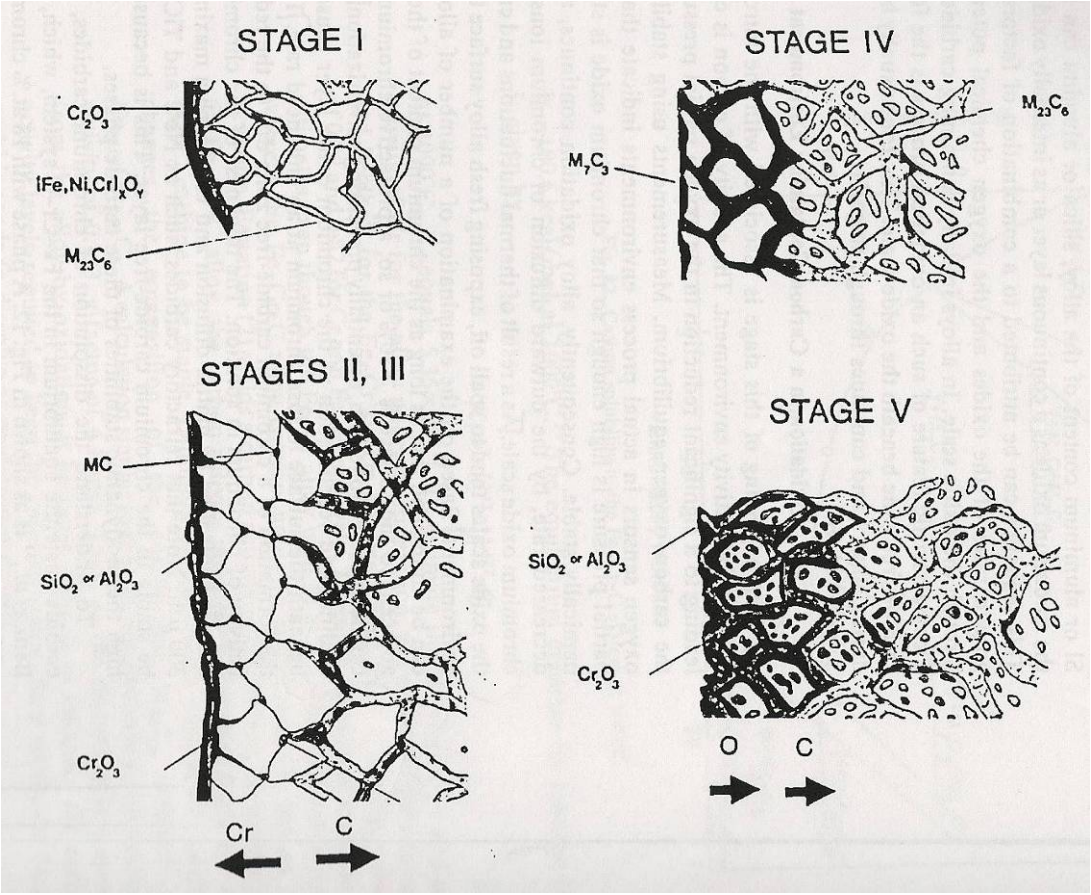

Figure 6-32 - Schematic representation of the five stages of microstructural degradation in carbon-oxygen-containing environments[67]

Evidence of the microstructure evolution/degradation outlined in Figure 6-32 is seen in failed samples analysed in this chapter. The high temperatures experienced in the firing leg contribute to this oxidation process, but can also break down the oxide layer[4,61,71]. The heat resistant stainless steel materials protect the base metal through the formation of a passive Cr_2O_3 oxide layer, which resists further oxidation. At service temperatures of above 1010°C, the Cr_2O_3 layer breaks down to a volatile CrO_3 layer, which doesn't provide the necessary protection. High gas flow rates also greatly accelerate this process[71].

An increasing oxide layer thickness, either through normal or accelerated oxidation, creates further problems as the differences in thermal expansion coefficients between the base metal and oxide film can accelerate attack through spalling. Contributing to this detrimental effect is the temperature cycling of the material[65,71]. The continuous

change in temperature or rapid cooling can accelerate the spalling of the oxide layer through the generation of internal stresses[76], which promotes small sections of oxide layer to break away from the base metal.

An increase in the oxidation rate of the material results in less cross sectional area of base metal available to provide the necessary strength required. This increases stress in the structure and can promote failure due to creep. Evidence of voids formed at the grain boundaries were seen in all samples, some had greater levels than others. This shows that creep is having an effect on the material and is promoting cracking along the thickness of the material.

Creep is a function of stress and temperature. The higher these values are, the less service life available from a particular component. Radiant tube temperature within the furnace has previously been discussed and found to be excessive in certain regions of the tube. Stress has not been quantified, but the attack of the material through oxidation and spalling increases the magnitude of stress in the structure by reducing the cross sectional area available of base metal, which is required to support the tube structure.

Evidence of high service temperatures is also provided by the change in the microstructure of the base metal. The coarse nature of the carbides and their agglomeration provide an indication that the metal has been exposed to high temperatures. Further to this, is evidence of continuous network of grain boundary carbides, which form due to exposure to elevated temperatures[4,6].

6.6 Summary

In summary, the radiant tube material is subjected to excessive service temperatures, which is accelerating the oxidation rate and breaking down the passive oxide layer, increasing the formation of scale and reducing the tube wall thicknesses. The changes in temperature and differences in expansion coefficients between the base metal and scale promote spalling, which allows fresh base metal to be exposed to further oxidation.

Cracks can develop under the scale and can grow along the grain boundaries where voids have formed through creep movement. The high service temperature also changing the structure of the base metal and producing continuous network of carbides at the grain boundaries, which has a detrimental effect on material creep strength.

The continuous annealing line, CAPL at the case study site, must consider the balance of heat input into the furnace and reduce radiant tube temperature in certain zones. This coupled with careful tube and support design could also reduce the stress generated in the material. Achieving both would have a considerable effect on the service life of a radiant tube.

7 Finite Element Modelling of a Radiant Tube

7.1 Introduction

This chapter discusses the finite element model produced using a Simulia Abaqus FEA programme to emulate the different designs of radiant tubes used at CAPL Port Talbot. Using collated data, gathered as part of the project, for temperature and material properties an accurate model was built and analysed. Results for the various tests conducted are discussed hereafter.

Having already analysed the temperature and failure types of the radiant tubes in chapters 5 and 6, it was decided to analyse the stresses within the structure due to the weight of the material and stresses induced from thermal expansion. Understanding the location and magnitude of the stresses can aid in determining the failure type and help to improve the design of future radiant tubes.

Stress plays a major role in the life of a radiant tube as it can increase deformation due to creep and in severe cases can cause material failure. Temperature has a significant effect on stress, as differences in thermal expansion can induce stresses within the material. As discussed in chapter 5, the radiant tubes have a temperature profile with maximum temperatures in the vicinity of the end of the firing leg and a difference of approximately 60-70°C is observed between the firing leg and exhaust leg under normal operating conditions.

Computational modelling of stress has been conducted previously in radiant tubes to either determine the stress values[77], determine the life of a radiant tube[4], or used as a comparison between different burner systems[78].

7.1.1 Building the Model

Simulia Abaqus FEA version 6.7 was utilised for the finite element modelling of the radiant tube. The software allows the formation of a structure in 3D mode and then boundary conditions and properties can be applied to the structure to replicate real life scenarios.

Models were built in parts, using 3D sketch tools, to form the various items of a W type radiant tube. The inner and external diameters of the tubes were sketched and then extruded to the various lengths to form the tubes, while the return bends had to be extruded along a path of known radius of curvature.

Various supports were built onto the return bends, to replicate the different designs used at Port Talbot CAPL. All parts were joined together to form a radiant tube, using a 'mating' tool, ensuring that all parts behaved and reacted as a single entity.

To create a more realistic model, furnace wall supports were built and fixed in position, with displacement constraints, to provide a support for the return bends. These supports were not subjected to thermal or displacement loadings, but did restrict the movement of the return bends in certain planes.

Material properties, at a range of temperatures, were entered into the software and applied to various parts of the tube according to the design. Meshes were then applied to each part and refined in areas of intricate detail. Finally, displacement restraints were entered for selected surfaces, to restrict movement in certain planes.

7.1.2 Designs

As previously documented, CAPL Port Talbot has modified the radiant tube design several times since the commissioning of the line. There has been various designs used, and although the modifications have been minimal, the failure mechanisms observed have been varied.

To understand the effect of the design changes on stress within the structure, all design changes were built into the model. Figure 7-1 highlights some of the modifications made to the model. Image (A) shows the saddle support utilised by Stein Heurtey to support the centre bend. (B) displays the sliding channel as used by Almor. (C) depicts the Stein Heurtey designed tube and (D), highlights the new support position for the centre return bend.

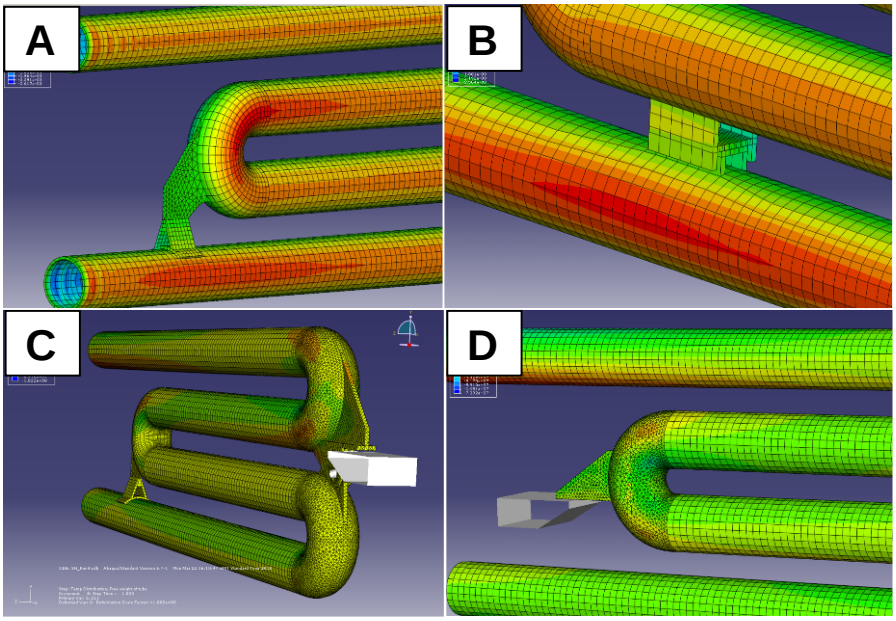

Figure 7-1 - Images of the various supports used as part of the development of the radiant tube undertaken by Port Talbot CAPL.

7.1.3 Boundary Conditions

Boundary conditions are required to subject the model to similar conditions as seen in operation. The boundary conditions applied to the model were deflection constraints to simulate mounting positions, material properties, which allowed the model to expand and deform according to material properties and temperature profiles, so that the model simulated the radiant tube in operating conditions within the furnace.

Two different material properties were used for the material constraints to ensure the model deflected and expanded in a similar manner as a real tube. Two different alloy compositions are utilised for the production of a radiant tube to minimise cost. The lower specification alloy is used in the lower temperature regions of the exhaust leg and third leg. The higher specification alloys are used for the lower half of the tube and all return bends.

Material properties were kept constant for all analyses with HP grade chosen for the higher temperature region, being the lower two tubes and lower return bend and HK-40 for the lower temperature region; upper two tubes and central and upper return bends. To ensure accurate material properties at the higher temperatures, data was

entered according to temperature range. Data sheets for both alloys are included in appendix F and G.

Lateral and rotational constraints were enforced on the end surfaces of both the firing leg and exhaust leg. These constraints mimic the flange attachments to the furnace wall, which fix the radiant tube in place. A gravitational acceleration was applied to the whole model to ensure forces were generated due to gravity.

Three different temperature profiles were used to represent the normal working conditions of the radiant tube. Figure 7-2, displays 3 temperature profiles, 800, 900 and 1000°C respectively, which were taken from the multi thermocouple tube installed in zone 7. This ensured that the model was subjected to exact profiles seen in the furnace to provide an accurate representation.

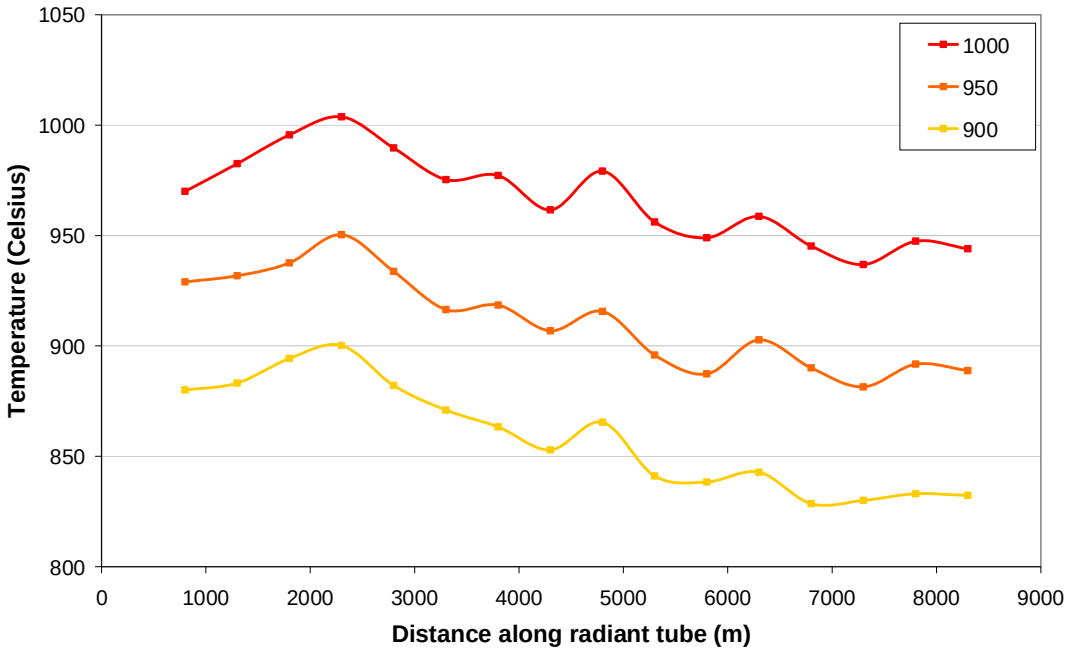

Figure 7-2 - Displaying the three temperature profiles used to simulate radiant tube conditions within the furnace. Temperature profiles were taken from multi thermocouple tube installed in zone 7

Meshing was applied in parts, with the element type selected, seeding was applied to each part and finally the mesh was produced. Each straight leg was meshed using hexahedron elements, with a global element size of 0.025. Due to the greater

complexity of the return bends, partitions were created to divide the part into simpler shapes. Seeding distance was also reduced in areas of complexity to refine the applied mesh. Tetrahedron elements were selected for the return bends, with a global element size of 0.0125. All elements were linear 3D stress.

7.2 Results and Discussion

7.2.1 Deformation

By applying a temperature field to the boundary conditions and running the analysis, the model could predict the expansion of the material due to the heat input. Figure 7-3 shows the expansion of the radiant tube due to the temperature profile applied to the structure.

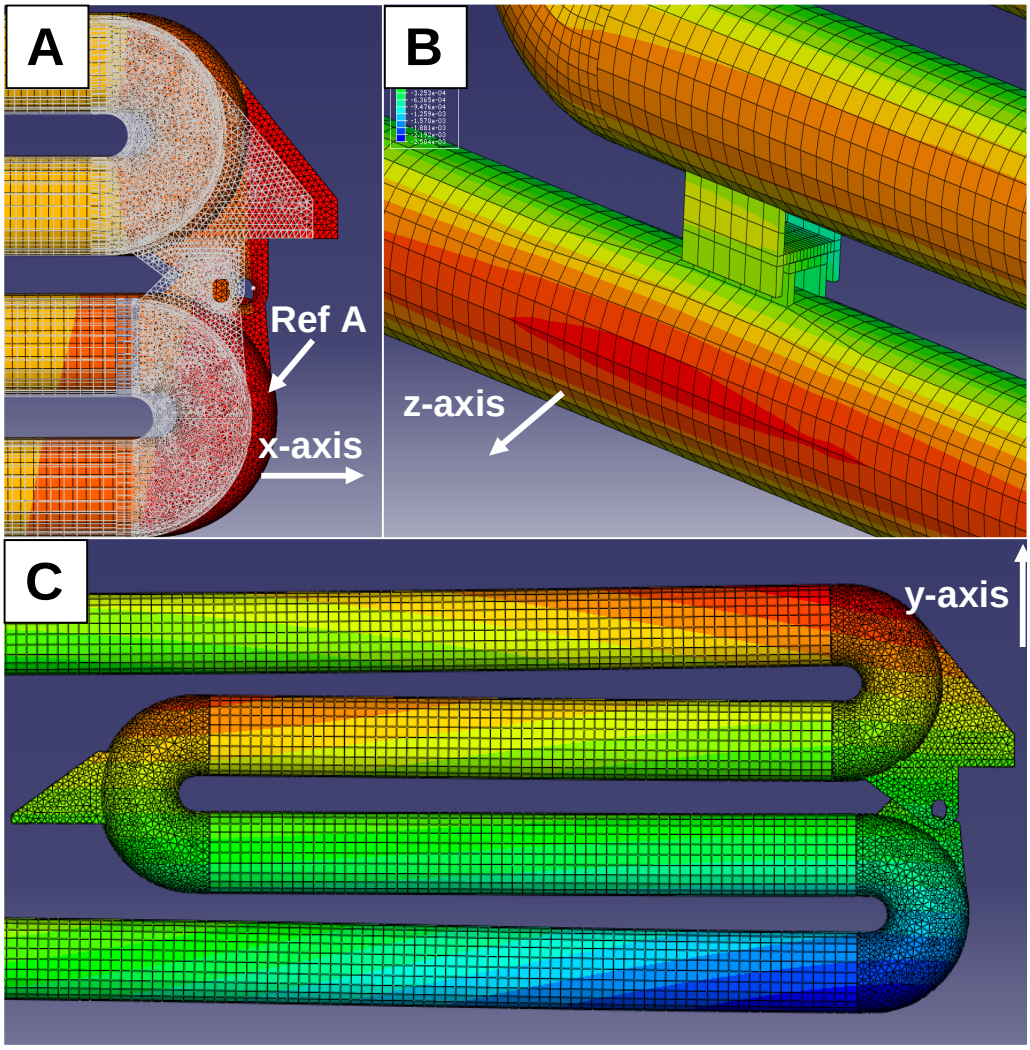

Figure 7-3 - Figure shows the expansion of the radiant tube structure due to applied temperature fields. Expansion along the x-axis (length of tube) A, expansion in the z-axis, B and deformation in the y-axis, C. Ghost image showing original position in image A

In Figure 7-3, image A shows the expansion in the x-axis, which is along the length of the radiant tube. Due to having the highest temperatures, the firing leg deformed the most. Figure 7-4 shows the maximum displacement for the end of the firing leg (Ref A on Figure 7-3) at the various temperature profiles. At 900°C, the firing leg end moved approximately 44mm from its original position. This increasing to 47.5mm and 50.5mm at 950 and 1000°C temperature profiles respectively.

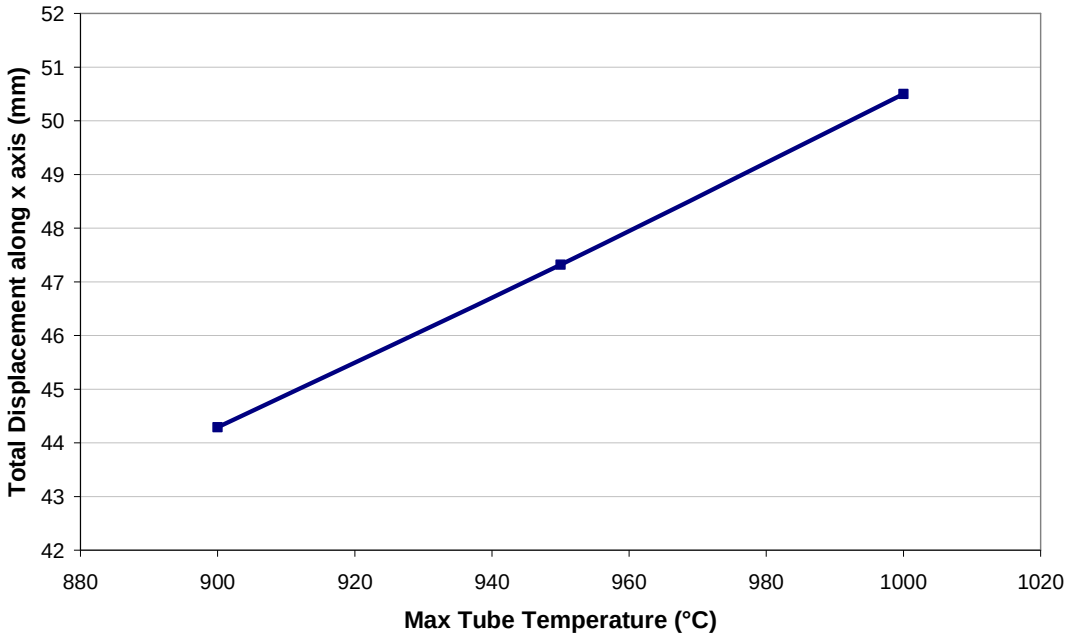

Figure 7-4 - Total displacement in the x axis with varying tube temperature profiles

Image B highlights the growth of the radiant tube along the z-axis, which is the growth on the radius of the tube. The tube expands approximately 1.7mm, 1.85mm and 2mm at the maximum point with temperature profiles of 900, 950 and 1000°C respectively, Figure 7-5.

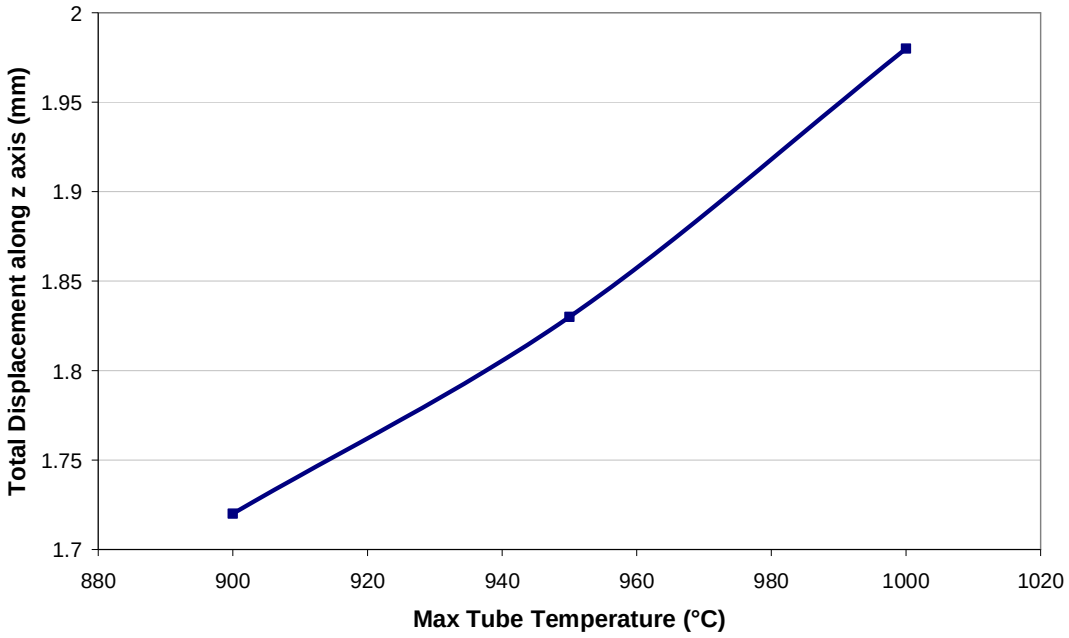

Figure 7-5 - Total displacement along the z axis with varying tube temperature profile

Finally, image C shows how the tube deformation in the y-axis; here gravity has an effect as well as the temperature field. The two outer return bends see the greatest deformation with both bends expanding in the positive and negative y-axis directions.

The shelf support on the opposite furnace wall, does not provide any support to the upper return bend initially, as the radiant tube lifts off the shelf due to the differences in thermal expansion. Only with time and creep deformation, would the return bend sit on the shelf, providing the necessary support.

7.2.2 Stress Analysis

Stresses were calculated for the whole model, but for ease of comparison it was decided to focus on the firing leg alone, as this is the location for all failures experienced at Port Talbot CAPL.

Figure 7-6 displays the stress produced in the bottom surface of the firing leg for all designs of radiant tubes. The stress direction is along the x-axis; therefore any high tension (positive stress) would promote cracking. Compression is indicated by negative stress respectively.

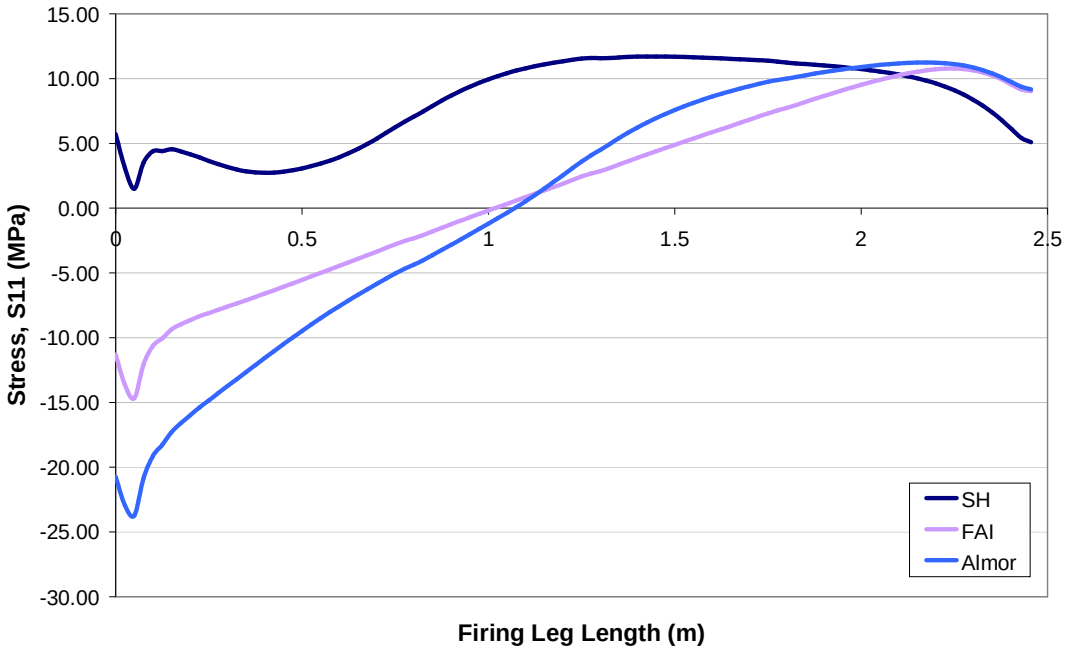

Figure 7-6 - Stress generated in the bottom surface of the firing leg. The location for all failure types experienced at Port Talbot CAPL

From Figure 7-6, the stress profile produced in the firing leg varies according to design. It shows that the design and position of the support for the centre bend has an effect on the stresses produced in the firing leg. The Stein Heurtey saddle support produces tension all along the lower surface of the firing leg, with a maximum tension of 11.7MPa at approximately 1.5m from the firing leg flange. But, in contrast to the other two designs, the stress decreases to 5.1MPa towards the weld join of the return bend.

Interestingly no failures were ever reported for Stein Heurtey tubes at the first weld region. But, nearly all Stein designed tubes failed from severe deformation in the firing leg, which resulted in the tube coming into the path of the strip. Figure 7-7 highlights the degree of deformation in the latter half of the firing leg of Stein Heurtey designed tubes.

The large tension force calculated for Stein tubes, tabulated in Figure 7-6, identifies why the two tubes in Figure 7-7 have deformed so badly. This failure could be due to creep deformation, a failure type which is governed by stress and temperature, the higher the stress and temperature the faster and more severe the deformation.

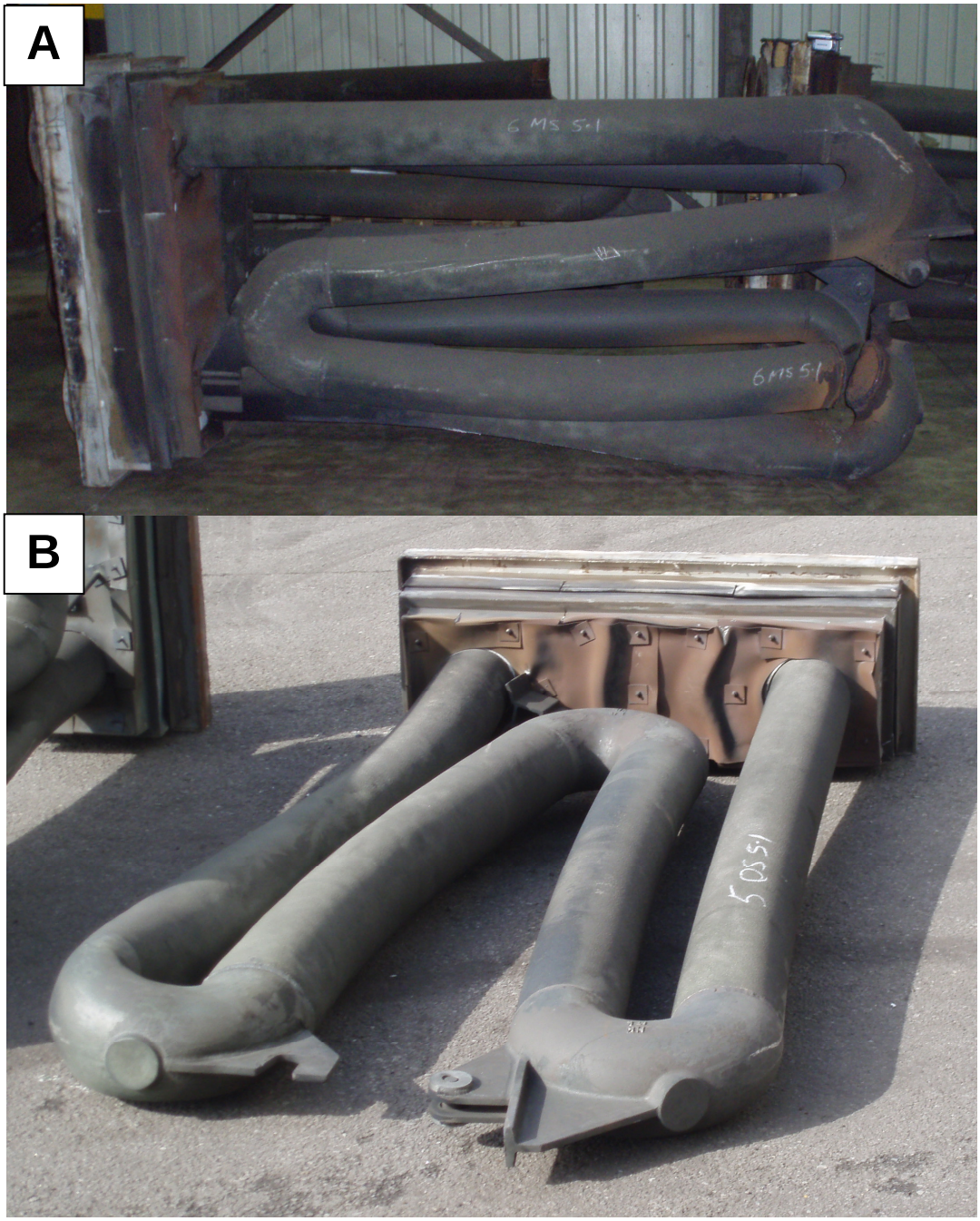

Figure 7-7 - Failure type of Stein Heurtey designed tubes at Port Talbot CAPL

The Almor channel support produces a large variance in stress along the firing leg, with a compression of approximately -24MPa near the flange, which increase to a tension of 11.2MPa at approximately 20cm from the return bend weld. At the firing leg/bend join the tension decreases to 9.2MPa, although this is lower than the maximum level it is still relatively high and is an area of high failure rates associated with poor welding.

This stress profile, Figure 7-6, correlates with failures observed in Almor designed tubes, with deformation and cracks forming towards the end of the firing leg, Figure 7-8. The area of high tension in the bottom of the firing leg, towards the first return bend has deformed the tube with a crack forming approximately 0.5m length from the weld region, very near to where the maximum tension occurs.

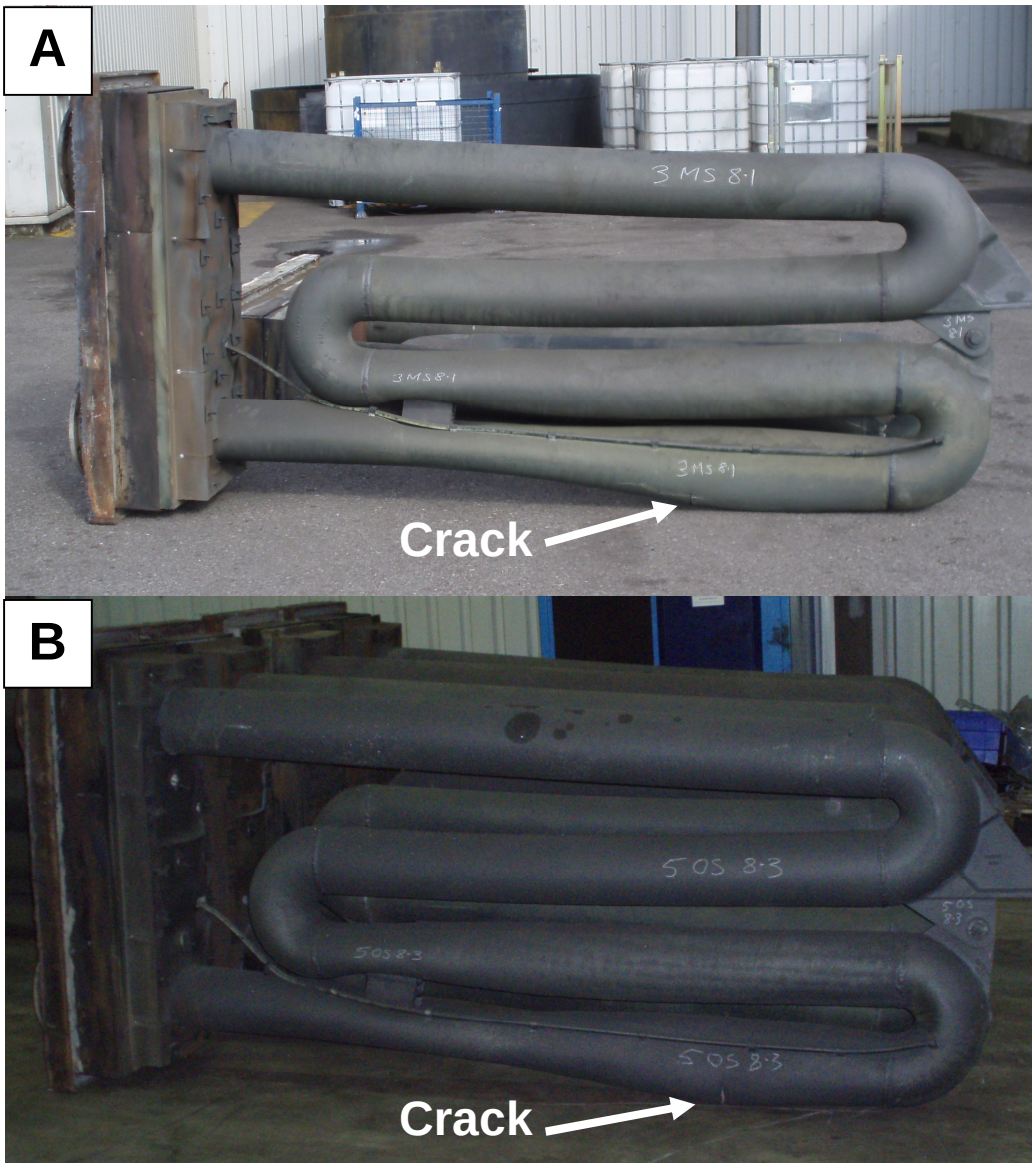

Figure 7-8 - Failure type of Almor designed tubes at CAPL Port Talbot

The new FAI design centre support, which relies on the furnace wall for support rather than the firing leg, has a maximum tension of 10.8MPa, also at 20cm from the join and a tension of 9MPa at the join interface. Although no failures have been

recorded in similarly designed tubes, it is considered a better design as it does not create any extra force or stress on the firing leg due to the support.

Stress, even at relatively low levels (compared to yield stress), plays a key role in the operating life of objects placed under elevated temperatures for prolonged periods of time. Reducing stress would reduce the deformation due to creep and ultimately prolong tube life.

Overall, the stress analysis of the firing leg has provided some evidence as to why and how the differently designed radiant tubes have failed. The stress profiles produced from the finite element calculation correlates to the failures observed at Port Talbot CAPL furnace, indicating that stress is a dominant factor in determining the ultimate life expectancy of a radiant tube.

7.2.3 Temperature

Figure 7-9 below displays the difference in stress along the bottom of the firing leg for temperature profiles of 900, 950 and 1000°C respectively. When the temperature profiles are applied, the stress profiles of each temperature distribution are identical with a compression experienced towards the flange and an area of tension towards the end of the firing leg.

Interestingly, the 1000°C profile has the smallest tension of 9.03MPa at the firing leg/first return bend join, while the 950 and 900 profiles have tensions of 9.41 and 9.83MPa respectively at the same position.

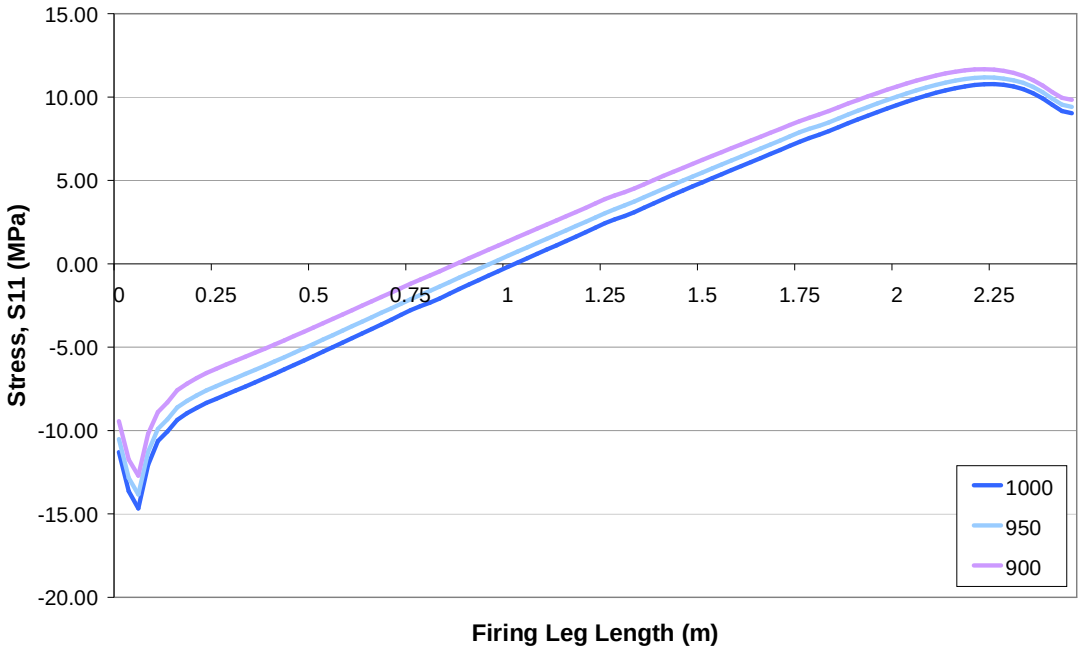

Figure 7-9 - Stress generated in the lower surface of the firing leg at various profile temperatures

7.2.4 Heating and Cooling

In all previous modelling simulations, the stress was calculated at the steady state maximum temperature profiles. During the heating and cooling of the radiant tube, the temperature profile can vary drastically and produce large gradients in temperature.

Typically during steady state production, the difference in temperature along the length of the tube can differ by up to 70°C. But, as discovered in chapter 5, during furnace heating from ambient conditions, the difference in temperature can increase to approximately 250°C, resulting in the firing leg expanding at a greater magnitude than the exhaust leg.

It was decided to analyse the stress generated in the radiant tube during furnace heating and cooling to determine the effect of the large temperature gradients seen. Ten temperature profiles were taken from recorded data, for both the heating and cooling phase, to portray the differences experienced in temperature gradients. The modelling was undertaken in steps as a result, with a new temperature profile applied to each step.

During the heating phase, as the temperature gradients reach 250ºC it can be seen that this has a detrimental effect on the stress loading in the lower firing leg surface, Figure 7-10. The stress reaches a maximum tension stress of 33MPa near the flange and as the gradients decrease, the stresses follow suit.

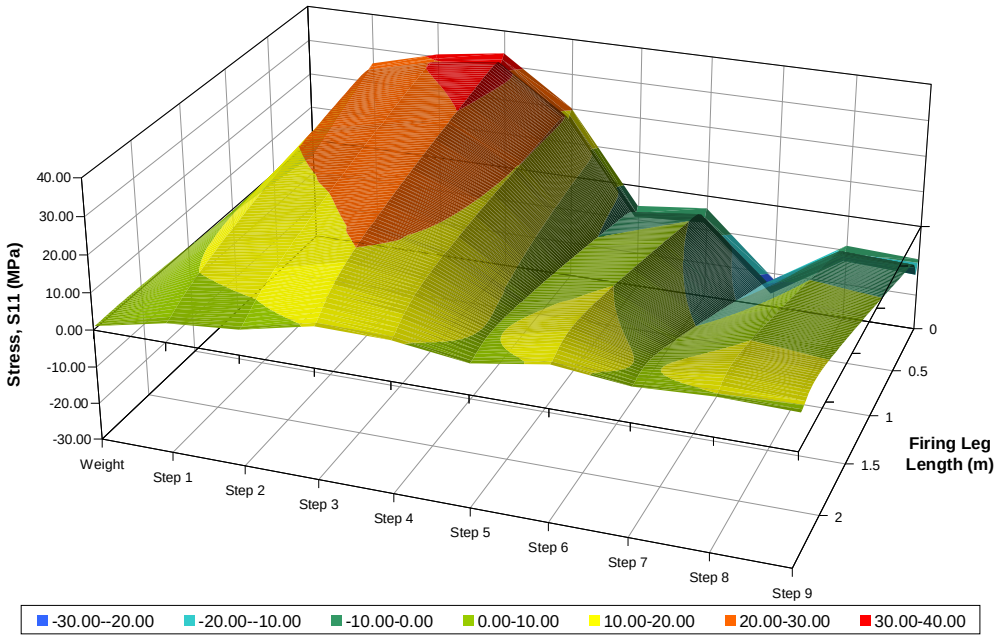

Figure 7-10 - Profile of the stresses generated in the lower surface of the firing leg during the heating phase of the radiant tube from ambient temperatures

In contrast, during the cooling phase, the temperature gradient along the length of the tube decreases from the operational gradients (~70ºC) to no gradient (i.e. the temperature is even throughout the length of tube). The stress as a result reduces in the firing leg during cooling, with the maximum tension reducing from 11.9MPa to 2.9MPa, Figure 7-11.

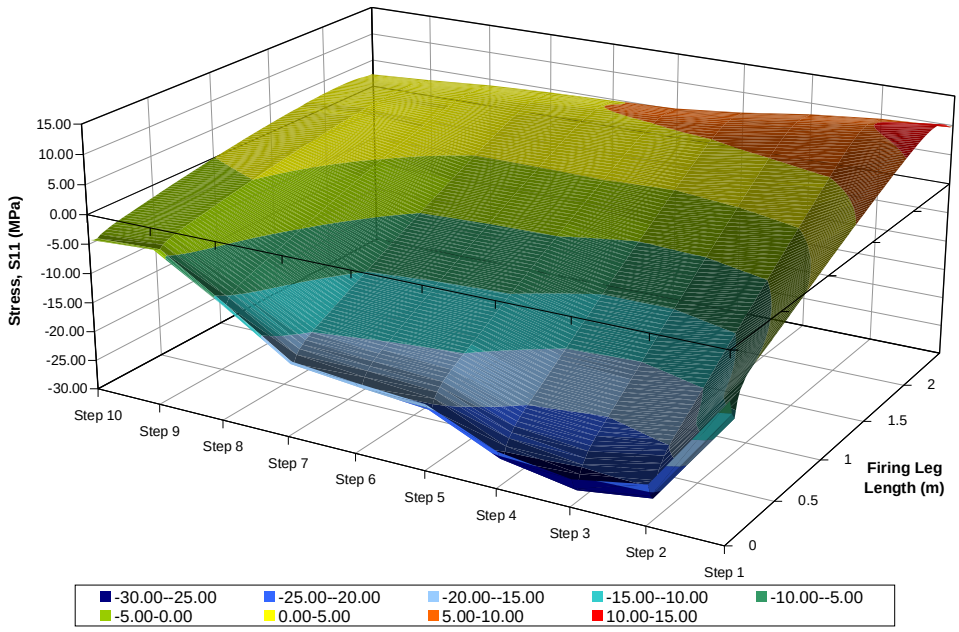

Figure 7-11 - Profile of stresses generated in the lower surface of the firing leg during the cooling cycle of the radiant tube

Tension developed in the material ultimately leads to cracking failures, where in comparison a compressive stress generates local bulging and distortion. Cracks in radiant tubes dictate the end of the tube life and requires replacement at the first available maintenance stop. Bulges and distortion are far more tolerable, and do not require replacement unless the distortion is so severe it leads to strip marking.

7.3 Design Development

With the aid of the finite element software, the assessment of suggested design modifications/improvements could be undertaken in the virtual sense to provide an indication if the changes could help reduce stress and improve tube life.

7.3.1 New Support Design

From chapter 4 (furnace comparisons) and discussions with radiant tube suppliers, it was understood that many radiant tube furnaces utilise supports on each return bend for W shape tubes.

To assess the affect of having a support on each return bend, the model was adapted to replicate such a radiant tube design and simulated with a temperature profile of 1000°C, Figure 7-12.

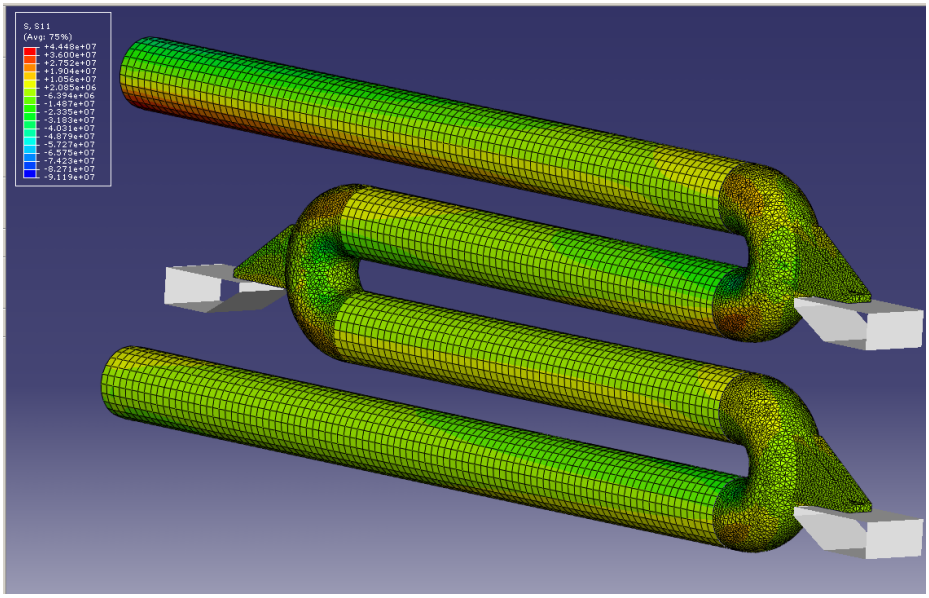

Figure 7-12 - The modelling software allows the simulation of new radiant tube designs and supports. Here a support is trialled at all return bends

Figure 7-13 displays the results of the stress in the firing leg compared to the current design utilised in the CAPL furnace. As can be seen, the results are practically identical. Initially the bottom shelf does not provide any support for the lower firing leg because the bend lifts up from the shelf by approximately 10mm due to differences in thermal expansion. Only with deformation due to creep, would the bend come to contact the shelf allowing it to provide the necessary support.

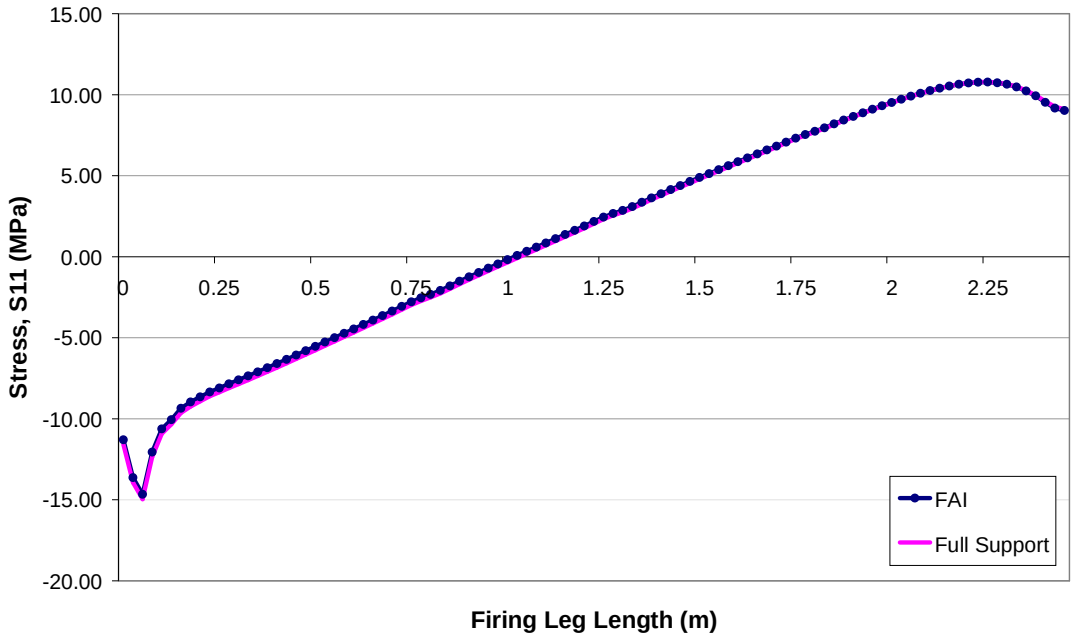

Figure 7-13 - Stress generated in new design displayed in Figure 7-12 compared with the current tube design used at CAPL

Without analysing creep conditions over a period of time, it is difficult to predict the effectiveness and advantage, if any, of having a separate support for each shelf. To adapt an existing furnace to include a support for each bend, such as Port Talbot CAPL would have to do, would be difficult, expensive and require a long downtime. But, if designing a new furnace, then having a support for each bend seems practicable. Manufacturing costs associated with mould patterns is simplified and reduced, due to all bends having identical patterns.

Having return bends with identical supports allows the tubes to be rotated in the furnace to minimise the effects of creep deformation, such as identified in chapter 4, the effect of which could prolong tube life.

7.3.2 Expansion Bellows

Another method, utilised by radiant tube manufactures, in trying to prolong tube life is to adopt the fitment of expansion bellows between the bung wall and the tube flanges. Thus, allowing a minimal amount of free movement along the length of the

tube to compensate for differences in thermal expansion and potentially reducing stresses in the tube structure.

During the benchmarking discussions (Chapter 4), expansion bellows proved to be reliable in operation, but, there is disagreement as to the number needed and where to position them. For example, an expansion bellow can be fitted to both flanges together or to only one flange, either to the top or bottom. Figure 7-14 shows the position where the expansion bellows can be fitted.

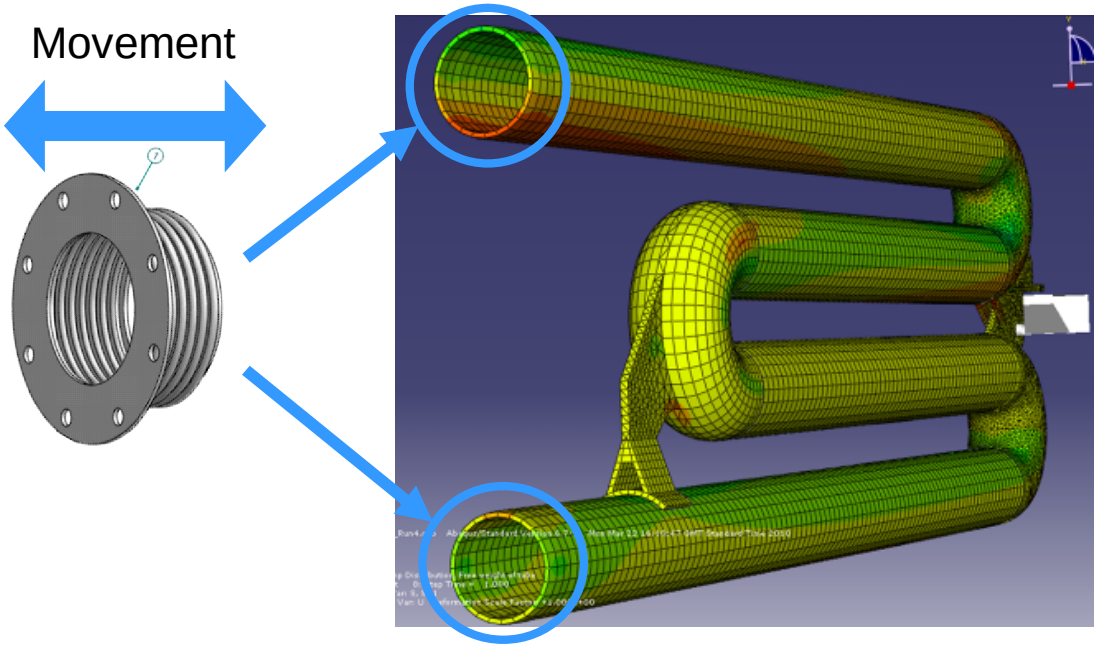

Figure 7-14 - The model allowed for the analysis of expansion bellows which can be fitted to the end of the flanges

To determine if there was any advantage to fitting an expansion bellow, the boundary conditions of the radiant tube was modified to reflect the allowance in movement of an expansion bellow. Effectively, four analyses were completed, where an expansion bellow was fitted to the top flange, bottom flange, both flanges and no expansion bellows fitted condition.

Figure 7-15 displays the results for the aforementioned analyses. Where no bellows was fitted, the stress profile replicates that of the current design used by CAPL. By fitting a bellow to the upper flange, the exhaust leg, the stress in the firing leg reduces.

Approximately 1.75m of the firing leg is under compression as opposed to 1m with no bellow fitted, while the maximum tensile stress reduces from 10.77MPa to 5.45MPa.

In fitting a bellow to the lower firing leg, the stress profile changes drastically. Initially at the flange the firing leg is under compression, but at a position of 1.25m from the flange the firing leg is under tension, which increases to a maximum tension of 2.61MPa at a position of 1.75m from the flange.

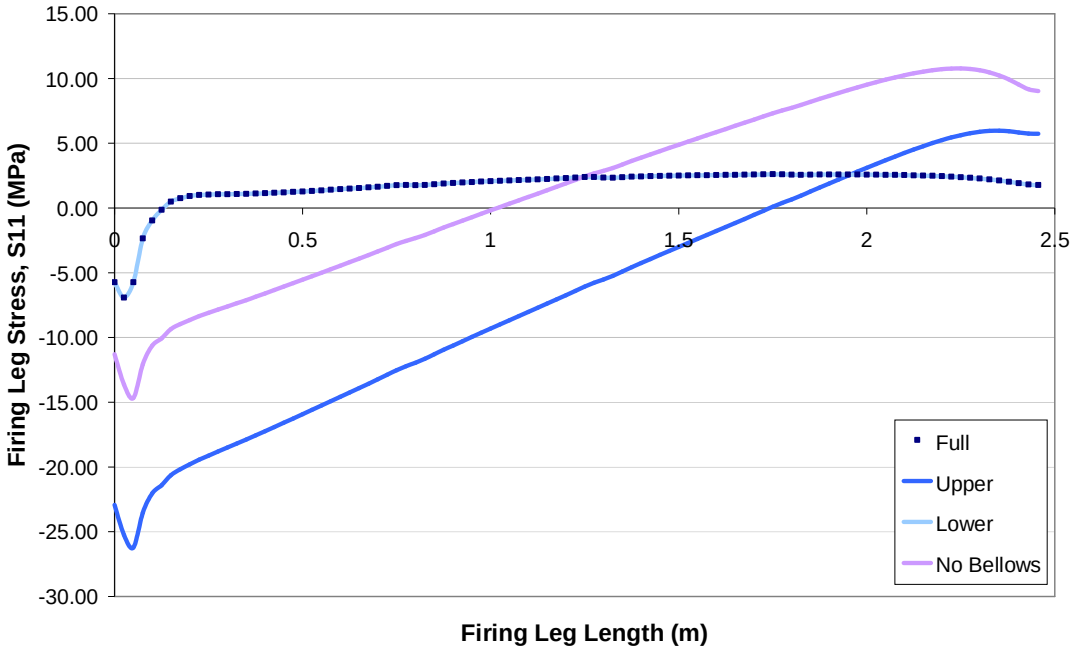

Figure 7-15 - A comparison of the stress generated in the firing leg with and without the attachment of expansion bellows at the firing and exhaust leg

On the fitment of both bellows, the stress in the firing leg is identical to when only a lower below was attached. What was noticeable in the model is that the stress in the exhaust leg also lowered, but as this is an area where temperatures are lower, creep has less of an effect and throughout CAPL history; no radiant tube has failed in this area.

7.4 Radiant Tube Life Prediction and Comparison

The stresses derived from the computational analysis can be compared with material creep data, which is widely documented for this category of materials, as creep is the predominant failure mode in service.

Figure 7-16 displays the relationship between creep rupture life for material grade HP and stress at various temperatures. When plotting the maximum stress of 11.7MPa observed in 7.2.2 at a temperature of 982°C, the figure indicates the life to rupture of just less than 4 years.

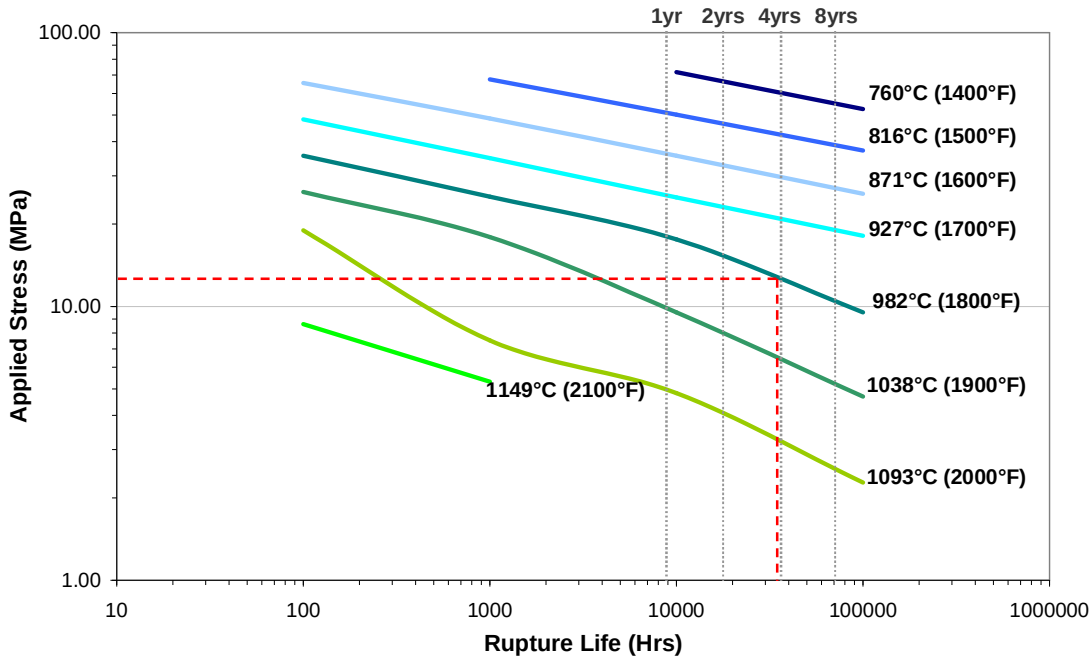

Figure 7-16 - A prediction of the tube material life from documented creep rupture data for material grade HP

This result correlates with the average age to failure in the final zones of the furnace, zones 7 and 8 in particular. Where, the average of failed tube is 200 and 226 weeks in zone 8 and 7 respectively. Average temperature of the tube material in these zones have been reported in chapter 5 to be approximately 940°C and reach maximums of above 1000°C.

What is interesting to note is the large differences in rupture life with temperature. If the whole radiant tube structure was constructed from the same material throughout, submitted to the same stress magnitude at current temperature profiles, where a difference of up to 70°C is recorded in steady state, then the cooler portion of the radiant tube would last over twice the life of the hotter region before rupture.

If the total heat output from a radiant tube can be achieved, with a higher average temperature and at a lower maximum temperature, then the material would last longer before rupture from creep. Also, if a lower temperature profile could be used, this would have the same effect, but the net heat output from the tube would be reduced.

This theory explains why the radiant tubes have remained in service for far longer periods in the initial zones compared to the latter furnace zones. The zone temperatures are much lower, thus radiant tube maximum temperatures are lower, which reduces the creep rate in the material, resulting in longer rupture lives.

Another method of increasing rupture life is to change the material grade for one which has a slower creep rate at the same temperatures. Figure 7-17 shows how a higher grade of material can prolong tube life. The two materials in comparison are grade HP and KHR48N (material composition can be found in appendix G and H respectively) at a temperature of 982°C. At the maximum stress of 11.7MPa, the HP grade has a rupture life of just less than 4 years, where the KHR48N grade has a rupture life of over 8 years, a substantial doubling of the lifetime of the material.

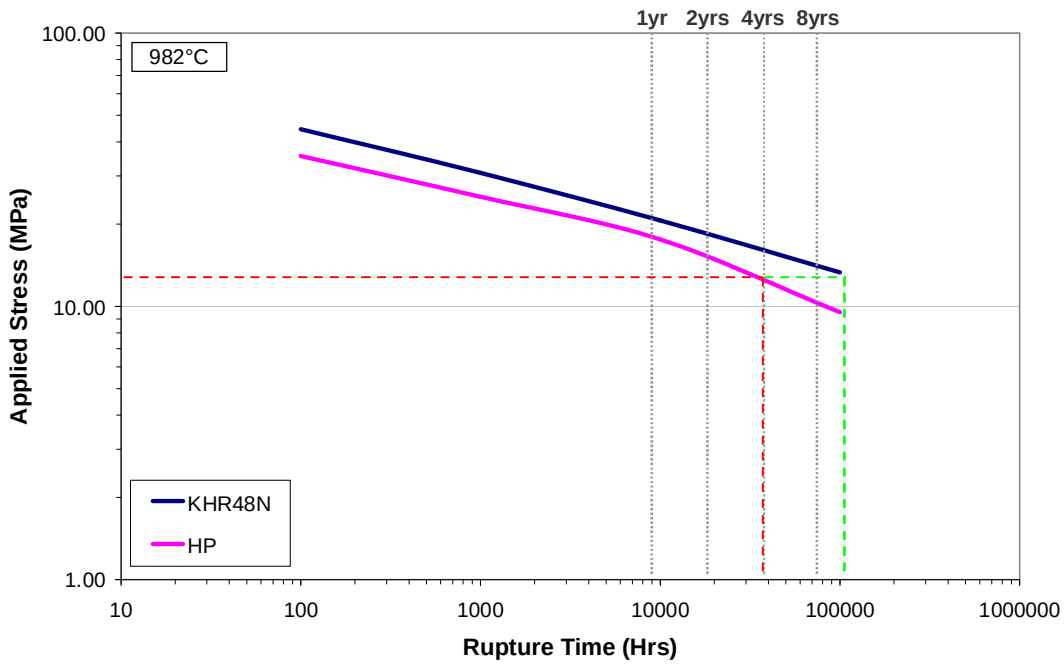

Figure 7-17 - A comparison of tube rupture life for various material specifications at a particular stress magnitude

The attachment of expansion bellows to the flanges of the radiant tube identified a significant reduction in stresses along the firing leg, section 7.3.2. Figure 7-18 shows the results of the stress analysis with the fitment of various expansion bellows on a rupture life chart of HP grade material.

With a maximum stress of 11.7MPa when no bellows are fitted, the expected rupture life at 982°C would be just under 4 years and approximately 6 months at 1038°C. With the fitment of bellows to the exhaust leg, the stress reduces to 5.45MPa; and at 1038°C this would give a rupture life of just over 4 years. When bellows are fitted to both flanges the stress reduces to 2.61MPa, at 1038°C the rupture life would by far exceed 8 years.

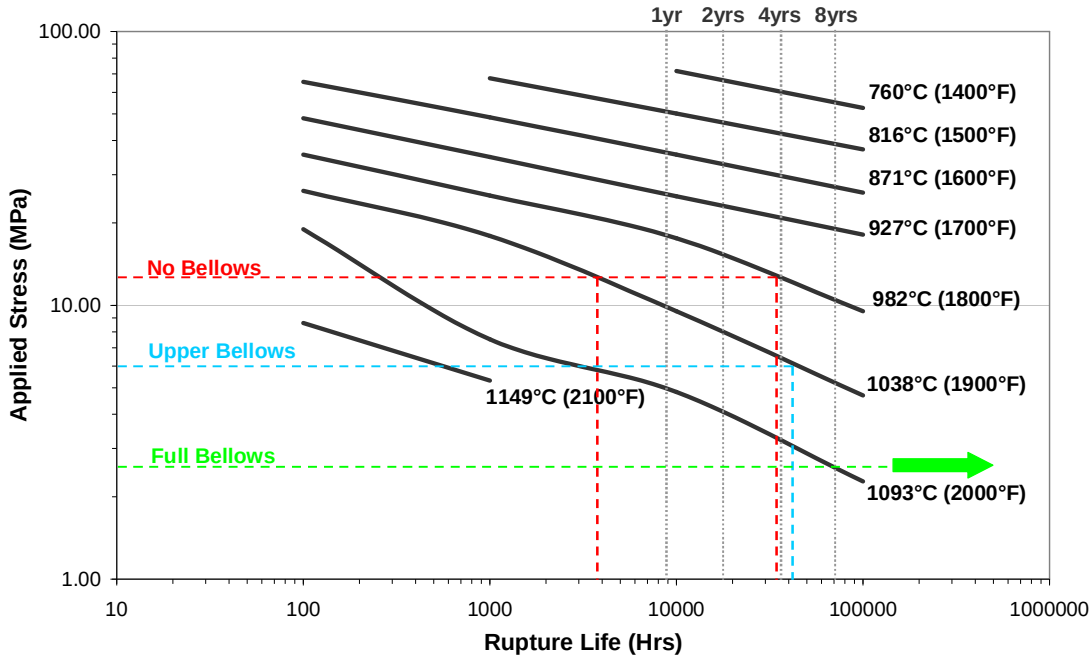

Figure 7-18 - A comparison of tube life prediction with and without the attachment of expansion bellows, for material grade HP

In summary, the life of a radiant tube is dependant upon the operating temperature, inherent stress and the ability of the material to withstand deformation at the elevated temperatures. Reducing temperature and stress and choosing a high creep strength alloy can, in theory, produce a long lasting radiant tube.

7.5 Summary of Findings

Under a maximum temperature of 1000ºC, the firing leg expands 50mm along the length of the tube and an area of high stress occurs at the bottom surface at the end of the firing leg, a feature that does not change with the different support designs.

By introducing the new central return bend support, the load previously put onto the firing leg is now supported by the bund wall. This reduces the stress and the level of deformation in the firing leg, thus reducing the effect of creep. The large area of tension, developed in the bottom surface of the firing leg, from a saddle type support (as employed by Stein Heurtey) could explain why all failed Stein Heurtey tubes featured bowed firing legs.

The fitment of expansion bellows at either flange can prolong tube life by reducing stress and increasing the time to rupture. Introducing a bellow to the upper flange can reduce the stress in the firing leg by up to 49%, when bellows are fitted to both flanges the stress reduction increases by as much as 75%.

Comparing the stress values of various bellow options on a rupture life chart can provide an indication of the expected life of a radiant tube. With the current tube designs used at CAPL and at a temperature of 982ºC, a time to rupture of approximately 4 years is expected. This result correlates with the radiant tube life expectancy experienced in zones 7 and 8 respectively. At a temperature of 1038ºC, this rupture life reduces to approximately 6 months. This highlights the importance of reducing material temperatures.

When fitting a bellow to the upper flange, the stress reduces in the firing leg and as a result the time to rupture at 1038ºC has increased from 6 months to just over 4 years. When both bellows are fitted, the time to rupture exceeds 8 years, resulting in a major improvement on tube life. This, coupled with a reduction in temperature, could provide even longer tube lives.

Other methods of increasing tube life are the use of more exotic material grades, which contain higher levels of nickel and chromium and addition of elements such as

cobalt. These additions help increase the creep strength of the material and as a result increase the rupture life. At the stress levels observed in the firing leg of the radiant tube, a material grade with a higher creep strength can double the life to rupture.

Ultimately, stress plays a key role in the operating life of a radiant tube. Every measure should be undertaken to try and reduce the stress levels generated in the hottest regions of the tube.

7.5.1 Future Work

Further work that could be undertaken is modelling of creep behaviour to understand how the radiant tube deforms with time and temperature given the stresses produced in the structure. The various design modifications suggested in this chapter can be compared in more detail and an understanding of how the stresses develop with time and deformation can be achieved.

Other models which could be trialled are to analyse how a fabricated radiant tube performs against its cast counterpart. Also, with new techniques being used in reducing temperature gradients in radiant tubes, for example ceramic inserts (See chapter 9.2), the model can predict the effect of increasing temperature and weight in the exhaust leg can have on the life of a radiant tube.

8 Temperature Cycling of Heat Resistant Material

8.1 Introduction

The temperature analysis of a radiant tube conducted in chapter 5 identified that the tube material was subjected to various temperatures ranges during operation.

Predominantly, the firing leg was operating near its limits at temperatures of over 1000ºC, in the region of the end of the firing leg. Also, during furnace heating, data showed that the lower half of the radiant tube was subjected to severe temperature cycling in maintaining temperature and during furnace cooling, a procedure known as 'Fast Cooling' was used to reduce furnace temperatures quickly.

This chapter focuses on the design and build of a testing rig capable of subjecting radiant tube material to the high temperatures and conditions, experienced at Port Talbot CAPL and under various temperature cycling operations to determine the effect on the material.

8.2 Test Rig Design and Manufacture

The test rig was designed and built in-house at Cardiff University School of Engineering and was situated in the combustion testing lab. The main structure of the rig was manufactured from Inconel heat resistant stainless steel and lined with thermal insulation to minimise the heat loss, which would make operating in and around the test rig more comfortable.

On one end of the rig, a natural gas burner was located to provide the necessary operating temperatures and conditions experienced in a radiant tube. On the other end, was an exhaust duct taking combustion products away from the rig and into the main exhaust system of the combustion lab, Figure 8-1.

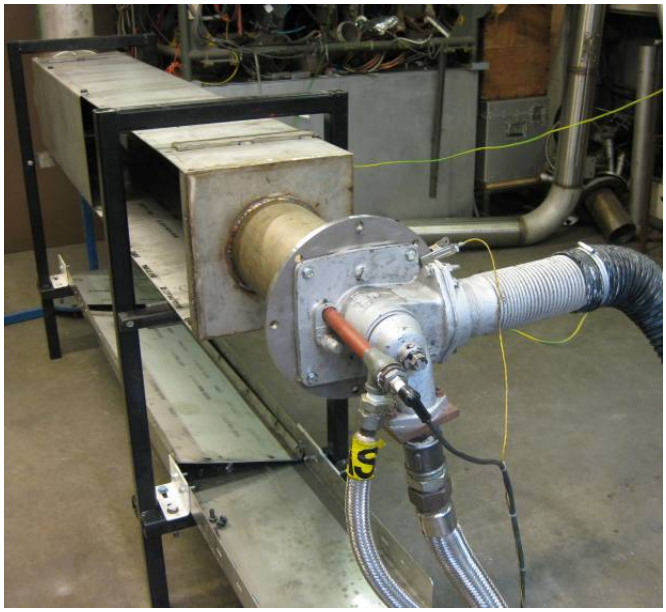

Figure 8-1 - Image showing the heat cycling test rig fitted with a natural gas burner, but without thermal insulation

The rig was of sufficient size and length to allow full size samples to be positioned in the combustion chamber and provide access for thermocouples to be installed for monitoring purposes, Figure 8-2. To allow ease of access into the rig, an access door was built into one side of the rig with quick release latches, which also contained an inspection window to allow a line of sight into the flame development and ignition procedures.

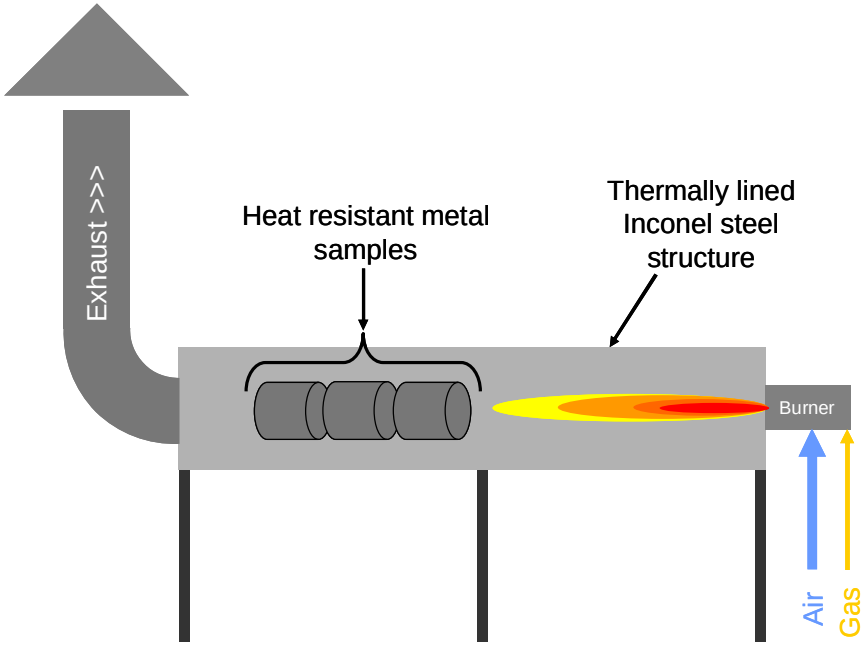

Figure 8-2 - Schematic displaying the general layout of the heat cycling testing rig

The burner was piped up into the main control panel, which provided control over the gas and air flow rates to both the pilot burner and main burner. Solenoid valves fitted to the pilot and main burner gas pipes controlled the ignition procedure. Firstly, the pilot gas was enabled to allow the pilot burner to be ignited via the electrode. Once, the pilot burner had ignited and was stable, detected via the ionisation probe, the main solenoid fitted to the main gas line, allowed the main burner gas to flow. The main gas along with the main combustion air would then be ignited by the pilot flame.

The burner control ensured that gas could not be emitted into the chamber without the pilot flame being lit and stabilised. This ensured that no un-ignited gas could accumulate in the chamber, which could potentially explode if an ignition source was present. Emergency stop push buttons fitted to the control panel allowed the closure of both gas solenoid valves in the event of an emergency. Also, the combustion lab was fitted with emergency push buttons to stop the flow of gas into the lab. These, precautions ensured that the test rig was able to operate in a safe manner and mitigated the potential for harmful accidents. A safe start up procedure for the testing rig was produced and is included in appendix I.

To cool the test rig, the gas solenoid valve was closed via the emergency stop valve, which ensured that the burner flame extinguished and no gas was able to pass into the burner. The combustion air fan continued to operate and provided ambient temperature air to the main burner and through the rig chamber. After a period of duration, the chamber was cool enough to ensure safe access into the chamber to monitor and change samples.

8.3 Equipment

8.3.1 Test Rig Equipment

To provide air for the main burner, a 3-phase fan was fitted with two rotameters, which was capable of delivering up to 4500L/min of air to the main burner, Figure 8-3. Hand valves were fitted before the rotameters to allow accurate adjustment of air flow to ensure the correct air to gas ratio was achieved. Pilot air was supplied by the

School of Engineering's compressed air supply, which was set by an individual rotameter located on the control panel.

Figure 8-3 - Electric fan fitted with rotameters, capable of delivering 4500L/min of air

The test rig was situated in the combustion lab, where access and connection to a natural gas supply was possible. Again, the main gas header, fitted with an emergency shut off solenoid valve, was connected to two rotameters, one for the pilot burner and the other for the main burner, Figure 8-4. Gas flows were controlled via hand valves located below the rotameters. Shut-off valves located in both lines, allowed the gas flows to be isolated. This allowed the pilot flame to be extinguished after the main flame was ignited and stable.

Figure 8-4 - Natural gas rotameters to indicate pilot gas and main burner gas flows (L/min)

The combustion was enabled via a natural gas radiant tube burner, Figure 8-5, manufactured by Hauck, rated at 310kW (Maximum input @ 10% excess air) and capable of maximum air flows of just over 5400L/min. The burner was not fitted with heat recuperation of any form; as a result, combustion air was entered at ambient air temperature. Burner specification is included in appendix J.

Figure 8-5 - Natural gas burner fitted with pilot burner for main burner ignition

8.3.2 Monitoring Equipment

Six type-K Inconel thermocouples were installed into the rig to monitor chamber and sample temperature throughout the duration of the experiments. Three thermocouples

measured the sample temperatures, where the end of the thermocouple was located into a pre-drilled hole in the sample and the other three thermocouples measured chamber temperature at 50cm spacing from the burner head, Figure 8-6. Each thermocouple was wired into an eight-channel selector, which was connected to a display unit. By selecting the appropriate channel, the display unit would indicate the temperature recorded via the connected thermocouple. Each channel or thermocouple signal was replicated to a data logger, where each signal was recorded at every 10 seconds interval.

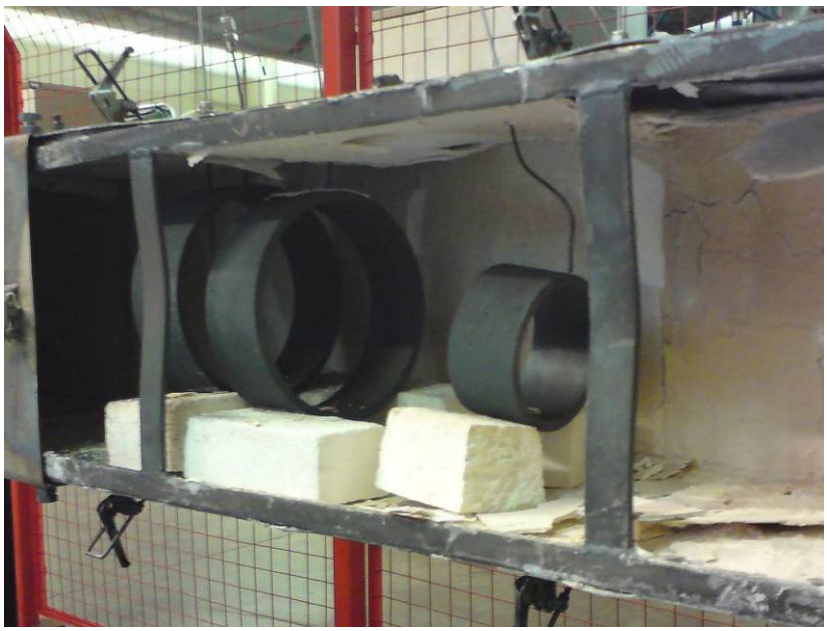

Figure 8-6 - Image displaying the layout of the samples within the test rig

The data logger was a 62 channel unit from Delta T Devices (DL2e model) and was calibrated to display thermocouple temperature in ºC from a mV signal (Calibration chart included in appendix L). Data logger calibration was confirmed with a calibrated handheld thermocouple meter. The six temperature signals were recorded, along with an ambient air temperature measurement (made on-board the data logger), during each experiment and the data was downloaded into Microsoft Excel, where data could then be easily manipulated and displayed.

8.4 Test Samples

For the temperature cycling tests, new as-cast samples were kindly donated by Kubota Metals Corporation, Ontario, Canada. The samples were off-cuts of spun cast tubes used for radiant tube manufacture.

Three cast sections were provided, designated KHR35H, KHR48N and HK40, each having a different chemical composition, Table 8-1, but representative of the grades used at CAPL, Port Talbot. The HK40 grade is used as part of the exhaust legs, while KHR35H is the same grade of steel used originally on the Stein Heurtey tubes, as part of the firing leg and second leg. Lastly, the KHR48N is the same grade as what the current firing leg is manufactured from.

Table 8-1 - Dimensions and chemical composition of the grades received from Kubota Metals

	HK 40	KHR35H	KHR48N
Dimensions			
Internal Dimater (mm)	90.5	177.8	183.4
Outside Diameter (mm)	118.3	193.7	200
Wall Thickness	13.9	7.95	8.3
Chemical Composition			
C	0.42	0.44	0.48
Mn	0.59	1	0.79
Cr	24.81	25.76	26.66
Ni	21.17	34.24	46.14
Si	1.27	0.85	0.83
Mo	0.017	1.19	0.001
W	0.008	0.004	4.89
Co	0.036	0.016	0.25

General condition of the samples was good, with constant sound wall thickness visible across the circumference of the tube. The KHR35H and KHR48N samples had the original as-cast inner surface visible, Figure 8-7 B and C respectively, where as the tube is spun during casting and cools, a small thickness of slag forms on the inner surface. This surface is acceptable for the manufacture of annealing furnace radiant tubes, but generally undesired in the manufacture of reforming tubes for the petrochemical industry.

The HK40 sample, Figure 8-7 A, was an off-cut from a tube designated for the petrochemical industry. Here, the surfaces of the inner bores of the tubes are prepared by machining. This ensures that the surface is clean and smooth, which helps prolong production campaigns before necessary maintenance is required. The extra costs associated with inner bore machining can be considerable in comparison to the total cost of the tube.

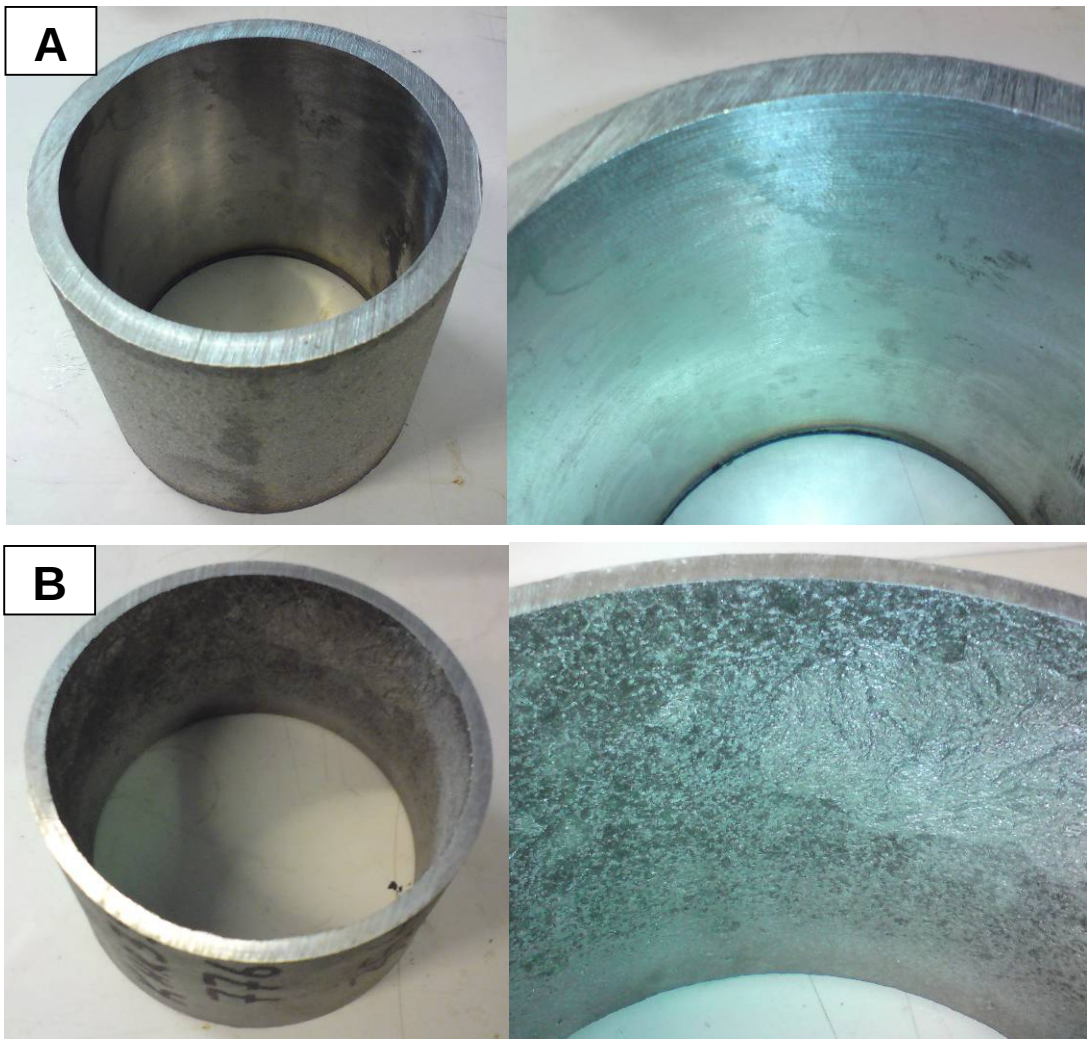

Figure 8-7 - Test Samples received from Kubota Metals for heat cycling experiments. A - HK40 with inner machined bore. B -KHR35H with as-cast inner surface. C - KHR48N with as-cast inner surface

For each experiment a 75mm long section was cut from each tube and located within the chamber. After a predetermined duration in the heating chamber a section of 20mm wide was cut from each sample and documented for further inspection.

8.5 Test Methods

Two different experiments were conducted to determine the effect of temperature and operation on the heat resistant stainless steel castings. The first experiment was a temperature cycling between two set temperatures, the second experiment was a heat and hold, where the samples were heated to 1000ºC and held for a period of duration.

8.5.1 Temperature Cycling

A 75mm wide sample of each material grade was subjected to a temperature cycling of between 1000ºC and 500ºC sequentially for a 100 cycles. 75mm by 20mm samples were cut from each sample after 1, 5, 10, 25, 50 and 100 cycles respectively, to determine the effect on the material with time. A figure indicating the duration of each cycle is included in appendix L.

During the heating phase the air and gas flow rates were set to 1700L/min and 137L/min respectively. This ensured a 20% excess air condition, which CAPL

operates at during periods of high fire. The heating cycle continued until all three samples recorded temperatures of 1000ºC at which point the gas supply to the burner was terminated and the flame extinguished.

On termination of the heating phase, the primary air flow was set to 600L/min to represent a fast-cool condition. The cooling cycle continued until all material temperatures had lowered to 500ºC. Once complete, the ignition process was initiated to relight the burner flame and start another heating cycle.

8.5.2 Heat and Hold

During the heat and hold experiment the 75mm wide cast samples were heated to approximately 1000ºC and held for duration of 5 hours. The heat and hold experiment was repeated 5 times to equal the time taken for the heat cycling experiments (25 hours total). This enabled a comparison to be made between the two different experimental samples.

The initial heating phase was identical to the heat cycle experiments, with an air to gas ratio of 20% and volumetric flow rates of 1700L/min of air and 137L/min of gas. Once the samples had reached a temperature of 1000ºC, the air and gas flow rates were controlled and altered to maintain the 1000ºC temperature, whilst keeping an air to gas ratio of 20%. The primary air and gas flows were set to 1400L/min and 113L/min respectively. Appendix M outlines the variance of gas and air flows according to the requirement of 20% excess air.

After the 5 hour holding period, the burner was extinguished by shutting off the gas supply and cooling was initiated via the primary air fan at a volumetric flow rate of 600L/min. Samples of 20mm width were taken from each sample at the end of the experiment for further analysis.

8.6 Results

8.6.1 Test Rig Problems

Problems were encountered with the test rig during preliminary testing of the burner and during normal operation of the rig. Firstly, the pilot flame could not stay lit, which resulted in the main gas solenoid remaining closed and subsequently not being able to light the main burner, as depicted in Figure 8-8. It was found that the pilot air pressure was too high and as a result insufficient gas was being entrained in the air to allow for a successful combustion.

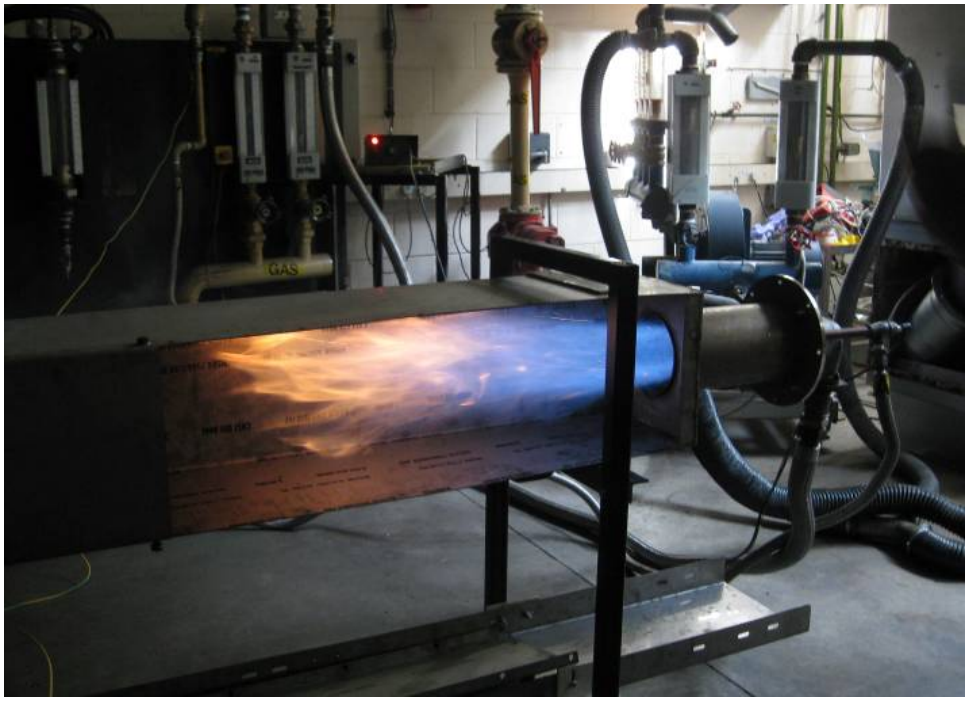

Figure 8-8 - Problems with lighting the main burner were experienced during preliminary tests

An insulation of thermal board and cement was applied to the inside of the rig to minimise the heat loss through the surfaces of the chamber and to reduce the effect of temperature on the stainless steel structure. The insulation also ensured that the area surrounding the rig did not get uncomfortably hot and allowed the operator to work in the area.

Unfortunately, the thermal lining had to be replaced quite frequently, due to the thermal cement cracking and the boards distorting and working loose form the metal

surface of the rig. This was especially a problem during the thermal cycling experiments, as the rig was subjected to large cyclical changes in temperature. An alternative solution was not found for the insulation problem; instead it was maintained and replaced as necessary.

Figure 8-9 - The thermal lining cracked, distorted and worked loose from the Inconel structure during thermal cycling experiments

8.6.2 Cyclical Temperature

The test samples were cycled between 1000ºC and 500ºC, Figure 8-10, for a 100 times with a total experimental time of 25 hours and 47 minutes. Samples were taken at cycle numbers 1, 5, 10, 25, 50 and 100 respectively, which were cut to size, mounted in conductive Bakelite and carefully ground then polished until the desired finish was achieved. Each sample was visually inspected then subsequently analysed using a light optical microscope.

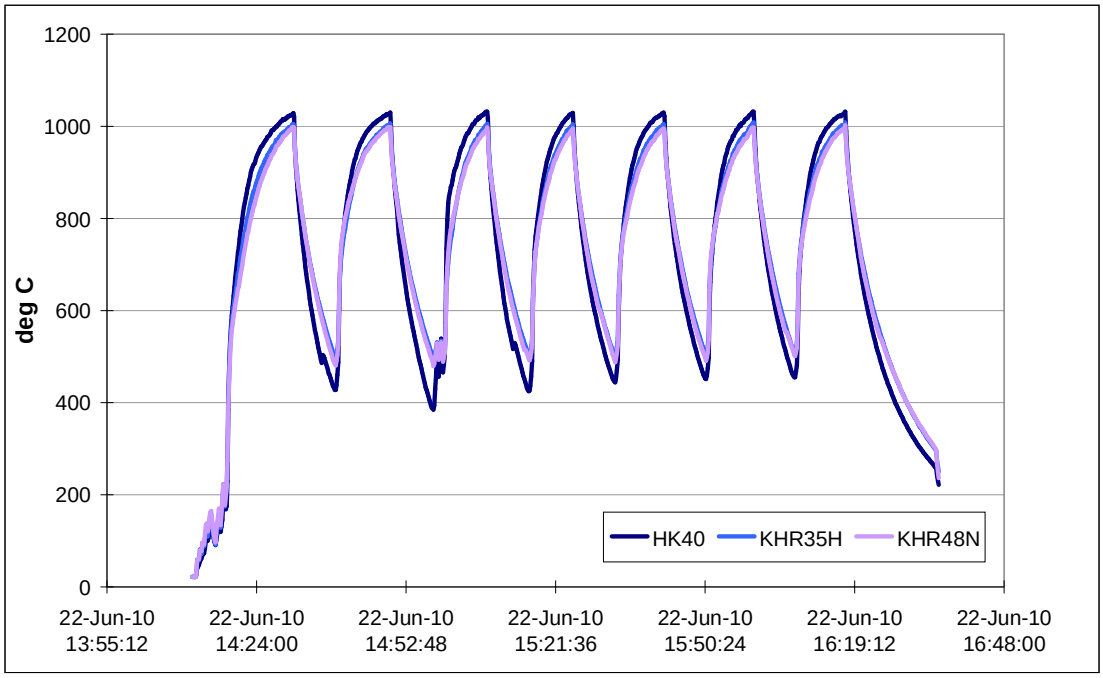

Figure 8-10 - Sample temperatures during heat cycling between 1000ºC and 500ºC. Cycles 11 to 17 shown.

Interestingly, the microstructure of the material had not changed during the heat cycling experiments. Figure 8-11 (A) displays the microstructure of the HK40 sample after 100 cycles and in comparison (B) displays an as cast microstructure of a HP material previously analysed in chapter 6. The chromium carbides are in a lamellar form at the grain boundaries with no visible signs of secondary carbide precipitates.

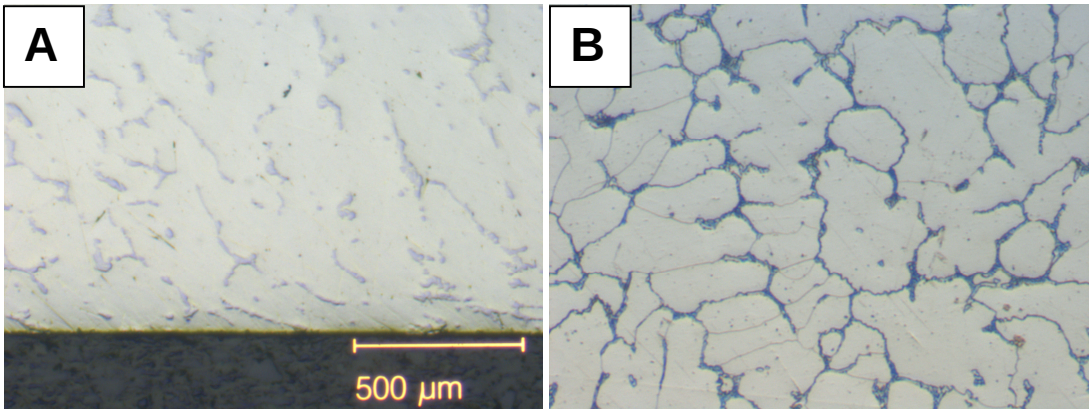

Figure 8-11 - Images displaying the microstructure of the HK40 sample (A) after 100 cycles compared to an as cast sample of HP material (B)

All samples, at all cycle rates showed similar microstructure with a slight oxidation film at the surfaces. By comparing each material's samples after 1 cycle and 100 cycles, visually there is no significant difference. What this suggests is that the samples did not have sufficient experimental time to display any significant changes and effects from the heating cycles.

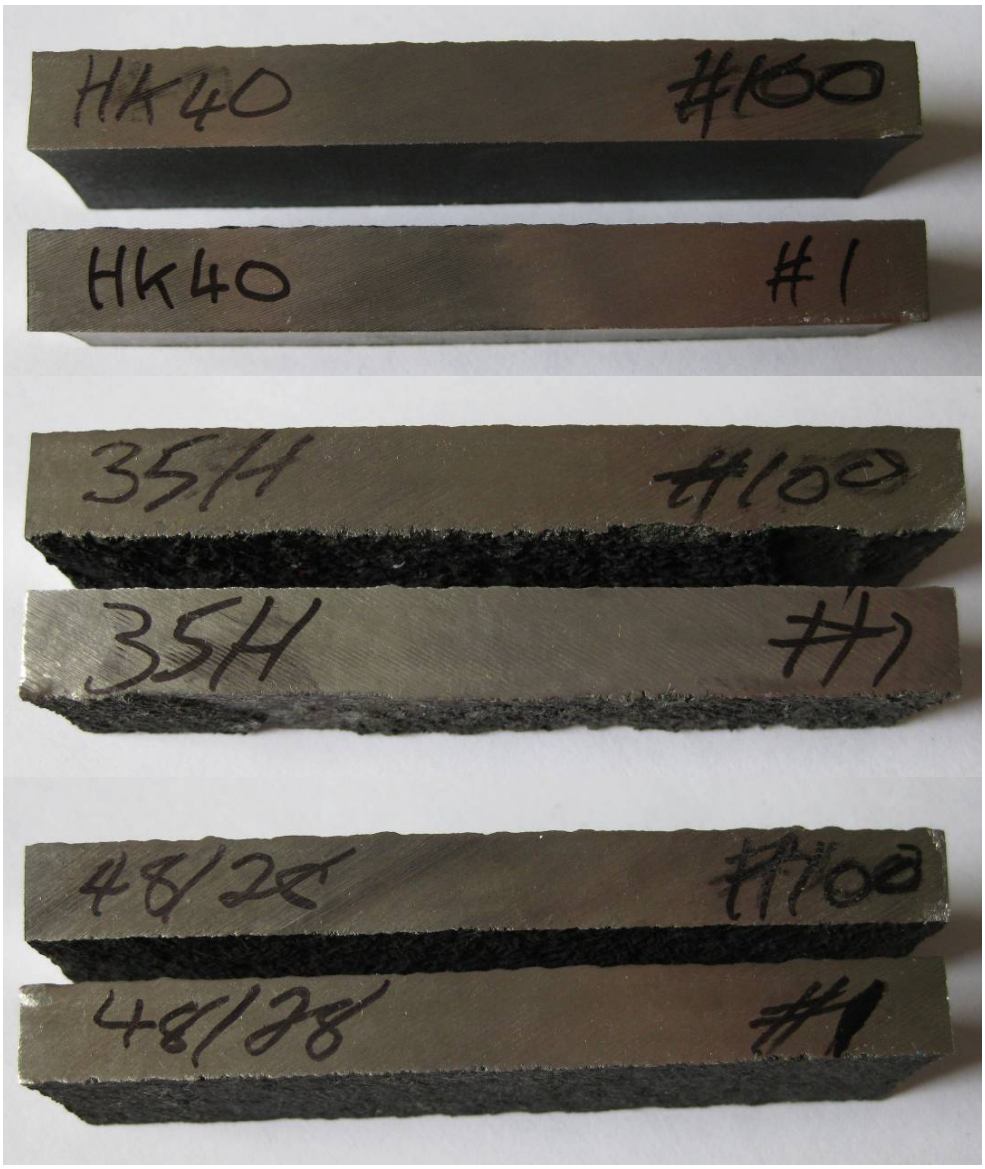

Figure 8-12 - Image displaying the comparison of samples of each material after 1 and 100 cycles

8.6.3 Heat and Hold

New test samples of each material, were cut and positioned in the test rig and subsequently heated to 1000ºC for a total period of 25 hours, which was achieved in five cycles of 5 hours each.

Figure 8-13 displays the constant temperature achieved throughout one of the 5 hour cycle. Slight differences in temperature were experienced due to the relative position of the samples within the chamber, but the effect of the slight variation in temperature was expected to be negligible. The samples were cooled at the end of the cycle with 600L/min of air through the primary air fan. Samples were cut at the end of the fifth cycle for further analysis.

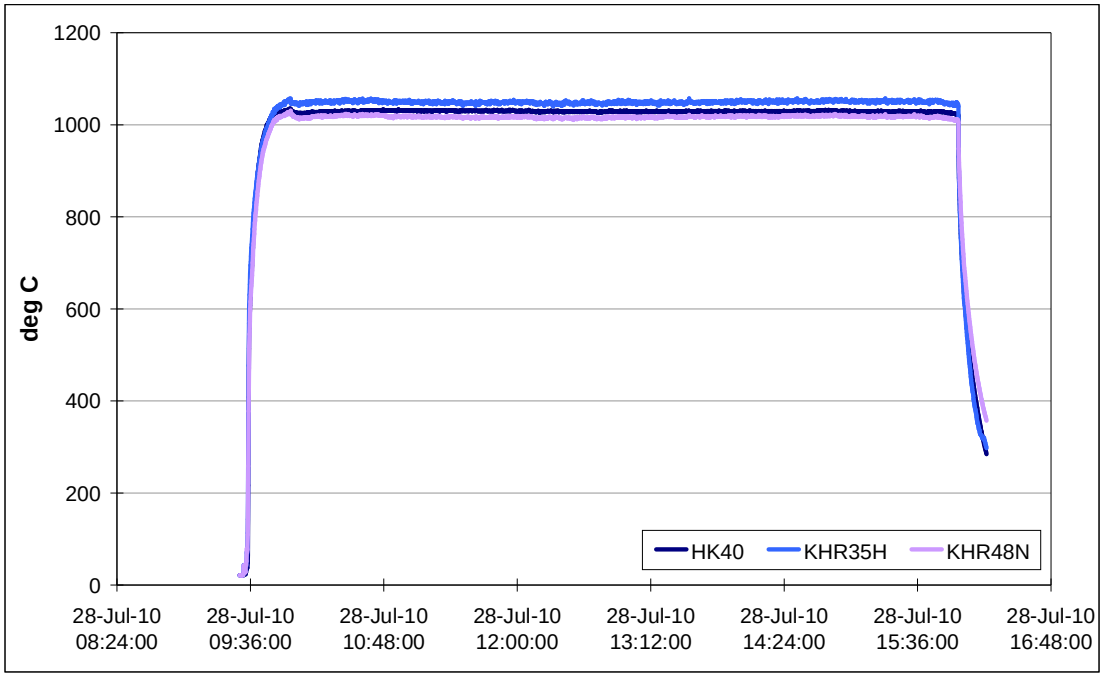

Figure 8-13 - Sample temperatures during the heat and hold experiment

Samples showed no difference in microstructure from an as cast sample as discussed earlier in the chapter and shown in Figure 8-11. But, what was interesting was the discovery of a dark coloured scale, littered on the chamber floor after the final cycle from 20 hours to 25 hours, as displayed in Figure 8-14 (A) and (B).

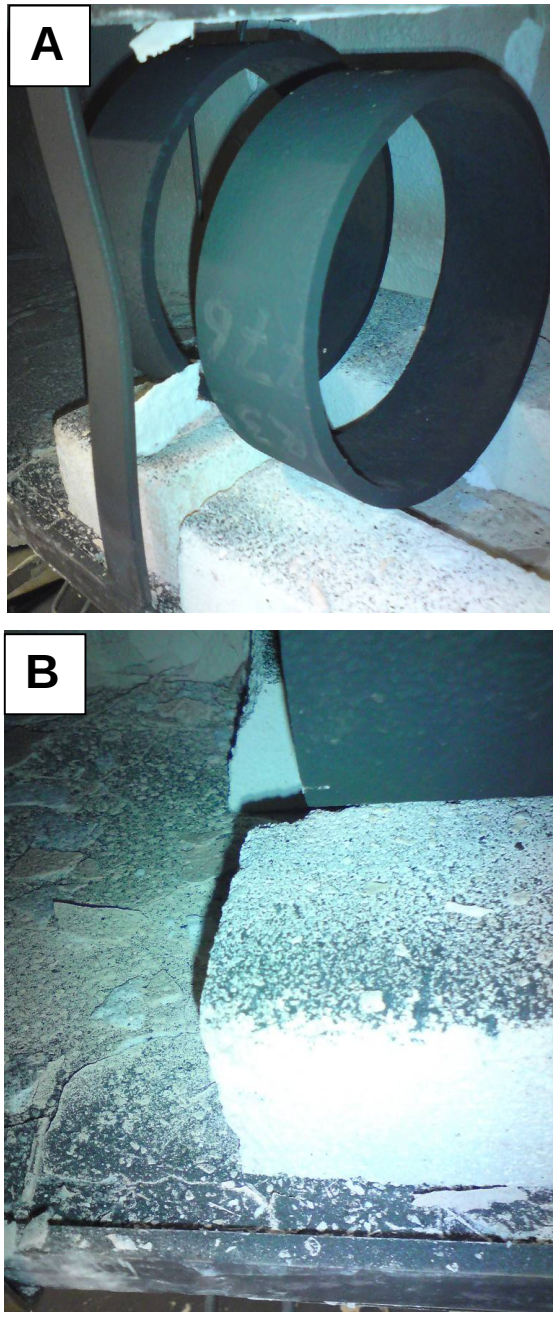

Figure 8-14 - Dark coloured scale littered on chamber floor after final heat and hold cycle. (A) General view of chamber, (B) Close up of scale

One hypothesis suggests that the scale is the oxide layer of the material being 'spalled' from the surface due to differences in surface stresses during the cooling phase[37,38]. During subsequent removal of the chamber door, immediately after the samples were cooled, scale was seen and heard to be propelled from the surface of the samples, which supports this theory.

8.7 Discussion

A testing rig capable of heating and cooling radiant tube material was successfully designed and built. The rig was capable of heating the material to temperatures of above 1000ºC and subsequent cooling with conditions akin to those experienced in an annealing furnace.

Samples of new as cast material, of various heat resistant stainless steel grades, were subjected to temperature cycling and heat and hold experiments to determine the effect, if any, on the material. During subsequent analysis on each sample, the microstructure was near identical to that of an as-cast sample with very thin oxide layer formed during both experiments.

Interestingly, at the end of the heat and hold experiment, dark coloured scale was found on the chamber floor. A viable hypothesis is that the scale is the 'spalling' of the oxide layer due to differences in surface stresses developed during the cooling cycle.

This could answer why, in most samples analysed in chapter 6, the bottom inside surface of the radiant tube was relatively smooth and seemed to have been filled with green oxide material. In comparison, all other surfaces of the inner bore displayed deep crevices and pits.

Worth noting also, is the difference shown between the inner surface of an as-cast sample and the surface of a machined inner bore sample, Figure 8-15. Sample KHR48 and KHR 35 display surfaces in an as-cast condition, which show the variability of the process and the formation of slag on the inner surface during the centrifugal casting. In comparison, the machined inner bore of sample HK40 has remained smooth even after experimentation.

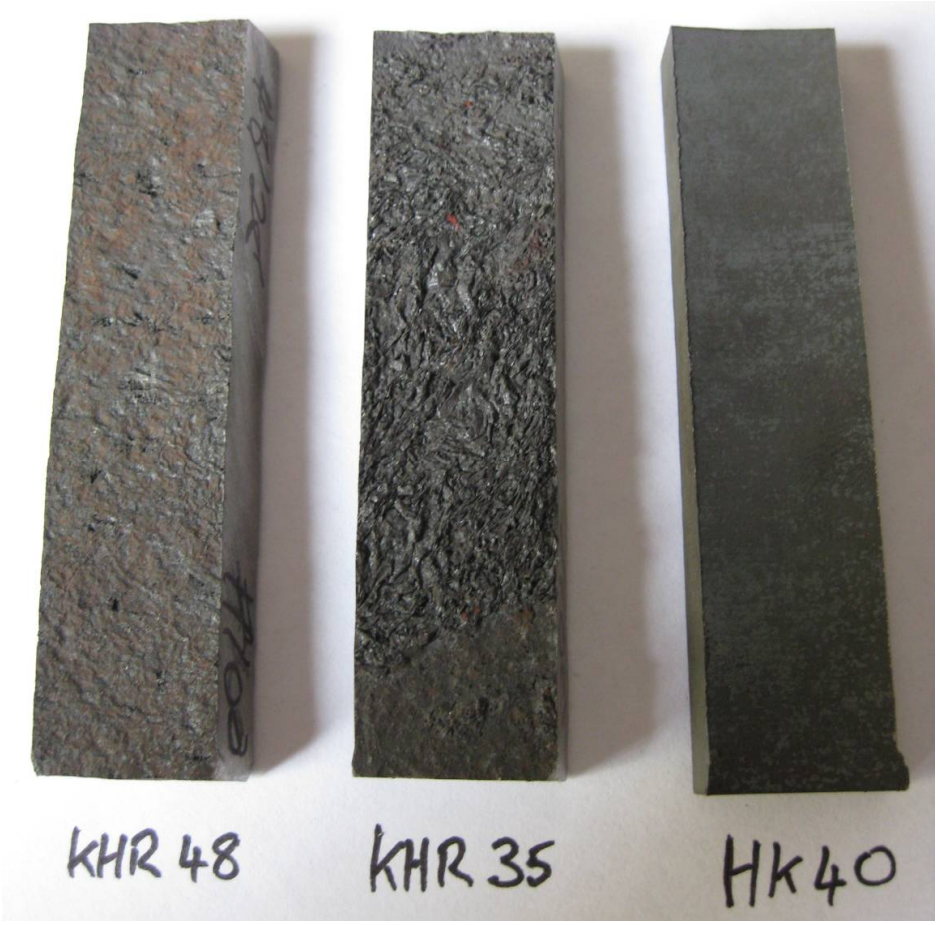

Figure 8-15 - Differences between an as-cast surface (KHR48 and KHR35) to a machined inner bore surface (HK40)

Sumitomo Metals now specify that all new radiant tubes have the inner bores machined to prolong tube life. As discussed in chapter 4, it is argued that the smooth surface reduces the rate of oxidation. Presumably, it accomplishes this through having a smaller surface area compared to a rough un-machined surface.

Further work could include experimenting with machined and as-cast inner surfaces for longer periods of time, to determine if a reduction in oxidation rate is observed with the smooth surface. Alternatively, it would be interesting to observe the longevity and inner surface of the trial tube, with the machined inner bore, installed in CAPL furnace in 2005. It should be in the interest of CAPL to have the trial tube analysed after failure.

8.8 Summary of Findings

In summary, the testing rig was successful in achieving heating and cooling heat resistant stainless steel samples to temperatures above 1000ºC and cool to low temperatures in quick succession. Also, samples were able to be held at elevated temperatures over long periods of time with consistency in material temperatures.

The experiments conducted did not change the microstructure of the material significantly to observe any effects. Although, visible signs of 'spalling' were observed at the end of the heat and hold experiment, which suggests that holding the sample at elevated temperatures was providing sufficient time for oxidation to occur and the resultant thermal stresses induced during the cooling phase resulting in the loss of material.

Longer experiments at elevated temperatures are required to allow changes to occur to the microstructure of the material, which should result in more prominent effects. Also, further experimentation is required to determine if machined inner bores prolong tube life through reduced oxidation rates.

9 Conclusions and Further Work

9.1 Conclusions

Radiant tube replacement and associated maintenance costs are one of CAPL's biggest annual expenditures, with on average 33 of the 338 furnace tubes changed every year since it was commissioned in 1998.

Tube longevity varies across the furnace, with the highest failure rates associated with the latter, hotter zones. Original tubes are still in service in zones 1, 2 and 3, where zone temperatures are up to 100ºC lower than zones 7 and 8. Tubes are on average expected to last 200 and 226 weeks in zone 8 and 7 respectively. In comparison, original tubes are still in service in zones 1, 2 and 3.

Radiant tube life is comparable across all furnaces surveyed, with most replacing at least 10% of the total radiant tubes every year. Segal galvanising line have increased material specification and added expansion bellows to the firing leg flange. Currently, they are replacing on average 8.5% of the furnace tubes every year.

Sumitomo Metals rotate their radiant tubes to counteract creep deformation. Also, recent material changes and machined inner bores have reported to increase tube life through reducing the oxidation rate.

Temperature analysis of a CAPL radiant tube highlighted that maximum temperatures of over 1000ºC occurred at the end of the firing leg. Differentials of up to 75ºC were achieved during normal operation, which increased to 250ºC during furnace heating from ambient conditions. Reducing the heating rate to 100ºC/hr during the initial heating phase, reduced the differentials to below 60ºC.

Analysis of failed radiant tube material identified that the tubes had been subjected to excessively high temperatures, evident from the coarsening and agglomeration of chromium carbides. This detrimental microstructure evolution decreases the material's capability of resisting creep rupture, resulting in excessive deformation and formation of cavities at the grain boundaries. Cracks developed at the inner surface,

due to spalling and breaking down of the passive oxide layer, travelled along the creep cavities resulting in tube failure.

Elevated temperatures also accelerate the rate of oxidation within the tube, compounded by the onerous duty, internal stresses develop between the oxide scale and the base metal, resulting in the oxide breaking away or spalling, allowing further base metal to be attacked. All failures observed at CAPL furnace were in the hottest region of the firing leg.

Stress analysis of the radiant tube design showed that stresses at the end of the firing leg were relatively high. The adoption of a new central bend support, reduced the local stresses induced in the firing leg and as a result reduced the overall deformation.

Tube life to rupture was calculated and was in the region of 4 years with current designs and maximum temperatures of 1000ºC. Installation of an expansion bellow to both flanges resulted in a significant stress reduction in the firing leg and as a result increased tube life to over 8 years. Increasing material composition also showed similar results. Combining these two design modifications could result in a significant increase in tube longevity.

Heat cycling of radiant tube material was achieved with a purpose built testing rig. Longer experimental time was required to identify significant changes in material microstructure. But, given sufficient time at temperature, the samples showed evidence of spalling under cooling, which confirmed the theory of metal loss and cavity forming in the failed radiant tubes.

Large differences were observed between the inner surfaces of as-cast samples and machined inner bore tubes. Sumitomo Metals argue that the smoother inner surface reduces the rate of oxidation and increases tube life. Presumably, this is achieved due to the smaller surface area for oxidation to occur.

Improvements have been made to the tube design and material specification throughout the project, which were based on the work conducted by this project. These modifications are now standard for all new radiant tubes supplied to CAPL.

But, further design modifications, for example the expansion bellows, are still being trialled, with the aim of confirming theories discussed in this thesis and improving tube longevity.

9.2 Further Work

9.2.1 Mixing Element Radiant Tube

The Mixing Element Radiant Tube (MERT) is a patented design offered by Kubota Fahramet, a company who manufacture high temperature alloy castings for the petrochemical and steel industry.

A MERT tube has a continuous weld bead fused to the inside surface of the tube in a spiral fashion to promote mixing within the tube, Figure 9-1. It does this by inducing turbulent flows and breaking down the laminar boundary layer which forms with the inner surface of the tube. The improved stirring within the tube, increases the heat transfer and improves efficiency.

Figure 9-1 - Image displaying a section of a MERT radiant tube showing the continuous weld bead on the inside of the tube surface[79]

The MERT design is only currently applied to radiant tubes used in the petrochemical industry. Here, the burners are mounted on the furnace walls heating the external surfaces of the tubes. The heat transfers energy to the petrochemical fluids within. The MERT weld bead mixes the fluids within the tube increasing the rate of reaction and improves the system efficiency.

It would be interesting to adopt a similar design on the inside of an annealing radiant tube, specifically in the exhaust legs of a 'W' tube design. Here, the combustion is complete and the hot exhaust gases are travelling along the tube, being drawn out to the exhaust stack by the eduction fan.

A weld bead acting as a spiral fin would break down the boundary layer which forms, promoting greater mixing, releasing more energy and also increasing convective heat transfer between the exhaust gases and the radiant tube material, due to increasing the surface area; thus improving heat transfer.

9.2.2 Ceramic Inserts

Ceramic inserts are positioned into the exhaust leg of a radiant tube and are reported to improve energy efficiency and radiant tube life[80-82]. The inserts, Figure 9-2, which have a high surface area, are heated by the exhaust gases. The ceramic inserts then re-radiate energy to the tube wall, raising the temperature of the exhaust leg and releasing greater amounts of heat energy from exhaust gases which would generally be lost to atmosphere.

The shape of the inserts plays a key role too, by inducing swirl flow; the effect of boundary layers is reduced. As a result, the convective heat transfer to the tube wall is increased and exhaust gas temperature leaving the tube is reduced. In prototype form, research by Wu[79] showed that exhaust leg temperatures could be increased by 25ºC, increasing the tube efficiency by up to 5%.

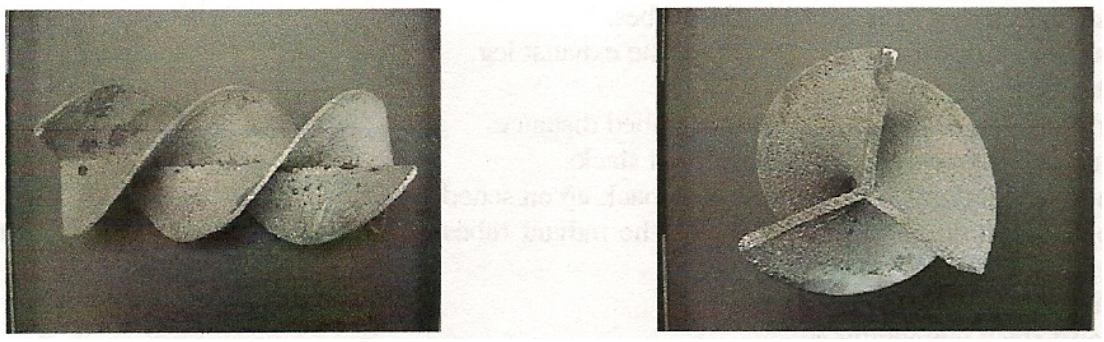

Figure 9-2 - Side and front views of the Spyrocor ceramic insert[81]

By increasing the amount of energy released from a combustion process, lesser amounts of fuel can be used. Also, if more energy can be released in the exhaust leg, Figure 9-3, then the maximum temperatures in the firing leg can be reduced. Lowering temperatures can have a beneficial effect on the longevity of the radiant tube, although the added weight of the inserts and increasing tube temperatures locally in the exhaust leg need to be considered.

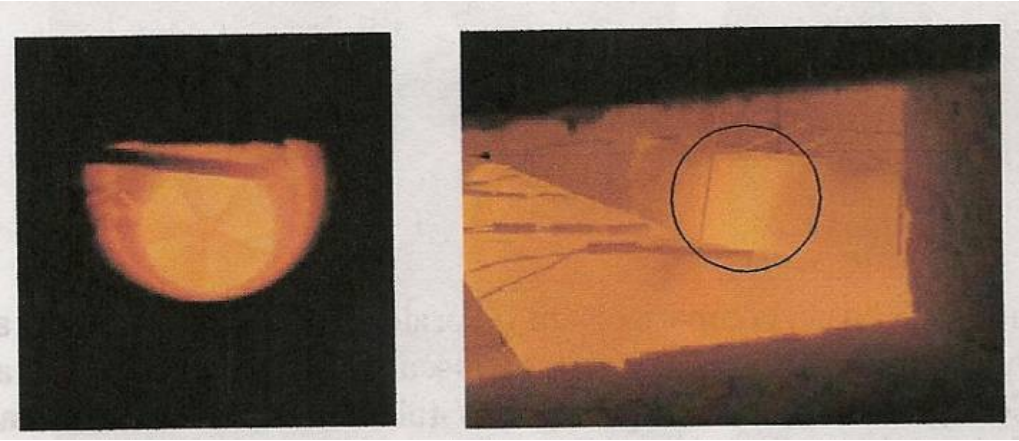

Figure 9-3 - The effect of installing a ceramic insert into an exhaust leg[81]

9.2.3 Radiant Tube Monitoring

There is great value in knowledge. Without it, new technologies and theories could not be proved. During the research conducted for this project, radiant tube monitoring was fundamental in understanding the behaviour of the radiant tube and its response to various furnace loading and demand.

If further technologies are to be trialled, for example the fitment of ceramic inserts, then tube monitoring through temperature thermocouples is essential to understand the differences to prove if the technology works. It is important that CAPL at Port Talbot continue to utilise the temperature monitoring installed during this project and increase the number of monitored tubes through the furnace to help with future developments.

9.2.4 Different Radiant Tube Designs and Burner Arrangements

With significant investment, different radiant tube designs and burner arrangements could be trialled at Port Talbot CAPL. In terms of design, a support for the lower return could be incorporated in the furnace wall, thus allowing the lower tubes to be independently supported from the upper half. Or a completely new design, such as a re-circulating tube design could be trialled in a high demand zone to see if the inherent better temperature uniformity prolonged tube life[83].

Experiences with such a re-circulating tube design have been outlined by Beck et al[83], where after 5 years of operation no visible signs of deformation were reported, while the re-circulating design along with regenerative burner installation allowed for very low NO_x levels.

Regenerative burners could be retrofitted to CAPL Port Talbot. Used with on-off firing, in the current W tube shape, better temperature uniformity has been reported[21,22,27]. It is argued that the better temperature uniformity across the length of the radiant tube lowers stresses developed in the tube material, which in turn prolongs tube life. Also, maximum temperatures can be reduced allowing the material to operate at higher creep strengths, minimising and delaying the effect of tube deformation from creep.

10 References

1. UK Steel Annual Review 2010. Publication by the EEF, Broadway House, London.

2. Shipley D.G. *Creep Damage in Reformer tubes.* International Journal for Pressure Vessels and Piping 1983, **14**: p. 21-34

3. Brear, J.M., Whittaker, M.T., Wilshire, B. *Creep Fracture of Centrifugally-Cast HK40 Tube Steel*. Materials Research Centre, School of Engineering, Swansea University. Pending Publication.

4. Dini, G., Vaghefi, S.M.M., Lotfiani, M., Jafari, M., Rad, M., Navabi, M., Abbasi, S. *Computational and Experimental Failure Analysis of Continuous-Annealing Furnace Radiant Tubes Exposed to Excessive Temperature*. Engineering Failure Analysis 2007. doi: 10.1016/j.engfailanal.2007.05.007

5. Hansel, M., Boddington, C.A., Young, D.J. *Internal Oxidation and Carburisation of Heat-resistant Alloys.* Corrosion Science 2003, **45**: p. 967-981

6. Ul-Hamid, A., Tawancy, H., Mohammed, A.I., Abbas, N.M. *Failure Analysis of Furnace Radiant Tubes Exposed to Excessive Temperature.* Engineering Failure Analysis, 2006. **13**: p. 1005-1021

7. El-Batahgy, A., Zaghloul, B. *Creep Failure of Cracking Heater at a Petrochemical Plant.* Materials Characterisation 2005, **54**: p. 239-245

8. Wen-Tai, H., Honeycombe, R. *Structure of Centrifugally Cast Austenitic Stainless Steels: Part 1, HK40 as cast and after creep between 750 and 1000ºC.* Materials Science and Technology 1985, **1**: p. 385-397

9. Rodriguez, J., Haro, S., Velasco, A., Colas, R. *A Metallographic Study of Aging in a Cast Heat-resisting Alloy.* Materials Characterisation 2000, **45**: p. 25-32

10. Kaya, A., Krauklis, P., Young, D. *Microstructure of HK40 Alloy after High Temperature Service in Oxidizing/Carburizing Environment.* Materials Characterisation 2002, **49**: p. 11-21

11. Xing, L., Zhao, J., Shen, F., Feng, W. *Reliability Analysis and Life Prediction of HK40 Steel During High Temperature Exposure.* International Journal of Pressure Vessels and Piping 2006, **83**: p. 730-735

12. Kaya, A. *Microstructure of HK40 Alloy after High Temperature Service in Oxidizing/Carburizing Environment.* Materials Characterisation 2002, **49**: p. 23-34

13. Shi, S., Lippold, J. *Microstructure Evolution During Service Exposure of Two Cast Heat Resisting Stainless Steels.* Materials Characterisation 2008, **59**: p. 1029-1040

14. Guan, K., Xu, H., Wang, Z. *Analysis of Failed Ethylene Cracking Tubes.* Engineering Failure Analysis 2005. **12**: p. 420-431

15. Mullinger, P. & Jenkins, B. *Industrial and Process Furnaces. Principles, Design and Operation.* Butterworth-Heinemann. Oxford, UK: p. 34

16. Baukal Jr, C.E. *Heat Transfer in Industrial Combustion*. CRC Press, Florida, USA: p. 42

17. Baukal Jr, C.E. *Heat Transfer in Industrial Combustion*. CRC Press, Florida, USA: p. 32

18. Baukal Jr, C.E. *Heat Transfer in Industrial Combustion*. CRC Press, Florida, USA: p. 491

19. Hekkens, R.H., Speets, R.C.J. & Veld, L. *Regenerative Burners for Radiant Tubes, Experiments with Recuperative Radiant Tube Burner*. Tata Research, Development & Technology, Ijmuiden Technology Centre. Report code: IJTC/RMS R&A/CR/09393/2003/A. Ref Source no. 110727. December 2003

20. Hekkens, R.H. *Regenerative Burners for Radiant Tubes, Feasibility for Corus Annealing and Galvanizing lines.* Reference Source No. 114511. June 2005

21. Quinn, D.E. *Regenerative Radiant Tube Combustion Systems for Continuous Strip Annealing Furnaces.* Paper presented at the 91st Galvanizer's Association Conference. Mississippi, October 1999

22. Quinn, D., Mieloo, R. & Cochenour, J. *Stelco's Experience with a Regenerative Combustion System.* Presented at the Galvanizer's Association 96th Annual Meeting, October 2004

23. Baukal Jr, C.E. *Heat Transfer in Industrial Combustion*. CRC Press, Florida, USA: p. 486

24. Quinn, D.E. *Increasing the Production Rate of Radiant Tube Fired Furnaces.* Industrial Heating Journal, September 2007: p. 115-122

25. Wuenning, J.G. *Self Regenerative Burner for Single Ended, P and Double-P Radiant Tubes*. Industrial Heating Journal, June 2007: p.47 -49

26. Wuenning, J.G. *Radiant Tubes for Continuous Strip Processing Furnaces.* Industrial Heating Journal, September 2005: p. 117-123

27. Wunning, J.G. *Radiant Tube Heating Systems, what are the Options?* Paper presented at the 94th Galvanizer's Association Conference. Dearborn, October 2002

28. http://www.flox.com/documents/regemat_eng_2.swf (Visited February 2011)

29. http://www.industrialheating.com/Articles/Feature_Article/BNP_GUID_9-5-2006_A_10000000000000168596 (Visited July 2010)

30. Baukal Jr, C.E. *Heat Transfer in Industrial Combustion*. CRC Press, Florida, USA: p. 44

31. ASM Metals Handbook. *Volume 1 – Properties and selection of metals*. 8th Edition. Metals Park. Novelty, Ohio

32. Mullinger, P. & Jenkins, B. *Industrial and Process Furnaces. Principles, Design and Operation*. Butterworth-Heinemann. Oxford, UK: p. 438

33. Mullinger, P. & Jenkins, B. *Industrial and Process Furnaces. Principles, Design and Operation*. Butterworth-Heinemann. Oxford, UK: p. 440 & 441

34. Magnan, J. *Materials Selection for Radiant Heaters*. Kubota Metal Corporation, Fahramet Division. Paper presented at the Galvanizer's Association Annual Meeting.

35. Callister Jr, W.D. *Materials Science and Engineering, An Introduction, 7th Edition*. John Wiley and Sons Inc. New York: p. 237 to 241

36. Glen, J. *The Problem of the Creep of Metals. Murex Welding Processes Limited*. Waltham Cross, Hertfordshire, England. The Kynoch Press, Birmingham. January 1968

37. Mullinger, P. & Jenkins, B. *Industrial and Process Furnaces. Principles, Design and Operation*. Butterworth-Heinemann. Oxford, UK: p. 442

38. Birks, N., Meier, G.H. & Pettit, F.S. *Introduction to the High Temperature Oxidation of Metals, Second Edition*. Cambridge University Press, 2006: p. 133-143

39. Wuenning, J.G. *Gas Fired Radiant Tube Heating Systems.* Heat Treating Progress, Volume 5, September 2005: p. 76-80

40. Georgiew, A., Bonnet, U. & Milani, A. Next Generation of Radiant Tubes for Vertical Galvanising Lines. Millennium Steel Journal, 2008: p. 223-226

41. http://www.industrialheating.com/IH/Home/Images/ih0607-igc-self-fig.1-lg.jpg (Visited July 2010)

42. Beck, E., Schonenberg, R., Zeizinger, S. & Wuenning, J. *Operating Experience with Regard to New Double-P Radiant Tube Technology in a Vertical Galvanising line.* Paper presented at the Galvanizer's Association Annual Meeting

43. Lewis, D.W., Adams, W.T.J. & John, I.H. *Combustion Stoichiometry and Other Factors which Influence Radiant Tube Life at CAPL Trostre.* Report No. WL/EG/TN/5609/1/94/D. May 1994.

44. Callister Jr., W.D. *Materials Science and Engineering, An Introduction, 6th Edition*. John Wiley and Sons Inc. New York.

45. Wilshire, B. *Processing of Uncoated Sheet Steels.* Lecture Notes, Materials Research Centre, University of Wales Swansea, 2006

46. McManus, G.J. *Batch Annealing Stages Comeback, but Continuous Annealing Gains Ground too*. Iron and Steel Engineer, September 1997. p. 58-59.

47. Abe, H. & Satoh, S. *Progress of Continuous Annealing Technology for Cold-Rolled Sheet Steels and Associated Product Development.* Kawasaki Steel Technical Report No. 22, May 1990

48. *Corus Strip Products UK, Making a Difference Brochure, Port Talbot and Llanwern Works.* Brochure Reference No. CSPUK01:3000:UK:06/2002

49. *Stein Heurtey, Technical Drawing of CAPL Process Sections.* 1997

50. *Stein Heurtey, Furnace Description Manual, CAPL, Port Talbot.* Manual 1, Vol. 1 of 3. 1997.

51. Veld, L. *CAPL Port Talbot; Radiant Tube Life Time*. Corus RD&T, Ijmuiden Technology Centre. Report Code: IJTC/RMS R&A/C/06516/2003/A. November 2003

52. T. Nakagawa, M. Kohashi et al. *Development of Radiant Tube and Burner for High Temperature and High Intensity Combustion.* 27th April 1992.

53. Chakrabarti, S., Sarkar, S., Kumar, S., Singh, G.R.P. & Maheshwari, M.D. *Failure of Radiant Tubes in a Continuous Galvanizing Furnace*. Tata Steel, Jamshedpur – 831 001. India

54. Yoon, K.B. & Jeong, D.G. *Oxidation Failure of Radiant Heater Tubes.* Engineering Failure Analysis, 1998. **6**: p. 101 - 112

55. Lewis, D.W., Uzzaman, R. & Bowen, R. *Radiant Tube Life & Temperature Assessment on CAPL Furnace at Trostre 1996.* British Steel Technical Report. Report No. WL/PP/TN/8003/3/96/D. October 1996.

56. Lewis, D.W., Adams, W.T.J. & Jones, M.B.L. *Continuous Annealing (CAL) Furnace Improvement Programme at Trostre Works.* British Steel Technical report. Report No. WL/EG/TN/8005/2/95/D. August 1995.

57. *Recent Developments in Annealing*. Special Report 79, Iron and steel institute. 1963. Percy Lund, London.

58. Lewis, D.W., James, W.M., Morgan, G. *Segal – Site Visit Report on Radiant Tube Failure/Improvement Programme, Liege, Belgium.* Report No. VR/PT/WMJ/08/0012. Feburary 2008.

59. American Society for Metals, Metals Handbook. *Volume 8, Metallography, Structures and Phase Diagrams.* Metals Park, Ohio 44073

60. Wulpi, D.J. *Understanding How Components Fail*. American Society for Metals. Metals Park, Ohio 44073

61. Yoon, K.B., Jeong, D.G. *Oxidation Failure of Radiant Heater Tubes.* Engineering Failure Analysis, 1998. **6**: p. 101-112

62. de Lima, B.B., Conte, R.A. & Nunes, C.A. *Analysis of Nickel-Niobium Alloys by Inductively Coupled Plasma Optical Emission Spectrometry.* Talanta, 2003. **59**: p. 89-93

63. Einhauser, T.J. *ICP-OES and SEM-EDX Analysis of Dust and Powder Produced by the Laser-Processing of CR-Ni-Steel alloy*. Mikrochimica Acta, 1997. **127:** p. 265-268

64. British Standards Document. *BS EN 10295:2002*

65. Hänsel, M., Boddington, C.A., Young, D.J. *Internal Oxidation and Carburisation of Heat-Resistant Alloys*. Corrosion Science, 2003. **45:** p. 967-981

66. British Standards Document. *BS EN ISO 6507-1:2005*

67. Petkovic-Luton, R., Ramanarayanan, T.A. *Mixed Oxidant Attack of High Temperature Alloys in Carbon and Oxygen Containing Environments.* Oxidation of Metals, 1990. **34**: p. 381-400

68. Branza, T., Deschaux-Beaume, F., Velay, V., Lours, P. *A Microstructural and Low-Cycle Fatigue Investigation of Weld Repaired Heat-Resistant Cast Steels.* Journal of Materials Processing Technology, 2009. **209**: p. 944-953

69. Henrique de Almeida, L., Ribiero, A.F., May, I.L. *Microstructural Characterization of Modified 25Cr-35Ni Centrifugally Cast Steel Furnace Tubes*. Materials Characterization, 2003. **49**: p. 219-229

70. Glen, J. *The Problem of the Creep of Metals. Murex Welding Processes Limited*. Waltham Cross, Hertfordshire, England. The Kynoch Press, Birmingham. 1968

71. ASM Speciality Handbook. *Heat Resistant Materials*. ASM international, Metals Park, Ohio 44073, p. 43

72. Alvino, A., Lega, D., Giacobbe, F., Mazzocchi, V., Rinaldi, A. *Damage Characterization in Two Reformer Heater Tubes After Nearly 10 Years of Service at Different Operative and Maintenance Conditions*. Engineering Failure Analysis, 2010. doi 10.1016/j.engfailanal.2010.03.003

73. El-Batahgy, A., Zaghloul, B. Creep Failure of Cracking Heater at a Petrochemical Plant. Materials Characterization, 2005. **54:** p. 239-245

74. May, L., da Silveira, T.L., Vianna, C.H. *Criteria for the Evaluation of Damage and Remaining Life in Reformer Furnace Tubes*. International Journal of Pressure Vessels and Piping, 1996. **66**: p. 233-241

75. Balikci, E., Mirshams, R.A., Raman, A. *Fracture Behaviour of Superalloy IN738LC with Various Precipitate Microstructures*. Materials Science and Engineering, 1999. **A265**: p. 50-62

76. Birks, N., Meier, G.H., Pettit, F.S. *Introduction to the High Temperature Oxidation of Metals, Second Edition*. Cambridge University Press, 2006. p. 133-143

77. Irfan, M.A., Chapman. W. *Thermal Stresses in Radiant Tubes due to Axial, Circumferential and Radial Temperature Distributions*. Applied Thermal Engineering 2009. **29**: p. 1913 – 1920.

78. Irfan, M.A., Chapman, W. *Thermal Stresses in Radiant Tubes: A Comparison between Recuperative and Regenerative Systems.* Applied Thermal Engineering 2009. doi: 10.1016/j.applthermaleng.2009.08.002

79. Picture taken from Kubota website: http://www.kubotametal.com/products/mert.html (Visited 2009)

80. Hardy, R. & Briselden, T. *Resulting Energy Savings Using Radiant Heat Transfer Systems.* Paper presented at the Galvanizer's Association 100th Conference, Baltimore. October 2008

81. Winger, C & Hardy, R. *Innovative Energy Savings in Continuous Annealing Furnace*. 7th International Conference on Zinc and Zinc Alloy Coated Steel Sheet: Galvatech '07, Osaka, Japan. November 2007

82. Wu, H. *Continuous Annealing Radiant Tube Inserts – Prototype Development.* Tata Research, Development & Technology. Ref Source No. 147584. November 2009

83. Beck, E., Schonenberg, R., Zeizinger, S., Wuenning, J.G. *Operating Experience with Regard to New Double P Radiant Tube Technology in a Vertical Galvanizing Line.* http://www.flox.com/documents/06_GA.pdf. (Visited 2008)

11 Appendices

11.1 Appendix A

Table 11-1 - Material composition of radiant tube material

Material	Designation	C (%)	Cr (%)	Ni (%)	Mo (%)	N (%)	Other (%)	ASTM
1.4848	GX40CrNiSi25-20	0.4	25	20			Si: 2	HK HK-40
1.4857	GX40CrNiSi35-25	0.4	25	35			Si: 2	HP
1.4849	GX40CrNiSiNb38-19	0.4	18	37			Si: 2 Nb: 1.5	HT50C HT50 HAT
2.4879	G-NiCr28W	0.4	28	48			Si: 2 W: 4.5	

11.2 Appendix B

Average thermocouple temperature calculated with the following formula:

$$Arithmetic\ Mean = \frac{1}{n}\sum_{i=1}^{n} a_i = \frac{a_1 + a_2 + ... + a_n}{n}$$

Where:

a = thermocouple temperature at any given sample

n = number of samples taken

11.3 Appendix C

Furnace Cooling:

- Primary Cooling

Time / Mins	Temperature		
	10th Mar	16th Mar	31st Mar
75	744	683	724
225	457	438	466

For 10th Mar:

$$\frac{(744-457)}{(225-75)} = 1.91°C/\min$$

For 16th Mar:

$$\frac{(683-438)}{(225-75)} = 1.63°C/\min$$

For 31st Mar:

$$\frac{(724-466)}{(225-75)} = 1.72°C/\min$$

- Secondary Cooling

Time / Mins	Temperature		
	10^{th} Mar	16^{th} Mar	31^{st} Mar
300	N/A	386	434
450	N/A	279	327

For 16^{th} Mar:

$$\frac{(386-279)}{(450-300)} = 0.71°C / \min$$

For 31^{st} Mar:

$$\frac{(434-327)}{(450-300)} = 0.72°C / \min$$

11.4 Appendix D

Furnace Heating:

13th Mar		20th Mar		2nd Apr	
Time	Temperature	Time	Temperature	Time	Temperature
225	82	510	156	900	161
330	440	585	402	1005	393

For 10th Mar:

$$\frac{(440-82)}{(330-225)} = 3.41°C/\min$$

For 16th Mar:

$$\frac{(402-156)}{(585-510)} = 3.28°C/\min$$

For 31st Mar:

$$\frac{(393-161)}{(1005-900)} = 2.21°C/\min$$

11.5 Appendix E

Table 11-2 - Semi-quantitative EDS microanalysis results of sample 5 OS 6.1

	Approximate Weight QA % Elements																
	C	O	Na	Mg	Al	Si	P	S	Cl	K	Ca	Ti	V	Cr	Mn	Fe	Ni
1						<1								9	tr	64	26
2						1								9	<1	63	26
3						<1								45	tr	40	14
4						tr								94		5	<1
5	D					<1		tr						7		13	4
6	D					tr		<1						13		9	3
7	D					2		tr	14					2		2	<1
8						81			1					10		6	2
9		10			tr	tr								60	26	3	<1
10		13				<1								3	1	54	27

Note.

The quantification procedure strictly applies to polished surfaces and therefore the results on rough surfaces such as particles may only be considered semi-quantitative. Carbon can be detected but not quantified i.e. d = detected and D = detected in significant amounts. For other elements:- blank cell = element not detected, tr = trace amounts (<0.5%). The above results indicate only the relative proportions of each element.

11.6 Appendix F

HK-40 data sheet

Kubota METAL CORPORATION
25 Commerce Road, Orillia, Ontario, Canada L3V 6L6
Phone (705) 325-2781 Fax (705) 325-5887

ALLOY DATA SHEET
HK

HEAT RESISTANT ALLOY

REVISION: 04/91

DESCRIPTION

HK alloy, more well known as HK 40, is an austenitic Fe-Cr-Ni alloy that has been a standard heat resistant material for over four decades. With moderately high temperature strength, oxidation resistance and carburization resistance the alloy is used in a wide variety of industrial applications.

COMPOSITION

	C	Mn	Si	Cr	Ni	P	S
Min %	0.35	0.4	0.5	23	19	-	-
Max %	0.45	1.5	1.5	27	22	0.03	0.03

APPLICATIONS

Ammonia, methanol and hydrogen reformers; ethylene pyrolysis coils and fittings; steam superheater tubes and fittings; tube supports and hangers; tube sheets; heat treatment fixtures and trays; refractory supports; furnace skids; furnace rolls; rabble arms.

PRODUCT FORMS

Horizontal and vertical centrifugal castings; static castings.

PHYSICAL PROPERTIES

Density (lbs/in^3)	0.280	
Melting Point(^{o}F)	2540	
Thermal Conductivity	7.9	@ 212^{o}F
(Btu/h/ft^2/ft/^{o}F)	15.7	@ 1600^{o}F
	17.1	@ 1800^{o}F
Thermal Expansion	9.8	@ 70-1400^{o}F
(10^{-6}in/in ^{o}F)	10.0	@ 70-1600^{o}F
	10.2	@ 70-1800^{o}F

CARBURIZATION RESISTANCE

(Gas-1064 hours @ 1760^{o}F)

ALLOY GRADE	WEIGHT GAIN mg/mm^2
H F	0.81
H H	0.58
H K	**0.56**
H P	0.20

MECHANICAL PROPERTIES (Typical Values)

		Centrifugal Castings					Static Castings
		70	1400	1600	1800	2000 ^{o}F	70 ^{o}F
U.T.S.	K.S.I.	84	38	24	15	5.6	74
Y.S.	K.S.I.	44	24	16	9	5	45
El.	%	20	13	16	42	55	17

SERVICE TEMPERATURE

The alloy is suitable for service at temperatures up to approximately 2000^{o}F.

COMPARATIVE OXIDATION RATES (mm / year)
(500 hour cyclic tests)

GRADE	1832	1922	2012	2102	2204 ^{o}F
H H	<0.1	0.22	0.92	3.9	
H K	**<0.1**	**0.22**	**0.95**	**3.5**	**12.7**
H T	0.20	0.54	1.4	3.2	7.2

WELDABILITY

HK40 alloy has good weldability by the SMAW, GTAW and GMAW processes using filler metal of matching composition.

CREEP-RUPTURE PROPERTIES

Long term creep-rupture properties were extrapolated from Larson-Miller Parameter versus stress plots.

RUPTURE-STRESS-KSI

HOURS		1400	1500	1600	1700	1800	1900	°F
1,000.	AVG.	11.9	8.75	6.18	4.34	3.05	2.09	
	MIN.	9.39	6.97	4.98	3.48	2.35	1.54	
10,000.	AVG	8.75	6.04	4.10	2.67	1.74	1.05	
	MIN	6.96	4.84	3.27	2.10	1.34	0.85	
100,000	AVG.	6.11	4.12	2.58	1.59	0.96		
	MIN.	4.84	3.20	2.06	1.28	0.78		

CREEP-STRESS-KSI

%/HOUR		1400	1500	1600	1700	1800	1900	°F
0.01	AVG.	-	11.8	9.9	8.0	6.35	4.75	
0.001	AVG.	11.6	9.5	7.4	5.7	3.93	2.68	
0.0001	AVG	9.0	6.85	5.0	3.35	2.05	1.05	

Note: Creep and rupture stresses are subject to periodic revisions as the results from long term tests become available.

RELATED SPECIFICATIONS

ASTM: A 297 (HK); A 351(HK30 and HK40); A 567 (HK40 and HK50 - specification discontinued in 1987); A608 (HK30 and HK40)

Nearest wrought grade: AISI 310. The composition of the wrought grade differs from that of the cast alloy and has different properties. The cast alloy designation should always be used to identify castings.

HEAD OFFICE, FOUNDRY & INTERNATIONAL SALES
Kubota Metal Corporation, Fahramet Division
25 Commerce Road, P.O. Box 1700,
Orillia, Ontario, Canada, L3V 6L6.
Phone (705) 325-2781
Fax (705) 325 5887

11.7 Appendix G

HP data sheet

Kubota METAL CORPORATION
25 Commerce Road, Orillia, Ontario, Canada L3V 6L6
Phone (705) 325-2781 Fax (705) 325-5887

ALLOY DATA SHEET
HP

HEAT RESISTANT ALLOY

REVISION: 04/91

DESCRIPTION

HP alloy is a fully austenitic iron-nickel-chromium heat resisting steel. It has much higher creep-rupture strength, carburization resistance and oxidation resistance than HK 40 alloy and consequently is used at higher service temperatures. This alloy also forms the base of an extensive family of Kubota alloys which are modified by single or multiple additions of cobalt, molybdenum, niobium, titanium and tungsten. These higher strength alloys are extensively used in reformer and pyrolysis furnaces in the petrochemical industry.

COMPOSITION

	C	Mn	Si	Cr	Ni	P	S
Min %	0.35			24	33	-	-
Max %	0.75	2.0	2.0	28	37	0.03	0.03

APPLICATIONS

Ammonia, methanol and hydrogen reformers; ethylene pyrolysis coils and fittings; steam superheaters; tube supports and hangers; tube sheets.

PRODUCT FORMS

Horizontal and vertical centrifugal castings; static castings; formed fittings and sweeps.

PHYSICAL PROPERTIES

Density (lbs/in^3)	0.284	
Melting Point(°F)	2450	
Thermal Conductivity	7.5	@ 212°F
(Btu/h/ft^2/ft/°F)	14.5	@ 1600°F
	15.7	@ 1800°F
Thermal Expansion	10.0	@ 70-1600°F
(10^{-6}in/in °F)	10.3	@ 70-1800°F
	10.6	@ 70-2000°F

CARBURIZATION RESISTANCE

(Gas-1064 hours @ 1760°F)

ALLOY GRADE	WEIGHT GAIN mg/mm^2
H K	0.56
H N	0.43
H P	**0.20**
H T	0.38

MECHANICAL PROPERTIES (Typical Values)

		Centrifugal Castings				Static Castings
		70	1600	1800	2000 °F	70 °F
U.T.S.	K.S.I.	71	26	15	7.5	66
Y.S.	K.S.I.	38	18	11	6	36
El.	%	11	27	46	69	11

SERVICE TEMPERATURE

The alloy is suitable for long term service at temperatures up 2050°F.

COMPARATIVE OXIDATION RATES (mm / year)
(500 hour cyclic tests)

GRADE	1832	1922	2012	2102 °F
H H	<0.1	0.22	0.92	3.9
H K	<0.1	0.22	0.95	3.5
H P	**<0.1**	**0.25**	**0.64**	**1.5**

WELDABILITY

HP alloy has good weldability by the SMAW, GTAW and GMAW processes.

CREEP-RUPTURE PROPERTIES

Long term creep-rupture properties were extrapolated from Larson-Miller Parameter versus stress plots.

RUPTURE-STRESS-KSI

HOURS		1400	1500	1600	1700	1800	1900	2000	2100	°F
100.	AVG.			9.5	7.0	5.15	3.8	2.75	1.25	
	MIN.			9.0	6.6	4.9	3.6	2.6	1.1	
1,000.	AVG.		9.8	7.05	5.05	3.65	2.6	1.09	0.77	
	MIN.		9.2	6.6	4.8	3.5	2.4	0.98	0.68	
10,000.	AVG.	10.4	7.28	5.15	3.63	2.55	1.38	0.70		
	MIN.	9.5	6.9	4.9	3.45	2.4	1.25	0.62		
100,000	AVG.	7.63	5.38	3.74	2.63	1.38	0.68	0.33		
	MIN.	7.25	5.1	3.57	2.5	1.25	0.62	0.30		

CREEP-STRESS-KSI

%/HOUR		1400	1500	1600	1700	1800	1900	2000	2100	°F
0.01	AVG.		11.7	8.55	6.65	4.95	3.7	2.08	1.67	
0.001	AVG.	12.8	8.8	6.2	4.5	3.6	2.05	1.6	0.92	
0.0001	AVG.	9.7	7.05	5.2	3.78	2.45	1.56	0.90	0.53	

Note: Creep and rupture stresses are subject to periodic revisions as the results from long term tests become available.

RELATED SPECIFICATIONS

ASTM: A 297 (HP).
Nearest wrought grade: None

HEAD OFFICE, FOUNDRY & INTERNATIONAL SALES
Kubota Metal Corporation, Fahramet Division
25 Commerce Road, P.O. Box 1700,
Orillia, Ontario, Canada, L3V 6L6.
Phone (705) 325-2781
Fax (705) 325 5887

11.8 Appendix H

KHR 48 N

Kubota METAL CORPORATION
25 Commerce Road, Orillia, Ontario, Canada L3V 6L6
Phone (705) 325-2781 Fax (705) 325-5887

ALLOY DATA SHEET
KHR48N

HEAT RESISTANT ALLOY

REVISION : 06/99

DESCRIPTION

KHR48N is a nickel-chromium-iron alloy with an addition of 5% tungsten, designed for high strength at elevated service temperatures. The alloy is produced in two types, KHR48N in which the composition is balanced to optimize creep-rupture strength; and KHR48N Hi Si which is adjusted to maximize carburization resistance.

COMPOSITION

	C	Mn	Si	Cr	Ni	W	P	S
Min %	0.4	0.0	0.0	25	45	4.0	-	-
Max %	0.6	1.5	1.5	30	50	6.0	0.03	0.03

APPLICATIONS

Radiant heater tubes and fittings, hangers and tube supports, hydrogen reformer assemblies, catalyst tubes; furnace rolls, steel mill skid conveyor systems, heat treatment furnace fixtures.

PRODUCT FORMS

Horizontal and vertical centrifugal castings; static castings.

PHYSICAL PROPERTIES

Density (lbs/in^3)	0.296	
Melting Solidus	2390	°F
Thermal Conductivity	5.98	@ 212 °F
(Btu ft/ft^2 hr °F)	16.9	@ 2012 °F
Thermal Expansion	7.92	@ 100-800 °F
(x 10^{-6}in/in °F)	8.33	@ 100-1100 °F
	8.61	@ 100-1600 °F
	8.75	@ 100-1800 °F

CARBURIZATION RESISTANCE

(Gas-100 hours @ 1922°F)

ALLOY GRADE	WEIGHT GAIN mg/mm^2
H K	0.33
KHR35C	0.23
KHR48N	0.21*
KHR48N HiSi	0.18

*Calculated value

OXIDATION LOSS (mm/yr)

	KHR 35H	**KHR 48N**	KHR SA	KHR S2	KHR S3
1832 °F	0.30	**0.22**	0.06	0.26	
2012 °F	0.81	**0.77**	0.10	0.37	0.23

MECHANICAL PROPERTIES (Typical Values)

		Centrifugal Castings					Static Castings
		70	1600	1800	2000	2100 °F	70 °F
U.T.S.	K.S.I.	75	30	19	11	8	66
Y.S.	K.S.I.	42	16	11	7	5	36
El.	%	10	27	46	55	47	10

SERVICE TEMPERATURE

The combination of high strength and excellent resistance to oxidation and carburization make this alloy suitable for long term service at temperatures up to 2100 °F and for shorter times and less critical loading for temperatures of 2200 °F

WELDABILITY

KHR48N is welded by the GTAW process using filler metal of matching composition.

CREEP-RUPTURE PROPERTIES

Long term creep-rupture properties were extrapolated from Larson-Miller Parameter versus stress plots.

RUPTURE-STRESS-KSI

HOURS		1400	1500	1600	1700	1800	1900	2000	2100	2200	°F
100	AVG.	-	-	12.03	8.93	6.45	4.51	3.06	2.00	1.27	
	MIN.	-	-	9.93	7.39	5.36	3.93	2.58	1.70	1.09	
1,000	AVG.	-	12.41	9.11	6.49	4.47	2.97	1.90	1.18	0.72	
	MIN.	-	10.24	7.54	5.40	3.74	2.50	1.61	1.01	0.62	
10,000	AVG	13.13	9.55	6.73	4.58	2.99	1.88	1.14	0.68	0.39	
	MIN	10.82	7.90	5.58	3.83	2.53	1.60	0.98	0.58	0.34	
100,000	AVG.	10.28	7.19	4.84	3.13	1.93	1.15	0.67	0.38	-	
	MIN.	8.50	5.98	4.05	2.63	1.64	0.98	0.58	0.33	-	

CREEP-STRESS-KSI

%/HOUR		1400	1500	1600	1700	1800	1900	2000	2100	2200	°F
0.0001	AVG.	-	-	-	4.35	3.15	2.07	1.29	0.67	0.31	

Note: Creep and rupture stresses are subject to periodic revisions as the results from long term tests become available.

HEAD OFFICE, FOUNDRY & INTERNATIONAL SALES
Kubota Metal Corporation, Fahramet Division
25 Commerce Road, P.O. Box 1700,
Orillia, Ontario, Canada, L3V 6L6.
Phone (705) 325-2781
Fax (705) 325 5887

11.9 Appendix I

Safe Operational Procedure for Radiant Tube Heating Rig

Visual and Operational Checks

- Ensure rig and components are in place and that all safety guarding are present
- Make sure that safety signage in place (i.e. hot equipment, test ongoing)
- Ensure all pipes are connected to correct locations
- Check that extraction unit is working
- Ensure that safety valves are in place and are fully functioning and are turned off
- Check that test rig access doors/hatches are closed
- Check that primary air blowers are working. Set to 250 L/min
- Check compressed air is on and set to 15 L/min
- Check that CO monitor is on
- Turn on gas solenoid on main board and check if working
    - Leave disengaged
- Turn on control unit and check if working

Start Up

- Turn on mains gas. D/B 1M/Switch
- Check that all emergency stop switches are disengaged (x3)
- Turn on extraction unit
- Turn on local main gas. Big red handle
- Turn on low level gas valve
- Turn on main board gas solenoid
- Turn on main control unit and press flashing button
- Adjust pilot gas feed to 2 L/min
- Wait for ignition to occur
- Watch for pilot light to be established via sight glass and T/C
- Once stable pilot flame has been achieved primary gas solenoid will activate
- Turn on primary air blowers and set rotameter to 250 L/min
- Once primary gas solenoid has activated adjust primary gas to desired flow
- Stable flame should have been achieved
- Rig now ready for experimental procedure

Shut Down

- To kill all gas supply hit main board gas emergency stop button
- Switch off main control unit
- Set primary air rotameter to maximum flow
- Monitor thermocouple readings for temperature and continue main air flow until temperatures are low

11.10 Appendix J

METRIC CAPACITIES

RTG RADIANT TUBE GAS BURNERS

			3450 Pa			6900 Pa		
			MODEL NUMBER			MODEL NUMBER		
SPECIFICATIONS			102	104	106	102	104	106
LONG FLAME	Max. Input @ 10% Excess Air	(kW)	97.1	178	310	143	254	432
	Max. Air Flow	(nm^3/hr)	102	187	325	150	267	454
	Min. Input @ Max. Air Flow	(kW)	13.2	13.2	17.1	13.2	13.2	17.1
	Max. Excess Air	(%)	710	1,390	1,890	1,100	2,030	2,680
SHORT FLAME	Max. Input @ 10% Excess Air	(kW)	143	238	402	196	346	564
	Max. Air Flow	(nm^3/hr)	150	250	422	205	364	592
	Min. Input @ Max. Air Flow	(kW)	23.7	39.4	53.1	23.7	39.4	53.1
	Max. Excess Air	(%)	560	560	730	810	870	1,070

NOTES:

1. Capacities based on natural gas with LHV of 36.74 MJ/nm^3 , 0.59 S.G., and a stoichiometric air/gas ratio 9.74:1 with burner firing into radiant tube.
2. Air and gas flows based on 0°C @ sea level; capacities for preheated air will differ from those shown.
3. Total air pressures measured 6 pipe diameters from burner air inlet.
4. All data based on industry standard air and gas piping practices.
5. Flame detection available via flame rod or UV scanner.

11.11 Appendix K

Table 11-3 - Calibration chart for the thermocouple voltages

°C	mV	°C	mV
0	0	680	27.88
40	1.64	720	29.52
80	3.28	760	31.16
120	4.92	800	32.8
160	6.56	840	34.44
200	8.2	880	36.08
240	9.84	920	37.72
280	11.48	960	39.36
320	13.12	1000	41
360	14.76	1040	42.64
400	16.4	1080	44.28
440	18.04	1120	45.92
480	19.68	1160	47.56
520	21.32	1200	49.2
560	22.96	1240	50.84
600	24.6	1280	52.48
640	26.24		

11.12 Appendix L

Table 11-4 - Temperature cycling log

Temperature Cycling Log

Index	
	Samples Cut
	Rig re-lined

Cycle #	Date	Heat-Up Start	Cool-Down Start	Cool-Down Finish	Duration	Cycle #	Date	Heat-Up Start	Cool-Down Start	Cool-Down Finish	Duration
1	16/06/2010	12:53	13:10	13:17	00:24	51	08/07/2010	10:55	11:10	11:16	00:21
2	17/06/2010	10:02	10:13	10:17	00:15	52	08/07/2010	11:17	11:24	11:30	00:13
3	17/06/2010	10:24	10:32	10:40	00:16	53	08/07/2010	11:31	11:37	11:43	00:12
4	17/06/2010	10:45	10:53	10:59	00:14	54	08/07/2010	11:45	11:52	11:59	00:14
5	17/06/2010	11:02	11:09	11:16	00:14	55	08/07/2010	12:00	12:06	12:13	00:13
6	21/06/2010	14:48	15:02	15:09	00:21	56	08/07/2010	12:14	12:20	12:22	00:08
7	21/06/2010	15:10	15:19	15:26	00:16	57	08/07/2010	12:23	12:34	12:41	00:18
8	21/06/2010	15:30	15:39	15:47	00:17	58	08/07/2010	12:42	12:49	12:56	00:14
9	21/06/2010	15:49	15:57	16:05	00:16	59	08/07/2010	12:57	13:02	13:08	00:11
10	21/06/2010	16:06	16:15	16:22	00:16	60	08/07/2010	13:09	13:15	13:21	00:12
11	22/06/2010	14:18	14:31	14:39	00:21	61	08/07/2010	13:22	13:29	13:35	00:13
12	22/06/2010	14:40	14:49	14:57	00:17	62	08/07/2010	13:36	13:43	13:50	00:14
13	22/06/2010	15:00	15:08	15:15	00:15	63	08/07/2010	13:51	13:57	14:03	00:12
14	22/06/2010	15:17	15:25	15:32	00:15	64	08/07/2010	14:04	14:10	14:16	00:12
15	22/06/2010	15:34	15:42	15:50	00:16	65	08/07/2010	14:17	14:24	14:30	00:13
16	22/06/2010	15:51	16:00	16:07	00:16	66	08/07/2010	14:31	14:38	14:45	00:14
17	22/06/2010	16:08	16:17	16:25	00:17	67	08/07/2010	14:46	14:53	15:00	00:14
18	23/06/2010	12:31	12:43	12:51	00:20	68	08/07/2010	15:01	15:06	15:13	00:12
19	23/06/2010	12:52	13:00	13:07	00:15	69	08/07/2010	15:13	15:20	15:26	00:13
20	23/06/2010	13:08	13:17	13:24	00:16	70	08/07/2010	15:27	15:34	15:41	00:14
21	23/06/2010	13:26	13:34	13:42	00:16	71	12/07/2010	10:02	10:14	10:21	00:19
22	23/06/2010	13:43	13:52	13:59	00:16	72	12/07/2010	10:22	10:28	10:36	00:14
23	23/06/2010	14:00	14:08	14:16	00:16	73	12/07/2010	10:37	10:43	10:50	00:13
24	23/06/2010	14:17	14:24	14:31	00:14	74	12/07/2010	10:51	10:58	11:05	00:14
25	23/06/2010	14:33	14:41	14:49	00:16	75	12/07/2010	11:06	11:12	11:19	00:13
26	05/07/2010	09:52	10:06	10:12	00:20	76	12/07/2010	11:20	11:27	11:35	00:15
27	05/07/2010	10:13	10:21	10:27	00:14	77	12/07/2010	11:36	11:43	11:50	00:14
28	05/07/2010	10:29	10:38	10:47	00:18	78	12/07/2010	11:51	11:58	12:05	00:14
29	05/07/2010	10:48	11:00	11:07	00:19	79	12/07/2010	12:06	12:14	12:21	00:15
30	05/07/2010	11:08	11:16	11:25	00:17	80	12/07/2010	12:22	12:29	12:36	00:14
31	05/07/2010	11:26	11:36	11:45	00:19	81	12/07/2010	12:37	12:45	12:52	00:15
32	05/07/2010	11:47	11:55	12:03	00:16	82	12/07/2010	12:53	13:00	13:07	00:14
33	05/07/2010	12:04	12:15	12:24	00:20	83	12/07/2010	13:08	13:15	13:22	00:14
34	05/07/2010	12:25	12:35	12:44	00:19	84	12/07/2010	13:23	13:30	13:37	00:14
35	05/07/2010	12:45	12:58	13:08	00:23	85	12/07/2010	13:38	13:45	13:52	00:14
36	05/07/2010	13:09	13:19	13:27	00:18	86	12/07/2010	13:53	14:00	14:07	00:14
37	05/07/2010	13:28	13:37	13:45	00:17	87	12/07/2010	14:08	14:17	14:25	00:17
38	05/07/2010	13:46	13:56	14:04	00:18	88	12/07/2010	14:26	14:35	14:43	00:17
39	05/07/2010	14:05	14:12	14:20	00:15	89	12/07/2010	14:44	14:52	14:59	00:15
40	05/07/2010	14:21	14:29	14:37	00:16	90	12/07/2010	15:00	15:07	15:13	00:13
41	05/07/2010	14:38	14:46	14:54	00:16	91	12/07/2010	15:15	15:22	15:28	00:13
42	05/07/2010	14:55	15:02	15:10	00:15	92	12/07/2010	15:29	15:35	15:42	00:13
43	05/07/2010	15:11	15:19	15:27	00:16	93	16/07/2010	09:30	09:45	09:52	00:22
44	05/07/2010	15:28	15:35	15:43	00:15	94	16/07/2010	09:53	10:00	10:07	00:14
45	05/07/2010	15:44	15:52	16:00	00:16	95	16/07/2010	10:08	10:15	10:22	00:14
46	06/07/2010	09:43	09:57	10:03	00:20	96	16/07/2010	10:23	10:30	10:37	00:14
47	06/07/2010	10:04	10:12	10:19	00:15	97	16/07/2010	10:38	10:46	10:53	00:15
48	06/07/2010	10:20	10:27	10:35	00:15	98	16/07/2010	10:54	11:01	11:08	00:14
49	06/07/2010	10:36	10:43	10:50	00:14	99	16/07/2010	11:09	11:16	11:23	00:14
50	06/07/2010	10:51	11:00	11:06	00:15	100	16/07/2010	11:24	11:31	11:38	00:14
				Total	14:01					Total	11:46

Total	25hrs 47mins

11.13 Appendix M

Assuming complete oxidation of Methane:

$$CH_4 + 2O_2 \rightarrow CO_2 + 2H_2O$$

The number of molecules of Oxygen for every molecule of Methane:

Atomic weights:

Carbon (C) = 12.01

Oxygen (O) = 16

Hydrogen (H) = 1

So:

1 molecule of Methane has a molecular weight of:

$$CH_4 = (1 \text{ x } 12.01) + (4 \text{ x } 1) = 16.01$$

1 Oxygen molecule weighs:

$$O_2 = 2 \text{ x } 16 = 32$$

Therefore, Air : Fuel mass ratio:

$$\frac{Air}{Fuel} = \frac{2 \times 32}{16.01} = 3.99$$

Thus, we need 3.99kg of Oxygen for every 1kg of Methane

Since 23.2% mass of Air is Oxygen,

We need:

$$3.99 \times \frac{100}{23.2} = 17.2 \,\text{kg of Air}$$

Assuming Air density of 1.2kg/m^3:

$$\rho = \frac{m}{V}$$

Where:

ρ = Density

m = Mass

V = Volume

$$V = \frac{17.2}{1.2} = 14.33\,\text{m}^3$$

Assuming Methane gas density of 0.717kg/m^3:

$$V = \frac{1}{0.717} = 1.39\,\text{m}^3$$

Therefore, Stoichiometric Air : Fuel volumetric ratio:

$$\frac{14.33}{1.39} = 10.3$$

Under high fire conditions, CAPL operate their furnace combustion with a λ = 1.2,

Where, $$\lambda = \frac{Actual\ Air : Fuel\ Ratio}{Stoichiometric\ Air : Fuel\ Ratio}$$

So, Actual Air : Fuel Ratio (AFR_{Actual}):

$$AFR_{Actual} = \lambda \times AFR_{Stoich}$$

$$AFR_{Actual} = 1.2 \times 10.3 = 12.36$$

Actual Air volume needed:

$$14.33 \times 1.2 = 17.2\ \mathrm{m}^3$$

To confirm:

$$Excess\ Air\% = \frac{total\ air - \ stoichiometric\ \ air}{stoichiometric\ \ air} \times 100$$

$$Excess\ Air\% = \frac{17.2 - 14.33}{14.33} \times 100 = 20\%$$

Therefore, the following is to be considered for the heat cycling test rig:

Table 11-5 - Combustion ratios to be considered for the heat cycling test rig

λ	1.2
AFR_{Stoich}	10.3
AFR	12.36

Gas L/Min	**Air** L/Min
80	989
100	1236
120	1483
140	1730
160	1978
180	2225
200	2472
220	2719
240	2966
260	3214
280	3461
300	3708